Dissertation

THE ROLE OF miR-451 DURING NEURONAL DIFFERENTIATION IN VITRO

submitted by

Mag.rer.nat.

Christa Maria Erika TRATTNIG, MSc

for the Academic Degree of

Doctor of Medical Science

(Dr. scient. med.)

at the

Medical University of Graz

Research Unit for Experimental Neurotraumatology

Department of Neurosurgery

under the Supervision of

Prof. Dr. Ute SCHÄFER

2015

Statutory Declaration

I hereby declare that this thesis is my own original work and that I have fully acknowledged by name all of those individuals and organisations that have contributed to the research for this dissertation. Due acknowledgement has been made in the text to all other material used. Throughout this thesis and in all related publications I followed the “Standards of Good Scientific Practice and Ombuds Committee at the Medical University of Graz”.

(Date, Place) (Christa Trattnig)

Acknowledgements

I would like to express my innermost gratitude to my PI Professor Dr. Ute Schäfer for providing this fascinating topic and for agreeing to supervise my dissertation. Together with PD Dr. Silke Patz Professor Dr. Ute Schäfer guided and advised me with encouragement, concern, patience and strong believe in my abilities.

Moreover I would like to record my appreciation to the members of my dissertation committee for their abundant academic assistance: Professor Dr. Peter Holzer, PD Dr. Gerd Leitinger, Dr. Gord von Campe and with special regard PD Dr. Silke Patz.

I would like to thank Professor Dr. Josef Smolle, Professor Dr. Michael Mokry and Dr. Christian Gülly for the opportunity to develop this dissertation at the Medical University of Graz and the Centre for Medical Research Graz.

Furthermore it is a pleasure to thank the members of the Research Unit of Experimental Neurotraumatology, the Institute of Histology, Embryology and Cell Biology, the Core Facilities of the Centre for Medical Research, the Biostatistics department at the Centre for Medical Research, the Institute of Pathology, the University Clinic of Orthopaedy and Orthopaedic Surgery and the University Clinic of Neurosurgery for their qualified and inspiring academic, experimental and personal support.

I owe my deepest gratitude to BMA Gerda Grünbacher, Muammer Ücal, MSc, Sepideh Mostofi, MSc, BMA Jennifer Ober, Samuel Schäfer, Vanessa Mair, BSc and Benedikt Sandner for their assistance during experiments and analyses.

I would like to thank BMA Markus Absenger-Novak and Mag. Kristin Öhlinger for support, assistance and help with the CellIQ, LSM and other microscopes.

With extraordinary respect I would like to thank Mag. Ulrike Zefferer, Mag. Andrea Groselj-Strele and Mag. Katharina Eberhard for their cooperativeness and help with statistical data analysis and data processing.

I would like to extend thankfulness to Dr. Monika Palt.

With special regard I would like to thank my friends for their friendship, motivating discussions and for helping me to achieve an efficient work-life-balance.
Particularly I would like to gratefully acknowledge Gerald Maurer, Verena Krischan, BSc, MMag. Katharina Stöttinger, Stefan Haubenwallner, MSc, Verena Müller, Mag. Angela Steinberger, Mag. Rosa Maria Lugger, Mag. Anna Maria Krainer, Elisabeth Krainer, Mag. Elisabeth Hermetter and Anna-Maria Gross.

Finally I would like to thank Monika and Thomas Trattnig, my parents, for their omnipresent and loving support and my brother Thomas and my sister Sarah, who helped me through difficult periods during my academic studies and my dissertation, with all my heart.

For Thomas and Sarah

Table of Contents

Abbreviations and Definitions

18S rRNA	18s ribosomal RNA
451+	miR-451 overexpressing cells
Ago2	Argonaute 2
AKT1	Serine-threonine protein kinase
AP	Action potential
ATP	Adenosintriphosphate
BM2	Beta-2-microglobulin
Ca++	Calcium
CAB39	Calcium-binding protein 39 (MO25)
CD133	Prominin-1
CD29	Integrin-ß1
CDKN2D	Cyclin-dependent kinase 4 inhibitor D
cDNA	Complementary DNA
CNS	Central nervous system
CNS	Central nervous system
CO_2	Carbon dioxide
CSF	Cerebrospinal fluid
Ct	Control cells (transduced control cells)
CTEN	C-terminal tensin-like
CXCL16	Chemokine (C-X-C motif) ligand 16
DCX	Doublecortin
ddH_2O	Double distilled water
DEPC	Diethyl pyrocarbonate
DG	Dentate gyrus
DGCR8	Di George syndrome critical region gene 8
DMEM	Dulbecco's Modified Eagle Medium
DMSO	Dimethylsulfoxid
DNA	Deoxyribonucleic acid
EDTA	Ethylenediaminetetraacetic acid
EF1a	Elongation factor 1 alpha
eGFP	Enhanced green fluorescent protein
ELISA	Enzyme linked immuno-sorbent assay

ESC	Embryonic stem cell
FACS	Fluorescent activated cell sorting
FBS	Fetal bovine serum
FGFR1	Fibroblast growth factor receptor 1
GAPDH	Glyceraldehyde 3-phosphate dehydrogenase
GFAP	glial fibrillary acidic protein
GFP	Green fluorescent protein
HEK293T	Human embryonic kidney 293T
hESC	Human embryonic stem cell
IL6R	Interleukin-6 receptor
KIF24	Kinesin family member 24
LB	Luria Broth
LP	Lentiviral particle
LSM	Laser Scanning Microscope
MAP2	Microtubule-associated protein 2
MIF	Macrophage migration inhibitory factor (glycosylation-inhibiting factor)
miR-	MicroRNA
miR-451+	miR-451 overexpressing cells
miRNA	MicroRNA
MM	Mastermix
MOPS	[N-morpholino]propanesulfonic acid
MP	Mikroparticle
MYC	c-Myc
NaOH	Natrium hydroxide
NEAA	Non-essential amino acids
Nest	Nestin
NeuN	Neuronal nuclear antigen
NF	Neurofilament
nm	Nanometer
NPC	Neural progenitor cell
NSC	Neural stem cell
NSPC	Neural stem/progenitor cell

nt	Nucleotides
NT2	Ntera-2 cl.D1
OB	Olfactory bulb
OSR1	Odd-skipped related 1 (Drosophila)
PBS	Phosphate Buffered Saline
PBS	Phosphate buffered saline
PNS	Peripheral nervous system
POU3F2	POU class 3 homeobox 2
pre-miRNA	Precursor miRNA
pri-miRNA	Primary miRNA
PSMB8	Proteasome (prosome, macropain) subunit, beta type, 8 (large multifunctional peptidase 7)
qRT-PCR	Quantitative Reverse Transcription Polymerase Chain Reaction
RA	Retinoic acid
RA	retinoic acid
RAB14	Ras related protein Rab-14
RanGTP	Ras-related Nuclear protein Guanosine triphosphate
RISC	RNA induced silencing complex
RMS	Rostral migratory stream
RNA	Ribonucleic acid
RNP	Ribonucleoprotein particle
RPL13A	Ribosomal protein L13A
RT	Room temperature
S1PR2	Sphingosine-1-phosphate receptor 2
SDHA	Succinate dehydrogenase complex
SDS	Sodiumdodecylsulfate
SGZ	Subgranular zone of dentate gyrus
SOB	Super optimal broth
SOC	Super optimal broth with glucose
SOX2	SRY (sex determining region Y)-box 2
SVZ	Subventricular zone of the lateral ventricle
TBI	Traumatic brain injury

TBIP	Traumatic brain injured patients
TBIP-CSF	Cerebrospinal fluid from patients with TBI
TNS4	Tensin 4
TOP1	Topoisomerase (DNA) 1
TRBP	Transactivating response RNA-binding protein
TSC1	Hamartin, Tuberous sclerosis 1
Tuj1	class III beta-tubulin 1
UBC	Ubiquitin C
VAPA	Vesicle-associated membrane protein
VSVG	Vesicular stomatitis virus Glycoprotein
YWHAZ	14-3-3 protein zeta/delta, Protein kinase C inhibitor protein 1

List of Figures

List of Tables

Zusammenfassung

Micro-RNA (miRNA, miR) sind 19-25 Nukleotide kurze, endogene nicht-codierende RNS-(Ribonukleinsäure) Moleküle, die die Genexpression auf post-transkriptionaler Ebene regulieren. miR-451 wird in Mikropartikeln aus cerebrospinaler Flüssigkeit von Patienten mit Schädelhirntrauma exprimiert, jedoch nicht in Mikropartikeln aus der Cerebrospinalflüssigkeit von Kontrollen ohne Schädelhirntrauma. Die Aufnahme von Mikropartikeln, die aus der cerebrospinalen Flüssigkeit von Patienten mit Schädelhirntrauma stammen, durch humane Zellen in vitro resultierte in einer miR-451 spezifischen verminderten Expression von FGFR1 (Fibroblast growth factor receptor 1) und CD133 (Prominin-1). Sowohl FGFR1 als auch CD133 sind mit verletzungsbedingt induzierter adulter Neurogenese, der Neubildung von Nervenzellen im adulten Gehirn, assoziiert. Ein erhöhter zerebraler Wert von miR-451 könnte somit frühe Prozesse der adulten Neurogenese regulieren und mit einer reiferen neuronalen Phase gekoppelt sein. Die Hypothese und Basis der vorliegenden Arbeit ist die Annahme, dass miR-451 eine wesentliche Rolle in der Proliferation und Induktion der neuronalen Differenzierung von humanen Zellen in vitro spielt. Das Ziel dieser Dissertation ist es, die Funktion von miR-451 während der Differenzierung zu neuronalen Zellen zu analysieren.

Dazu wurden humane NT2 Zellen (Ntera-2 cl.D1) mit einem lentiviralen Vektor, der die Sequenz von miR-451 enthält, transduziert, wodurch die Überexprimierung von miR-451 erreicht wurde. Die neuronale Differenzierung dieser Zellen und Zellen, die mit einem Kontrollvektor transduziert wurden, wurde durch die 2-wöchige Zugabe von Retinsäure in einer frei schwimmenden Aggregatkultur (Bildung von Neurosphären) und der anschließenden Behandlung der später adhärenten Neurosphären mit Mitoseinhibitor bewirkt. Die Zellen wurden zu verschiedenen Differenzierungszeitpunkten mit diversen Methoden analysiert (Immunfluoreszenz (Visualisierung der neuronalen Differenzierung), CellIQ (Beobachtung der sich bildenden Zellausläufer), qRT-PCR (Expression der verschiedenen Differenzierungsmarker und Zielgene), Western Blot (Validierung der potentiellen Zielgene)).

miR-451 überexprimierende undifferenzierte Zellen zeigten eine verzögerte Spaltschließung beim Scratch-Assay und morphologische Veränderungen während der Migration (signifikante Zellelongation). Während der Differenzierung von nicht transduzierten NT2 Zellen kommt es zu einer gesteigerten Expression von miR-451, was möglicherweise auf eine Beteiligung von miR-451 in der neuronalen Differenzierung von NT2 Zellen hindeutet. Bei der Differenzierung von miR-451 überexprimierenden NT2 Zellen kommt es im Vergleich zu den transduzierten Kontrollzellen zu einer signifikant veränderten Expression neuronaler Differenzierungsmarker, einer beschleunigten morphologischen Veränderung zum neuronalen Phänotyp und zu einem erhöhten Ausmaß des Neuritenauswuchses. Das spricht für eine Beteiligung von miR-451 in Reifungsprozessen der neuronalen Differenzierung in vitro.

Weiters wurden in der vorliegenden Arbeit AKT1, CAB39, RAB14, TSC1 und YWHAZ als Zielgene von miR-451 im Kontext der neuronal Differenzierung in vitro mittels qRT-PCR validiert.

Abstract

Micro-RNAs (miRNA, miR) are small, endogenous noncoding RNA molecules, which regulate gene expression post-transcriptionally. miR-451 is present in microparticles (MPs) isolated from cerebrospinal fluid (CSF) of traumatic brain injured (TBI) patients and not in MPs derived from CSF of non-injured controls. Uptake of MPs derived from CSF of TBI patients by human NT2 cells in vitro results in a miR-451 specific down-regulation of FGFR1 (Fibroblast growth factor receptor 1) and CD133 (Prominin-1) expression. These factors are linked to injury induced neurogenesis. High cerebral miR-451 levels might regulate neurogenic processes and could be associated to more mature differentiation states. We hypothesise that miR-451 plays a role in the induction of neurogenesis. The aim of this dissertation is to analyse the role of miR-451 during neuronal differentiation of NT2 (Ntera-2 cl.D1) cells in vitro.

NT2 cells were transduced with a miR-451 overexpression and control vector using lentiviruses. Neuronal differentiation was induced by addition of retinoic acid in free floating aggregates (neurospheres) and mitotic inhibitor in adherent neurospheres. Cell migration and development was monitored at different developmental time points using CellIQ and qRT-PCR; miRNA expression was examined using qRT-PCR; immunofluorescence was performed to visualize neuronal extensions; target genes were validated by qRT-PCR and western blot.

Expression levels of miR-451 significantly increase during later stages of neuronal differentiation in NT2 cells. Neurite outgrowth from NT2 neurospheres and mobility of precursor cells was significantly enhanced in miR-451 overexpressing cells. Delay of gap closure in scratch assays in undifferentiated miR-451+ cells, increased miR-451 expression levels during neuronal differentiation in vitro, enhanced elongation of miR-451 overexpressing migrating cells and augmented outgrowth of neurites during neuronal differentiation indicate a role of miR-451 in neurogenic maturation processes in vitro. Furthermore we succeeded in validating AKT1, CAB39, RAB14; TSC1 und YWHAZ as target genes for miR-451 via qRT-PCR.

1. Introduction

Adult neurogenesis in vivo is defined as the generation of new functional neurons from multipotent somatic precursor cells under the otherwise non-neurogenic conditions of the adult brain and was discovered initially in the early 1960s by Joseph Altman and colleagues (1-6), then almost disappeared in scientific literature (6) and was rediscovered in humans in 1998 by Eriksson and colleagues (7). The presence of adult neurogenesis and its functional significance in memory, plasticity, behaviour (8) and regeneration (reviewed by (9)) has now been accepted and is researched intensely in vivo and in vitro, as highlighted by Prof. Dr. Gerd Kempermann in the cover of his book “Adult Neurogenesis 2”:

“Research on adult neurogenesis and neural stem cell biology is among the fastest growing and most dynamic fields in neuroscience.”

(Gerd Kempermann, Adult Neurogenesis – Stem Cells and Neuronal Development in the Adult Brain, 2011, Oxford University Press, New York, USA).

The term neurogenesis alone, especially in older literature on embryonal and fetal neuronal development, is often still referred to the division of precursor cells leading to neuronal development ((6), chapter 1, page 5). This definition is inaccurate in the adult system, as the division of precursor cells alone does not imply the presence of new functional neurons in the end (10).

In vitro models of adult neurogenesis are grounded on cell culture experiments with pluripotent embryonic stem cells (ESCs) or embryonic carcinoma cells (ECCs) ((6), chapter 1, page 57), for example neuronal differentiation of human Ntera2 (NT2) cells in free-floating aggregates by addition of retinoic acid (11).

MicroRNAs, tiny post-transcriptional regulators of gene expression (12) and adult neurogenesis share a historical path of underestimation and non-observance (6, 12). But in the last 15 years these two fascinating topics gained scientific importance as demonstrated by altogether thousands of publications in the last 5 years in Pubmed (National Library of Medicine, National Center for Biotechnology Information, www.ncbi.nlm.nih.gov/pubmed (11); keyword *microRNA:* over 30000 publications in the last 5 years of over 40000 in the last 10 years, compared to only 5 publications in the year 2001; keyword *"adult neurogenesis":* over 1200 in the last 5 years of over 1900 in the last 10 years, compared to 317 publications in the year 2001, keyword *"neuronal differentiation"*: over 2000 publications over the last 5 years out of over 4000 in the last 10 years, compared to 216 publications in the year 2001. The common scientific impact expressed as the number of publications related to these two topics becomes evident when searching via Pubmed for the keywords *microRNA and neurogenesis* (out of 352 hits 278 papers were published in the last 5 years and almost all within the last 10 years) or *microRNA and neuronal differentiation* (out of 422 hits 309 papers were published in the last 5 years and nearly all were published within the last 10 years, data from Pubmed queries performed on 27th August 2015, www.ncbi.nlm.nih.gov/pubmed, National Library of Medicine, NCBI, National Center for Biotechnology Information (13)).

This dissertation is concerned with the role of a specific microRNA (miRNA, miR-), namely miR-451, in neuronal differentiation of human Ntera2 (NT2) cells in vitro. In order to develop and address the rationale, hypothesis and aims of this work it is crucial to provide and discuss answers to the following questions:

1.1. What are the key aspects of adult neurogenesis and neuronal differentiation of human NT2 cells?

1.1.1. Cells of the nervous system

The mammalian nervous system consists of morphologically and functionally specialized cells called neurons (nerve cells, neuronal cells) and supporting glial cells (glia) (14). Neurons transmit, receive and conduct signals electrically or electrochemically and enable complex behaviour through their regulated cooperation and interaction with each other and the inner and outer environment (14, 15). A neuronal cell consists of a cell body (soma), neurites (dendrites and axon) and presynaptic nerve terminals (boutons) (14) (Figure 1). Each morphological unit has a certain functionality in the generation and transmission of signals between neurons, sensory cells and neurons or nerve cells and effector cells (muscle, gland or organ cells (14)). Most neurons have only one tubular axon extending from the axon hillock, from where the signal transmission in terms of action potentials (APs) to other neurons or effector cells takes place (14, 15). Axons are wrapped with an insulating myelin sheath, which is interrupted at regular intervals by uninsulated spots (Nodes of Ranvier), where an AP becomes regenerated (14). Extending from the soma, several shorter branching dendrites receive input from sensory cells or other neurons via synapses (15). These specialized communication locations at boutons of dendrites and branching axons facilitate signal transmission chemically or electrically (14). Electrical synapses are formed via gap junctions (2-4 nm cell distance) and allow fast signal transmission (14). In the circle in Figure 1 a chemical synapse is shown. Upon action potential arrival at the presynaptic nerve terminal, neurotransmitter release is stimulated via increase of intracellular Ca^{++} into the synaptic cleft (20-40nm wide gap between the pre- and postsynaptic cell) by fusion of synaptic vesicles with the cell membrane at the active zone of the presynaptic bouton (exocytosis) (14). The released transmitter molecules diffuse across the synaptic cleft to the receptors in the membrane of the postsynaptic nerve cell(s) (14). Transmitter-receptor binding causes the postsynaptic cell to generate a postsynaptic potential, which can be either inhibitory or excitatory, depending on the kind of receptors in the postsynaptic membrane (14).

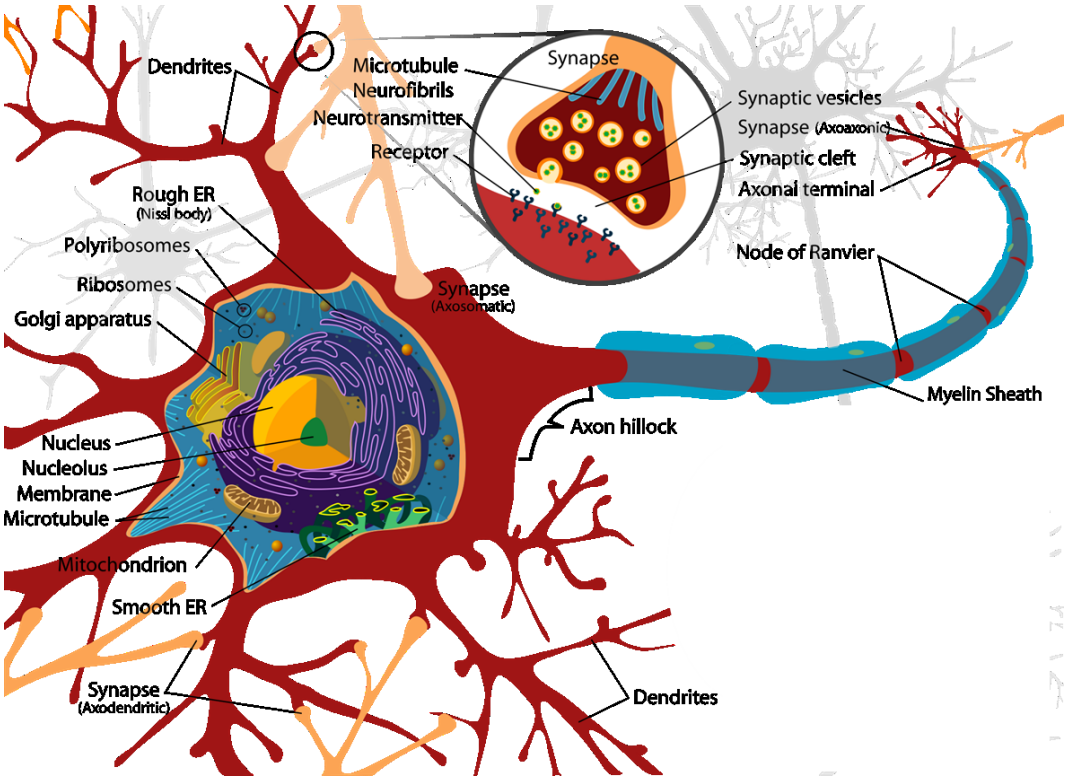

Figure 1[1]

Schematic scheme of a neuron

1.1.2. Short overview of (neuronal) development

From the fertilized egg onwards there is a characteristic order of hierarchically subsequent arising cell types (Figure 2, (6), chapter 3, page 57). Cells of the fertilised egg are totipotent, which means, that they are able to give rise to a various number of different cell types. They give rise to trophoblast cells and cells of the inner cell mass, where embryonic stem cells reside ((6), chapter 3, page 57). These cells are pluripotent and have lost some developmental potential in comparison to cells of the fertilized egg. Trophoblast cells differentiate into cells of the placenta. ESCs develop into somatic stem cells of the endoderm, mesoderm, ectoderm and neuro-ectoderm, which are multipotent, which means, that they are able to give rise to at least 2 different cell types. The neuro-ectoderm gives rise to neuro-epithelial cells, which then differentiate into neural crest stem cells (development of the autonomous and peripheral nervous system) and CNS precursor cells, which facilitate through their regionalised occurrence the development of the brain and spinal cord ((6), chapter 3, page 61).

[1] with permission of Geralt/pixabay.com, modified; August 26th 2015

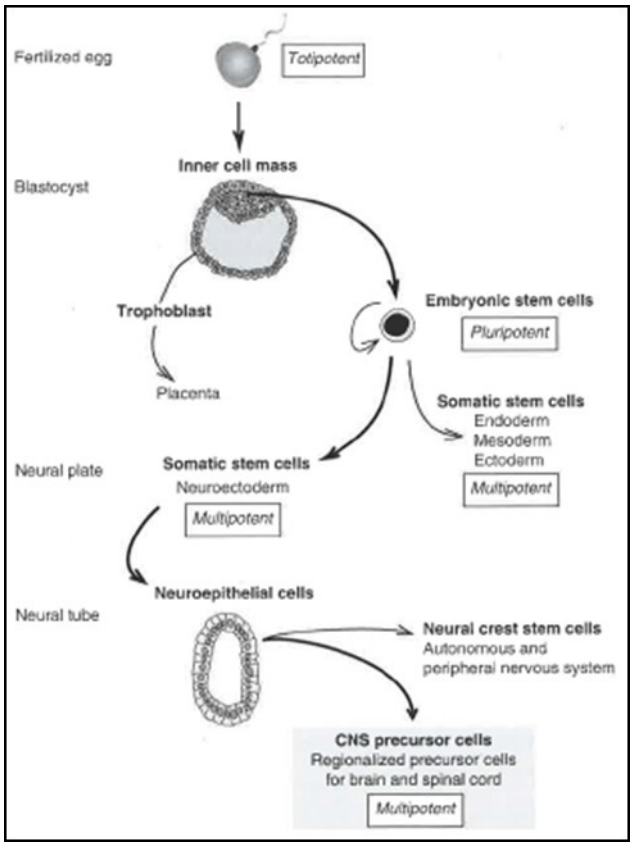

Figure 2[2]

During embryonal development there is a hierarchically sequence of different cell type varying in level of proliferation and developmental potential.

1.1.3. Adult neurogenesis

Adult neurogenesis is neuronal development under otherwise non-neurogenic conditions of the adult brain and is just as embryonal and fetal neuronal development based on multipotent somatic precursor cells (adult neural stem cells), which arise from neuro-epithelial cells during development (1-5, 7). Adult neural stem/progenitor cells (neural stem cells (NSCs), neural progenitor cells (NPCs)) exhibit, like all stem cells, the capability of unlimited self-renewal by division and are multipotent (16). That means, that they are able to differentiate into any neural cell type by symmetric and asymmetric cell divisions (17, 18). NPCs (Neural progenitor cells) are proliferative cells with a limited capacity for self-renewal and are often considered as unipotent (17, 18). Figure 3 shows the principal, simplified theory, how NSCs are differentiating over NPCs, neuroblasts (immature neuronal cells) and glioblasts (immature glial cells) to neuronal and glial cells.

[2] 6. Kempermann G. Adult neurogenesis 2. New York: Oxford University Press; 2011. 601 p. chapter 3, page 57. with permission of Prof. Dr. Gerd Kempermann

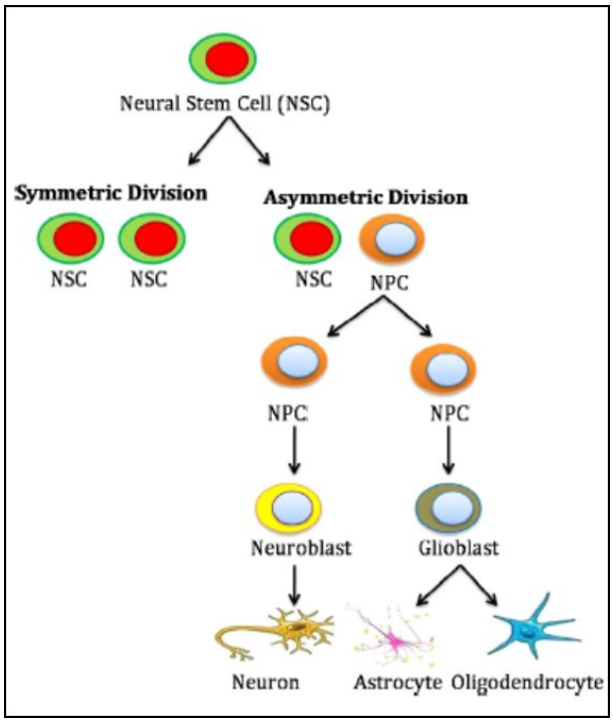

Figure 3[3]

Schematic scheme of the self-renewal and proliferation of neural stem cells adapted from (9).

1.1.4. Neurogenic niches

Neurons are primarily created from early embryonic development until the early postnatal age (5). In a few specialised regions of the adult brain there is a complex and highly dynamic process of neuron generation (5). In the mouse and human brain, these neurogenic niches are the subgranular zone (SGZ) of the hippocampal dentate gyrus (DG) (7, 19) and the subventricular zone lining the lateral ventricles (SVZ) (20) (Figure 4A and B). Furthermore in rodents adult neurogenesis has been reported also in the hypothalamus (21, 22) and its occurrence in the neocortex is under disputation (23-25). NSPCs in the SVZ generate restricted neural progenitor cells that migrate via the rostral migratory stream towards the olfactory bulb (OB) and contribute there to new neurons ((26, 27) Figure 4A). The maturation and migration of neuronal cells in/to the olfactory bulb is not very prominent in adult humans (28, 29). In contrast, the SVZ contributes new neurons to the human striatum (7, 16, 30, 31), reviewed by (32), represented in Figure 4B.

[3] 9. Vishwakarma SK, Bardia A, Tiwari SK, Paspala SA, Khan AA. Current concept in neural regeneration research: NSCs isolation, characterization and transplantation in various neurodegenerative diseases and stroke: A review. Journal of advanced research. 2014;5(3):277-94. modified

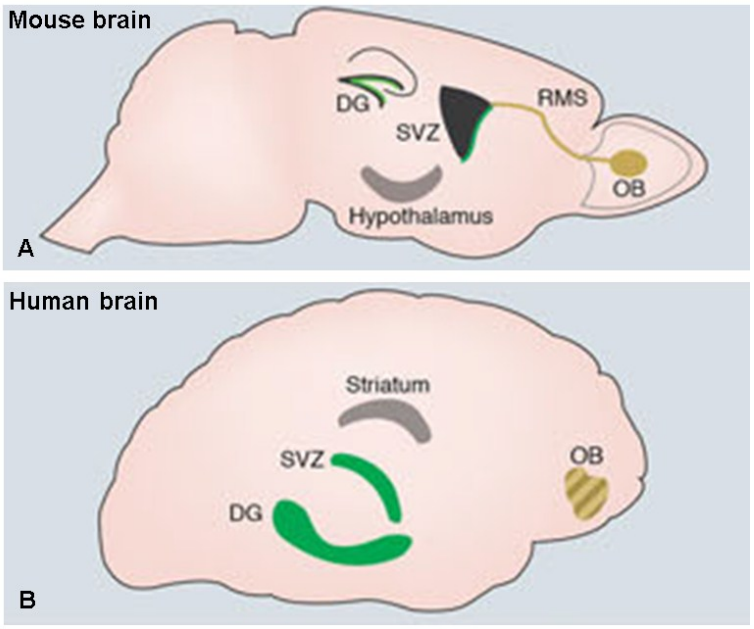

Figure 4[4]

Schematic scheme of neurogenic sites in the mouse (A) and human brain (B). (DG = dentate gyrus, SVZ = subventricular zone, RMS = rostral migratory stream, OB = olfactory bulb)

Figure 5 and Figure 6 show the in-vivo situation of adult neurogenesis in the SGZ and SVZ in mice.

NSPCs (neural stem/progenitor cells) in the dentate gyrus (DG) are also called type-1 cells or radial glia-like cells (DG); in the SVZ they are called B-cells (16). The first step of the maturation process to an integrated and functional neuron requires the activation of the quiescent NSPCs to proliferating, non-radial transit-amplifying cells (TAPs) which are named type-2 cells in the DG and C-cells in the SVZ (reviewed by (27, 33)). In the SVZ these cells differentiate into immature neurons (A-cells), which migrate in rodents to the olfactory bulb and differentiate into mature olfactory neurons (26, 27). In the DG type-2 cells give rise to neuroblasts, immature neurons, which migrate up into the granule cell layer and differentiate over a period of 3 weeks to excitatory granule cell neurons (34, 35)

It has to be taken into account, that the described mechanisms of neurogenesis in the SVZ and SGZ are mostly based on research performed with animals (rodents) (16). To overcome the disparity between animal and human models, there is currently much effort to study human adult neurogenesis in vitro in human cell culture models and to develop novel methods to measure levels of adult neurogenesis in the human brain for example by using non-invasive magnetic resonance imaging (MRI) (36).

[4] 16. Braun SM, Jessberger S. Adult neurogenesis: mechanisms and functional significance. Development. 2014;141(10):1983-6.; modified

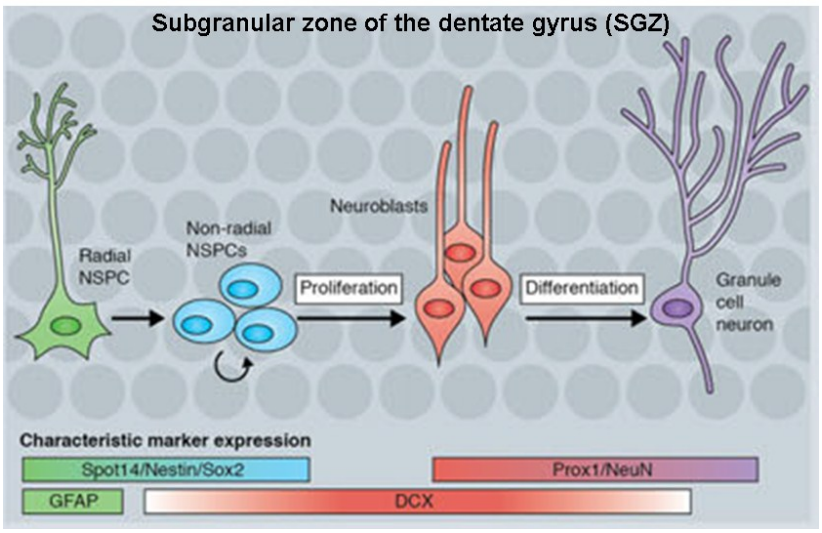

Figure 5[5]

Adult hippocampal neurogenesis in the dentate gyrus and characteristic marker expression (see text) during proliferation and differentiation to mature granule cells

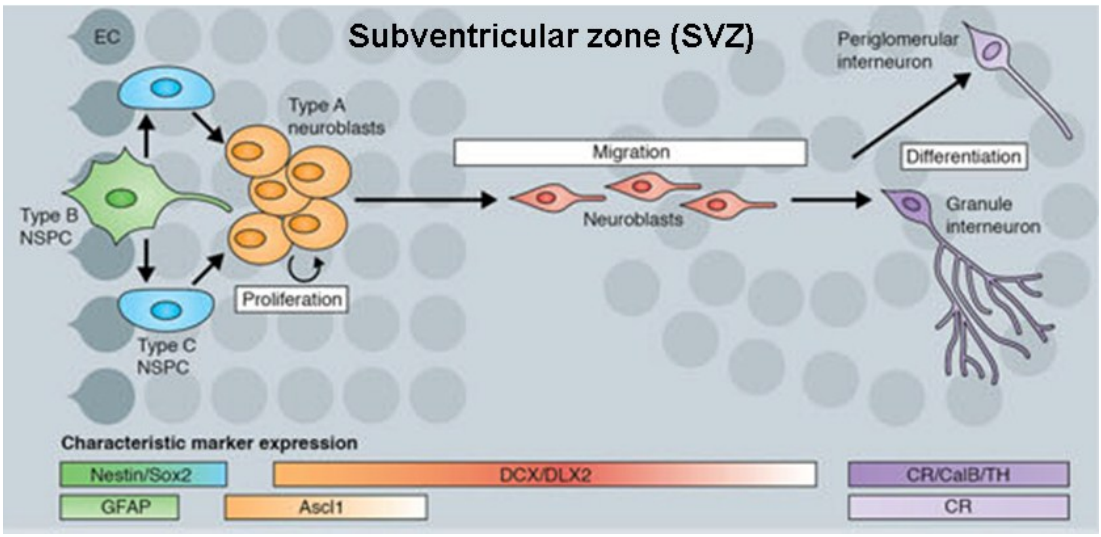

Figure 6[6]

In the subventricular zone of the lateral ventricle maturation of the neural stem progenitor cells into neuroblasts and proliferation of neuroblasts takes place. Cells migrate via the rostral migratory stream to the olfactory bulb, where terminal differentiation takes place. Characteristic marker expression is also shown (see text).

[5] 16. Ibid.; modified
[6] 16. Ibid.; modified

1.1.5. Neural stem cell marker and neuronal differentiation markers

NSCs in the SVZ and DG show certain characteristics at molecular and cellular level (37). NSCs express intermediate filament nestin (marker for early neuronal precursors and early stage neuronal development) (38-41), Sox2 (SRY-2 related transcription factor) (41-46) and GFAP, a marker for cells of the glial lineage and cells at early neuronal development stage (37, 47, 48), Figure 5 and Figure 6.

In addition, new-born neurons at an intermediate differentiation status express the microtubuli-associated protein Doublecortin (DCX), which is expressed in neuronal precursor cells and in post-mitotic immature neuronal cells (49-53).

Neuron-specific class III beta-tubulin1 or also called Tuj1 is an isotype of tubulin, one of the major constituent of the cytoskeleton ((6), chapter 7, page 242), is used as a neuron-specific marker of newly generated cells and is expressed in early post-mitotic and differentiated neurons and in some mitotically active neuronal precursors (54-56).

MAP2 (Microtubule associated protein 2) is an early marker neuron-specific cytoskeletal protein that is enriched in dendrites implicating a role in determining and stabilizing dendritic shape during neuron development (57, 58).

Neurofilament (NF) proteins are early to intermediate markers of neuronal cells (59, 60).

1.1.6. Neuronal differentiation in vitro

Neuronal differentiation in vitro, which is the generation of neurons in cell culture conditions, can be mainly achieved by differentiating embryonic stem cells (ESC), which are pluripotent cells found in the inner layer of the blastocyst (61, 62). Obtainment of hESC (human embryonic stem cells) is ethically, legally and politically critical and sustainment and characterisation is difficult, time consuming and expensive (63, 64).

NT2 cells are a human teratocarcinoma cell line that was originally derived from a testicular germ cell tumour (11). In order to understand the functional significance of neuronal differentiation of NT2 cells in vitro it is crucial to examine the origin of NT2 cells, which leads us to the discussion of teratocarcinomas, as NT2 cells are an immortalised cell line derived from this kind of tumour .

Human teratocarcinomas, also known as mixed germ cell tumours or nonseminomatous germ cell tumours, are malignant germ cell tumours, that occur in most cases in the gonads (65).

Teratocarcinomas contain malignant stem cells, so called embryonal carcinoma cells (ECC), which exhibit similar characteristics as normal pluripotent embryonic cells from preimplantation stage embryos (66, 67).

ECCs resemble ESC cells in antigen expression patterns, developmental potential, and global gene expression including common gene expression patterns for both ‘‘stemness’’ and pluripotency (68-73). ECC have the potential to differentiate into many somatic cell types because of their pluripotency. Upon appropriate treatment with retinoic acid ECC lose their malignancy and differentiate into non-proliferating terminally differentiated nerve cells (11). NT2 cells exhibit similar properties as ECC and show characteristics of committed neuronal precursors at an early stage of development (74). Upon treatment with retinoic acid (RA) NT2 cells are, as they are an immortalized cell line of ECCs, induced to differentiate into fully functional postmitotic neurons and other cell types of the neuronal lineage displaying a variety of neurotransmitter phenotypes and expressing neuron-specific proteins as for example neurofilaments providing therefore a corresponding model for human neuronal development in the adult and embryonal brain (11, 64, 69, 74-76). Neuronal differentiation of NT2 cells seems to be a trustable model of neurogenesis in vivo, as high levels of retinoic acid have been found in the embryonic CNS (77-79).

1.2. What are microRNAs and what is their function?

microRNAs were viewed for a considerably long time as being part of non-functional “junk” repetitions in the genome (12). Comprising a class of endogenous, 19-25 nt (nucleotides) small non-coding RNA molecules microRNAs have gained more and more physiological, biological and functional relevance as regulators of cell biology and behaviour, novel biomarkers and potential targets for therapeutic approaches in the last twenty years since their first description in 1993 (80) and their first citation by name in 2001 (12, 80-85).

To date, more than 2500 different mature miRNAs are described for the human genome (according to the microRNA database miRBase; www.mirbase.org (12, 86-90). A large fraction is expressed in the human brain (12, 91, 92). More than 80% of conserved miRNAs are tissue specific and it is estimated that more than 60% of human protein coding genes are regulated by miRNAs (93, 94)

Changes in tissue specific miRNA expression patterns or in the expression of the miRNA processing machinery are closely associated to disease induction and progression (94).

1.2.1. Function and biogenesis

microRNAs regulate gene expression mostly negatively at the post-transcriptional level by base-pairing to the complementary 3' untranslated region (3'UTR) of their target messenger RNA (mRNA) (85). This causes translational repression and/or degradation of the respective target mRNA (80, 85, 95). miRNAs modulate protein expression and therefore fine-tune many cellular processes, which impacts on cellular function at a network level and on the phenotype of cells in eukaryotic organisms (96). One single miRNA is estimated to interact with several hundreds of target mRNAs and their dysregulation is associated with disease induction and progression. The biogenesis of miRNAs is shown in Figure 7.

miRNAs are transcribed mostly by RNA polymerase II or sometimes by RNA polymerase III as hundreds to thousands nucleotides long primary transcripts (pri-miRNAs) (12, 83, 85). These pri-miRNAs, which contain large portions of secondary hairpin structures, are then cleaved in the nucleus by the RNase III enzyme Drosha and its cofactor DiGeorge syndrome critical region gene 8 (DGCR8) to 70-80 nt long, stem-looped precursor miRNAs (pre-miRNAs) (85, 97, 98). Pre-miRNAs are exported actively to the cytoplasm by exportin-5/RanGTP and cleaved there by the RNase III enzyme Dicer to form double-stranded mature miRNAs (99-102). One strand of the mature miRNAs (guide miRNA strand) is then loaded into the RNA-induced silencing complex (RISC), a ribonucleoprotein complex that is composed of 3 proteins: the human immunodeficiency virus trans-activating response RNA-binding protein (TRBP), Argonaute 2 (Ago2) and Dicer. Incorporated into the RISC, the mature miRNA binds to the target mRNA and modulates gene expression post-transcriptionally (83, 85, 103).

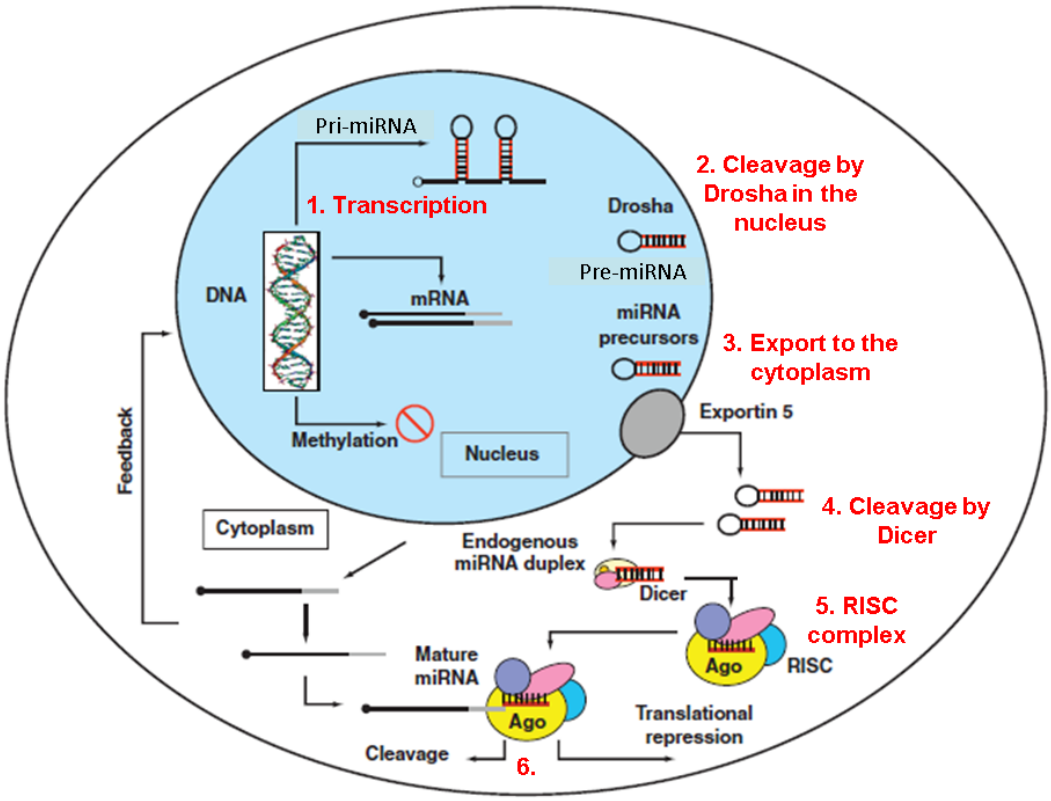

Figure 7[7]

Canonical miRNA processing pathway

1.2.2. miRNAs and adult neurogenesis

miRNA expression is particularly high in the brain and there they have been shown to have important regulatory functions in neuronal development and dysfunction (92). miRNAs regulate neural development (neural induction, progenitor expansion, differentiation and neural subtype specification), neuronal migration, neuronal function, neurite outgrowth and synaptic plasticity. Alteration in the tissue specific miRNA expression pattern or changes in the expression of the miRNA processing machinery are linked to the induction and progression of cerebral disease and degeneration (104-111). The expression pattern in physiological and pathophysiological cerebral processes has been best described for miR-9 (112), miR-124 (113) and let-7 (114).

[7] 93. Ross JS, Carlson JA, Brock G. miRNA: the new gene silencer. Am J Clin Pathol. 2007;128(5):830-6., modified

1.3. What evidence suggests a role of miR-451 in neuronal differentiation?

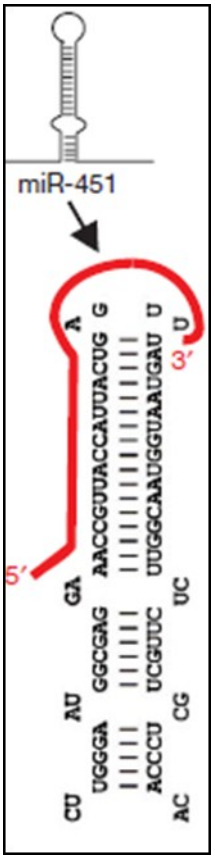

In humans the miR-451 gene is located on chromosome 17 at 17q11.2 (GeneID: 574411) 100bp downstream to the miR-144 gene in a polycistronic unit (94).

Due to its specific pre-miRNA secondary structure (Figure 8), the maturation of pre-miR-451 does not require Dicer (Figure 9).

Figure 8[8]

Structure of pre-miRNA-451, Marked in red is the mature sequence of miR-451 (5'-3')

Instead the pre-miRNA is cleaved by the argonaut-2 catalytic centre to generate an intermediate 3' end, which is then further trimmed (115-117). The miR-451 gene and the enzymatic activity of argonaute proteins are deeply conserved in higher eukaryotes ((115, 117, 118), Figure 10) indicating the importance of argonaute-miRNA-451 interaction for post-transcriptional gene regulation in eukaryotes. MiR-451 has primarily been associated with erythropoiesis (119-129), but has recently been shown to play a role in tumorigenesis and tumour progression (reviewed by (94)) and in modulations of cerebral function, for example during traumatic brain injury and more specific in injury induced adult neurogenesis, damage or disease induced cerebral modulations (130-133). For example, some studies deal with miRNA expression change after traumatic brain injury (81, 130-132), having reported altered miR-451 expression in hippocampus (130) and cortex (131) after experimental traumatic brain injury. Furthermore a role of miR-451 in maintenance and multipotential differentiation capacity of stem cells and cancer stem cells has been described (129, 134-137). Cell processes regulated by miR-451 comprise cell growth and survival (138-152) as well as differentiation of epithelial cells while establishment of basolateral polarity (153).

[8] 115. Cheloufi S, Dos Santos CO, Chong MM, Hannon GJ. A dicer-independent miRNA biogenesis pathway that requires Ago catalysis. Nature. 2010;465(7298):584-9.

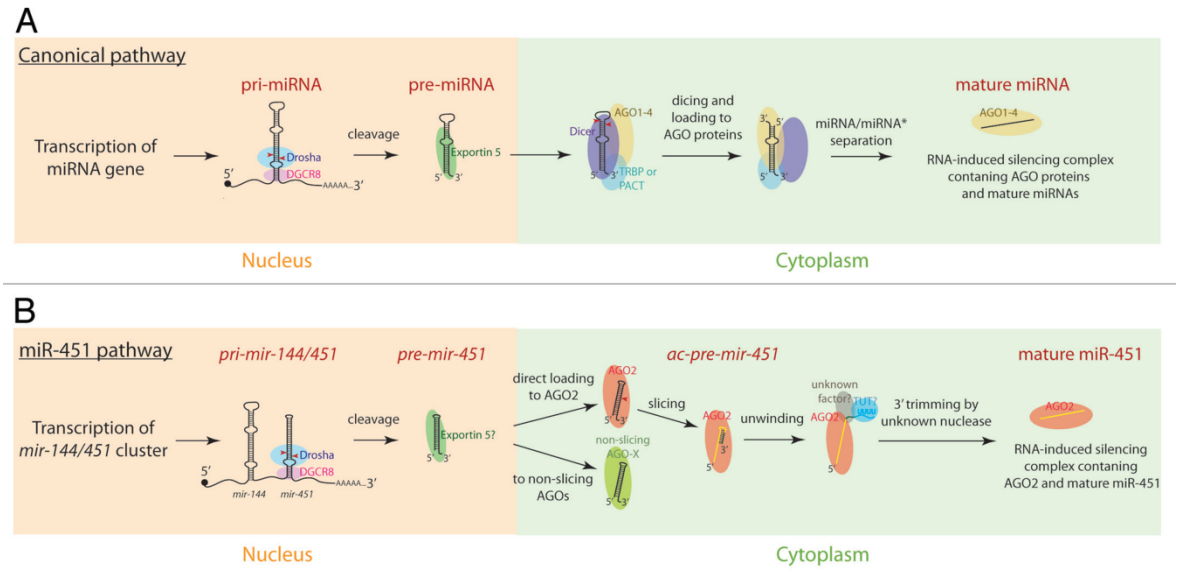

Figure 9[9]

miRNA processing pathway and miR-451 pathway

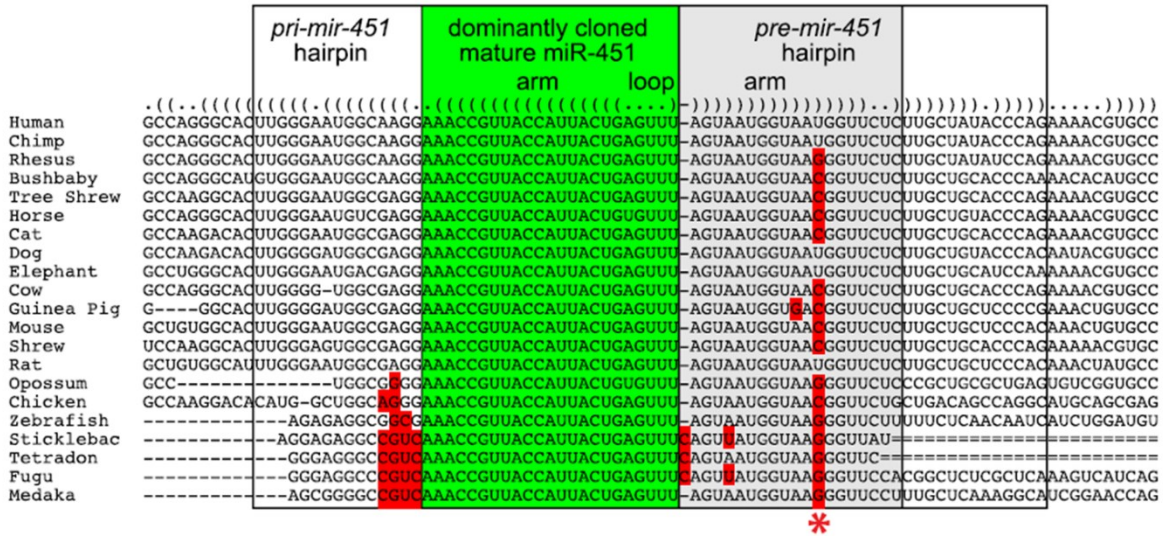

Figure 10[10]

miR-451 is highly conserved among species, especially the mature sequence of miR-451. Marked in red are deviations from the human miR-451 sequence.

[9] 93. Ross JS, Carlson JA, Brock G. miRNA: the new gene silencer. Am J Clin Pathol. 2007;128(5):830-6., modified

[10] 117. Yang JS, Maurin T, Robine N, Rasmussen KD, Jeffrey KL, Chandwani R, et al. Conserved vertebrate mir-451 provides a platform for Dicer-independent, Ago2-mediated microRNA biogenesis. Proc Natl Acad Sci U S A. 2010;107(34):15163-8.

In a recent study from Patz et al. in 2013 miR-451 was identified to be present only in the cerebrospinal fluid (CSF) of traumatic brain injured patients (TBIP) (154), (Figure 11). Patz et al. also showed miR-451 specific down-regulation of neural stem cell genes FGFR-1 (Fibroblast growth factor receptor 1) and CD133 after uptake of TBIP-CSF derived microparticles (MPs) by undifferentiated NT2 cells (154) (Figure 12). FGFR-1 and CD133 play an important role in the regulation of injury induced neurogenesis (155-157).

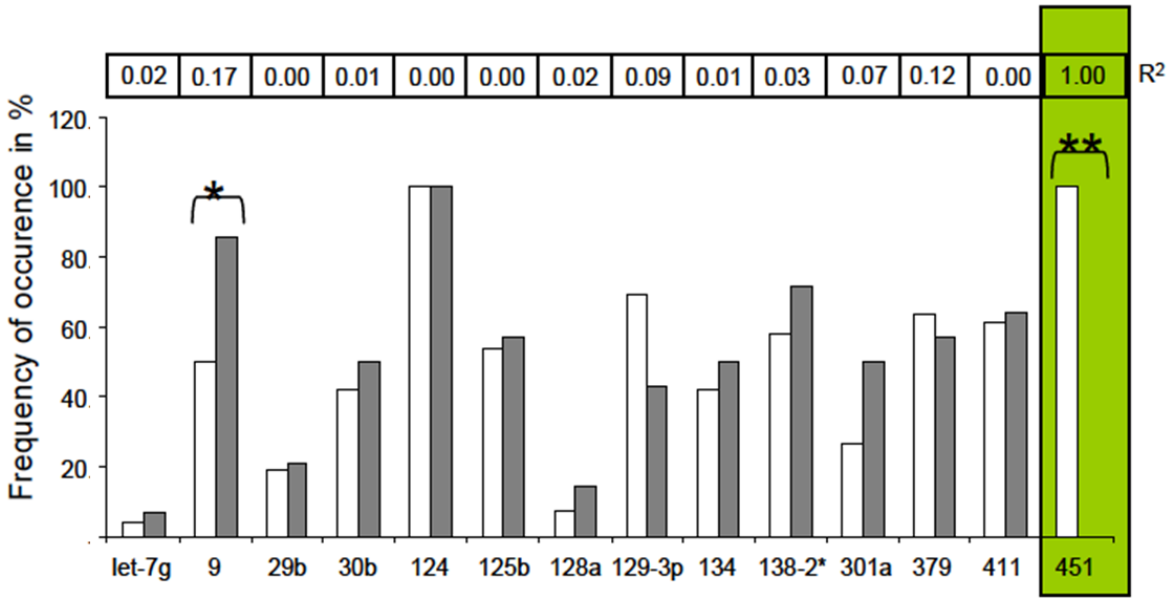

Figure 11[11]

Frequency of occurrence on the y-axis of different miRNAs in the MPs derived from CSF of traumatic brain injured patients (white bars) and healthy controls (grey bars).

[11] 154. Patz S, Trattnig C, Grunbacher G, Ebner B, Gully C, Novak A, et al. More than cell dust: microparticles isolated from cerebrospinal fluid of brain injured patients are messengers carrying mRNAs, miRNAs and proteins. J Neurotrauma. 2013. modified

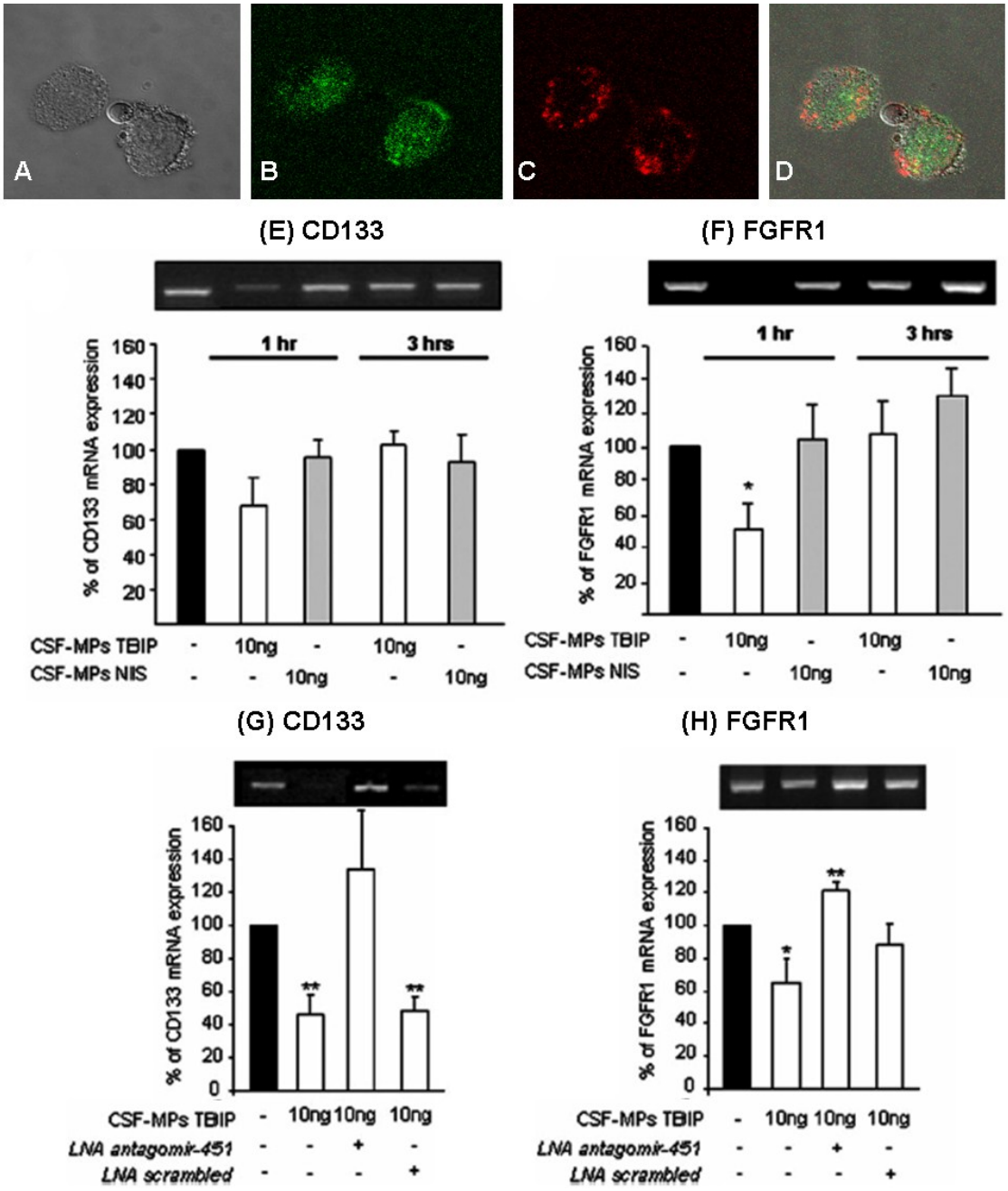

Figure 12[12]

miR-451 specific down-regulation of neural stem cell genes FGFR-1 (Fibroblast growth factor receptor 1) and CD133 after uptake of TBIP-CSF derived microparticles by human Ntera cells.

[12] 154. Ibid. modified

1.4. Hypothesis and aims

Taken into consideration previously described processes that are regulated by miR-451 (proliferation, cell survival, stem cell maintenance and differentiation capacity), we hypothesize that miR-451 mediated gene regulation supports regenerative processes following brain injury. High cerebral levels of miR-451 expression might be linked to a more mature differentiation state. We aim to investigate the role of miR-451 in in-vitro cell polarisation, migration, neurite formation and maturation of the cell line Ntera-2 cl.D1 (NT2) via stable overexpression of miR-451.

2. Material and Methods

Recipes for all used buffers, media and solutions are listed in the Appendix.

2.1. Cell culture of Ntera-2 cl.D1 (NT2) and HEK293T cells

All cell culture techniques were performed under a laminar flow (Kendro Laboratory Products, Langenselbold, Germany). Ntera-2 cl.D1 (NT2) (ATCC, LCG standards, Wesel, Germany) and HEK293T cells (Human embryonic kidney cells, gift from Dr. Alexander Deutsch, Division of Hematology, Medical University Graz) were cultured and maintained in complete high glucose DMEM (Dulbecco's modified Eagle Medium, Sigma-Aldrich Handels GmbH, Vienna) under an atmosphere of 5% CO_2 in a 37°C incubator (Galaxy R CO_2 Incubator, RS Biotech, Irvine, Ayrshire, United Kingdom). NT2 and HEK293T cells were passaged every 2-4 days or when having reached near 100% confluency in new 75cm^2 or 175cm^2 flasks (PAA Laboratories GmbH, Cölbe, Germany). Medium was aspirated and cells were rinsed with sterile 1xPBS (Phosphate buffered saline, Sigma-Aldrich Handels GmbH, Vienna, Austria). Then 1ml per 75cm^2 flask or 2ml per 175cm^2 flask accutase (Sigma-Aldrich Handels GmbH, Vienna, Austria) was or were added and incubated for 5 to 10min in a 37°C CO_2 incubator in order to loosen the cells from the surface of the flask. Then the cells were taken up in 10ml complete medium and 1ml of the cell suspension was added to a new flask with 11ml (75cm^2) or 20ml (175cm^2) fresh complete medium.

2.2. Differentiation of NT2 cells

Undifferentiated NT2 cells were maintained and cultivated as stated under 2.1 and described in (11). The differentiation protocol of free-floating aggregates (neurospheres) was adapted from (158), but changes were applied. Briefly, 5x10^6 undifferentiated non-transduced or transduced NT2 cells were seeded into ultra-low attachment flasks (VWR International, Vienna, Austria). 10µM retinoic acid Sigma-Aldrich Handels GmbH, Vienna, Austria) of a 10mM stock solution was added on the same day (Day 1 of differentiation). Every 2 days until day 15 the medium was changed by sedimentation of the resulting neurospheres and addition of fresh complete medium plus 10µM retinoic acid.

On day 15 medium was changed without adding retinoic acid and the neurospheres were left in ultra-low attachment flasks. On day 17 neurospheres were plated from ultra-low attachment flasks onto matrigel coated 75cm^2 flasks plus mitotic inhibitor every two days until day 28 (10µM 5-Fluoro-2-Desoxyuridine (Sigma-Aldrich Handels GmbH, Vienna, Austria), 1µM Cytosine-β-D-Arabinofuranoside (Sigma-Aldrich Handels GmbH, Vienna, Austria) and 10µM Uridine (Sigma-Aldrich Handels GmbH, Vienna, Austria)).

On Day 28 the cells were selectively trypsinised and plated on Matrigel coated 75cm^2 flasks (Geltrex^{TM} hESC – qualified, ready-to-use, reduced growth factor basement membrane matrix, Life Technologies, Paisley, United Kingdom).

2.3. Lentiviral vectors

The lentiviral vector for overexpression of miR-451 (AB.G.451, miR-451+) and control vector (AB.G.ct (Ct)) were a gift from Dr. Papapetrou (129), Figure 13A and B. Small amounts of the vectors were spotted on filter paper. The respective area was cut out, put in 200µl TE buffer and incubated overnight at 37°C. Lentiviral DNA amount was measured with a photometer (Eppendorf, Vienna, Austria).

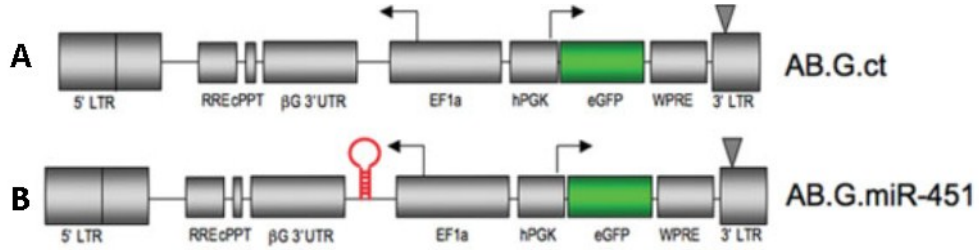

Figure 13[13]

Lentiviral vectors were a gift from Dr. Papapetrou (129). (A) The control vector AB.G.ct (hereafter termed Ct) encodes no miRNA. (B) Bidirectional vector driving expression of miR-451 (AB.G.miR-451, hereafter termed miR-451+) under the EF1a promoter. All vectors encode eGFP and ampicillin.

[13] 129. Papapetrou EP, Korkola JE, Sadelain M. A genetic strategy for single and combinatorial analysis of miRNA function in mammalian hematopoietic stem cells. Stem Cells. 2009;28(2):287-96.

2.4. Transformation

For transformation of the lentiviral vectors GCI-5α and GCI-L3 super-competent strains (THP Medical Products, Vienna, Austria) were used. 100µl of the competent cells were transferred into pre-chilled polypropylene tubes (PAA Laboratories GmbH, Cölbe, Germany). Then 100-200ng of lentiviral vector DNA or 1µl of the pUC19 control were added. The tubes were mixed cautiously and incubated for 30min on ice. Every 10 minutes the tubes were mixed gently. Then the cells were heat-shocked in a 42°C water bath for 45 seconds and placed immediately on ice for 2-5min. Then 500µl pre-warmed SOC medium (42°C) was added to each tube. The cells were incubated for 1h in a 37°C shaker at 100-200rpm (HT infors, Bartelt, Graz, Austria). Different aliquots of transformation culture (50-200µl) were spread onto pre-warmed selective LB-plates (recipe see Appendix). The plates were incubated 12-16h in a 37°C incubator (Binder, Tuttlingen, Germany) and examined for bacterial colonies. The colonies were picked into selective LB medium and grown overnight in a 37°C shaker. Minipreps (see 2.5), control digestions (see 2.6), maxipreps (see 2.7) and/or glycerol stocks (see 2.8) were performed.

2.5. Miniprep

Minipreps were performed according to the manufacturer's instructions (Qiagen, Hilden, Germany). The selective antibiotic is ampicillin.

2.6. Control digestion

The identity of the different lentiviral plasmids was confirmed using restriction digestion (Figure 44). 500ng miR-451+ vector DNA (AB.G.miR-451) and control vector DNA (AB.G.ct, Ct) were digested for 1h at 37°C with 0,5µl each of *Eco*RI and *Xho*I in a 50µl reaction (New England Biolabs, Ipswich, Massachusetts, United States of America). The theoretical restriction digestion pattern was created with Serial Cloner 2.1[14] (theoretical restriction digestion pattern for Ct: 6260bp, 1869bp, 1239bp, 253bp and 18bp, for miR-451+: 6260bp, 1869bp, 1256bp, 545bp) and then compared to the restriction pattern seen on a 1% agarose gel (Figure 44B). 1g Agarose (Biozym, Hessisch Oldendorf, Germany) was melted in 100ml 0,5xTBE+100µl/L GelRed buffer by heating in a microwave until the solution was completely clear.

[14] http://www.neudownload.com/download/11038/Serial-Cloner-21.html

The solution was cooled down by cold water, poured into an appropriate gel form (see 2.15) and a comb (Biozym, Hessisch Oldendorf, Germany) was plunged in.
The set gel was put into an electrophoresis chamber (EasyPhor Medi Gelelectrophoresis chamber 15x15cm, Biozym, Hessisch Oldendorf, Germany), which had been filled with 0,5xTBE buffer.
For evaluation of restriction digestion 50µl were mixed with 5µl 1x DNA-loading buffer. 10µl of the mix were loaded onto the gel and voltage was applied (80V, 45min, powersupply Power Pac HC^{TM} Bio-Rad Laboratories, Hercules, California, United States of America).

2.7. Maxiprep

Maxipreps were done according to the manufacturer's instructions (Qiagen, Hilden, Germany). Starter cultures (2-5ml LB medium supplemented with 100µg/ml ampicillin) were inoculated with the different bacterial glycerol stocks (see 2.8). 500µl of the starter culture were inoculated into 250ml LB medium supplemented with 100µg/ml ampicillin.

2.8. Glycerol stocks

Glycerol stocks were generated from all the bacterial cultures transformed with lentiviral vectors. A single colony of bacteria was picked, inoculated in 2-3ml LB medium containing 100µg/ml ampicillin and then incubated in a shaker incubator at 225rpm and 37°C for 8-12h (HT infors, Bartelt, Graz, Austria). 100-200µl of this culture were inoculated in 100ml LB medium containing 100µg/ml ampicillin then incubated in a shaker incubator at 225rpm and 37°C for 12-18h (HT infors, Bartelt, Graz, Austria). 0,75ml of the bacterial culture were aliquoted into 1,5ml or 2ml tubes tubes (Eppendorf, Vienna, Austria) and 0,25ml of 50% (vol/vol) Glycerol (Sigma-Aldrich Handels GmbH, Vienna, Austria) were added to each tube. The glycerol stocks were stored at -80°C. For inoculating a starter culture, a pipette tip was scratched on top of the still frozen glycerol stock and then the tip was brought into 2-3ml of LB medium containing 100µg/ml ampicillin.

2.9. Transfection of HEK293T cells for production of viral particles

HEK293T (gift of Dr. Alexander Deutsch, Division of Hematology, Medical University Graz) cells were transfected with lentiviral DNA of the different vectors. On day 1, $5x10^6$ cells were seeded out in a 10cm dish (Szabo Scandic, Vienna, Austria). Cells reached 80-90% confluence on the day of transfection (day 2). A transfection complex consisting of Solution A and B, was prepared. In solution A 20µg DNA plasmids (10µg miR-451+ vector or control vector DNA and 10µg of Packaging Mix (ABM good, Applied Biological Materials Inc, Richmond, Canada) were diluted in 1ml serum-free high glucose DMEM. medium.

In Solution B 80µl Lentifectin™ reagent (ABM good, Applied Biological Materials Inc, Richmond, Canada) were diluted in 1ml serum-free high glucose DMEM (Sigma-Aldrich Handels GmbH, Vienna, Austria). Solution A and B were incubated separately at room temperature (RT) for 5min, mixed together and incubated at RT for 20min. Medium was removed from HEK293T cells, the transfection complex (completed with 4,5ml medium) was added and the cells were incubated in a 37°C CO_2 incubator overnight. On day 3 medium was removed from the cells and 10ml complete medium was added. On day 4 the supernatant was collected. 10ml of complete medium were added to the cells after the first harvest. The second harvest was done on day 5, repeating the steps mentioned above. The combined supernatant was centrifuged at 3000rpm for 15min at 4°C in order to pellet cell debris. The cleared supernatant was filtered with a low-protein binding 0,45µm sterile filter (VWR International, Vienna, Austria) and transferred into a new 50ml tube (PAA Laboratories GmbH, Cölbe, Germany). The virus was used for transduction or was stored in aliquots as viral stock at -80°C for future applications.

2.10. Determination of the viral titer

Determination of the viral titer was done with an ELISA based method, the Lenti-x p24 Rapid Titer Kit according to the manufacturer's instructions (Clontech Laboratories, Inc., Mountain View, California, USA). A p24 standard curve was included in every measurement (see example in Figure 45). A trend line was plotted through the data points and the resulting equation was used to determine the concentration of p24 lentiviral protein in the sample. In the manual there were values and calculations given for the determination of approximate titers.

This is based on the observation that each lentiviral particle (LP) contains approximately 2000 molecules of p24. 1 LP contains $8x10^{-5}$ pg of p24 (derived from (2000)x($24x10^{3}$Da)/($6x10^{25}$). 1ng p24 is equivalent to $1,25x10^{7}$ LPs. For a typical lentiviral vector, 1 IFU (infectious unit) stands for every 100-1000 LPs.

2.11. Transduction of NT2 cells with viral particles

On day 1 $5x10^{5}$ NT2 cells were seeded out in a 75cm^{2} flask incubated overnight in a 37°C CO_2 incubator. The cells should reach 30-50% confluence. On day 2, transduction was performed by using 10^{8} viral particles/ml.

The transduction complex contained 2ml of the viral stock, 3ml of complete medium and 6µg/ml Polybrene (ABM good, Applied Biological Materials Inc, Richmond, Canada). The resulting MOI (multiplicity of infection) is calculated by the following formula: MOI = (volume [viral stock] * concentration [virus])/(Volume [cell culture] * cell number [cell culture]). We used a MOI of approximately 80 for our experiments.

The transduction complex was added to the cells and then incubated for 1 day in a 37°C CO_2 incubator. On day 3 and 4 the procedure was repeated. On day 5 medium was changed and cells were left to grow. Appearance of fluorescence was checked under a fluorescence microscope on day 6 or 7 (Figure 46A and B).

2.12. FACS of the transduced NT2

To generate a pure cell population of transduced cells, we sorted them according to the magnitude of fluorescence of eGFP (enhanced green fluorescent protein) in high, middle and low eGFP expressing cells (Figure 46C). FACS was done with FACS Aria IIu (BD Biosciences, Schwechat, Austria) by the Core Facility Flow Cytometry (Center for Medical Research, Medical University of Graz, Austria).

Briefly, GFP fluorescence was excited with 488nm and detected with a filter for FITC (530/30 BP). GFP negative NT2 cells were used for set up of the basic adjustments. Then the cells were sorted in a 4-Way sort (maximal purity) into low, middle and high fluorescent GFP positive cells. Cell aggregates were excluded to prevent sorting of false positive cells (Sort adjustments: 100 µM Nozzle, pressure: 20 psi, frequency: 27 kHz, flow rate: 1-2, 4-Way sort (maximal purity).

2.13. RNA isolation of the different cell pellets

RNA, microRNA (miRNA) and proteins were isolated from one cell pellet using mirVana Paris kit for miRNA and RNA isolation (Applied Biosystems, Darmstadt, Germany).

Cell pellets were done of all transduced cells (cells transduced with lentiviral vectors overexpressing miR-451 (AB.G.miR-451, miR-451+) or the control vector AB.G.ct (Ct)).

Transduced and non-transduced cells were differentiated and cell pellets were taken at different time points of differentiation (0, 8, 17, 22 and 27 days). Cells were treated with accutase (see 2.1). After taking up the cells in 10ml complete medium the cell suspension was centrifuged for 5min at 1000rpm (multifuge 3 L-R, Heraeus, Hanau, Germany). The medium was aspirated and then the cell pellet was re-suspended in 1400µl complete medium.

700µl of this suspension were centrifuged for 3min at 13000rpm (biofuge fresco, Heraeus, Hanau Germany) and the medium was aspirated. The resulting cell pellet was shock-frozen in liquid N_2 and stored at -80°C (Herafreeze, Kendro Laboratory Products GmbH, Hanau, Germany). The remaining 700µl of the cell suspension were pipetted in a 2ml cryotube^{TM} vial (Thermo Fisher Scientific, Vienna, Austria). Then 700µl of freezing medium (see Appendix) were added by pipetting carefully up and down. The cryotube containing the cells was put in a CoolCell box (Biozym, Hessisch Oldendorf, Germany) and was stored at -80°C. After 1 day at -80°C cells were frozen in liquid N_2. For RNA, miRNA and protein isolation cell pellets were put on ice and 100-600µl of ice cold lysis buffer supplemented with RNA spike-in mix I (UniSp2, UniSp4 and UniSp5) were added (usually 600µl were used, 1µl RNA spike-in mix I per 600µl Lysis Buffer, see 2.19). Cells were re-suspended and homogenized by vortexing (IKA Laboratory Products, Staufen, Germany) and treatment with ultrasound in an Ultrasons H (3x5s, in between 1min incubation on ice; JP Selecta, Barcelona, Spain). Half of the sample was processed immediately for RNA and miRNA isolation according to the manufacturer's instructions. The other half was used for protein analysis. After 5-10min incubation on ice the sample, if not used immediately, was snap-frozen in liquid N_2 and stored at -80°C for long-term storage or at -20°C for short term storage.

2.14. RNA and miRNA concentration

RNA and miRNA concentration was determined in ng/µl with a biophotometer from Eppendorf (Vienna, Austria) by measurement of the absorption at 260/280nm after adjustment to the Blank.

2.15. RNA quality

At least 200ng RNA and/or 30ng miRNA were loaded on a denaturing RNA formaldehyde Gel in order to determine the quality of the isolated RNA/miRNA. 1,2g/100ml Agarose (Biozym, Hessisch Oldendorf, Germany) and 10ml 10x formaldehyde gel buffer (recipe see Appendix) were mixed. The volume was adjusted to 100ml with DEPC-treated water (Diethylpyrocarbonate, Sigma-Aldrich Handels GmbH, Vienna, Austria). The agarose was melted in a microwave (Siemens, Linz, Austria), the solution was cooled down to 60°C and then 1µl GelRed (GelRedTM Nucleic Acid Gel Stain, VWR international, Vienna, Austria) and 1,8ml 37% formaldehyde solution (Merck, Hohenbrunn, Germany) were added. The solution was poured into a gel form (small gel pouring form for EasyPhor Medi, 15x7cm, Biozym, Hessisch Oldendorf, Germany). For generating a 200ml gel, the double amount of each ingredient was used and the gel was poured into a big gel form (15x15cm, Biozym, Hessisch Oldendorf, Germany). One to three (for big gels) 20-lane comb(s) (Biozym, Hessisch Oldendorf) was or were plunged in and the gel was allowed to set. The set gel was put equilibrated for at least 30min in an electrophoresis chamber (EasyPhor Medi Gelelectrophoresis chamber 15x15cm, Biozym, Hessisch Oldendorf, Germany) filled with 1x Formaldehyde Agarose Gel Running Buffer (recipe in the Appendix). RNA samples were mixed with 5x RNA loading buffer (recipe in the Appendix, 1 volume 5x RNA loading buffer per 4 volumes of RNA sample), incubated 3-5min at 65°C in a thermomixer (Eppendorf, Vienna, Austria) and chilled on ice. This mixture was then loaded onto the equilibrated formaldehyde agarose gel and voltage was applied (100V, 20min, powersupply Power Pac HC^{TM} from Bio-Rad Laboratories, Hercules, California, USA).

2.16. cDNA synthesis

cDNA synthesis from isolated RNA was done with First Strand cDNA synthesis kit from Thermo Fisher Scientific Bioscience GmbH (St. Leonrot, Germany) according to the manufacturer's instructions. 100ng of RNA were used for each reaction.

cDNA synthesis from miRNA was performed with miRCURY^{TM} LNA Universal cDNA Synthesis Kit II from Exiqon (Vedbaek, Denmark) according the manufacturer's instructions. 20ng of miRNA were used for each reaction. For data normalisation RNA spike-in mix II (UniSp6 and cel-miR-39-3p) was used. This mix was spiked-in before cDNA synthesis (1µl spike-in mix per 20µl reaction).

2.17. PCR

2.17.1. SYBR green based PCR (qPCR)

KAPA SYBR FAST LightCycler 480 kit from VWR International (Vienna, Austria) was used for SYBR green based PCR. For one 10µl reaction 4µl diluted cDNA (1:80 for cDNA from miRNA, 1:20 for cDNA from RNA) and 6µl master mix (5µl/reaction of SYBR green kit and 1µl/reaction of the forward-reverse primer mix) were pipetted together in a white 96- or 384-well plate (Roche Applied Science, Vienna, Austria).

qPCR was done with LightCycler 480 (Roche Applied Science, Vienna, Austria). Negative controls were included in each experiment. The used program for miRNA expression analysis was 1) Pre-incubation: 95°C, 10min, 2) Amplification: 45 cycles: a) 95°C, 10s; b) 60°C 1min). mRNA analysis was done with 1) Pre-incubation: 95°C, 5min, 2) Amplification: 45 cycles: a) 95°C, 30sec; b) Annealing: 60°C (depends on the primer, but mostly 60°C was used), 30sec; c) Extension: 72°C, 30sec. Melting curve analysis was done according to the suggestions of the instruction manual of the LC480 (Roche Applied Science, Vienna, Austria), where additional information concerning the used ramp rates is found. Gene expression was evaluated by using the $2^{-\Delta\Delta Ct}$ method without PCR efficiency correction (159). Experiments were conducted 3 times in quadruplets unless stated otherwise.

2.17.2. Primers

In general, primers for PCR were searched in the literature, ordered at companies (Qiagen, Hilden, Germany; Origene, Rockville, Maryland, USA; Exiqon, Vedbaek, Denmark; Primerdesign, South Hampton, United Kingdom) or were designed with Primer3Output (Table 3, appendix) and then ordered at Eurogentec, Seraing, Belgium.

2.18. Standard curves for absolute quantification of miRNA

A Standard curve using defined copy numbers of miRNA mimics of miR-451 (Ambion mirVana miRNA mimic for miR-451a, Thermo Fisher, Vienna, Austria) was created using qRT-PCR. We calculated the molecular weight of the miR-451a mimic with equations from the Thermo Fisher Website[15] as the sequence of the mimics was known (AAACCGUUACCAUUACUGAUU)[16]. The starting copy number was calculated per 1µl. Then a series of dilution was prepared, starting with undiluted mimics (10^{13} molecules/µl) to 10^{2} molecules/µl including 7 dilutions. These series of dilutions were converted into cDNA using miRNA Universal cDNA Synthesis Kit II from Exiqon (Vedbaek, Denmark). Then SYBR based qPCR was done as described in 2.17.1. The standard curves were designed by plotting the measured Ct-values on the y-axis against natural logarithmic (ln) value of the specific copy number of mimic used as described in (160).

This was done with Microsoft Excel 2010 (Microsoft Corporation, Redmont, Washington, USA). A trend line was plotted through the data points and the resulting formula was used to calculate the copy number per 20ng used miRNA.

2.19. Normalisation of data with synthetic RNA spike-ins

2.19.1. Copy number

The copy number/20ng miRNA, which was calculated from the formula of the standard curve (Figure 54), was normalized by multiplication with a normalisation factor. The normalisation factor was determined with the Ct-values of the spiked-in synthetic control templates according to (160).

[15] http://www.thermofisher.com/at/en/home/references/ambion-tech-support/rna-tools-and-calculators/dna-and-rna-molecular-weights-and-conversions.html, August 2015
[16] http://www.thermofisher.com/order/genome-database/details/mirna/MC10286, August 2015

Instead of using the synthetic RNA spike-ins described by (160) we used the RNA spike-in kit from Exiqon (Vedbaek, Denmark). Three RNA spike-in templates (UniSp2, UniSp4 and UniSp5) are premixed in one vial, each at a different concentration with 100-fold increments. This mix, hereafter termed RNA spike-in mix I, was designated as RNA isolation control. A second vial contained a synthetic version of *Caenorhabditis elegans* microRNA, cel-miR-39-3p. This template was meant to be used in combination with the UniSp6 RNA Spike-in template provided with the miRCURY LNA™ Universal cDNA synthesis kit II (see 2.16). This mix, termed hereafter RNA spike-in mix II, was intended as cDNA synthesis control.

2.19.2. miRNA analyses

For undifferentiated transduced and non-transduced NT2 (NT2, miR-451+ and Ct) analysis was performed regarding the suitability of different housekeeping genes as normalisation genes concerning mRNA studies by qRT-PCR (SNORD38b, 48 49A, 66, U1, U6, GAPDH, S14). The resulting Ct-values were compared statistically with the program MultiD for variability (GeNorm and NormFinder analysis, Figure 48A and B). SNORD38b and SNORD49A were chosen as the best normalisation combination in GeNorm. NormFinder selected YHWAZ as the least variable gene. Figure 47A shows the mean Ct-values together with the standard deviation as error bars of the different housekeeping genes in undifferentiated transduced and non-transduced cells. RNA spike-in mix I (mix of UniSp2, UniSp4 and UniSp5) was added to the Lysis Buffer before starting with RNA isolation (1µl RNA/amount of Lysis Buffer needed per sample, normally 600µl). When preparing the master mix for cDNA synthesis, the Spike-in mix II (UniSp6 and cel-39-3p) was added (see 2.16).

2.19.3. mRNA analyses

For undifferentiated transduced and non-transduced NT2 (NT2, miR-451+ and Ct) analysis was performed regarding the suitability of different housekeeping genes as normalisation genes concerning mRNA studies by qRT-PCR (YWHAZ, U6, UBC, SDHA, GAPDH, RPL13A, B2M, TOP1).

The resulting Ct-values were compared statistically with the program MultiD for variability (GeNorm and NormFinder analysis, Figure 52A and B).
UBC and YHWAZ were chosen as the best normalisation combination in GeNorm. NormFinder selected YHWAZ as the least variable gene. Figure 51A shows the mean Ct-values together with the standard deviation as error bars of the different housekeeping genes in undifferentiated transduced and non-transduced cells.
UBC and Spike-in were chosen for further studies in differentiated transduced and non-transduced cells (Figure 51B).
For mRNA analyses we also used a spike-in for normalization (Tataa Biocenter, Saarbrücken, Germany). 2µl spike-in per 20µl master mix spike-in was added when preparing the master mix for mRNA cDNA synthesis (see 2.16).

2.20. Microscopy and CellIQ

All transduced cells were observed with a microscope (Olympus, Hicksville, New York, USA). Pictures of different passages of transduced cells were taken. During differentiation pictures of cells at different time points were taken under a microscope (Olympus, Hicksville, New York, USA). Living cells were observed with CellIQ (Cell IQ V2 MLF Cell Imaging and Analysis System, Imagen, Massachusetts, USA). On the one hand differentiating neuronal precursor cells were plated in 6-well plates at day 17 under addition of mitosis inhibitor.
Cells were then observed for 10 consecutive days while performing medium change and addition of mitosis inhibitor every 2 days. On the other hand scratch assays were performed. $5x10^5$ cells were seeded out in 6-well plates and were incubated for 72h at 37°C and 5% CO_2. After 72h of incubation cells were scratched with a pipette tip according to the scheme shown in Figure 14A and observed in the CellIQ for approximately 72-90h.

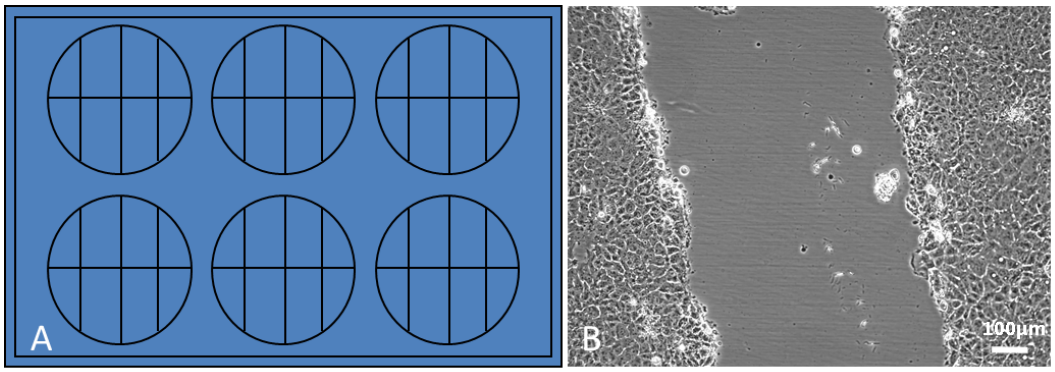

Figure 14

Cells were seeded out at a specific density and were then scratched according to (A) (picture by Verena Müller) with a 1000µl pipette tip. (B) shows one of the created gaps (10x, Olympus, Hicksville, New York, USA).

2.21. Indirect immunofluorescence

Non-transduced and transduced cells were plated on day 17 on Matrigel coated glass slides (Menzel, Thermo Fisher Scientific, Braunschweig, Germany) in 6 well plates (VWR International, Vienna, Austria) and differentiated. At various differentiation stages they were fixed with 4% Paraformaldehyde (in 1x PBS, VWR International, Vienna, Austria) for 20min and then subjected to different indirect immunofluorescence stainings according to a standard protocol. Indirect immunofluorescence is based on the detection of a primary antibody, which has bound specifically to the protein of interest, by a fluorochrome conjugated secondary antibody (Figure 15). Briefly, cells were washed with 1xPBS (Phosphate buffered saline, Sigma-Aldrich Handels GmbH, Vienna, Austria) 3 times for 5min. Then they were incubated 30min in 0,3% Triton X-100 (in 1xPBS, Sigma-Aldrich Handels GmbH, Vienna, Austria), washed 3 times for 5min each in 1x PBS and then blocked in 1% BSA-PBS solution for 60min at RT (recipe in the Appendix, Sigma-Aldrich Handels GmbH, Vienna, Austria).

After blocking incubation with the primary antibody (Table 4) was done overnight at 4°C. Afterwards, the cells were washed 3 times with 1xPBS for 5min. Then the secondary antibody (Table 5, dilution according to the manufacturer's instructions, but mostly 1:1000 was used) is applied for 1h at RT. After 2 washing steps for 5min with 1xPBS the cells are covered with Fluoroshield (with DAPI, Sigma-Aldrich Handels GmbH, Vienna, Austria).

Cells were then analysed with a fluorescence microscope (Olympus, Hicksville, New York, USA, used objective: 20x), a Zeiss Laser Scanning Microscope (LSM 510 META, Zeiss, Oberkochen, Germany; integrated lasers are UV 405nm, multiline Argon 458/477/488/514nm, Helium-Neon 543nm as well as Argon 514 and Helium-Neon 633nm, used objective: EC Plan-Neo 40x/1.3 Oil with DIC capability) or an Ultra-Fast Spectral Scanning Confocal Microscope (Nikon A1R, Nikon, Melville, New York, USA, integrated lasers are Violet diode 405nm, multiline Argon 457-514nm, DPSS laser 561nm, Diode Laser system 642nm, used objective: CFI Plan Apochromat Lambda 40x/0.95).

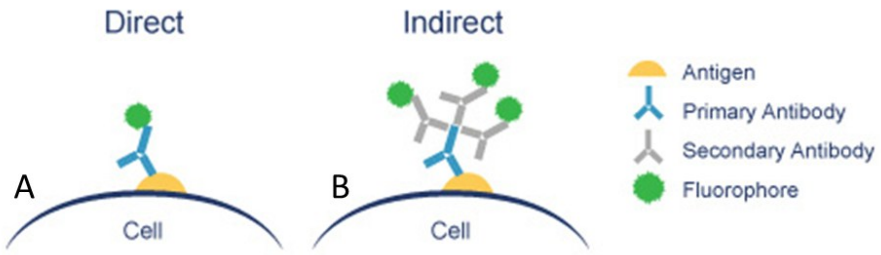

Figure 15[17]

The principles of direct (A) and indirect (B) immunofluorescence are shown. In direct immunofluorescence, an antigen (protein, yellow) is specifically recognized by an antibody conjugated with a fluorophore F (green). Binding and signal detection happens in one step. In indirect immunofluorescence, a protein (yellow) is specifically recognized by a primary antibody (blue). Signal detection is carried out by a secondary antibody (grey) specific for the primary antibody which is conjugated with a fluorophore F (green). Picture taken from the Abcam website (www.abcam.com).

2.22. Western Blot

Western blots were performed with the assistance of BMA Gerda Grünbacher and PD Dr. Silke Patz from the Research Unit of Experimental Neurotraumatology.

Protein samples were separated according to their molecular mass by SDS-PAGE on 8% or 12,5% ready-to-use gels (Bio-Rad, Vienna, Austria) and transferred onto a nitrocellulose membrane (Amersham, GE Healthcare Vienna, Austria) for immunodetection.

[17] http://www.abcam.com/secondary-antibodies/direct-vs-indirect-immunofluorescence, August 2015

The samples were prepared with 1x XT Sample Buffer (Bio-Rad, Vienna, Austria) and 1x XT Reducing Agent (Bio-Rad, Vienna, Austria) and heated for 5 minutes at 95°C. A total protein amount of 10-20 µg was loaded on the gel and electrophoresis was performed for approximately 2h at 160 V (Pre-run at 80V for 15min) in 1x XT MES Buffer (Bio-Rad, Vienna, Austria) with a Criterion electrophoresis chamber unit from Bio-Rad (Vienna, Austria). As a molecular weight marker the Spectra Multicolour Broad Range Protein Ladder (5 µl, Thermo Scientific, Braunschweig, Germany) was used.

Next, the separated proteins were transferred onto a nitrocellulose membrane (Amersham, GE Healthcare Vienna, Austria) using a Trans Blot Cell Unit (Bio-Rad, Vienna Austria) at 40 V for 1 hour and 15min. Prior to electro-transfer the membrane was equilibrated together with the filter paper (Thermo Scientific, Braunschweig, Germany) and sponges (Thermo Scientific, Braunschweig, Germany) in 1x transfer buffer (recipe see Appendix). Successful transfer was checked by NBB staining (3-5min in NBB staining solution, rinsing with water, 3-5min NBB destaining solution, rinsing with water, recipe see Appendix). For immunodetection, the membrane was blocked in 5% BSA-TBS (Sigma-Aldrich, Vienna, Austria) for 30min. Then the membrane was incubated with the primary antibody (dilution see Table 4 in 5% BSA-TBS) overnight at 4°C, agitating. The following day, the membrane was washed 3 times with TBS-Tween (0.1%, VWR, Vienna, Austria) for 5 minutes and then incubated with the secondary antibody, which was conjugated to HRP (dilution see Table 5 in 1xTBS). Detection was performed by detecting HRP using the Super Signal West Pico Chemiluminescent Substrate (Thermo Scientific, Braunschweig, Germany) and exposure to Fuji Super RX Films (A. Hartenstein, Würzburg, Germany).

2.23. Data analysis

Expression data was analysed with Microsoft Excel 2010 (Microsoft Corporation, Redmont, Washington, USA), IBM SPSS Statistics 22 (Armonk, New York, United States of America) and GenEx (MultiD Analyses AB, Göteborg, Sweden).

Pictures obtained from immunofluorescence stainings were analysed with the plugin NeuronJ (161-163) within the program ImageJ. (Bethesda, Maryland, USA; (163, 164). Imaging data (neurite length) was analysed with Imaris software (Bitplane, Concord, USA). Statistical analysis was done with IBM SPSS Statistics 22 with the support of Mag. Katharina Eberhard from the Biostatistics department at the Centre for Medical Research, Medical University of Graz. As the size of the biological replicates was only 3 in qRT-PCR expression data, we performed non-parametric tests. We used the Friedman's test for comparing different differentiation time points within the mRNA expression profile. For detecting significant differences between Ct cells and transduced miR-451+ cells, we used the Mann-Whitney U-Test.

3. Results

3.1. Neuronal differentiation of NT2 cells

Successful neuronal differentiation of NT2 cells was verified by morphological, immunofluorescent and molecular analysis of different time points of differentiation. Three different protocols were tested with NT2 cells (data not shown) and protocol 3 which was based on the protocol described by Paquet-Durand in 2003 (158) was used for further studies after obtaining neurite building cells, which develop into post-mitotic neurons. The morphological changes during neuronal differentiation of NT2 cells are shown in Figure 16a-e. Seeded out in ultra-low attachment flasks cells build free floating aggregates (neurospheres). 10µM retinoic acid was added every two days until day 15. One day 17 neurospheres were plated on matrigel coated flasks and mitosis inhibitor was added. From day 18 onwards (data not shown), cells started to build neurites. On day 2 a branched network of neurite building cells growing out of the neurospheres had developed (Figure 16d and Figure 17A), which was more pronounced and elongated at day 27 (Figure 16e, and Figure 17B).

3.1.1. Analysis of developmental markers by qRT-PCR

The expression profiles of (A) Sox2, (B) Nestin, (C) DCX, (D) Tuj1, (E) MAP2, (F) NF and (G) GFAP compared to day 0 during neuronal differentiation of NT2 cells is shown in Figure 16A-G

As already described in the introduction, there is a characteristic expression pattern of specific markers in adult neurogenesis and neuronal differentiation in vitro respectively, and the down-regulation of Sox2 and Nestin and the up-regulation of DCX, Tuj1, MAP2 and NF with advanced differentiation status was verified.

In detail the expression of **Sox2** decreases over the time of differentiation, being significantly lowest at day 27 compared to day 0 (pairwise non-parametric statistical testing of related samples, Friedman's test, * = $p \leq 0{,}05$, Figure 16A)

Nestin expression is first upregulated until day 17 but at day 22 and 27 down-regulated and is significantly different between day 17 and day 27 (Friedman's test, * = $p \leq 0,05$, Figure 16B)

The expression of **DCX** and **Tuj1** is higher at day 8, 17, 22 and 27 compared to day 0 during neuronal differentiation of NT2. The overall statistical test was significant, but after correction for the number of pairwise comparisons the values rose above the significance level (Figure 16C and D).

During neuronal differentiation of NT2 the expression of **MAP2** rises and there is a significant difference between day 0 and day 22 (Friedman's test, * = $p \leq 0,05$, see Figure 16E)

NF and **GFAP** are not expressed significantly different during differentiation of NT2, but there is an obvious trend of up-regulation compared to day 0 (Figure 16F and G).

3.1.2. Analysis of neuronal differentiation by morphological observation

Immunofluorescent staining of markers DCX (A, B), Tuj1 (C, D), MAP2 (E, F) and NF (G, H) at day 22 (A, C, E, G) and 28 (B, D, F, H) show the successfully implemented neuronal differentiation of NT2 cells in vitro (Figure 18 and Figure 19). Pictures were taken at 20x (Figure 18) and 40x (Figure 19). In the appendix all immunostainings are shown together with negative controls, which are negative for all the different markers except for negative controls of DCX, where weak, unspecific and fuzzy staining of the cell body is visible.

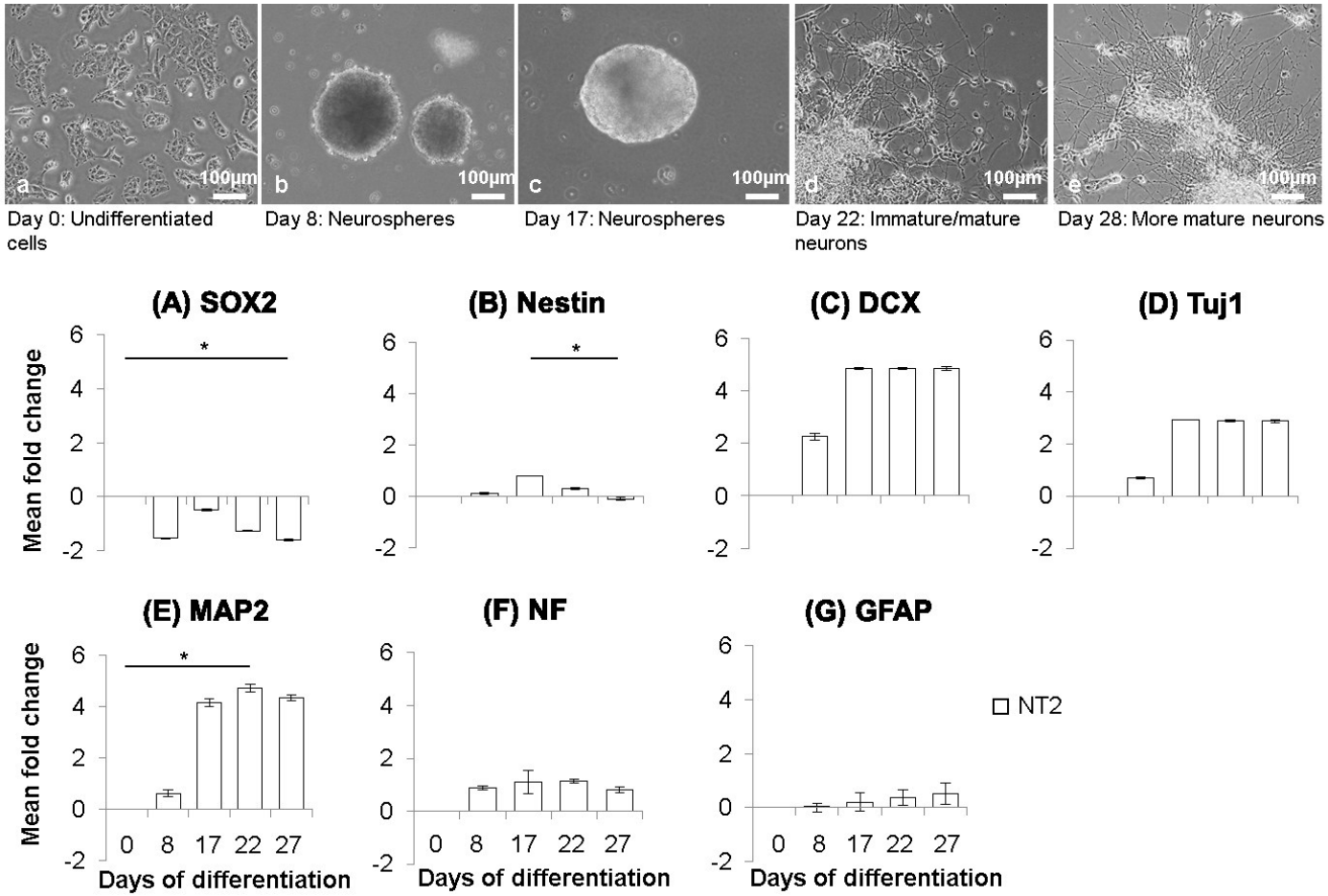

Figure 16

Morphological changes of undifferentiated NT2 cells (a) during neuronal differentiation; Neurosphere formation at day 8 (b) and day 17 (c); Neurite growth and differentiation at day 22 (d) and day 27 (e); (10x, Olympus, Hicksville, New York, USA).

Expression pattern of markers (A) Sox2, (B) Nestin, (C) DCX, (D) Tuj1, (E) MAP2, (F) NF and (G) GFAP during neuronal differentiation of NT2 (n=3). Error bars indicate the standard error mean (SEM); Friedman's test (* = $p \leq 0{,}05$).

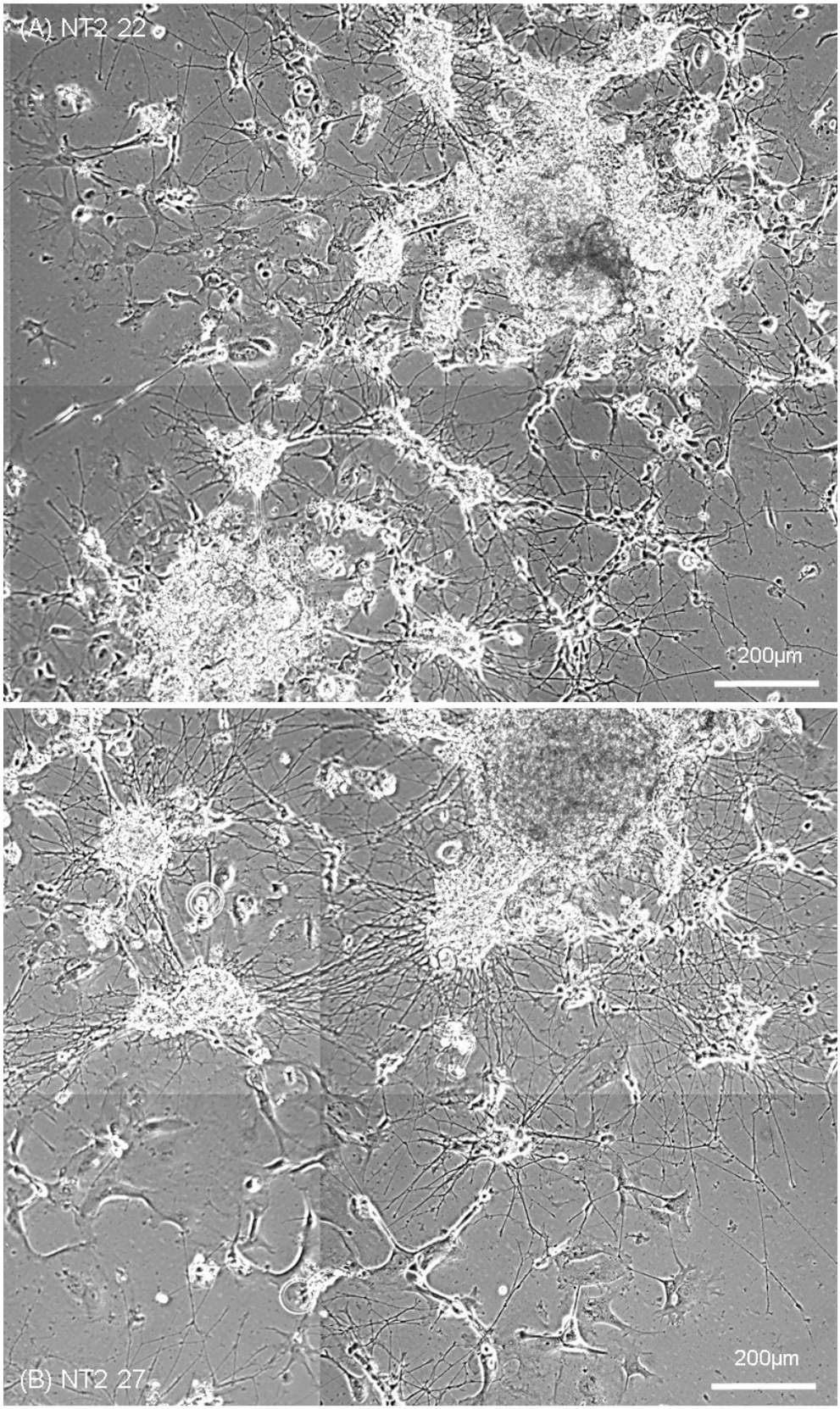

Figure 17

Neuronal differentiation of NT2 is shown at day 22 and day 27 (10x, CeIIIQ, Imagen, Massachusetts, USA).

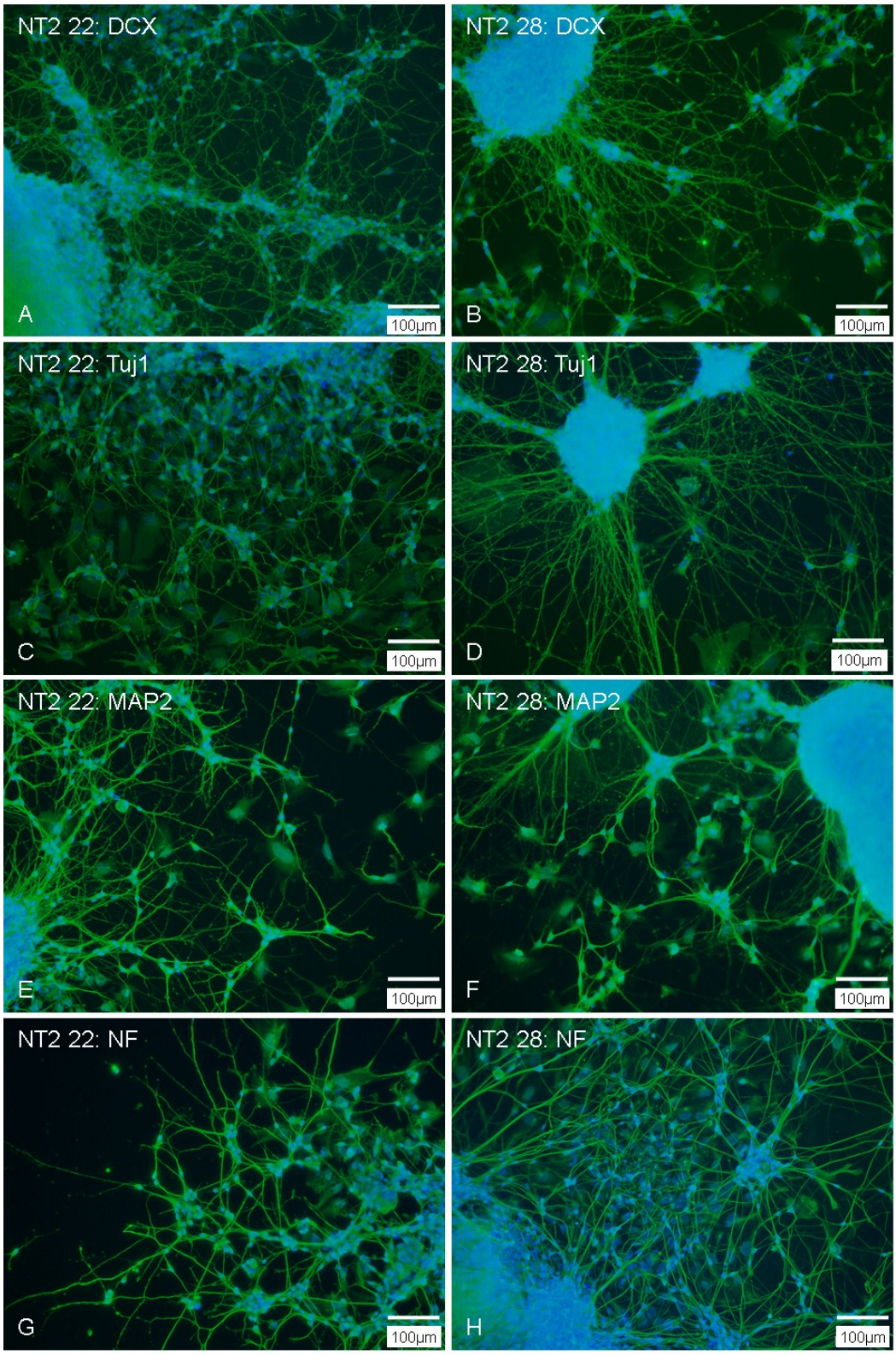

Figure 18

Immunostaining of DCX (A, B), Tuj1 (C, D), MAP2 (E, F) and NF (G, H) in NT2 cells is shown at day 22 (A, C, E, G) and 28 (B, D, F, H) of neuronal differentiation (20x, Olympus, Hicksville, New York, USA).

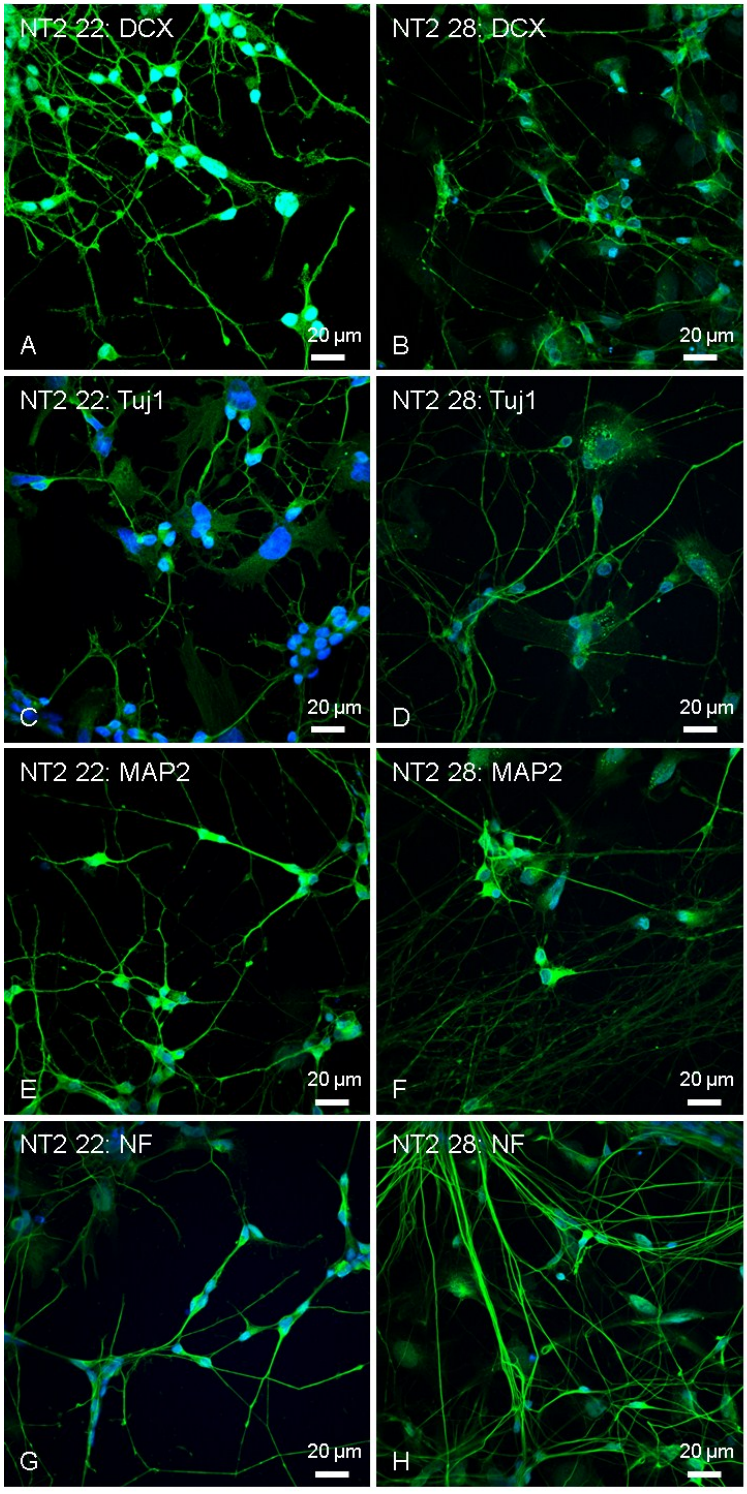

Figure 19

Immunostaining of DCX (A, B), Tuj1 (C, D), MAP2 (E, F) and NF (G, H) in NT2 cells is shown at day 22 (A, C, E, G) and 28 (B, D, F, H) of neuronal differentiation (40x, LSM, Nikon, Vienna, Austria)

Neuronal differentiation of NT2 was implemented successfully, as shown by down-regulation of Sox2 and Nestin and up-regulation of DCX, Tuj1, MAP2 and NF and the appearance of neurite building cells and cells with neuronal phenotype.

3.2. Endogenous expression of miR-451 during neuronal differentiation

To judge the possible relationship of miR-451 and neuronal differentiation endogenous miR-451 expression in undifferentiated and differentiating NT2 cells was analysed. MiR-451 expression was significantly higher at day 27 compared to day 0 and day 8 respectively during neuronal differentiation of NT2 (Friedman's Test, $p \leq 0,05$, Figure 20A). We also calculated the endogenous copy number of miR-451 on the basis of a standard curve with miR-451 mimics. The normalised copy number per 20 ng used miRNA is significantly different between day 8 and 22 or 27 respectively during neuronal differentiation of NT2 (Friedman's Test, $p \leq 0,05$, Figure 20B)

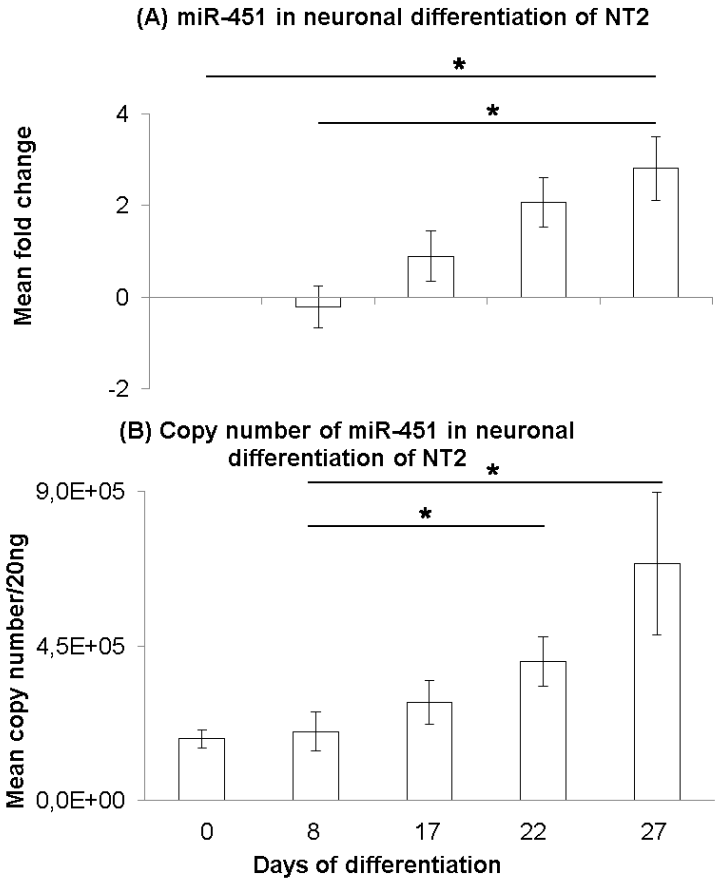

Figure 20

(A) Expression of miR-451 represented as mean fold change compared to day 0.

(B) The normalised mean copy number/20ng used miRNA during neuronal differentiation of NT2 in vitro is shown (n=3). The error bars indicate the standard error mean (SEM); n=3; * $p \leq 0,05$, Friedman's Test.

During neuronal differentiation of NT2 endogenous miR-451 expression increases, which could imply a function of miR-451 in the maturation of neuronal cells.

3.3. Neuronal differentiation of Ct cells (transduced with AB.G.ct)

To analyse the effect of control vector transduction (AB.G.Ct transduced cells, termed hereafter as Ct cells) on the potential of NT2 cells to differentiate into neuronal lineages regular neuronal differentiation of Ct cells was evaluated by morphological, immunofluorescent and molecular analysis of various differentiation time points.

The description of the vector and the transduction protocol are described in the methods section and the results of the transduction are summarized in the appendix.

The morphological changes during neuronal differentiation of Ct cells are shown in Figure 21a-e. The expression profiles of (A) Sox2, (B) Nestin, (C) DCX, (D) Tuj1, (E) MAP2, (F) NF and (G) GFAP compared to day 0 in Ct are shown in Figure 21A-G. Down-regulation of Sox2 and up-regulation of DCX, Tuj1, MAP2, NF and GFAP were observed with advanced differentiation.

Sox2 expression decreases over time of differentiation, being significantly lowest at day 27 compared to day 0 (Friedman's test, * = $p \leq 0,05$, Figure 21A).

In Ct cells **Nestin** expression is first up-regulated until day 8, down-regulated at day 17, increases again at day 22 and 27 and is significantly different between day 17 and 27 (Friedman's test, * = $p \leq 0,05$, Figure 21B).

The expression of **DCX** is higher at day 8, 17, 22 and 27 compared to day 0 in Ct, being significantly different between day 0 and 22 (Friedman's test, * = $p \leq 0,05$, Figure 21C).

There is a trend of up-regulation of **Tuj1** during neuronal differentiation of Ct compared to day 0 (Figure 21D).

During neuronal differentiation the expression of **MAP2** increases in Ct showing a significant difference between day 8 and day 17 (Friedman's test, * = $p \leq 0,05$, Figure 21E).

NF expression is up-regulated in Ct during neuronal differentiation showing a significant difference between day 0 and 22 (Friedman's test, * = $p \leq 0,05$, Figure 21F).

GFAP expression is up-regulated in Ct during neuronal differentiation in vitro. There is a significant difference in expression between day 0 and day 27 (Figure 21G).

Neuronal differentiation of Ct cells leads to neurite building cells and the development of neuronal cells, meaning that in vitro neuronal differentiation was also successfully implemented in control vector transduced NT2.
There are differences in neurite network density especially at day 27 and differences in marker expression (appendix), but as the formation of neurite networks and neurite building cells was observed and the patterns of the marker expression profiles were comparable, we concluded, that the general neuronal differentiation capacity was not changed in Ct cells because of the transduction process. Therefore Ct is used as control for analysis of miR-451+ cells in neuronal differentiation.

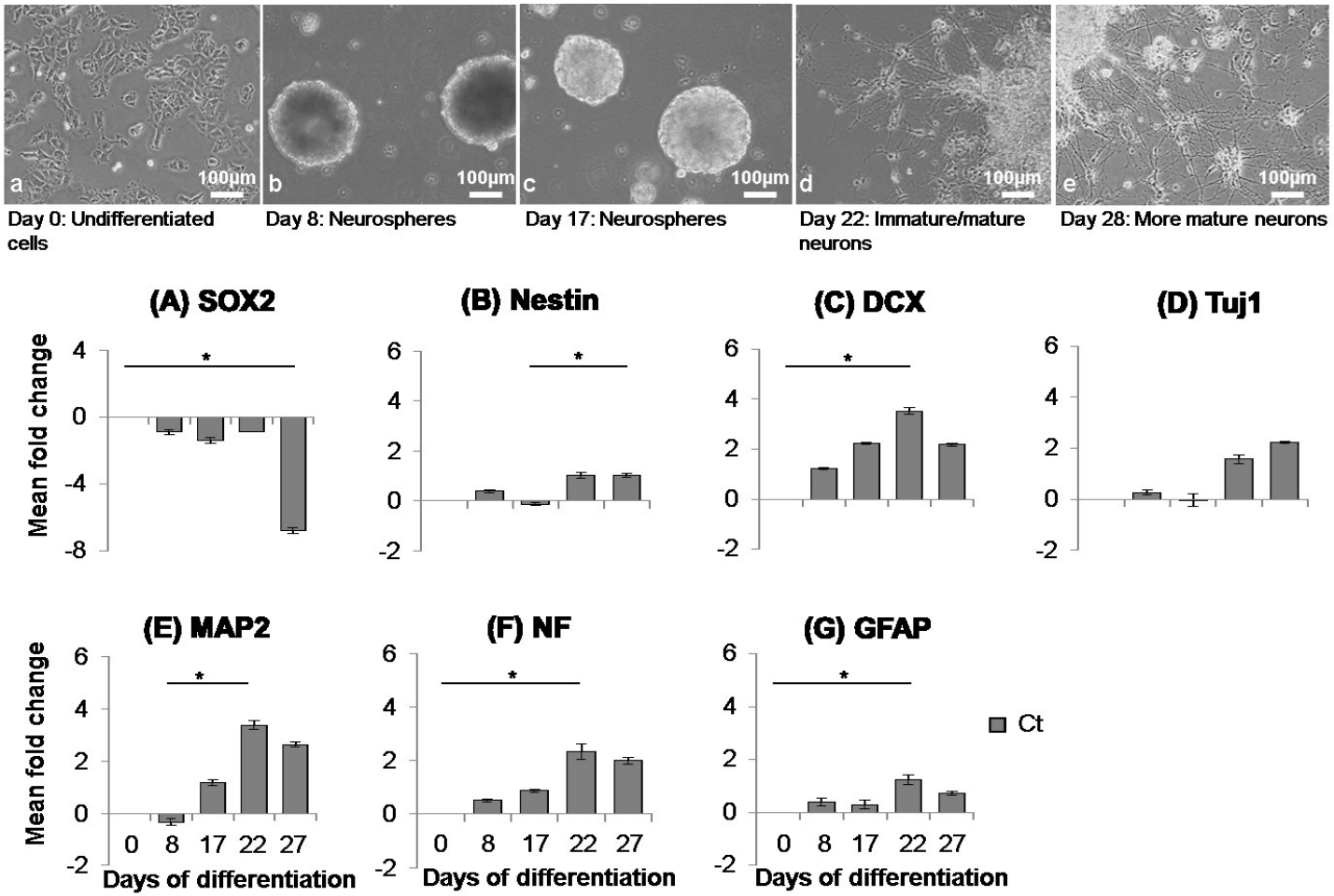

Figure 21

Morphological changes of undifferentiated Ct cells (a) during neuronal differentiation; Neurosphere formation at day 8 (b) and day 17 (c); Neurite growth and differentiation at day 22 (d) and day 27 (e); (10x, Olympus, Hicksville, New York, USA).

Expression pattern of markers (A) Sox2, (B) Nestin, (C) DCX, (D) Tuj1, (E) MAP2, (F) NF and (G) GFAP during neuronal differentiation of Ct. (n=3). Error bars indicate the standard error mean (SEM); Friedman's test (* = $p \leq 0{,}05$).

3.4. MiR-451 expression in transduced cells

To prove the efficiency of transduction the copy number of miR-451 in undifferentiated transduced cells and the fold change of miR-451 expression by referring to day 0 of neuronal differentiation of miR-451+ cells was determined.

A standard curve with known copy numbers of miR-451 mimics by qRT-PCR was established (Figure 54). A trend line was fitted through the data points. The resulting equation was used to calculate the copy number/20ng miRNA which was normalized by multiplication with a normalisation factor (calculated as described by Mitchell in the supplemental data (160)). The normalised copy number is illustrated in Figure 22 and Figure 23B). The copy number for miR-451 in undifferentiated Ct cells is approximately $2x10^5$ copies/20ng used miRNA, whereas overexpression of miR-451 results in a copy number of about $9x10^6$ in miR-451+ h (high eGFP expressing cells). miR-451+ h, med (medium eGFP expressing cells) and l (low eGFP expressing cells) were sorted according the magnitude of eGFP fluorescence by FACS. The expression of miR-451 expressed as normalised copy number/20ng used miRNA is significantly higher in miR-451+ h and med cells compared to Ct cells (Figure 22A, * = $p \leq 0,05$, Kruskal-Wallis-Test). The expression of miR-451 correlates with the magnitude of eGFP fluorescence, meaning high eGFP expressing cells also show the highest overexpression of miR-451. MiR-451 expression was not increased during later stages of neuronal differentiation of Ct (data not shown).

There is an overexpression of miR-451 in miR-451+ cells compared to Ct (Figure 23A). MiR-451 overexpression in miR-451+ cells is highest at day 0 and 17 of differentiation (about 10 and 8 fold) and is lower at day 8, 22 and 27 (about 7, 6 and 5 fold respectively, Figure 25A). In miR-451+ cells the normalised copy number of miR-451 per 20ng used miRNA decreases at day 22 and 27 (Figure 23A).

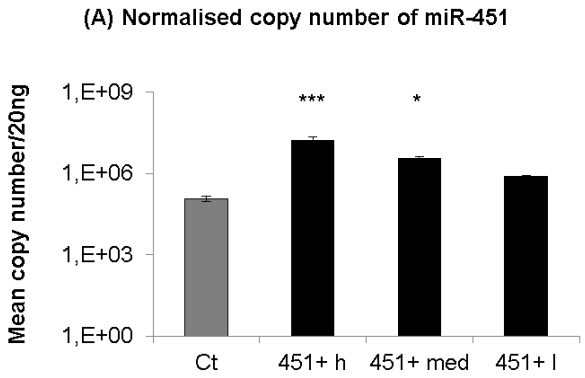

Figure 22

(A) Calculated normalized copy number of miR-451 in transduced undifferentiated NT2 (Ct and miR-451+ high, middle and low GFP expressing cells). * p ≤ 0,05 (Kruskal-Wallis-Test).

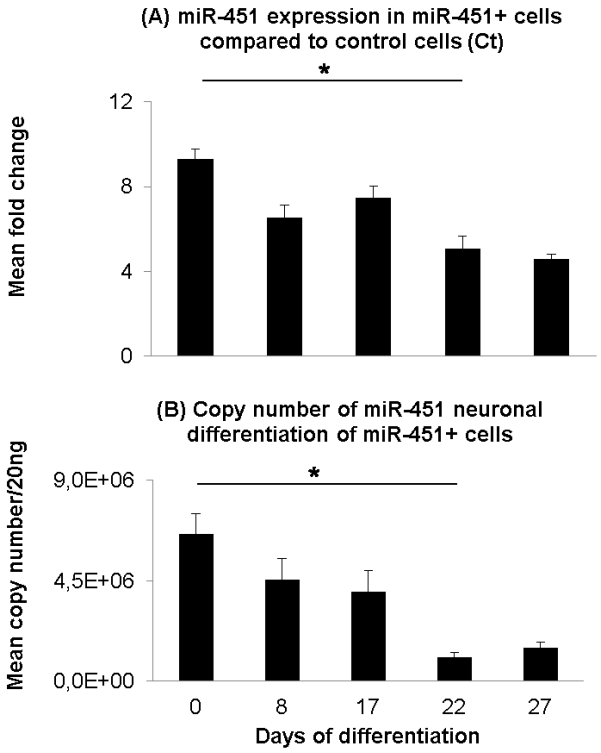

Figure 23

(A) Expression of miR-451 represented as mean fold change during neuronal differentiation of miR-451+ compared to Ct is shown (n=3). (B) Copy number per 20ng used miRNA during differentiation of miR-miR-451+ cells. The error bars indicate the standard error mean (SEM). n=3, * p ≤ 0,05 (Friedman's test).

There is a significant overexpression of miR-451 in undifferentiated and differentiated miR-451+ cells. The decrease of miR-451 overexpression during neuronal differentiation of miR-451+ cells might be the consequence of an endogenous regulatory mechanism during neuronal differentiation in vitro.

3.5. Neuronal differentiation miR-451 overexpressing cells

To avoid false negative results of further experiments by transduction of the vector AB.G.miR-451 (termed hereafter as miR-451+ cells) regular neuronal differentiation of transduced cells was determined by morphological, immunofluorescent and molecular analysis of various differentiation time points.

The morphological changes during neuronal differentiation of miR-451+ cells are shown Figure 24a-e. The expression profiles of (A) Sox2, (B) Nestin, (C) DCX, (D) Tuj1, (E) MAP2, (F) NF and (G) GFAP compared to day 0 in miR-451+ cells are shown in Figure 24A-G). Down-regulation of Sox2 and Nestin and up-regulation of DCX, Tuj1, MAP2 and NF were observed with advanced differentiation.

Sox2 expression decreases over time of differentiation, being significantly lowest at day 27 compared to day 0 (Friedman's test, * = $p \leq 0,05$, Figure 24A).

In miR-451+ cells there is a trend of down-regulation of **Nestin** (Figure 24B).

There is an up-regulation of **DCX** and **Tuj1** expression during neuronal differentiation of miR-451+ compared to day 0, being significantly different between day 0 and 17 in DCX (Friedman's test, * = $p \leq 0,05$, Figure 21C and D).

During neuronal differentiation the expression of **MAP2** increases in miR-451+ cells showing a significant difference between day 0 and 22 (Friedman's test, * = $p \leq 0,05$, Figure 24E).

In miR-451+ cells **NF** expression increases until day 17 of neuronal differentiation. A down-regulation at day 22 and 27 compared to day 0 during differentiation of miR-451+ cells is seen. There is a significant difference in expression at day 17 and 27 (Friedman's test, * = $p \leq 0,05$, Figure 24F).

GFAP expression is up-regulated in miR-451+ cells during neuronal differentiation in vitro. There is a significant difference in expression between day 17 and 27 in miR-451+ cells (Figure 24G).

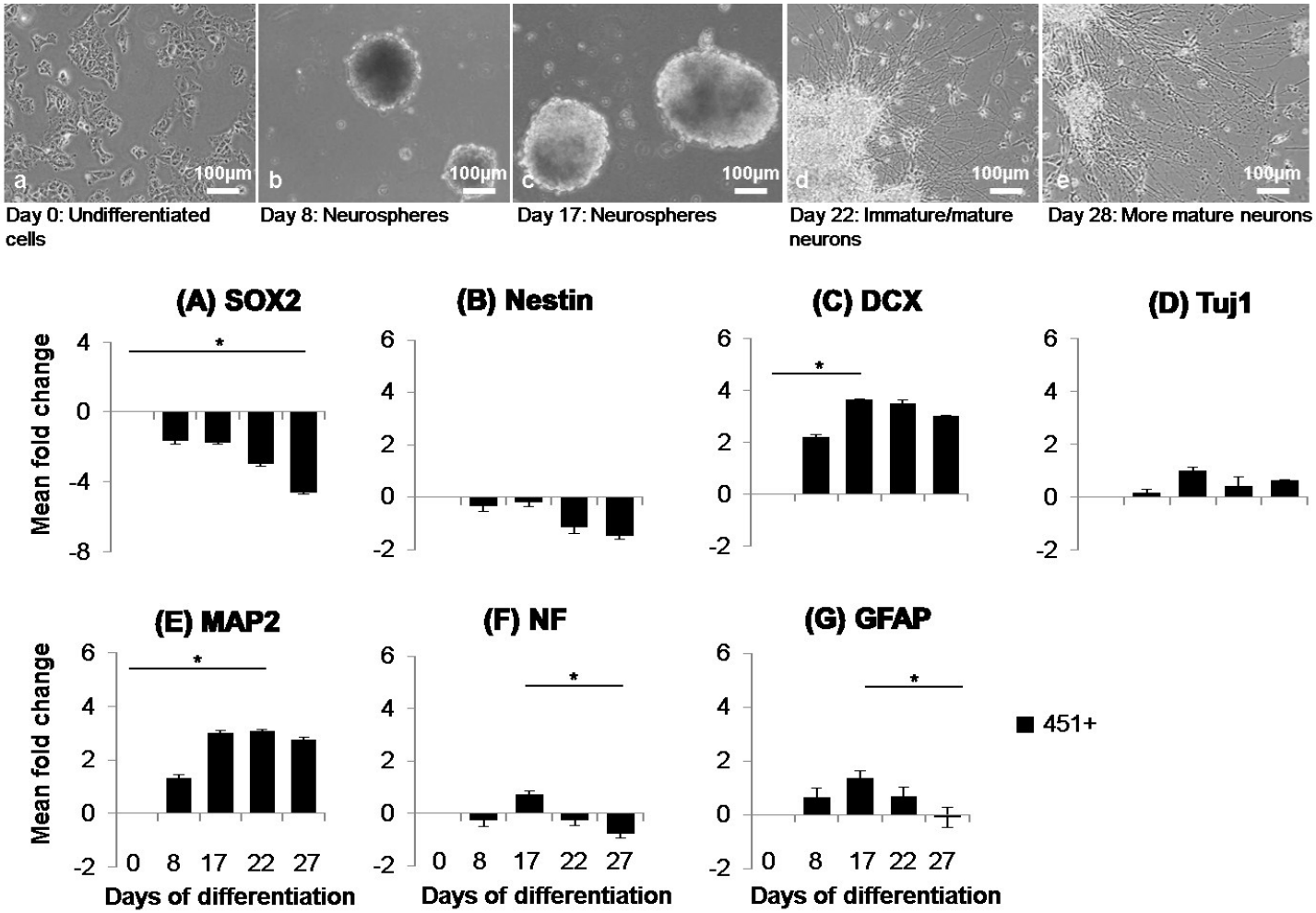

Figure 24

Morphological changes of undifferentiated miR-451+ cells (a) during neuronal differentiation; Neurosphere formation at day 8 (b) and day 17 (c); Neurite growth and differentiation at day 22 (d) and day 27 (e); (10x, Olympus, Hicksville, New York, USA).

Expression pattern of markers (A) Sox2, (B) Nestin, (C) DCX, (D) Tuj1, (E) MAP2, (F) NF and (G) GFAP during neuronal differentiation of miR-451+ cells (n=3). Error bars indicate the standard error mean (SEM); Friedman's test, * = $p \leq 0{,}05$).

Neuronal differentiation of miR-451+ cells leads to neurite building cells and characteristic marker expression profiles. Therefore neuronal differentiation of miR-451+ cells was implemented successfully.

3.6. Comparison of differentiation marker expression in Ct and miR-451+ cells

To analyse the impact of miR-451 overexpression on neuronal differentiation the expression of (A) Sox2, (B) Nestin, (C) DCX, (D) Tuj1, (E) MAP2, (F) NF and (G) GFAP during neuronal development is compared to Ct cells (Figure 25). Delta ct values of miR-451+ were referenced to the delta ct of day 0 of Ct cells in order to compare the marker expression between Ct and miR-451+ at day 0 and within the expression profile.

When comparing miR-451+ and Ct cells a significant up-regulation of **Sox2** in undifferentiated miR-451+ cells is seen (Figure 25A), Mann-Whitney U-Test, * = $p \leq 0,05$). At day 8 and 17, expression of Sox2 is not significantly different between Ct and miR-451+ cells. At day 22 there is a significant lower expression in Sox2 in miR-451+ cells compared to Ct cells (Mann-Whitney U-Test, * = $p \leq 0,05$). At day 27, this is reversed and there is a significant lower expression of Sox2 in Ct cells than in miR-451+ cells (Mann-Whitney U-Test, * = $p \leq 0,05$).

Nestin expression is significantly different between miR-451+ cells and Ct cells at day 0, 17, 22 and 27 (Figure 25B, Mann-Whitney U-Test, * = $p \leq 0,05$).

Expression of **DCX** at day 0 and day 22 is similar in Ct cells and miR-451+ cells (Figure 25C). At day 8, 17 and day 27 a significant higher expression of DCX in miR-451+ cells was observed (Mann-Whitney U-Test, * = $p \leq 0,05$).

Tuj1 expression is significantly different between miR-451+ and Ct cells at day 0, 8, 17 and 27 (Figure 25D, Mann-Whitney U-Test, * = $p \leq 0,05$).

There is a significant increase of **MAP2** expression in miR-451+ at day 8 and 17 and 27 compared to Ct (Figure 25E, Mann-Whitney U-Test, * = $p \leq 0,05$).

Comparing miR-451+ and Ct cells, an accelerated and earlier increase of **NF** expression in miR-451+ is seen, which is significantly higher at day 17 and significantly lower at day 22 and 27 (Figure 25F, Mann-Whitney U-Test, * = $p \leq 0,05$).

GFAP expression increases during neuronal differentiation of miR-451+ and Ct cells (Figure 25G). There is a significant higher expression in miR-451+ cells at day 0, 8, 17 and 27. (Mann-Whitney U-Test, * = $p \leq 0,05$).

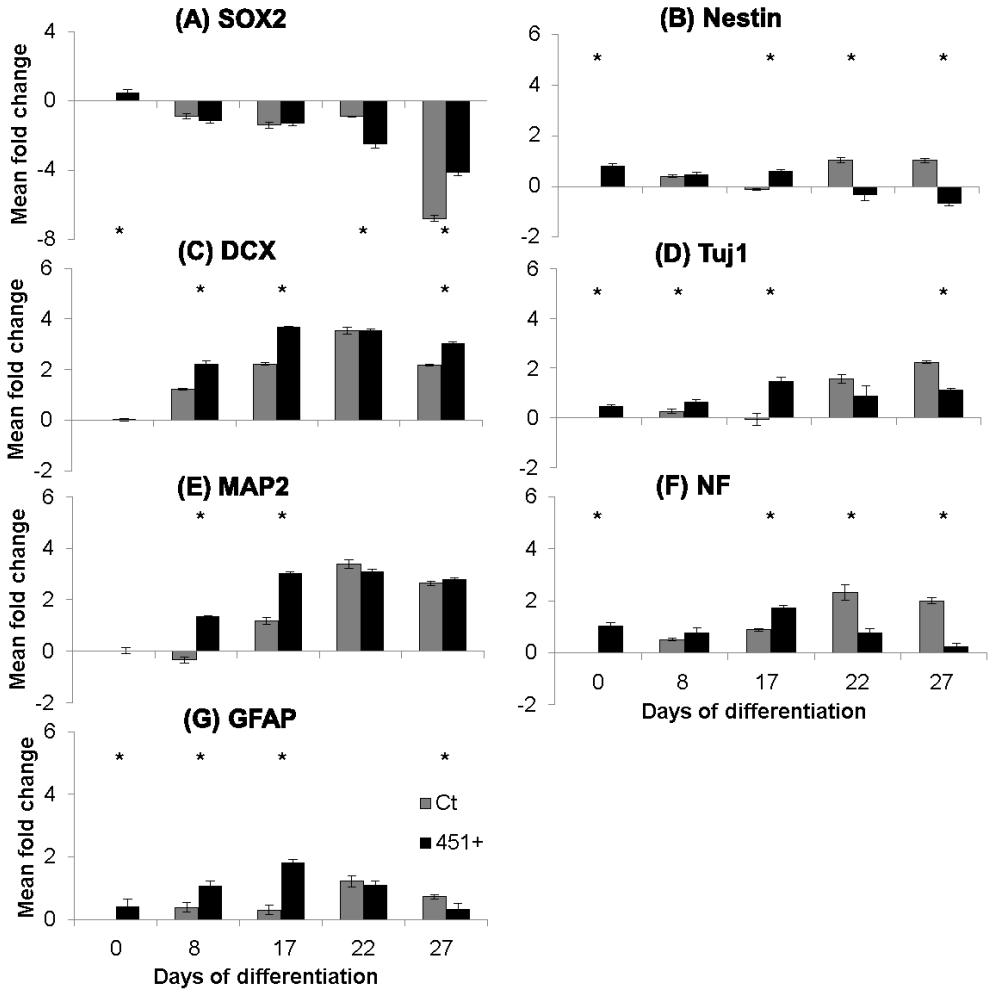

Figure 25

Expression pattern of neuronal differentiation markers (A) Sox2, (B) Nestin, (C) DCX, (D) Tuj1, (E) MAP2, (F) NF and (G) GFAP during of neuronal differentiation of transduced miR-451+ cells compared to Ct cells at day 0 (n=3). Mann-Whitney U-Test, * = $p \leq 0,05$.

During neuronal differentiation of Ct and miR-451+ cells there are significant differences in marker expression. miR-451+ cells show an earlier increase of marker expression, which is linked to a more differentiated cells status.

3.7. Morphological differences in the differentiation of Ct and miR-451+

3.7.1. Neurite network and neurite length

At day 22 differentiation neurite building cells in Ct and miR-451+ cells have established and maturate and expand their neurite network until day 27 (Figure 26A-D). This occurs within one day after cells have been plated on matrigel coated flasks (day 18, data not shown). While comparing differentiation day 22 and 27 of Ct (Figure 26A1, A2 and C) and miR-451+ cells (Figure 26A1, A2, and D) morphological differences between Ct cells and miR-451+ cells become obvious. miR-451+ cells establish a denser and more pronounced neurite network compared to Ct cells. Furthermore cells of enlarged size and different shape are seen in Ct.

These differences were quantified by calculating the ratio between neurite length and size of the core neurosphere from which the neurites had been growing out of with the Imaris software (Figure 27). The ratio between neurite length and neurosphere is size is significantly higher in miR-451+ cells at day 21 of neuronal differentiation (Mann Whitney U-Test, *** = $p \leq 0{,}001$).

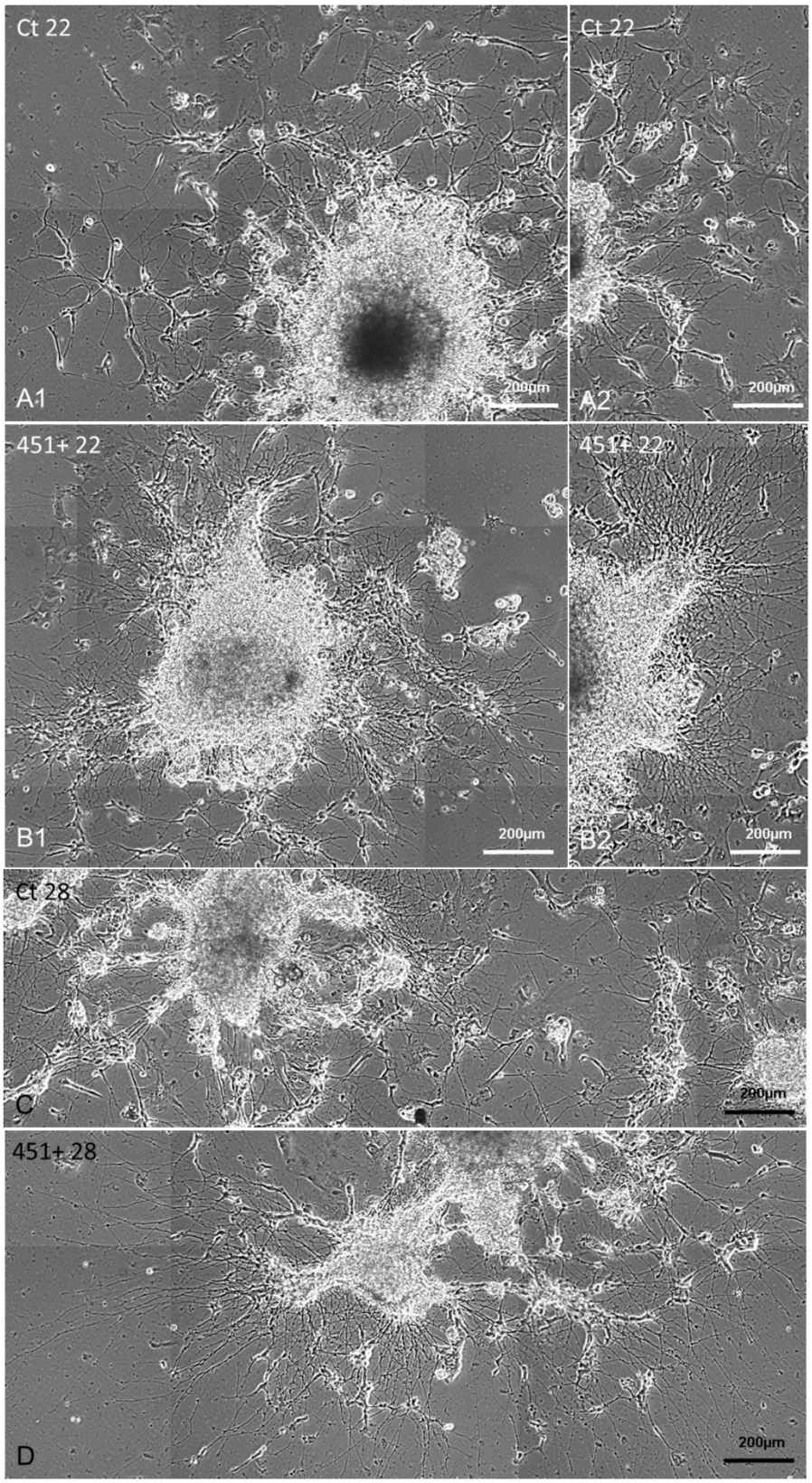

Figure 26

Neuronal differentiation of Ct (A1, A2, C) and miR-451+ (B1, B2 and D) at day 22 and 28 (10x, CellIQ, Imagen, Massachusetts).

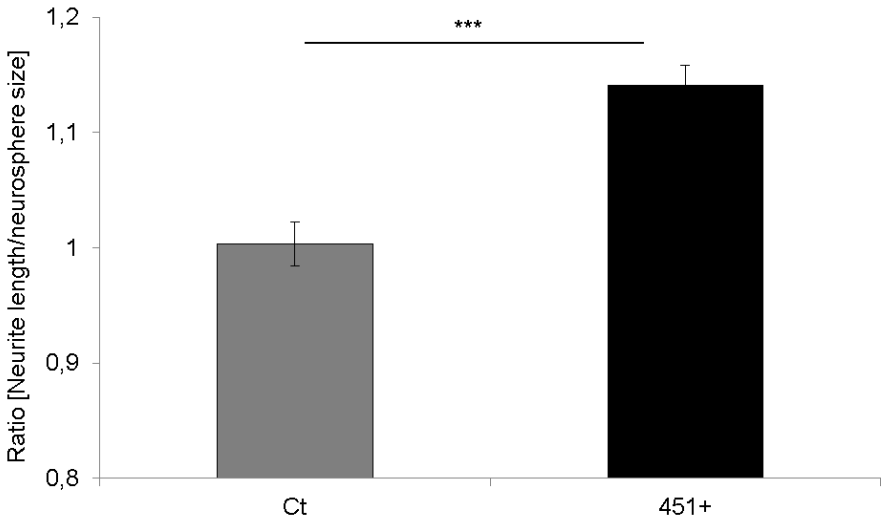

Figure 27

The ratio between neurite length and neurosphere size is represented in the different transduced cells at day 21 of neuronal differentiation (Ct = control vector, miR-451+ = miR-451 overexpressing cells, Mann Whitney U-Test, *** = $p \leq 0{,}001$)

miR-451+ cells show a denser neurite network and longer neurites compared to Ct, which could, together with the differences in neuronal marker expression, originate from a more differentiated cells status in miR-451+ cells.

3.7.2. Cell size and shape

To better visualise the morphological differences of Ct and miR-451+ cells TNS4 staining was chosen for immunohistochemistry (for further information please move to the discussion). Staining of TNS4 revealed extensive morphological differences in size and shape of Ct and miR-451+ cells at day 22 and 28 of neuronal differentiation (Figure 28 and Figure 29). Negative controls are shown in the Appendix.

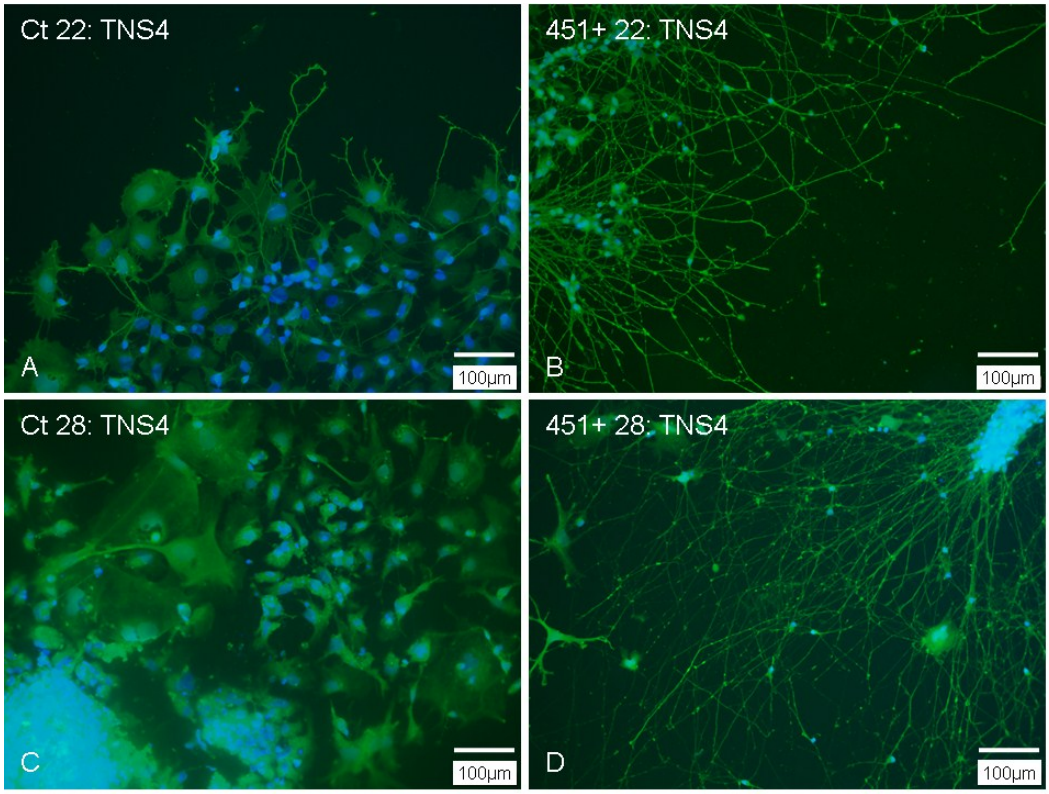

Figure 28

Immunostaining of TNS4 at day 22 and 28 in Ct (A, C) and miR-451+ cells (B, D), 20x, Olympus, Hicksville, New York, USA.

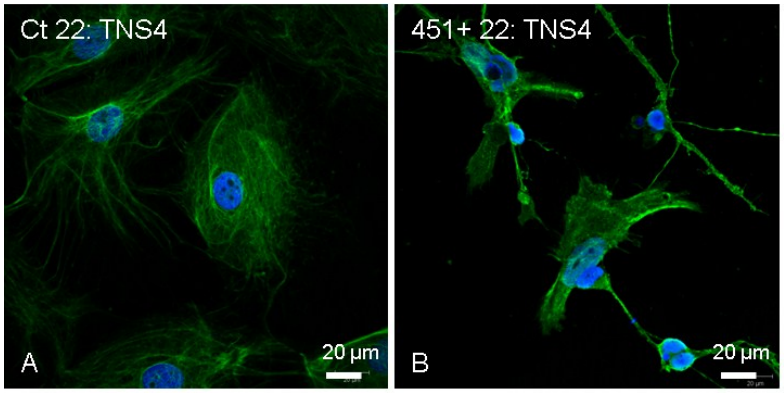

Figure 29

Immunostaining of TNS4 at day 22 and 28 in Ct (A, C) and miR-451+ cells (B, D), 40x, LSM Zeiss, Oberkochen; Germany.

Quantitative analysis of the cell area in Ct and miR-451+ cells showed that miR-451+ cells at day 22 (mean area 5000 μm^2) are significantly smaller in area than Ct cells (mean area 10000 μm^2) at day 22 of differentiation (Figure 30).

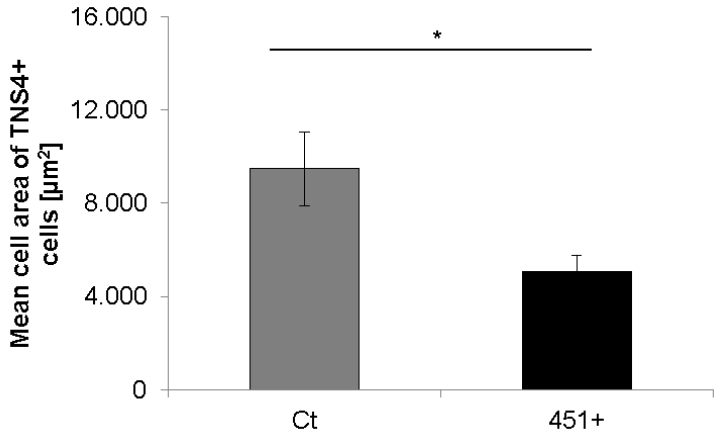

Figure 30

Mean area of TSN4-positive cells at day 22 (Ct = control cells, miR-451+ = miR-451 overexpressing cells, Mann Whitney U-Test, * = $p \leq 0,05$).

TNS4 staining shows a difference in morphology, which quantitatively evaluated. miR-451+ cells show the morphology of more differentiated cells than Ct cells.

3.8. Immunofluorescence of Ct and miR-451+

To underline the results revealed by qRT-PCR and visualize the differences in Ct and miR-451+ cell populations during development immunohistochemistry for selected markers was done. Immunofluorescent staining for DCX (Figure 31A-D, Figure 32A-D), Tuj1 (Figure 31E-H, Figure 32E-H), MAP2 (Figure 33A-D, Figure 34A-D) and NF (Figure 33E-H, Figure 34E-H were performed at day 22 (A, C, E, G) and 28 (B, D, F, H) of differentiation. Differentiating cells show differences according to their morphology, maturity and network building efficiency. Ct cells show a reduced neurite length and network density than miR-451+ cells at day 22 and day 28. Ct cells have a larger cell surface, whereas miR-451+ cells look more like mature neurons. Negative controls are shown in the Appendix.

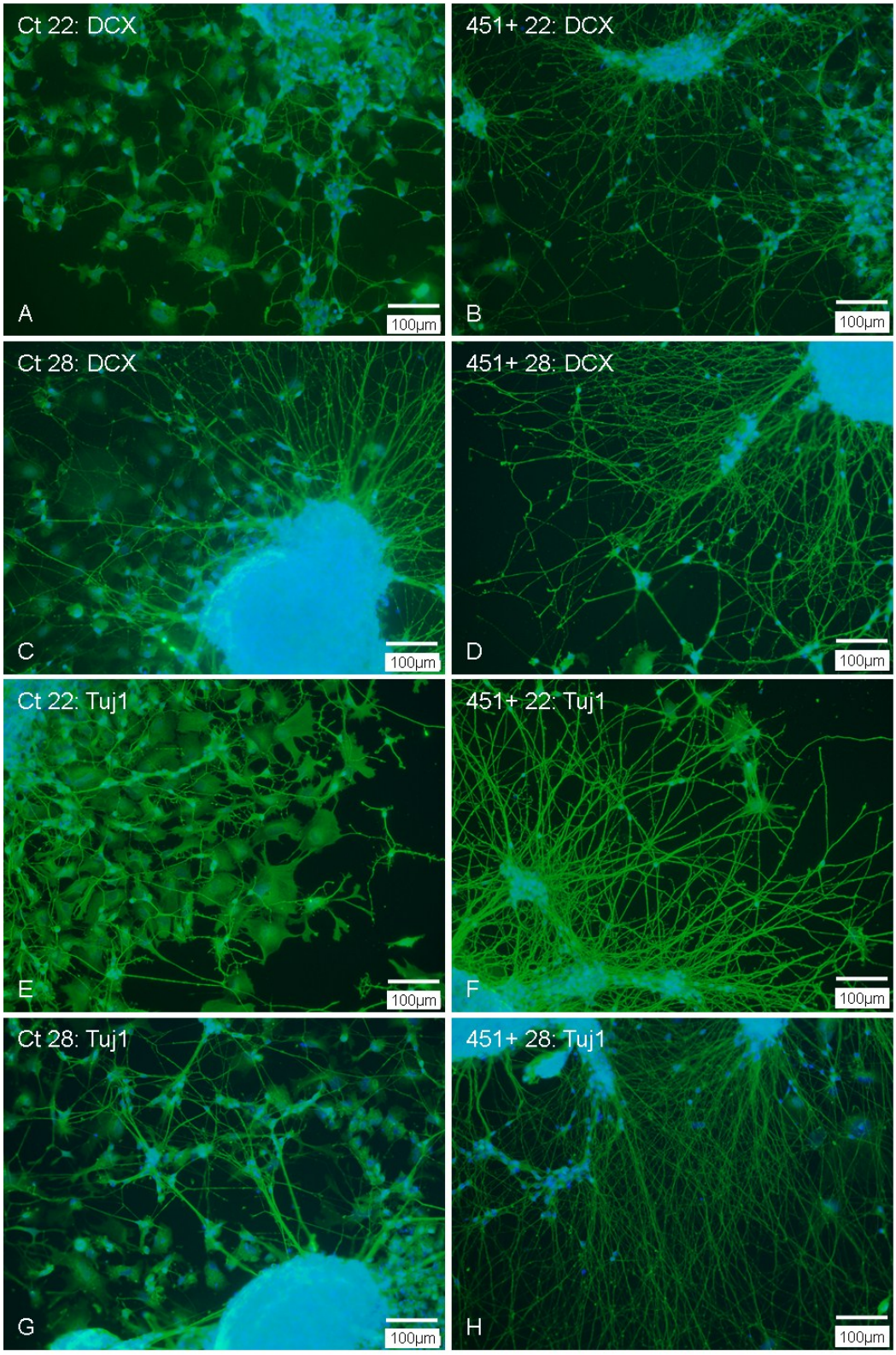

Figure 31

Immunostaining of DCX (A-D) and Tuj1 (E-H) is shown at day 22 (A, B, E, F) and 28 (C, D, G, H) of neuronal differentiation of Ct (A, C, E, F) and miR-451+ cells (B, D, F, H), 20x, Olympus, Hicksville, New York, USA.

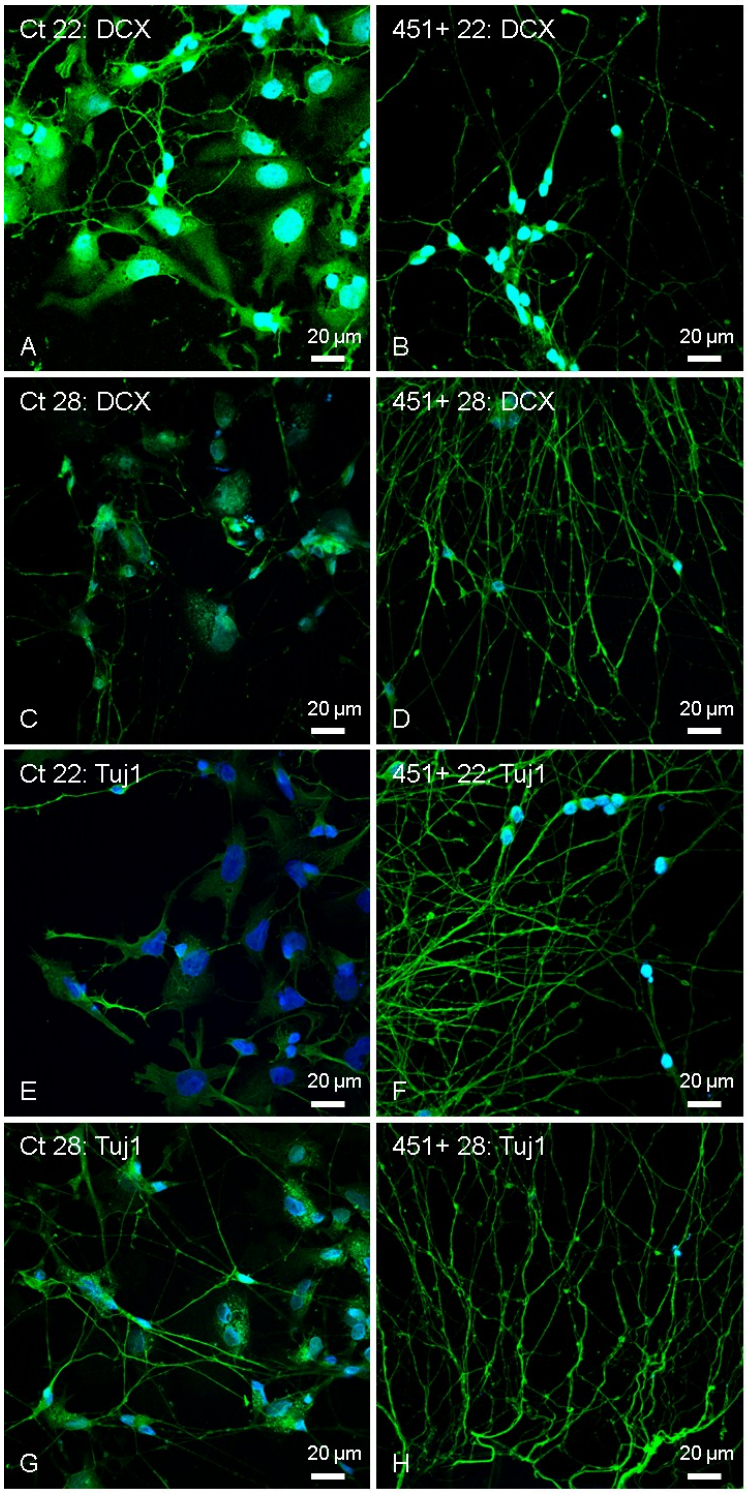

Figure 32

Immunostaining of DCX (A-D) and Tuj1 (E-H) is shown at day 22 (A, B, E, F) and 28 (C, D, G, H) of neuronal differentiation of Ct (A, C, E, F) and miR-451+ cells (B, D, F, H), 40x, LSM, Nikon, Vienna, Austria.

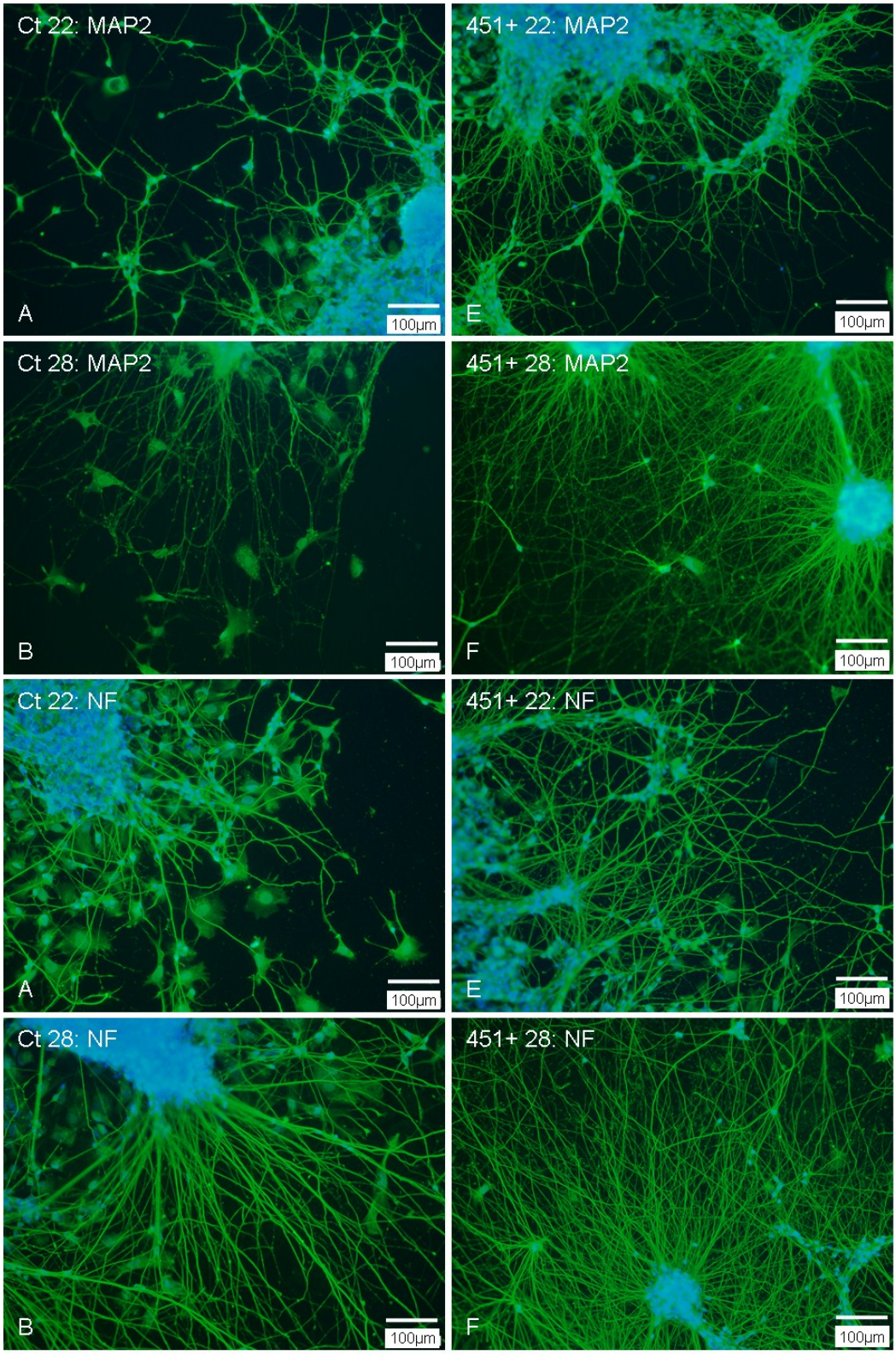

Figure 33

Immunostaining of MAP2 (A-D) and NF (E-H) is shown at day 22 (A, B, E, F) and 28 (C, D, G, H) of neuronal differentiation of Ct (A, C, E, F) and miR-451+ cells (B, D, F, H), 20x, Olympus, Hicksville, New York, USA.

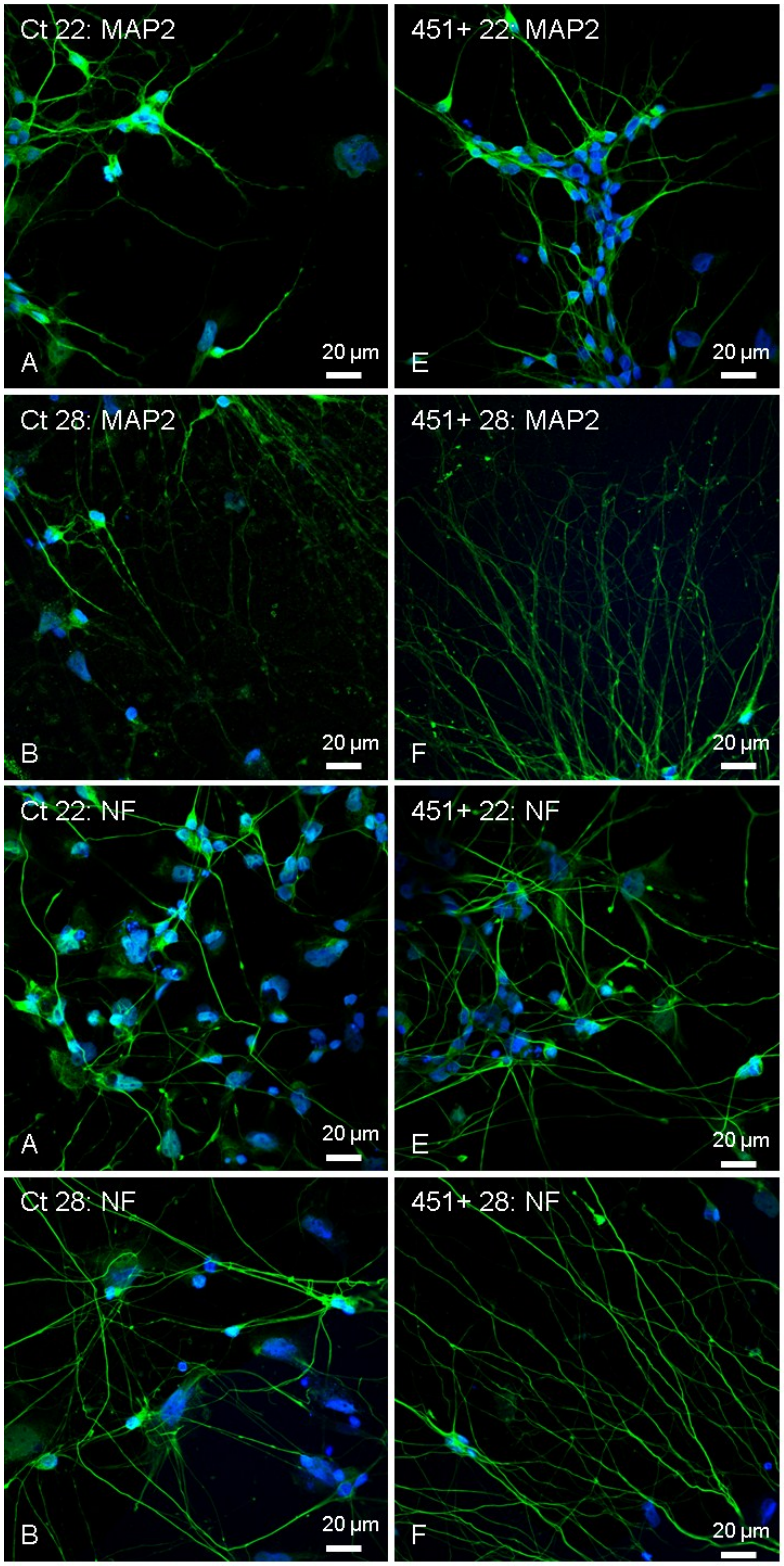

Figure 34

Immunostaining of MAP2 (A-D) and NF (E-H) is shown at day 22 (A, B, E, F) and 28 (C, D, G, H) of neuronal differentiation of Ct (A, C, E, F) and miR-451+ cells (B, D, F, H), 40x, LSM, Nikon, Vienna, Austria.

Figure 35 shows a quantitative evaluation of neurite length of immunofluorescent staining of NF. Differentiating Ct cells show a mean neurite length of approximately 200 µm at day 22, whereas miR-451+ cells show a mean length of about 300µm. Analysis was done with 3 different batches of staining, neurite lengths were measured in approximately 6 pictures of each condition.

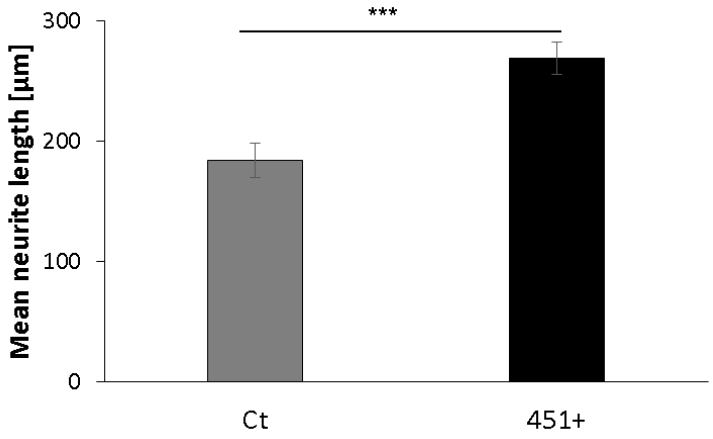

Figure 35
Length of NF+ neurites at day 22 of differentiation (Ct = control cells, miR-451+ = miR-451 overexpressing cells, Mann-Whitney-U-Test, *** = $p \leq 0{,}001$).

There are obvious differences in morphology, neurite network formation and neurite length in miR-miR-451+ cells compared to Ct cells at day 22 and 28 of neuronal differentiation. MiR-451 overexpression seems to influence neurite network, network density and morphology of the cells and therefore seems to have a role in neuronal differentiation in vitro.

3.1. Integrin-ß1 and Vimentin expression in Ct and miR-451+ cells

Integrin-ß1 (CD29, ITGB1, first described by Hynes in 1987 (165)) mediates adhesion, migration and differentiation of neural precursors (166), for further information please see discussion section). The intermediate filament protein Vimentin is initially expressed by nearly all neuronal precursors in vivo, and is replaced by neurofilaments shortly after the immature neurons become post-mitotic. Both Vimentin and NFs can be transiently detected within the same neurite, and Vimentin is essential for neuritogenesis at least in culture. Therefore CD29 and Vimentin are ideal candidates to study morphological changes and differences of differentiating cells.

Figure 36 shows the expression profiles of) Integrin-ß1 (A) and Vimentin (B) during neuronal differentiation of Ct and miR-451+ cells.

In Ct cells Integrin-ß1 expression is down-regulated at 8 and day 17 compared to day 0, but is then up-regulated at day 22 and 27, being significantly highest at day 27 (Friedman's test, * = p ≤ 0,05). Vimentin is first down-regulated at day 8 and 17 compared to day 0 and then up-regulated at the later differentiation days, being highest at day 27 and significantly different between day 17 and 27 (Friedman's test, * = p ≤ 0,05).

In miR-451+ cells Integrin-ß1 expression is down-regulated at all differentiation days compared to day 0, being lowest at day 27 and significantly different between 0 and 22 days (Friedman's test, * = p ≤ 0,05). Vimentin is first down-regulated at day 8, 17 and 22 compared to day 0 and then slightly up-regulated at day 27, being significantly different between 17 and 27 days (Friedman's test, * = p ≤ 0,05).

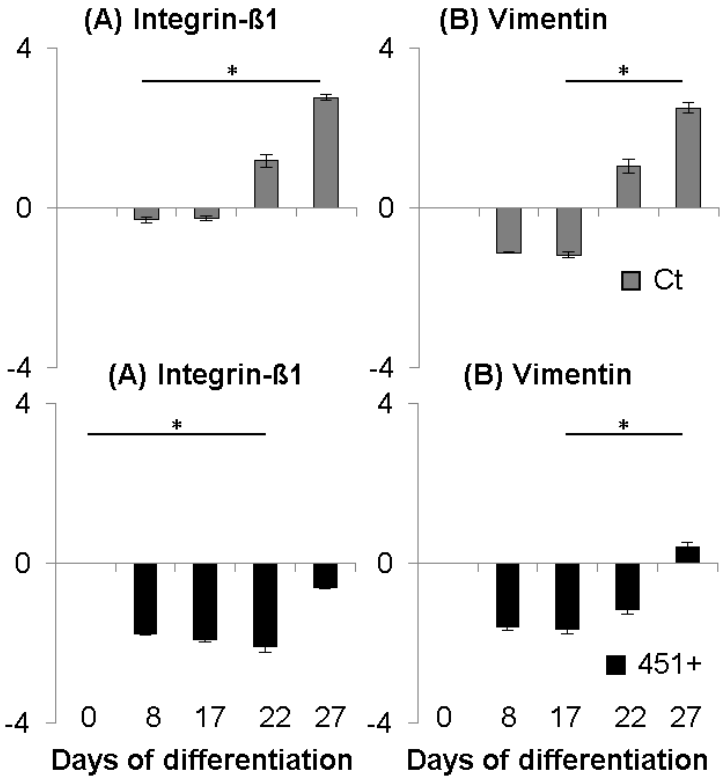

Figure 36
Expression profiles of Integrin-ß1 (A) and Vimentin (B) in the differentiation of Ct and miR-451+ cells. Error bars show the standard error mean (SEM), Friedman's test, * = p ≤ 0,05.

Figure 37 shows the comparison of the expression of Integrin-ß1 (A) and Vimentin (B) in miR-451+ and Ct cells. There is a significant difference in expression at day 0, 17 and 27 in Integrin-ß1 and at all examined differentiation time points of Vimentin. Delta ct values of miR-451+ were referenced to the delta ct of day 0 of Ct cells in order to compare the marker expression between Ct and miR-451+ at day 0 and within the expression profile.

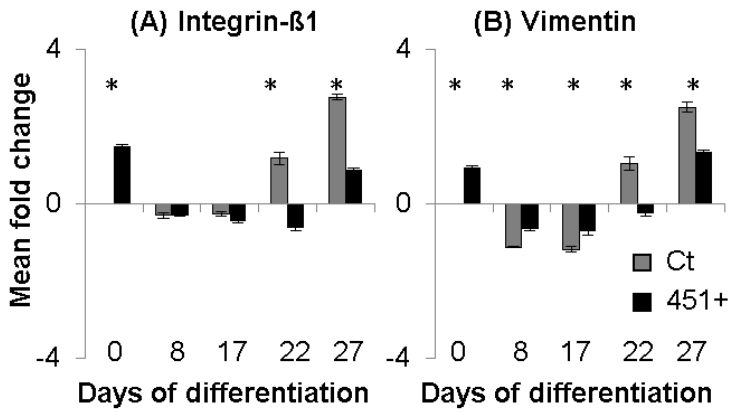

Figure 37
Expression of Integrin-ß1 (A) and Vimentin (B) in miR-451+ cells compared to day 0 of Ct cells. Error bars indicate the standard error mean (SEM), Mann Whitney U-Test, * = $p \leq 0,05$.

3.2. Differences in CD133 (Prominin 1) and FGFR1 expression

Former studies of our group revealed a miR-451 specific impact on CD133 and FGFR1 expression in NT2 cells via intake of miR-451 enriched microparticles. Uptake of microparticles from patients suffering from TBI, which are enriched with miR-451, by undifferentiated NT2 cells led to downregulation of CD133 and FGFR1. Moreover CD133 is known as stem cell marker, whereas FGFR1 signalling is involved in cell growth, migration, and differentiation, neuronal differentiation and survival (for further information please see the discussion section). Therefore the endogenous impact of increased miR-451 signalling in miR-451+ cells was investigated.

Figure 38 shows the expression profiles of CD133 (A) and FGFR1 (B) during neuronal differentiation of miR-451+ compared to day 0 of Ct cells (Ct)
In Ct cells CD133 expression is nearly similar at day 8 compared to day 0, is decreasing at day 17 (compared to day 0) and is then increasing at differentiation day 17 and 22 (compared to day 0). FGFR1 expression is down-regulated compared to day 0 in all consecutive differentiation days except for day 22.

In miR-451+ cells CD133 and FGFR1 expression are down-regulated at all consecutive differentiation days compared to day 0, being lowest at at day 27.

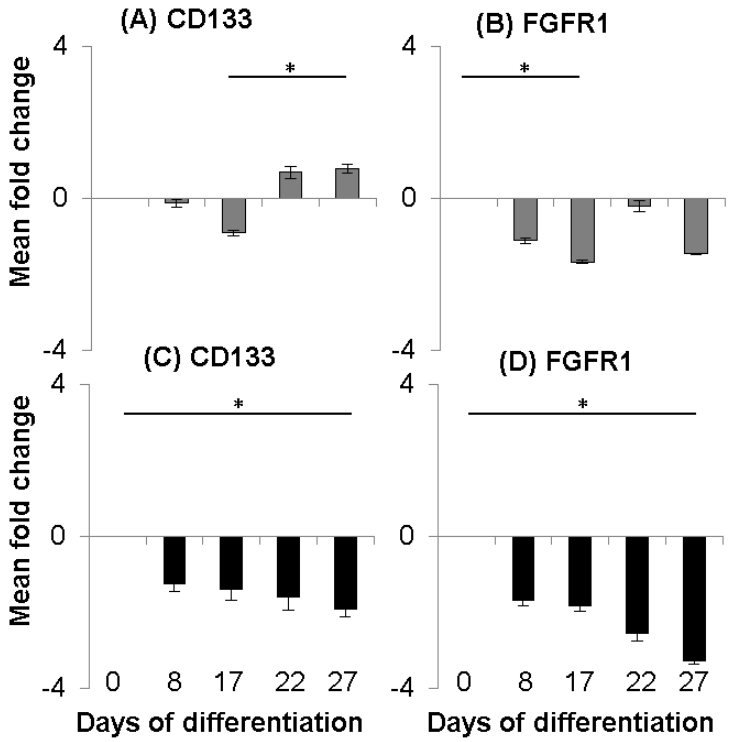

Figure 38

Expression profiles of CD133 (A) and FGFR1 (B) in differentiation of Ct and miR-451+ cells. Error bars indicate the standard error mean (SEM), Friedman's test, * = $p \leq 0{,}05$.

Figure 39 shows the comparison of the expression of CD133 (A) and FGFR1 (B) in miR-451+ and Ct cells. There is a significant difference in expression at day 0, 17, 22 and 27 in CD133 and at all examined differentiation time points of FGFR1. Delta ct values of miR-451+ were referenced to the delta ct of day 0 of Ct cells in order to compare the marker expression between Ct and miR-451+ at day 0 and within the expression profile.

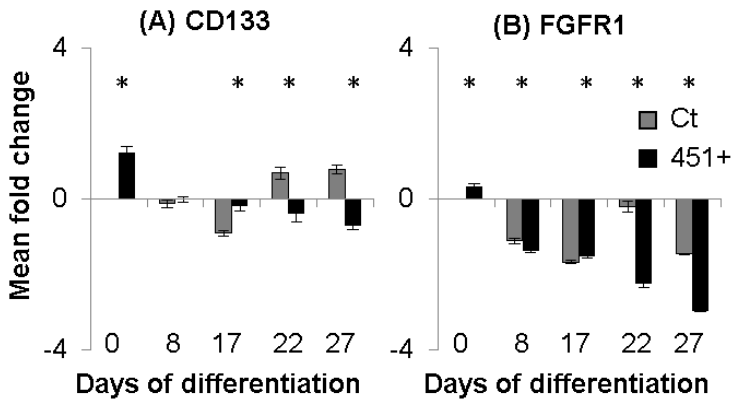

Figure 39

Expression of CD133 (A) and FGFR1 (B) in miR-451+ cells compared to day 0 of Ct cells. Error bars indicate the standard error mean (SEM); Mann Whitney U-Test, * = $p \leq 0,05$.

Significant differences in CD133 and FGFR1 expression at the different differentiation time points between Ct and miR-451+ indicate on the one hand enhanced loss of stemness (undifferentiated status) in miR-miR-451+ cells and on the other hand a direct or indirect influence of miR-451 overexpression on CD133 and FGFR1 expression.

3.3. List of miR-451 regulated target genes

MiRNAs bind to specific sequences of their target mRNA and suppress translation of their target mRNAs by different mechanisms (for further information please see the discussion section). A database and literature search for predicted and validated target genes of miR-451 was performed to get information potential binding partners of miR-451. 17 target genes were selected for analysis because of their validation status and/or function in neuronal development.

Table 1 lists references, release dates, resources and search results of 7 different used databases.

Table 1

List of databases used for search of validated and predicted target genes for miR-451

Name	Literature	Release	Resource	Results
miRanda	(167)	08/2010	www.microrna.org	1605 predicted targets
Target Scan 7.0	(168-174)	07/2015	www.targetscan.org	541 predicted targets, of which 28 have conserved sites
miRSearch V3.0	(168, 171)	?	https://www.exiqon.com/miRSearch	90 predicted target genes
DIANA microT	(175, 176)	2012	diana.imis.athena-innovation.gr/DianaTools/index.php?r=microT_CDS/index	37 predicted target genes, 3 validated target genes
MiRDB	(177-179)	03/2015	http://mirdb.org	23 predicted targets
TarBase v7.0	(180, 181)	2014	diana.imis.athena-innovation.gr/DianaTools/index.php?r=tarbase/index	37 validated target genes
Mirtarbase 4.5	(182)	11/2013	http://mirtarbase.mbc.nctu.edu.tw/php/detail.php?mirtid=MIRT000046#enrichment	23 validated target genes

Table 2 shows the selected predicted and validated target genes in alphabetical order.

Table 2

Selected validated and predicted target genes

Target gene	Status	Literature	Databases
AKT1	**validated**	(183-186)	TarBase, Mirtarbase
CAB39	**validated**	(141, 187-191)	miRanda, Target Scan, Diana MicroT, TarBase Mirtarbase
CDKN2D	**validated**	(192)	miRanda, Target Scan, miRDB
CXCL16	**validated**	(193)	miRanda, miRSearch
KIF24	predicted		miRanda, miRSearch
IL6R	**validated**	(194)	TargetScan, mirtarbase
MIF	**validated**	(138, 195, 196)	miRanda, miRSearch, Diana MicroT, mirtarbase
Myc	**validated**	(142-144, 146, 197)	Tarbase, mirtarbase
OSR1	predicted		miRanda, Target Scan, miRSearch, Diana Micro T, miRDB
POU3F2	predicted		miRanda, miRSearch,
PSMB8	**validated**	(198)	miRanda, Target Scan, miRSearch, DIANA microT, Tarbase
RAB14	**validated**	(140, 199)	miRanda, Diana microT, Tarbase, mirtarbase
S1PR2	predicted		miRanda, Target Scan, miRSearch
TSN4	Predicted in mouse	(200)	http://bioinformatics.sdstate.edu/gskb/get?label=MIRNA_MM_KREK_MMU-MIR-451
TSC1	**validated**	(134, 201)	miRanda, Target Scan, Diana MicroT, targetscan
VAPA	predicted		Target Scan
YWHAZ	**validated**	(128, 148, 202-206)	miRanda, Target Scan, miRDB

3.4. Validation of miR-451 target genes during neuronal differentiation

3.4.1. Validation by qRT-PCR

qRT-PCR analysis was performed to analyse the expression profile of 17 selected target mRNAs during differentiation of Ct and miR-451+ cells. Figure 40 shows the expression profile of (A) AKT1, (B) CAB39, (C) CDKN2D, (D) CXCL16, (E) IL6R, (F) KIF24, (G) MIF, (H) MYC and (I) OSR1 (J) POU3F2, (K) PSMB8, (L) RAB14, (M) S1PR2, (N) TNS4, (O) TSC1, (P) VAPA and (Q) YWHAZ during differentiation of miR-451+ cells in comparison to Ct cells. Mean fold changes at day 8, 17, 22 and 27 are referred to day 0 of Ct cells. Error bars show the standard error mean of 3 biological replicates. Delta ct values of miR-451+ were referenced to the delta ct of day 0 of Ct cells in order to compare the marker expression between Ct and miR-451+ at day 0 and within the expression profile.

There are significant differences in expression between Ct and miR-451+ during neuronal differentiation in vitro (Mann-Whitney U-Test, * = $p \leq 0{,}05$). AKT1, CAB39, RAB14, TSC1 and YWHAZ are down-regulated significantly in miR-451+ cells at all time points compared to Ct 0. The expression of all target genes except for MYC, MIF and VAPA is down-regulated at day 0 in miR-451+ compared to the expression in Ct. MYC and MIF are significantly up-regulated in miR-451+ cells at day 0 compared to Ct. VAPA is the only gene, which shows no significant differences in expression in miR-451+ and Ct.

3.4.2. Validation by western blot

MiR-451 target genes CAB39, MIF, MYC, RAB14 and YWHAZ were selected for western blot analysis because of our own qRT-PCR results and previous findings in the literature. In general, western blot analysis was very time consuming and is still in progress. Western blots for MYC, RAB14 and YWHAZ did not work (data not shown). The protein expression of CAB39 (A) and MIF (B) was analysed by western blot in the differentiation of Ct and miR-451+ cells (Figure 41). It should be taken into account that western blot data presented in this dissertation is very preliminary and has been performed only once. Therefore quantitative analysis was not performed. There is a down-regulation of protein expression of CAB39 and MIF at day 0, 8 and 17 during neuronal differentiation in miR-451+ cells compared to Ct. Data should be normalised against the loaded protein amount visualised by incorporation of a fluorescent dye during SDS-PAGE.

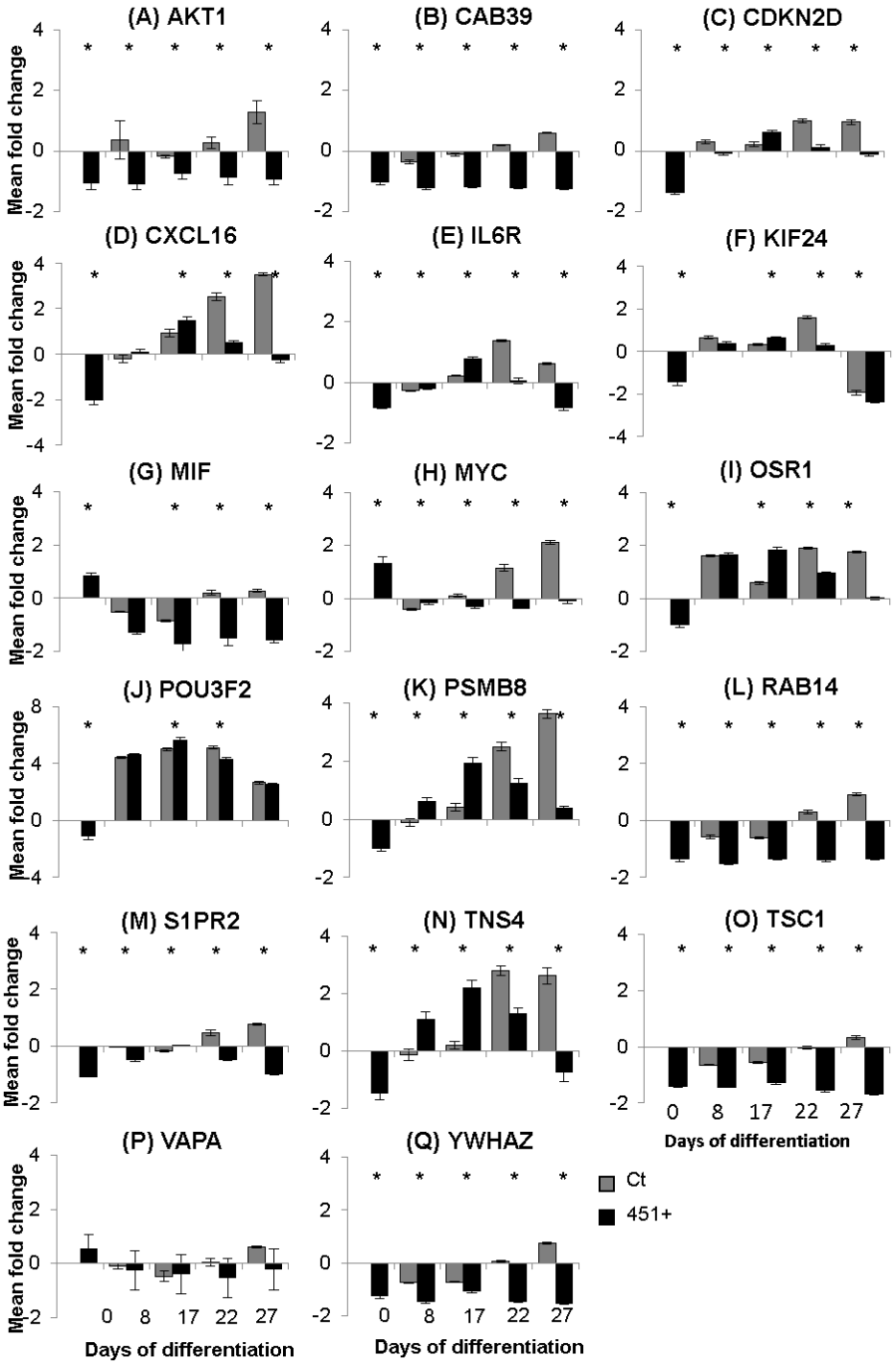

Figure 40

Expression pattern of various predicted and validated miR-451 target genes (A) AKT1, (B) CAB39, (C) CDKN2D, (D) CXCL16, (E) IL6R, (F) KIF24, (G) MIF, (H) MYC and (I) OSR1 (J) POU3F2, (K) PSMB8, (L) RAB14, (M) S1PR2, (N) TNS4, (O) TSC1, (P) VAPA and (Q) YWHAZ during neuronal differentiation of miR-451+ compared to Ct at day 0 (n=3). Mann-Whitney U-Test (* = $p \leq 0{,}05$).

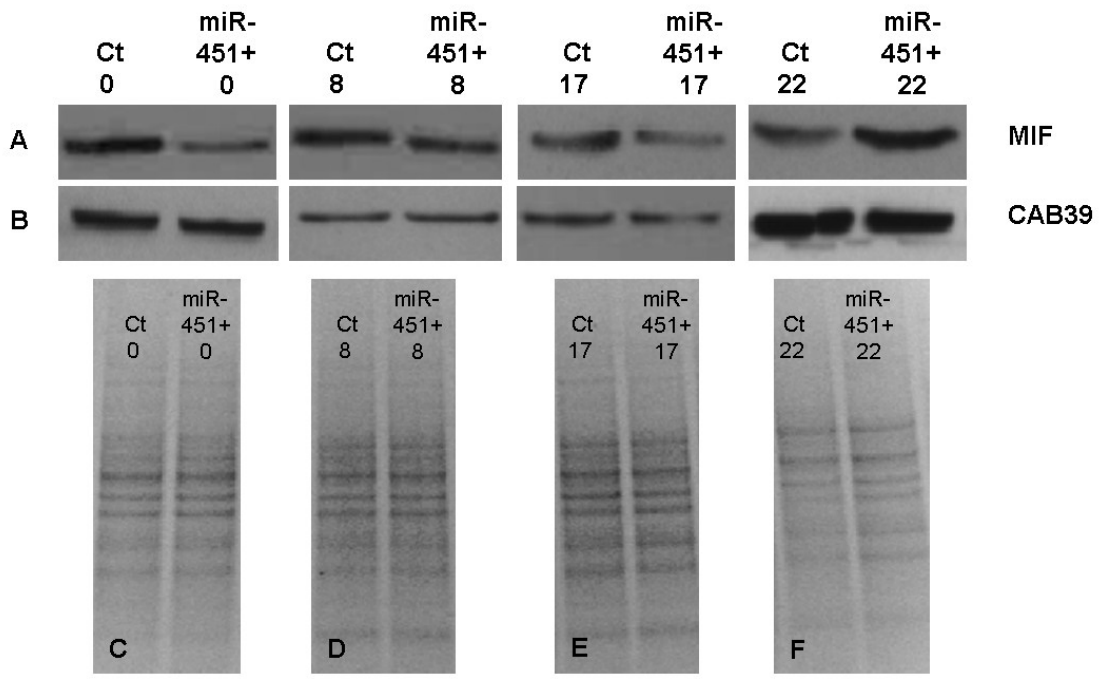

Figure 41

Western blot of CAB 39 (A) and MIF (B) during neuronal differentiation of Ct and miR-451+ cells. Data should be normalised against the loaded protein amount visualised by incorporation of a fluorescent dye during SDS-PAGE (C-F).

MiR-451 overexpression seems to influence mRNA expression of diverse target genes (most prominently AKT1, CAB39, RAB14, TSC1 and YWHAZ). Effects on the protein level were also observed for MIF and CAB39 although western blot analysis was performed only once. Therefore we propose further investigation of protein expression of above mentioned genes in neuronal differentiation in vitro.

3.5. CellIQ – effect on morphology and gap closure

It is widely described in the literature that miR-451 overexpression influences the migration and proliferation of cancer cells (for references and further information please see discussion section). As undifferentiated NT2 cells are a terato-carcinoma cell line, migration and proliferation capability are also important topics in adult neurogenesis and to test whether this migration and proliferation are also influences in our setup, we scratched undifferentiated confluent Ct and miR-451+ cells and gap closure was observed using CellIQ.

The gap closure in percent is shown in Figure 42A. miR-451+ cells proliferating and migrating in the gap show a different morphology compared to Ct cells (Figure 42B and C). Furthermore the length of the cells migrating and proliferating in the gap was measured and is shown in Figure 42D. The gap closure in % is reduced in miR-451+ cells compared to Ct cells.

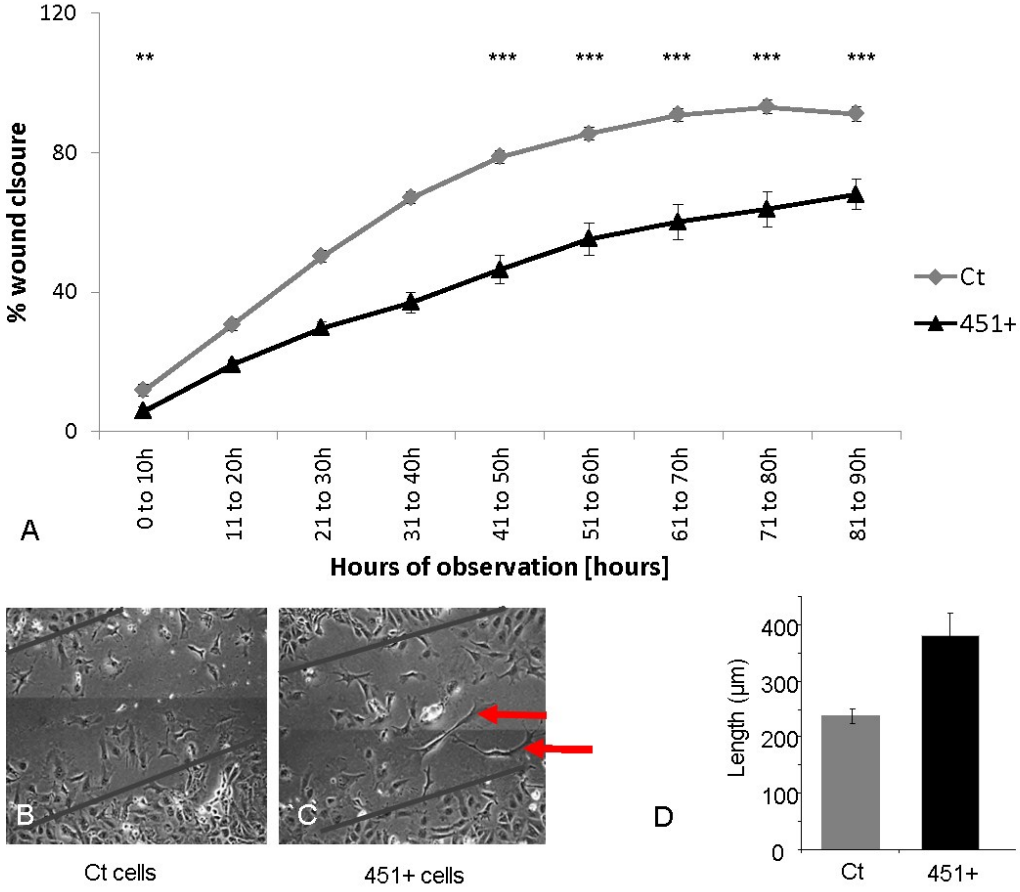

Figure 42

miR-451 overexpressing NT2 (miR-451+) and Ct were scratched and then observed using CellIQ. The gap closure in percent is lower in the cells, which overexpress miR-451 (miR-451+) compared to Ct (A). Furthermore miR-451+ cells (C) show morphological changes during the process of gap closure compared to Ct. The length of miR-451+ cells is increased compared to the control cells (D). Mann Whitney U-Test (** = $p \leq 0{,}005$, *** = $p \leq 0{,}001$).

4. Discussion

The fundamental results presented in this dissertation are:

- Successful neuronal differentiation by morphological, immunofluorescent and molecular analysis of various time points of differentiation in NT2, Ct and miR-451+ cells was verified. Cells express molecular and phenotypical properties of immature and maturating neurons and to some extent also glial cells.
- There is an endogenous upregulation of miR-451 expression during in-vitro differentiation of NT2 cells.
- Significant miR-451 overexpression was detected in cells transduced by viral particles containing the lentiviral vector AB.G.miR-451 (miR-451+ cells). This overexpression is decreasing during the in-vitro differentiation of transduced miR-451+ cells, but is still higher than in Ct cells (cells transduced with lentiviral particles containing the control vector AB.G.Ct).
- miR-451+ cells show accelerated differentiation to a neuronal phenotype compared to Ct cells. They show a denser outgrowth of neurites, longer neurites and more cells with neuronal morphology.
- qRT-PCR analysis revealed the down-regulation of many predicted and validated target genes (AKT1, CAB39, RAB14, TSC1 und YWHAZ).
- Preliminary results point out down-regulation of miR-451 targets CAB39 and MIF on the protein level.
- miR-451+ cells proliferate slower than Ct cells during gap closure and have a different behaviour and morphology during migration (elongated cells).

4.1. Scientific discussion

The important role of miRNAs in neuronal function, neural development (neural induction, progenitor expansion, differentiation and neural subtype specification), neuronal migration, neurite outgrowth and synaptic plasticity has been investigated intensely in the last 15 years and has been discussed in many reviews (12, 81, 85, 92, 207-214). Alteration in the tissue specific miRNA expression pattern or changes in the expression of the miRNA processing machinery are linked to the induction and progression of cerebral disease and degeneration (104-111).

The expression pattern in physiological and pathophysiological neurogenic processes and their functional implications have been described for **miR-9** ((112, 215), reviewed by (209, 216), **miR-124** ((113, 215), reviewed by (209, 217)), **let-7** ((114, 215), reviewed by (209, 218)), **miR-137** (reviewed by (219)), **miR-219** ((220), the **miR-17 family** (reviewed by (85)), the **miR-200 family** (reviewed by (85)), **miR-195** (reviewed by (85)), **miR-128** (221, 222), **miR-132** (223), **miR-125b** (reviewed by (12, 92), **miR-134** (reviewed by (12, 224), **miR-184** ((225), reviewed by (12)) and **miR-138** ((92, 226).

As already mentioned in the introduction, the hypothesis of this dissertation, namely that miR-451 influences neuronal differentiation in vitro, originated from findings of our research group (possible role in injury induced neurogenesis (154)) and findings described in the literature (possible role in traumatic brain injury and/or neurodegeneration (130-133), role in erythropoiesis (119-129), tumorigenesis (reviewed by (94)), differentiation of epithelial cells while establishing basolateral polarity (153), in cell growth and survival (138-152) and in self-renewal and multi-potential differentiation capacity of stem cells and cancer stem cells (129, 134-137).

Morphological observation, molecular analysis of markers, CD133, FGFR1, Integrin-ß1 and Vimentin as well as immunofluorescent staining were performed of specific differentiation time points in order to assess differences in neuronal differentiation of miR-451+ and Ct cells and a role for miR-451 during neuronal differentiation in vitro.

Conclusion 1: *A lot of research has been done and is currently been done concerning the elucidation of the role of specific miRNAs in neuronal differentiation and neurogenesis. The role of miR-451 has not been investigated in the context of neuronal differentiation. Findings in the literature speak for involvement of miR-451 in this process.*

4.1.1. Differentiation of used cell lines

There is a significant enrichment of neuronal-like cells during neuronal differentiation of NT2 as well as of Ct and miR-451+ cells, as is proven by morphological examination and marker expression analysis.

It should be taken into account that lentiviral transduction results in a permanent integration of the lentiviral genome as well as the transgene of interest into the host genome (NT2 cells) (227).

The permanent incorporation of the viral genome and the transgenes into the host is rather non-specific and can cause a disruption of a host gene at the site of incorporation or an abnormal expression of nearby host genes driven by the enhancer of the inserted viral DNA (227). This can lead to changes in the genotype and phenotype of the cells (227).

We have therefore primarily analysed the effect of transduction of NT2 cells with the control vector on the potential of NT2 cells to be stimulated into neuronal differentiation.

Induction of neuronal differentiation resulted in patterns of expression profiles of marker genes and time dependent changes of cell morphology that were comparable in untreated and transduced NT2 cells, indicating the transduction of NT2 cells with AB.G.Ct does not interfere with the neuronal differentiation potential of NT2 cells. Due to some differences in the extent of expression regulation of some of the markers (for example DCX) only the AB.G.Ct transduced cells were used as control cells for the analysis of miR-451 modulated neuronal differentiation.

Conclusion 2: *Slight differences in the genotype and phenotype of NT2 and Ct cells might be due to the non-specific integration of the lentiviral control vector DNA caused by the transduction process, but Ct cells are also able to build neurites and neuronal like cells and show similar expression profiles of markers compared to NT2 cells during neuronal differentiation in vitro. This leads to the conclusion, that Ct cells have a similar neuronal differentiation capacity and can be used as control cells for the analysis of miR-miR-451+ induced changes of neuronal differentiation.*

4.1.2. Endogenous miR-451 expression

In erythroid maturation, higher levels of miR-451 are associated with an advanced differentiation status of cells (described by (119, 122-125, 228) and reviewed in (94)). Abundant occurrence of miR-451 has been shown in mature erythrocytes (229). miR-451 was also shown to be elevated during differentiation of epithelial cells (153). But higher levels of miR-451 were reported to have no effect on murine osteoclast differentiation (230) and miR-451 was down-regulated during myogenesis (231). In this dissertation we show that endogenous miR-451 expression is up-regulated significantly at day 27 of neuronal differentiation in vitro assuming miR-451 has a role in neuronal differentiation as previously shown for erythroid differentiation.

Conclusion 3: *The significant increase of miR-451 at day 27 during neuronal differentiation suggests a role of miR-451 during the development of neuronal cells in vitro.*

4.1.3. MiR-451 overexpression accelerates neuronal differentiation

MiR-451 overexpression seems to accelerate differentiation into a neuronal phenotype. MiR-451+ cells show a denser outgrowth of neurites, longer neurites and more cells with neuronal morphology compared to Ct cells. This is shown by immunofluorescent staining (DCX, Tuj1, MAP2, NF and TNS4) and morphological analysis of Ct and miR-451+ cells. By comparison of marker expression between miR-451+ and Ct cells it becomes evident, that at the mRNA level markers (DCX, Tuj1, MAP2, NF and GFAP) are earlier and higher expressed in miR-451+ cells compared to Ct cells. Moreover there are significant differences in Nestin and Sox2 mRNA expression. This leads to the conclusion of more mature and differentiated cells in the miR-451+ condition.

Generally, the role of miR-451 has not been described in neuronal differentiation in the literature. But there is evidence that the endogenous level of miR-451 is elevated during erythroid differentiation in diverse systems (119, 122-125, 228, 232).

Pase and colleagues described in 2009, that miR-451 regulates erythroid maturation in vivo in zebrafish, as overexpression of miR-451 in mutants with miR-451 deficiency and impaired erythropoiesis rescued erythrocyte maturation partially (127). However, overexpression of miR-451 in wildtype zebrafish did not affect erythrocyte maturation or gross embryo morphology (127). In contrast, we describe that overexpression of miR-451 in the neuronal context in vitro enhances differentiation capacity of neuronal precursor cells.
Kouhkan and colleagues showed in 2013 that overexpression of miR-451 induced erythroid differentiation in CD133 positive cells (233) and furthermore concluded in 2014 on the basis of their own results and results from Masaki in 2007 that miR-451 is a lineage-specific miRNA which regulates erythroid differentiation and maturation (123, 234). In both publications it was not specified nor examined, whether overexpression of miR-451 had an accelerating effect on the maturation of erythrocytes. Therefore the results presented in this dissertation show a role for miR-451 in neuronal differentiation in a new context and also suggest that overexpression of miR-451 leads to acceleration of neuronal differentiation in vitro.
It has to be taken into account, that the verification of involvement of a certain molecule in a specific process also includes loss-of-function studies. Within this scope of this dissertation it was initially planned to perform inhibition of miR-451 by lentiviral transduction of inhibitory sequences. Preliminary results, which are not shown in this dissertation, indicate a deceleration of neuronal differentiation capacity by inhibition of miR-451 during neuronal differentiation of transduced NT2 cells. Unfortunately we had methodological problems while verifying the down-regulation of miR-451 by northern blot in transduced cells.

At day 27, we find a significant higher expression of DCX in miR-451+ cells compared to control cells. DCX is a marker for immature neuroblasts and is also expressed early post-mitotic neurons ((6), chapter 6, page 193). The general number of DCX higher expressing cells could be simply higher in miR-451+ cells, which also means, that there is a higher number of early neuronal cells available, whereas in the control condition are less immature neuronal cells, more neuronal precursor cells at a more immature differentiation status and less undifferentiated cells available at day 27 (higher Sox2 down-regulation).

The control condition (Ct cells) seems in fact to have more neuronal precursors at a more immature differentiation state (higher Nestin expression) and less undifferentiated cells (higher Sox2 down-regulation) but also some more mature neurons (less DCX expression). This could imply that in miR-451+ cells neuronal differentiation is accelerated as shown by marker expression, immunohistochemistry and morphological observations, but terminates at a certain time point. This assumption is speculative, because for the exact determination of the differentiation status of the cells it is necessary to perform double immunofluorescent staining with diverse neuronal markers and especially with late neuronal markers, as for example NeuN, Calretinin and Calbindin ((6), chapter 6, page 193). Furthermore DCX is expressed in broad range during neuronal differentiation and is therefore not a sensitive marker for exact evaluation of the differentiation status of differentiating cells ((6), chapter 7, page 229).

Conclusion 4: *There is a striking difference in the maturation status in miR-451+ and Ct cells. The results presented in this dissertation lead to the conclusion, that there is an accelerated differentiation of cells overexpressing miR-451. In order to investigate the exact differentiation status of the cells it is necessary to perform a double staining with different (late) neuronal markers.*

Tensins are scaffolding proteins, which regulate cell motility and growth (235). TNS4, also called CTEN, promotes cell migration by triggering the uncoupling of integrins from the actin cytoskeleton (236-238). Therefore we selected TSN4 for morphological analysis. There is an obvious difference in morphology in TSN4 positive miR-451+ and Ct cells. miR-451+ cells are often smaller than the control cells. Furthermore they show more pronounced neurite outgrowth and a denser spine quantity. TNS4 was found to be a predicted target gene of miR-451 in mouse (200)[18]. We wanted to confirm this by screening other databases for target gene prediction, but we could not find TNS4 as predicted target for mouse or humans in any of the other databases.

[18] 200. Krek A, Grun D, Poy MN, Wolf R, Rosenberg L, Epstein EJ, et al. Combinatorial microRNA target predictions. Nat Genet. 2005;37(5):495-500.
http://bioinformatics.sdstate.edu/gskb/get?label=MIRNA_MM_KREK_MMU-MIR-451

As we saw prominent morphological differences between miR-451+ and Ct cells, we included this gene in our target gene expression analysis, although we are aware of the fact, that TNS4 might not even be a predicted target gene in mouse, not to mention in humans.

There is a significant difference in expression of Integrin-ß1 (CD29, ITGB1, first described by Hynes in 1987 (165)) and Vimentin (VIM, reviewed by Chung and colleagues (239)) in neuronal differentiation of Ct and miR-451+ cells. Both vimentin and integrin-ß1 expression changes have been shown to influence the morphology of cells tremendously (240), which is why we chose these two genes for analysis in our set-up. There was no evidence found in the literature and in miRNA target gene search databases, that ITGB1 is a predicted or validated target gene of miR-451. But Tsuchiya and colleagues showed that during epithelial differentiation cells establish basolateral polarity, which is mediated by translocation of Integrin-ß1 (153) and was linked to elevated miR-451 and miR-338-3p levels. Gain of function studies by transfection of synthetic miR-338-3p and miR-451 promoted epithelial differentiation, although the introduction of individual synthetic microRNAs exhibited no effect (153). Therefore, the altered Integrin-ß1 gene expression in miR-451+ cells compared to Ct cells is mediated most likely via secondary effects of miR-451 overexpression.
Likewise, there was no evidence that Vimentin might be a target for miR-451 in target gene databases. Zeng and colleagues reported in 2014 significant up-regulation of vimentin expression after inhibition of miR-451 leading together with the up-regulation or down-regulation of other genes to inhibition of trans-differentiation and therefore invasion in bladder cancer (241). But gain of function with miR-451 mimics did not result in down-regulation of vimentin expression. Therefore differences in Vimentin expression in miR-451 overexpressing cells are most likely due to secondary effects of miR-451 overexpression.

Conclusion 5: *Differences in Integrin-ß1 and Vimentin expression between miR-451+ cells and Ct cells are most likely due to secondary effects of miR-451 overexpression and are linked to morphological differences seen between miR-451+ and Ct cells.*

Furthermore we assessed the expression profiles of CD133, FGFR1 in neuronal differentiation Ct and miR-451+ cells. Patz and colleagues showed a miR-451 specific down-regulation of CD133 and FGFR1 after microparticles isolated from patients with TBI which are enriched in miR-451 and are being taken up by undifferentiated NT2 cells (154)

The up-regulation of CD133 and FGFR1 in undifferentiated miR-451+ cells compared to Ct cells and the down-regulation of CD133 and FGFR1 in miR-451+ cells are indicative for a possible direct/indirect regulation mechanism of miR-451 on the expression of these two genes. Furthermore, as CD133 is a known marker for (cancer) stem cells (reviewed by (242)), the down-regulation of CD133 in the course of differentiation could possibly mean that there is a loss of the stem cell properties.

Conclusion 6: *Differences in CD133 and FGFR1 expression between miR-451+ cells and Ct cells are most likely due to secondary effects of miR-451 overexpression, although there is evidence that miR-451 directly influences CD133 and FGFR1 expression.*

4.1.4. Identification of key target genes of miR-451 during early neuronal differentiation

Literature and target gene database search was done in order to identify target genes. 17 target genes were selected because of their validated status and/or because of previous validation reports in the literature. Some target genes were chosen because of their function in neuronal differentiation context. We found significant differences between Ct and miR-451+ cells in mRNA expression in some of the target genes (AKT1, CAB39, MIF, MYC, RAB14, TSC1 and YHWAZ). Some of these examined target genes will be discussed concerning their role in neuronal differentiation in vitro or neurodevelopment in general.

AKT1 was listed as a validated target gene of miR-451 in tarbase (180, 181) and mirtarbase (182). Literature search revealed that AKT1 was shown to be down-regulated on the protein level after miR-451 overexpression or transfection with miR-451 mimics in various systems, but was not verified as a target gene by luciferase assay (183-186). In this dissertation we could verify AKT1 downregulation by qRT-PCR by overexpression of miR-451. AKT1 is present in nearly all tissues and has functions in cell growth and survival (243-245). AKT1 was shown to be involved in the differentiation to auditory hair cells in mice (246) and in exercise induced adult neurogenesis (247). Validation of AKT1 on the protein level is currently in progress.

Preliminary data suggests that MIF and CAB39 protein expression is down-regulation after miR-451 overexpression at specific time points of neuronal differentiation.

MIF (macrophage migration inhibitory factor) was validated as one of the first target genes for miR-451 in the literature (138, 195, 196). Graham and colleagues showed that MIF expression is inversely related to miR-451 expression in endometriotic tissue and they also confirmed MIF as a target gene of miR-451 by luciferase assay (196). There are many publications which relate MIF to the neuronal context, but only a few reports link MIF to neuronal development or neurogenesis. Arno and colleagues reported for example, that apoptosis in the murine developing forebrain initiates microglial proliferation, which is mediated by release of MIF (248). Conboy and colleagues reported that MIF is linked to antidepressant-induced hippocampal neurogenesis (249).

Ohta and colleagues showed in 2012 that MIF induces proliferation and regulates self-renewal of neural stem/progenitor cells (250). In fact, we see decreased proliferation and altered migration behaviour in undifferentiated miR-451+ cells when performing scratch assays. There might be a functional connection of MIF and miR-451, as we see a down-regulation of MIF at day 0, 8 and 17 in neuronal differentiation of miR-451 overexpressing cells. But this needs further investigation and confirmation via luciferase assays.

CAB39 was shown to be down-regulated by miR-451 in osteogenesis of mesenchymal stem cells (251). CAB39 has been shown to be a target of miR-451 in other studies as well, mostly in the context of cancer (141, 187-191). To our best knowledge, there are no reports available for **CAB39** in the context of neuronal differentiation.

Conclusion 7: *We show down-regulation of putative miR-451 targets AKT1, CAB39, RAB14, TSC1 and YWHAZ on the mRNA level miR-451 overexpressing cells in the context of neuronal differentiation. CAB39 and MIF are down-regulated on the protein level during neuronal differentiation of miR-451+ cells. MIF down-regulation could lead to reduced proliferation and regulation of self-renewal during neuronal differentiation. This suggestion remains speculative, as the direct connection of miR-451 and MIF in neuronal differentiation needs more evidence via luciferase assays and loss of function studies. A role for miR-451 in neuronal differentiation via targeting CAB39 would be novel in the context of neuronal differentiation.*

As we see a rise of miR-451 expression during later stages of neuronal differentiation in vitro we assume to observe a down-regulation of target gene expression in the course of differentiation of NT2. We could only see such an approximate pattern in TNS4, TSC1, VAPA and MYC.

Mechanisms of miRNA mediated post-transcriptional regulation of gene expression comprise 4 principal mechanisms (252). Binding of miRNA-RISC complex to a target mRNA can lead to inhibition of translation and therefore accumulation of the target mRNA (A). Furthermore, when the target mRNA and miRNA binding is perfectly complementary, degradation of the respective target mRNA can be initiated. This process called slicing is rather untypical in animals, but is common in plants (253), (B). A much more frequent mechanism in animals is the destabilisation and subsequent degradation of the target mRNA by binding of the miRNA-RISC complex and subsequent deadenylation and decapping (C). Furthermore upon miRNA-RSC binding target mRNAs can be transported in relatively large vesicles, so called P-bodies, where they are stored for later usage (D) (252, 254).

Because of the different existing post-transcriptional mechanisms mediated by mature miRNAs, as the mechanism by which miR-451 mediates its function is unknown and as the expression pattern of one target gene during neuronal differentiation of NT2 is not only influenced by the increase of miR-451 it might be explainable, why the expression patterns of most of the predicted and validated target genes seem to be not in negative accordance with internal miR-451 expression.

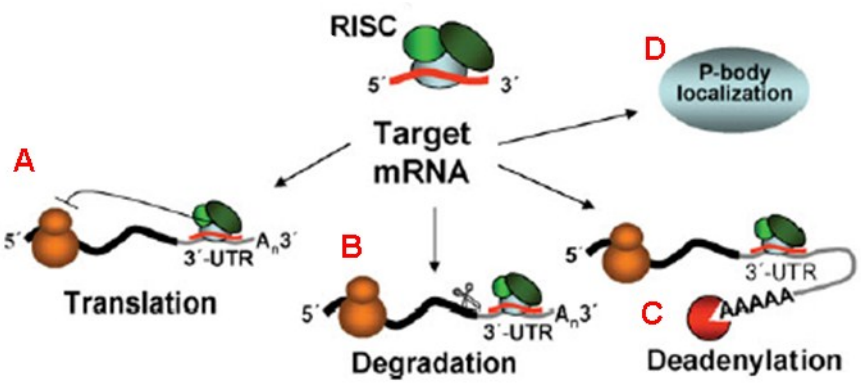

Figure 43[19]

There are 4 possible mechanisms of miRNA mediated post-transcriptional regulation of gene expression: (A) Inhibition of translation and concentration of the target mRNA, (B) Initiation of degradation of the target mRNA (slicing), (C) Deadenylation of the target mRNA, which leads to the degradation of the target mRNA in the end, (D) Initiation of storage in P-bodies for later use

Conclusion 8: *As miRNAs function at the post-transcriptional level (85) the functional detection of an miR-451 mediated down-regulation of a target gene is shown by analysis of the protein expression (western blot) and by subsequent proof of the miR-451 specific down-regulation by performing luciferase assays. As miRNAs also mediate the degradation of their target gene mRNAs directly or indirectly, it might be valid to use qRT-PCR to show down-regulation of the respective mRNA. But as mentioned above, miRNAs function post-transcriptionally and the down-regulation on the mRNA level might be associated with other processes as well and not be due to interaction with miRNAs.*

[19] 252. Fazi F, Nervi C. MicroRNA: basic mechanisms and transcriptional regulatory networks for cell fate determination. Cardiovasc Res. 2008;79(4):553-61.

After confirmation of the target gene-miRNA interaction by luciferase assay, it is important to knock down the respective miRNA and for the up-regulation of the respective target. But in most cases miRNA regulation of neuronal differentiation is a multifactorial process, which does not lead back to one specific target or miRNA, but is regulated by a network of proteins and miRNAs, which influence each other. Therefore miR-451 mediated processes can have minor effects on the protein expression of one specific protein, but major effects on the phenotype. This might be the reason, why we saw only minor effects in western blots. Moreover the validation of target genes of miR-451 seems to be context depending.

4.2. Conclusion

We see an accelerated differentiation, enhanced neurite outgrowth, elongated neurites and therefore more mature neuronal cells at an earlier time point in miR-miR-451+ cells compared to the control by various methods including molecular marker expression and immunofluorescent staining. We propose that the overexpression of miR-451 leads to accelerated differentiation and faster development of a neuronal phenotype, which is also detectable at the molecular level. This leads us to the conclusion, that miR-451 might be associated with the process of neuronal differentiation.

4.3. Methodological discussion

This dissertation comprises the establishment of many methods, as for example the set-up of transformation, transfection, transduction, neuronal differentiation in vitro and of a normalisation method for performing qRT-PCR. By discussing the results of this partly very time consuming processes novel aspects of the used methodologies will be highlighted.

4.3.1. Transformation

Because of the relatively large size of our vectors (approximately 10kbp) it is likely that the transformation efficiency was lower compared to transformation efficiency of the relatively small (approximately 2700bp) pUC19 control plasmid (255). The usage of commercially available competent cells, which were specifically created for the transformation of lentiviral constructs, yielded in the highest number of transformed colonies.

4.3.2. Transfection, lentiviral titer measurement and transduction

First, we used a calcium phosphate based transfection method with HEK293T cells, which already expressed viral structure proteins. Although a lot of time was spent to implement this method successfully, this process did not lead to fluorescent and viral particle producing HEK293T cells. Then, we switched to a transfection method based on the usage of Lentifectin and a 3rd generation packaging mix, which worked on the very 1st trial.

The viral titer of the collected supernatant was measured with an rapid, ELISA based method. The wells of a 96-well plate are coated with an anti-HIV-1 p24 capture antibody, which quantitatively binds the HIV-1 p24, an abundant HIV-1 virus core/capsid protein (source: user manual of the Lenti-X p24 Rapid Titer Kit). Specifically bound p24 is detected in a “sandwich” ELISA format using a biotinylated anti-p24 secondary antibody, a streptavidin-Horse radish peroxidase (HRP) conjugate and colour producing substrate. The determination of the lentiviral titer led to problems, as we could not generate a corresponding standard curve described in the user manual. One reason for the higher values measured at 0pg/ml could be that we would have needed to subtract the blank (absorbance of cell medium alone) from our values. But this was not mentioned in the user manual. The measured viral titers can hence be seen only as approximate values.

4.3.3. Neuronal differentiation of NT2 cells

As already described in the introduction, the process of (adult) neurogenesis can be modelled in vitro by retinoic acid induced neuronal differentiation of the human teratocarcinoma cell line Ntera-2 cl.D1 (NT2 cells) (11, 256). Previously differentiation of NT2 into post-mitotic neurons into took a time span of about 8 weeks (11, 74), but was shortened to up to 4 weeks by introducing a cell aggregation method (257). In this dissertation, neuronal differentiation of NT2 cells was established by performing 3 different protocols with NT2 cells. Protocol 3 (based on Paquet-Durand (158)) yielded a satisfying number of neurite building cells and is described in the results section. In this study it is shown, that the implemented protocol of neuronal differentiation of NT2 cells is leading to neurite building cells in an approximately time period of 3 weeks. Selective trypsination for purifying neuronal cells was performed, but in the course of this study it was decided to stop the differentiation protocol at day 28, because differences between miR-451 overexpressing cells and Ct cells were depicted relatively early during neuronal differentiation in vitro.

4.3.4. SYBR green based PCR

LNA modified primers for the detection of miR-451 were used in the end, as we encountered methodological difficulties when using non LNA modified primers (detection of unspecific extra products). LNA modifications of the used primers were very effective in increasing the duplex stability and affinity for complementary targets, as was described previously in the literature (258-260).

It has to be taken into account, that SYBR green based qRT-PCR, as it was used in our study, has limitations regarding detection of specific amplified products. (261). SYBR green, which has been used in qPCR since the mid-1990s (262, 263), is fluorescent dye binds double stranded DNA with high affinity but low specificity (261). A fluorophore-based primer-based technique (as for example TaqMan^{TM} assays) has several advantages compared to SYBR green based PCR. For example, probe and primer set offer maximal specificity and the reproducibility and sensitivity is higher.

Furthermore it is important to note that the used detection platform and selected pre-amplification workflows affect the relative levels of the detected miRNAs (261).

4.3.5. Normalisation method

The search for a valid data normalisation method is the first and major step when establishing a detection method of expression levels by qRT-PCR (261). There is no universally accepted control/normalisation method/house-keeping gene available, because this depends on the study question and study object, but there are various normalisation strategies (238). A common strategy is to use a stably expressed transcript as a normalisation gene, which we performed in our study. Another popular method for the normalisation of miRNA expression data is “global normalisation”, as it was described by Mestdagh in 2009 (264). As this method not recommended when analysing a limited set of miRNAs, we did not perform this method for normalisation. The usage of spike in for data normalisation is currently not commonly used, but is already described in the literature (160, 265).

4.3.5.1. miRNA analyses

We examined the suitability of various normalisation genes in miRNA analysis of transduced and non-transduced undifferentiated and differentiated cells.

GeNorm is an algorithm that selects an optimal pair of reference genes out of a larger set of candidate genes (266). It calculates and compares the so called M-value of all candidate genes, eliminates the gene with the highest M-value, and repeats the process until there is only two genes left (266). NormFinder is an algorithm that attempts to find the optimum reference genes out of a group of candidate genes (267). It also takes, in contrast to geNorm, information of groupings of samples into account. The result is an optimum (pair of) reference gene(s). The different examined normalisation genes partly showed a high variation in Ct-values in transduced and non-transduced cells, hence being unsuitable for normalisation usage in this context. SNORD38b and SNORD49A were found to be the best combination of normalisation genes in geNorm and NormFinder.

U6 is a widely used normalisation gene in studies of miRNA expression (268-272), but is, as described by Lim (273), not a valid normalizing gene for miRNA expression analysis in various models of neuronal in-vitro differentiation. In our study there seems to be no significant difference in Ct-values of U6 in neuronal in-vitro differentiation of NT2 cells, but there is, as mentioned above, a clear trend of rising Ct-values with increasing developmental time.

Furthermore there is a high standard deviation especially at day 0, 17 and 27 of the Ct-values in U6, meaning there is a high variation in the values at the different differentiation days.
Although the algorithm had chosen SNORD38b and SNORD49A as the best normalisation combination, although we found no significant difference in U6 expression during neuronal differentiation, because we detected high standard deviations in the Ct-values of U6 at the different differentiation days and because we found a relatively high difference in the mean Ct-values (sometimes more than 1 cycle), we decided to use Spike-ins as normalisers (160).
Although the standard deviation of the Ct-values of the Spike-in was quite low and we had excluded obvious outliers (if there was no given Ct-value at all for a sample, as this was a pipetting mistake at high chance) the spike-in was among the higher ranked and therefore more variable genes in GeNorm and NormFinder analysis. This cannot easily be explained and gave us reason to doubt the correctness of the results generated with those algorithms.

4.3.5.2. mRNA analyses

We searched for an optimal normalisation gene or an optimal set of normalisation genes respectively for normalisation by performing q-RT-PCR from RNA samples from transduced and non-transduced undifferentiated and differentiated NT2. YHWAZ and UBC were found to be the best combination of genes when comparing transduced and non-transduced undifferentiated NT2 cells. But YHWAZ was found to be a target gene of miR-451 (274), which is why we did not use this gene as normalisation gene. We analysed a selection of 4 potential normalisation genes in differentiated transduced and non-transduced NT2.
We found a relatively high variability of Ct-values in the different analysed genes. When looking at the data more intensively, we detected significant differences in Ct-values of Ct cells (Ct) and non-transduced differentiated cells and between Ct-values of non-transduced cells (NT2) and miR-451+ cells. Therefore we decided to use mRNA Spike-in for data normalisation (160, 265).

5. Bibliography

1. Altman J. Are new neurons formed in the brains of adult mammals? Science. 1962;135(3509):1127-8.
2. Altman J. Autoradiographic investigation of cell proliferation in the brains of rats and cats. Anat Rec. 1963;145:573-91.
3. Altman J, Das GD. Autoradiographic and histological evidence of postnatal hippocampal neurogenesis in rats. J Comp Neurol. 1965;124(3):319-35.
4. Altman J, Das GD. Post-natal origin of microneurones in the rat brain. Nature. 1965;207(5000):953-6.
5. Urban N, Guillemot F. Neurogenesis in the embryonic and adult brain: same regulators, different roles. Front Cell Neurosci. 2014;8:396.
6. Kempermann G. Adult neurogenesis 2. New York: Oxford University Press; 2011. 601 p.
7. Eriksson PS, Perfilieva E, Bjork-Eriksson T, Alborn AM, Nordborg C, Peterson DA, et al. Neurogenesis in the adult human hippocampus. Nat Med. 1998;4(11):1313-7.
8. Deng W, Aimone JB, Gage FH. New neurons and new memories: how does adult hippocampal neurogenesis affect learning and memory? Nat Rev Neurosci. 2010;11(5):339-50.
9. Vishwakarma SK, Bardia A, Tiwari SK, Paspala SA, Khan AA. Current concept in neural regeneration research: NSCs isolation, characterization and transplantation in various neurodegenerative diseases and stroke: A review. Journal of advanced research. 2014;5(3):277-94.
10. Kempermann G, Kuhn HG, Gage FH. Genetic influence on neurogenesis in the dentate gyrus of adult mice. Proc Natl Acad Sci U S A. 1997;94(19):10409-14.
11. Andrews PW. Retinoic acid induces neuronal differentiation of a cloned human embryonal carcinoma cell line in vitro. Dev Biol. 1984;103(2):285-93.
12. Stappert L, Roese-Koerner B, Brustle O. The role of microRNAs in human neural stem cells, neuronal differentiation and subtype specification. Cell Tissue Res. 2015;359(1):47-64.
13. Database resources of the National Center for Biotechnology Information. Nucleic Acids Res. 2015;43(Database issue):D6-17.

14. Kandel ER, Schwartz JH, Jessell TM. Principles of neural science. New York: McGraw-Hill, Health Professions Division; 2000.
15. Alberts B, Bray D, Lewis L, Raff M, Roberts K, Watson JD. Molecular biology of the cell. New York: Garland Publishing, New York and London; 1994. 1361 p.
16. Braun SM, Jessberger S. Adult neurogenesis: mechanisms and functional significance. Development. 2014;141(10):1983-6.
17. Potten CS, Loeffler M. Stem cells: attributes, cycles, spirals, pitfalls and uncertainties. Lessons for and from the crypt. Development. 1990;110(4):1001-20.
18. Weiss S, Reynolds BA, Vescovi AL, Morshead C, Craig CG, van der Kooy D. Is there a neural stem cell in the mammalian forebrain? Trends Neurosci. 1996;19(9):387-93.
19. Kuhn HG, Dickinson-Anson H, Gage FH. Neurogenesis in the dentate gyrus of the adult rat: age-related decrease of neuronal progenitor proliferation. J Neurosci. 1996;16(6):2027-33.
20. Lois C, Alvarez-Buylla A. Long-distance neuronal migration in the adult mammalian brain. Science. 1994;264(5162):1145-8.
21. Kokoeva MV, Yin H, Flier JS. Neurogenesis in the hypothalamus of adult mice: potential role in energy balance. Science. 2005;310(5748):679-83.
22. Lee DA, Bedont JL, Pak T, Wang H, Song J, Miranda-Angulo A, et al. Tanycytes of the hypothalamic median eminence form a diet-responsive neurogenic niche. Nat Neurosci. 2012;15(5):700-2.
23. Gould E, Reeves AJ, Graziano MS, Gross CG. Neurogenesis in the neocortex of adult primates. Science. 1999;286(5439):548-52.
24. Bhardwaj RD, Curtis MA, Spalding KL, Buchholz BA, Fink D, Bjork-Eriksson T, et al. Neocortical neurogenesis in humans is restricted to development. Proc Natl Acad Sci U S A. 2006;103(33):12564-8.
25. Zhao C, Deng W, Gage FH. Mechanisms and functional implications of adult neurogenesis. Cell. 2008;132(4):645-60.
26. Carleton A, Petreanu LT, Lansford R, Alvarez-Buylla A, Lledo PM. Becoming a new neuron in the adult olfactory bulb. Nat Neurosci. 2003;6(5):507-18.

27. Kempermann G, Jessberger S, Steiner B, Kronenberg G. Milestones of neuronal development in the adult hippocampus. Trends Neurosci. 2004;27(8):447-52.
28. Sanai N, Tramontin AD, Quinones-Hinojosa A, Barbaro NM, Gupta N, Kunwar S, et al. Unique astrocyte ribbon in adult human brain contains neural stem cells but lacks chain migration. Nature. 2004;427(6976):740-4.
29. Curtis MA, Kam M, Nannmark U, Anderson MF, Axell MZ, Wikkelso C, et al. Human neuroblasts migrate to the olfactory bulb via a lateral ventricular extension. Science. 2007;315(5816):1243-9.
30. Spalding KL, Bergmann O, Alkass K, Bernard S, Salehpour M, Huttner HB, et al. Dynamics of hippocampal neurogenesis in adult humans. Cell. 2013;153(6):1219-27.
31. Ernst A, Alkass K, Bernard S, Salehpour M, Perl S, Tisdale J, et al. Neurogenesis in the striatum of the adult human brain. Cell. 2014;156(5):1072-83.
32. Gage FH. Mammalian neural stem cells. Science. 2000;287(5457):1433-8.
33. Merkle FT, Alvarez-Buylla A. Neural stem cells in mammalian development. Curr Opin Cell Biol. 2006;18(6):704-9.
34. Zhao C, Teng EM, Summers RG, Jr., Ming GL, Gage FH. Distinct morphological stages of dentate granule neuron maturation in the adult mouse hippocampus. J Neurosci. 2006;26(1):3-11.
35. Toni N, Laplagne DA, Zhao C, Lombardi G, Ribak CE, Gage FH, et al. Neurons born in the adult dentate gyrus form functional synapses with target cells. Nat Neurosci. 2008;11(8):901-7.
36. Ho NF, Hooker JM, Sahay A, Holt DJ, Roffman JL. In vivo imaging of adult human hippocampal neurogenesis: progress, pitfalls and promise. Mol Psychiatry. 2013;18(4):404-16.
37. Bracko O, Singer T, Aigner S, Knobloch M, Winner B, Ray J, et al. Gene expression profiling of neural stem cells and their neuronal progeny reveals IGF2 as a regulator of adult hippocampal neurogenesis. J Neurosci. 2012;32(10):3376-87.
38. Lendahl U, Zimmerman LB, McKay RD. CNS stem cells express a new class of intermediate filament protein. Cell. 1990;60(4):585-95.

39. Lothian C, Lendahl, U. An evolutionarily conserved region in the second intron of the human nestin gene directs gene expression to CNS progenitor cells and to early neural crest cells. Eur J Neurosci 1997;9(3):452-62.
40. Michalczyk K, Ziman, M. Nestin structure and predicted function in cellular cytoskeletal organisation. Histol Histopathol. 2005;20(2):665-71.
41. Shin S, Mitalipova, M., Noggle, S., Tibbitts, D., Venable, A., Rao, R., Stice, S.L. Long-term proliferation of human embryonic stem cell-derived neuroepithelial cells using defined adherent culture conditions. Stem Cells 2006;24(1):125-38.
42. Adachi K, Suemori H, Yasuda SY, Nakatsuji N, Kawase E. Role of SOX2 in maintaining pluripotency of human embryonic stem cells. Genes to cells : devoted to molecular & cellular mechanisms. 2010;15(5):455-70.
43. Cai J, Wu, Y., Mirua, T., Pierce, J.L., Lucero, M.T., Albertine, K.H., Spangrude, G.J., Rao, M.S. Properties of a fetal multipotent neural stem cell (NEP cell). Dev Biol. 2002;251(2):221-40.
44. Ellis P, Fagan BM, Magness ST, Hutton S, Taranova O, Hayashi S, et al. SOX2, a persistent marker for multipotential neural stem cells derived from embryonic stem cells, the embryo or the adult. Dev Neurosci. 2004;26(2-4):148-65.
45. Komitova M, Eriksson, P.S. Sox-2 is expressed by neural progenitors and astroglia in the adult rat brain. Neurosci Lett. 2004;369(1):24-7.
46. Zappone MV, Galli R, Catena R, Meani N, De Biasi S, Mattei E, et al. Sox2 regulatory sequences direct expression of a (beta)-geo transgene to telencephalic neural stem cells and precursors of the mouse embryo, revealing regionalization of gene expression in CNS stem cells. Development. 2000;127(11):2367-82.
47. Doetsch F, Caille I, Lim DA, Garcia-Verdugo JM, Alvarez-Buylla A. Subventricular zone astrocytes are neural stem cells in the adult mammalian brain. Cell. 1999;97(6):703-16.
48. Seri B, Garcia-Verdugo JM, McEwen BS, Alvarez-Buylla A. Astrocytes give rise to new neurons in the adult mammalian hippocampus. J Neurosci. 2001;21(18):7153-60.
49. des Portes V, Pinard, J.M., Billuart, P., Vinet, M.C., Koulakoff, A., Carrié, A., Gelot, A., Dupuis, E., Motte, J., Berwald-Netter, Y., Catala, M., Kahn, A., Beldjord, C., Chelly, J. A novel CNS gene required for neuronal migration and involved in X-

linked subcortical laminar heterotopia and lissencephaly syndrome. Cell. 1998;92(1):51-61.

50. Gleeson JG, Lin, P.T., Flanagan, L.A., Walsh, C.A. Doublecortin is a microtubule-associated protein and is expressed widely by migrating neurons. Neuron. 1999;23(2):257-71.

51. Gleeson JG, Allen, K.M., Fox, J.W., Lamperti, E.D., Berkovic, S., Scheffer, I., Cooper, E.C., Dobyns, W.B., Minnerath, S.R., Ross, M.E., Walsh, C.A. Doublecortin, a brain-specific gene mutated in human X-linked lissencephaly and double cortex syndrome, encodes a putative signaling protein. Cell. 1998;92(1):63-72.

52. Francis F, Koulakoff, A., Boucher, D., Chafey, P., Schaar, B., Vinet, M.C., Friocourt, G., McDonnell, N., Reiner, O., Kahn, A., McConnell, S.K., Berwald-Netter, Y., Denoulet, P., Chelly, J. Doublecortin is a developmentally regulated, microtubule-associated protein expressed in migrating and differentiating neurons. Neuron 1999;23(2):247-56.

53. Couillard-Despres S, Winner B, Schaubeck S, Aigner R, Vroemen M, Weidner N, et al. Doublecortin expression levels in adult brain reflect neurogenesis. Eur J Neurosci. 2005;21(1):1-14.

54. Doetsch F, García-Verdugo, J.M., Alvarez-Buylla, A. Cellular composition and three-dimensional organization of the subventricular germinal zone in the adult mammalian brain. J Neurosci. 1997;17(13):5046-61.

55. Gould E, Vail, N., Wagers, M.,, Gross, C.G. Adult-generated hippocampal and neocortical neurons in macaques have a transient existence. Proc Natl Acad Sci U S A 2001;98(19):10910-7.

56. Parent JM, Yu TW, Leibowitz RT, Geschwind DH, Sloviter RS, Lowenstein DH. Dentate granule cell neurogenesis is increased by seizures and contributes to aberrant network reorganization in the adult rat hippocampus. J Neurosci. 1997;17(10):3727-38.

57. Riederer BM, Draberova. E., Viklicky, V., Draber, P. Changes of MAP2 phosphorylation during brain development. J Histochem Cytochem. 1995;43(12):1269-84.

58. Sarnat HB. Clinical neuropathology practice guide 5-2013: markers of neuronal maturation. Clin Neuropathol. 2013;32(5):340-69.

59. Eyer J, Peterson A. Neurofilament-deficient axons and perikaryal aggregates in viable transgenic mice expressing a neurofilament-beta-galactosidase fusion protein. Neuron. 1994;12(2):389-405.
60. Takahashi N, Ishizuka, B. The involvement of neurofilament heavy chain phosphorylation in the maturation and degeneration of rat oocytes. Endocrinology. 2012;153(4):1990-8.
61. Bongso A, Fong CY, Ng SC, Ratnam S. Isolation and culture of inner cell mass cells from human blastocysts. Hum Reprod. 1994;9(11):2110-7.
62. Andrews PW. From teratocarcinomas to embryonic stem cells. Philosophical transactions of the Royal Society of London Series B, Biological sciences. 2002;357(1420):405-17.
63. Serra M, Leite SB, Brito C, Costa J, Carrondo MJ, Alves PM. Novel culture strategy for human stem cell proliferation and neuronal differentiation. J Neurosci Res. 2007;85(16):3557-66.
64. Coyle DE, Li J, Baccei M. Regional differentiation of retinoic acid-induced human pluripotent embryonic carcinoma stem cell neurons. PLoS One. 2011;6(1):e16174.
65. Damjanov I. The road from teratocarcinoma to human embryonic stem cells. Stem Cell Rev. 2005;1(3):273-6.
66. Pierce GB. Teratocarcinoma: model for a developmental concept of cancer. Current topics in developmental biology. 1967;2:223-46.
67. Stevens LC. The biology of teratomas. Advances in morphogenesis. 1967;6:1-31.
68. Josephson R, Ording CJ, Liu Y, Shin S, Lakshmipathy U, Toumadje A, et al. Qualification of embryonal carcinoma 2102Ep as a reference for human embryonic stem cell research. Stem Cells. 2007;25(2):437-46.
69. Guillemain I, Alonso G, Patey G, Privat A, Chaudieu I. Human NT2 neurons express a large variety of neurotransmission phenotypes in vitro. J Comp Neurol. 2000;422(3):380-95.
70. Sperger JM, Chen X, Draper JS, Antosiewicz JE, Chon CH, Jones SB, et al. Gene expression patterns in human embryonic stem cells and human pluripotent germ cell tumors. Proc Natl Acad Sci U S A. 2003;100(23):13350-5.

71. Henderson JK, Draper JS, Baillie HS, Fishel S, Thomson JA, Moore H, et al. Preimplantation human embryos and embryonic stem cells show comparable expression of stage-specific embryonic antigens. Stem Cells. 2002;20(4):329-37.
72. Pal R, Ravindran G. Assessment of pluripotency and multilineage differentiation potential of NTERA-2 cells as a model for studying human embryonic stem cells. Cell Prolif. 2006;39(6):585-98.
73. Andrews PW, Matin MM, Bahrami AR, Damjanov I, Gokhale P, Draper JS. Embryonic stem (ES) cells and embryonal carcinoma (EC) cells: opposite sides of the same coin. Biochem Soc Trans. 2005;33(Pt 6):1526-30.
74. Pleasure SJ, Page C, Lee VM. Pure, postmitotic, polarized human neurons derived from NTera 2 cells provide a system for expressing exogenous proteins in terminally differentiated neurons. J Neurosci. 1992;12(5):1802-15.
75. Lee VM, Andrews, P.W. Differentiation of NTERA-2 clonal human embryonal carcinoma cells into neurons involves the induction of all three neurofilament proteins. J Neurosci 1986;6(2):514-21.
76. Pleasure SJ, Lee VM. NTera 2 cells: a human cell line which displays characteristics expected of a human committed neuronal progenitor cell. J Neurosci Res. 1993;35(6):585-602.
77. Rossant J, Zirngibl R, Cado D, Shago M, Giguere V. Expression of a retinoic acid response element-hsplacZ transgene defines specific domains of transcriptional activity during mouse embryogenesis. Genes Dev. 1991;5(8):1333-44.
78. Wagner M, Han B, Jessell TM. Regional differences in retinoid release from embryonic neural tissue detected by an in vitro reporter assay. Development. 1992;116(1):55-66.
79. Horton C, Maden M. Endogenous distribution of retinoids during normal development and teratogenesis in the mouse embryo. Dev Dyn. 1995;202(3):312-23.
80. Lee RC, Feinbaum RL, Ambros V. The C. elegans heterochronic gene lin-4 encodes small RNAs with antisense complementarity to lin-14. Cell. 1993;75(5):843-54.
81. Bhalala OG, Srikanth, M., Kessler, J.A. The emerging roles of microRNAs in CNS injuries. Nat Rev Neurol. 2013 9(6):328-39.

82. Carthew RWS, E.J. Origins and Mechanisms of miRNAs and siRNAs. Cell. 2009;136(4):642-55.
83. Bartel DP. MicroRNAs: genomics, biogenesis, mechanism, and function. Cell 2004;116(2):281-97.
84. Ambros V. The functions of animal microRNAs. Nature. 2004;431:350-5.
85. Sun E, Shi Y. MicroRNAs: Small molecules with big roles in neurodevelopment and diseases. Exp Neurol. 2015;268:46-53.
86. Kozomara A, Griffiths-Jones S. miRBase: annotating high confidence microRNAs using deep sequencing data. Nucleic Acids Research. 2014;42(D1):D68-D73.
87. Kozomara A, Griffiths-Jones S. miRBase: integrating microRNA annotation and deep-sequencing data. Nucleic Acids Research. 2011;39(suppl 1):D152-D7.
88. Griffiths-Jones S, Saini HK, van Dongen S, Enright AJ. miRBase: tools for microRNA genomics. Nucleic Acids Research. 2008;36(suppl 1):D154-D8.
89. Griffiths-Jones S, Grocock RJ, van Dongen S, Bateman A, Enright AJ. miRBase: microRNA sequences, targets and gene nomenclature. Nucleic Acids Research. 2006;34(suppl 1):D140-D4.
90. Griffiths-Jones S. The microRNA registry. Nucleic Acids Res. 2004;32:D109-11.
91. Shao NY, Hu HY, Yan Z, Xu Y, Hu H, Menzel C, et al. Comprehensive survey of human brain microRNA by deep sequencing. BMC Genomics. 2010;11:409.
92. Saba R, Schratt GM. MicroRNAs in neuronal development, function and dysfunction. Brain Res. 2010;1338:3-13.
93. Ross JS, Carlson JA, Brock G. miRNA: the new gene silencer. Am J Clin Pathol. 2007;128(5):830-6.
94. Pan X, Wang R, Wang ZX. The potential role of miR-451 in cancer diagnosis, prognosis, and therapy. Molecular cancer therapeutics. 2013;12(7):1153-62.
95. Yekta S, Shih IH, Bartel DP. MicroRNA-directed cleavage of HOXB8 mRNA. Science. 2004;304(5670):594-6.
96. le Sage C, Agami R. Immense promises for tiny molecules: uncovering miRNA functions. Cell Cycle. 2006;5(13):1415-21.

97. Denli AM, Tops BB, Plasterk RH, Ketting RF, Hannon GJ. Processing of primary microRNAs by the Microprocessor complex. Nature. 2004;432(7014):231-5.

98. Gregory RI, Yan KP, Amuthan G, Chendrimada T, Doratotaj B, Cooch N, et al. The Microprocessor complex mediates the genesis of microRNAs. Nature. 2004;432(7014):235-40.

99. Grishok A, Pasquinelli AE, Conte D, Li N, Parrish S, Ha I, et al. Genes and mechanisms related to RNA interference regulate expression of the small temporal RNAs that control C. elegans developmental timing. Cell. 2001;106(1):23-34.

100. Hutvagner G, McLachlan J, Pasquinelli AE, Balint E, Tuschl T, Zamore PD. A cellular function for the RNA-interference enzyme Dicer in the maturation of the let-7 small temporal RNA. Science. 2001;293(5531):834-8.

101. Ketting RF, Fischer SE, Bernstein E, Sijen T, Hannon GJ, Plasterk RH. Dicer functions in RNA interference and in synthesis of small RNA involved in developmental timing in C. elegans. Genes Dev. 2001;15(20):2654-9.

102. Knight SW, Bass BL. A role for the RNase III enzyme DCR-1 in RNA interference and germ line development in Caenorhabditis elegans. Science. 2001;293(5538):2269-71.

103. Kim VN. MicroRNA biogenesis: coordinated cropping and dicing. Nat Rev Mol Cell Biol. 2005;6(5):376-85.

104. Cuellar TL, Davis TH, Nelson PT, Loeb GB, Harfe BD, Ullian E, et al. Dicer loss in striatal neurons produces behavioral and neuroanatomical phenotypes in the absence of neurodegeneration. Proc Natl Acad Sci U S A. 2008;105(14):5614-9.

105. Wang G, van der Walt JM, Mayhew G, Li YJ, Zuchner S, Scott WK, et al. Variation in the miRNA-433 binding site of FGF20 confers risk for Parkinson disease by overexpression of alpha-synuclein. Am J Hum Genet. 2008;82(2):283-9.

106. Kim J, Inoue K, Ishii J, Vanti WB, Voronov SV, Murchison E, et al. A MicroRNA feedback circuit in midbrain dopamine neurons. Science. 2007;317(5842):1220-4.

107. Rademakers R, Eriksen JL, Baker M, Robinson T, Ahmed Z, Lincoln SJ, et al. Common variation in the miR-659 binding-site of GRN is a major risk factor for TDP43-positive frontotemporal dementia. Hum Mol Genet. 2008;17(23):3631-42.
108. Boissonneault V, Plante I, Rivest S, Provost P. MicroRNA-298 and microRNA-328 regulate expression of mouse beta-amyloid precursor protein-converting enzyme 1. J Biol Chem. 2009;284(4):1971-81.
109. Hebert SS, Horre K, Nicolai L, Papadopoulou AS, Mandemakers W, Silahtaroglu AN, et al. Loss of microRNA cluster miR-29a/b-1 in sporadic Alzheimer's disease correlates with increased BACE1/beta-secretase expression. Proc Natl Acad Sci U S A. 2008;105(17):6415-20.
110. Saba R, Goodman CD, Huzarewich RL, Robertson C, Booth SA. A miRNA signature of prion induced neurodegeneration. PLoS ONE. 2008;3(11):e3652.
111. Montag J, Hitt R, Opitz L, Schulz-Schaeffer WJ, Hunsmann G, Motzkus D. Upregulation of miRNA hsa-miR-342-3p in experimental and idiopathic prion disease. Mol Neurodegener. 2009;4:36.
112. Packer AN, Xing YI, Harper SQ, Jones L, Davidson BP. The biofunctional microRNA miR-9/miR-9* regulates REST and CoREST and is downregulated in Huntington's Disease. J Neurosci. 2008;28(53):14341-6.
113. Johnson MA, Ables JL, Eisch AJ. Cell-intrinsic signals that regulate adult neurogenesis in vivo: insights from inducible approaches. BMB Reports. 2009;42(5):245-59.
114. Junn E, Lee KW, Jeong BS, Chan TW, Im JY, Mouradian MM. Repression of alpha-synuclein expression and toxicity by microRNA-7. Proc Natl Acad Sci U S A. 2009;106(31):13052-7.
115. Cheloufi S, Dos Santos CO, Chong MM, Hannon GJ. A dicer-independent miRNA biogenesis pathway that requires Ago catalysis. Nature. 2010;465(7298):584-9.
116. Yang JS, Lai EC. Dicer-independent, Ago2-mediated microRNA biogenesis in vertebrates. Cell Cycle. 2010;9(22):4455-60.
117. Yang JS, Maurin T, Robine N, Rasmussen KD, Jeffrey KL, Chandwani R, et al. Conserved vertebrate mir-451 provides a platform for Dicer-independent, Ago2-mediated microRNA biogenesis. Proc Natl Acad Sci U S A. 2010;107(34):15163-8.

118. Hock J, Meister G. The Argonaute protein family. Genome Biol. 2008;9(2):210.
119. Bruchova-Votavova H, Yoon D, Prchal JT. miR-451 enhances erythroid differentiation in K562 cells. Leuk Lymphoma. 2010;51(4):686-93.
120. Rasmussen KD, Simmini S, Abreu-Goodger C, Bartonicek N, Di Giacomo M, Bilbao-Cortes D, et al. The miR-144/451 locus is required for erythroid homeostasis. J Exp Med. 2010;207(7):1351-8.
121. Svasti S, Masaki S, Penglong T, Abe Y, Winichagoon P, Fucharoen S, et al. Expression of microRNA-451 in normal and thalassemic erythropoiesis. Ann Hematol. 2010;89(10):953-8.
122. Zhan M, Miller CP, Papayannopoulou T, Stamatoyannopoulos G, Song CZ. MicroRNA expression dynamics during murine and human erythroid differentiation. Exp Hematol. 2007;35(7):1015-25.
123. Masaki S, Ohtsuka R, Abe Y, Muta K, Umemura T. Expression patterns of microRNAs 155 and 451 during normal human erythropoiesis. Biochem Biophys Res Commun. 2007;364(3):509-14.
124. Bruchova H, Yoon D, Agarwal AM, Mendell J, Prchal JT. Regulated expression of microRNAs in normal and polycythemia vera erythropoiesis. Exp Hematol. 2007;35(11):1657-67.
125. Patrick DM, Zhang CC, Tao Y, Yao H, Qi X, Schwartz RJ, et al. Defective erythroid differentiation in miR-451 mutant mice mediated by 14-3-3zeta. Genes Dev. 2010;24(15):1614-9.
126. Du TT, Fu YF, Dong M, Wang L, Fan HB, Chen Y, et al. Experimental validation and complexity of miRNA-mRNA target interaction during zebrafish primitive erythropoiesis. Biochem Biophys Res Commun. 2009;381:688-93.
127. Pase L, Layton JE, Kloosterman WP, Carradice D, Waterhouse PM, Lieschke GJ. miR-451 regulates zebrafish erythroid maturation in vivo via its target gata2. Blood. 2009;113(8):1794-804.
128. Yu D, dos Santos CO, Zhao G, Jiang J, Amigo JD, Khandros E, et al. miR-451 protects against erythroid oxidant stress by repressing 14-3-3zeta. Genes Dev. 2010;24(15):1620-33.

129. Papapetrou EP, Korkola JE, Sadelain M. A genetic strategy for single and combinatorial analysis of miRNA function in mammalian hematopoietic stem cells. Stem Cells. 2009;28(2):287-96.
130. Redell JB, Liu Y, Dash PK. Traumatic brain injury alters expression of hippocampal microRNAs: Potential regulators of multiple pathophysiological processes. J Neursci Res. 2009;87:1435-48.
131. Lei P, Li Y, Chen X, Yang S, Zhang J. Microarray based analysis of microRNA expression in rat cerebral cortex after traumatic brain injury. Brain Res. 2009;1284:191-201.
132. Truettner JS, Alonso OF, Bramlett HM, Dietrich DW. Therapeutic hypothermia alters microRNA responses to traumatic brain injury in rats. J Cereb Blood Flow Metab. 2011;epub ahead of print.
133. Cogswell JP, Ward J, Taylor IA, Waters M, Shi Y, Cannon B, et al. Identification of miRNA changes in Alzheimer's Disease brain and CSF yields putative biomarkers and insights into disease pathways. J Alzheimers Dis. 2008;14:27-41.
134. Du J, Liu S, He J, Liu X, Qu Y, Yan W, et al. MicroRNA-451 regulates stemness of side population cells via PI3K/Akt/mTOR signaling pathway in multiple myeloma. Oncotarget. 2015;6(17):14993-5007.
135. Bitarte N, Bandres E, Boni V, Zarate R, Rodriguez J, Gonzalez-Huarriz M, et al. MicroRNA-451 is involved in the self-renewal, tumorigenicity, and chemoresistance of colorectal cancer stem cells. Stem Cells. 2011;29(11):1661-71.
136. Qian S, Ding JY, Xie R, An JH, Ao XJ, Zhao ZG, et al. MicroRNA expression profile of bronchioalveolar stem cells from mouse lung. Biochem Biophys Res Commun. 2008;377(2):668-73.
137. Gal H, Pandi G, Kanner AA, Ram Z, Lithwick-Yanai G, Amariglio N, et al. MIR-451 and Imatinib mesylate inhibit tumor growth of Glioblastoma stem cells. Biochem Biophys Res Commun. 2008;376(1):86-90.
138. Bandres E, Bitarte N, Arias F, Agorreta J, Fortes P, Agirre X, et al. microRNA-451 regulates macrophage migration inhibitory factor production and proliferation of gastrointestinal cancer cells. Clin Cancer Res. 2009;15(7):2281-90.

139. Godlewski J, Bronisz A, Nowicki MO, Chiocca EA, Lawler S. microRNA-451: A conditional switch controlling glioma cell proliferation and migration. Cell Cycle. 2010;9(14):2742-8.
140. Wang R, Wang ZX, Yang JS, Pan X, De W, Chen LB. MicroRNA-451 functions as a tumor suppressor in human non-small cell lung cancer by targeting ras-related protein 14 (RAB14). Oncogene. 2011.
141. Godlewski J, Nowicki MO, Bronisz A, Nuovo G, Palatini J, De Lay M, et al. MicroRNA-451 regulates LKB1/AMPK signaling and allows adaptation to metabolic stress in glioma cells. Mol Cell. 2010;37(5):620-32.
142. Wang R, Chen DQ, Huang JY, Zhang K, Feng B, Pan BZ, et al. Acquisition of radioresistance in docetaxel-resistant human lung adenocarcinoma cells is linked with dysregulation of miR-451/c-Myc-survivin/rad-51 signaling. Oncotarget. 2014;5(15):6113-29.
143. Chen D, Huang J, Zhang K, Pan B, Chen J, De W, et al. MicroRNA-451 induces epithelial-mesenchymal transition in docetaxel-resistant lung adenocarcinoma cells by targeting proto-oncogene c-Myc. European journal of cancer (Oxford, England : 1990). 2014;50(17):3050-67.
144. Li HPZ, X.C., Zhang; B., Long, J.T.; Zhou, B.; Tan, G.S.; Zeng, W.X.; Chen, W.; Yang, J.Y. miR-451 inhibits cell proliferation in human hepatocellular carcinoma through direct suppression of IKK-β. Carcinogenesis. 2013;34(11):2443-51.
145. Lv G, Hu Z, Tie Y, Du J, Fu H, Gao X, et al. MicroRNA-451 regulates activating transcription factor 2 expression and inhibits liver cancer cell migration. Oncol Rep. 2014;32(3):1021-8.
146. Huang JY, Zhang K, Chen DQ, Chen J, Feng B, Song H, et al. MicroRNA-451: epithelial-mesenchymal transition inhibitor and prognostic biomarker of hepatocelluar carcinoma. Oncotarget. 2015;6(21):18613-30.
147. de Los Reyes VA, Jung E, Kim Y. Optimal control strategies of eradicating invisible glioblastoma cells after conventional surgery. Journal of the Royal Society, Interface / the Royal Society. 2015;12(106).
148. Bergamaschi A, Katzenellenbogen BS. Tamoxifen downregulation of miR-451 increases 14-3-3zeta and promotes breast cancer cell survival and endocrine resistance. Oncogene. 2012;31(1):39-47.

149. Liu X, Zhang X, Xiang J, Lv Y, Shi J. miR-451: potential role as tumor suppressor of human hepatoma cell growth and invasion. Int J Oncol. 2014;45(2):739-45.
150. Xu H, Mei Q, Shi L, Lu J, Zhao J, Fu Q. Tumor-suppressing effects of miR451 in human osteosarcoma. Cell Biochem Biophys. 2014;69(1):163-8.
151. Liu N, Jiang N, Guo R, Jiang W, He QM, Xu YF, et al. MiR-451 inhibits cell growth and invasion by targeting MIF and is associated with survival in nasopharyngeal carcinoma. Mol Cancer. 2013;12(1):123.
152. Heinzelmann J, Henning B, Sanjmyatav J, Posorski N, Steiner T, Wunderlich H, et al. Specific miRNA signatures are associated with metastasis and poor prognosis in clear cell renal cell carcinoma. World J Urol. 2011;29:367-73.
153. Tsuchiya S, Oku M, Imanaka Y, Kunimoto R, Okuno Y, Terasawa K, et al. MicroRNA-338-3p and microRNA-451 contribute to the formation of basolateral polarity in epithelial cells. Nucleic Acids Res. 2009;37(11):3821-7.
154. Patz S, Trattnig C, Grunbacher G, Ebner B, Gully C, Novak A, et al. More than cell dust: microparticles isolated from cerebrospinal fluid of brain injured patients are messengers carrying mRNAs, miRNAs and proteins. J Neurotrauma. 2013.
155. Fagel DM, Ganat Y, Cheng E, Silbereis J, Ohkubo Y, Ment LR, et al. Fgfr1 is required for cortical regeneration and repair after perinatal hypoxia. J Neurosci. 2009;29(4):1202-11.
156. Götz M, Hutter WB. The cell biology of neurogenesis. 2005. 2005;6(10):777-88.
157. Kosodo Y, Röper K, Haubensak W, Marzesco AM, Corbeil D, Huttner HB. Asymmetric distribution of the apical plasma membrane during neurogenic divisions of mammalian neuroepithelial cells. EMBO J. 2004;23(11):2314-24.
158. Paquet-Durand F, Tan, S., Bicker, G. Turning teratocarcinoma cells into neurons: rapid differentiation of NT-2 cells in floating spheres. Brain Res Dev Brain Res. 2003 142(2):161-7.
159. Pfaffl MW. A new mathematical model for relative quantification in real-time RT-PCR. Nucleic Acids Res. 2001;29(9).

160. Mitchell PS, Parin RK, Kroh EM, Fritz BR, Wyman SK, Pogosova-Agadjanyan EL, et al. Circulating microRNAs as stable blood-based markers for cancer detection. PNAS. 2008;105(30):10513-8.
161. Meijering E. Neuron Tracing in Perspective. Cytometry Part A. 2010;77(7):693-704.
162. Meijering EJ, M.; Sarria, J.-C. F.; Steiner, P.; Hirling, H. ; Unser, M.;. Design and Validation of a Tool for Neurite Tracing and Analysis in Fluorescence Microscopy Images. Cytometry Part A. 2004;58(2):167-76.
163. Abramoff MDM, P.J.; Ram, S.J. Image Processing with ImageJ. Biophotonics International. 2004;11(7):36-42.
164. Schneider CAR, W.S.; Eliceiri, K.W. . NIH Image to ImageJ: 25 years of image analysis. Nature Methods. 2012;9:671-5.
165. Hynes RO. Integrins: a family of cell surface receptors. Cell. 1987;48(4):549-54.
166. Tate MC, Garcia AJ, Keselowsky BG, Schumm MA, Archer DR, LaPlaca MC. Specific beta1 integrins mediate adhesion, migration, and differentiation of neural progenitors derived from the embryonic striatum. Mol Cell Neurosci. 2004;27(1):22-31.
167. John B, Enright AJ, Aravin A, Tuschl T, Sander C, Marks DS. Human MicroRNA targets. PLoS Biol. 2004;2(11):e363.
168. Lewis BP, Burge CB, Bartel DP. Conserved seed pairing, often flanked by adenosines, indicates that thousands of human genes are microRNA targets. Cell. 2005;120(1):15-20.
169. Friedman RC, Farh KK, Burge CB, Bartel DP. Most mammalian mRNAs are conserved targets of microRNAs. Genome Res. 2009;19(1):92-105.
170. Grimson A, Farh KK, Johnston WK, Garrett-Engele P, Lim LP, Bartel DP. MicroRNA targeting specificity in mammals: determinants beyond seed pairing. Mol Cell. 2007;27(1):91-105.
171. Garcia DM, Baek D, Shin C, Bell GW, Grimson A, Bartel DP. Weak seed-pairing stability and high target-site abundance decrease the proficiency of lsy-6 and other microRNAs. Nat Struct Mol Biol. 2011;18(10):1139-46.
172. Agarwal V, Bell GW, Nam JW, Bartel DP. Predicting effective microRNA target sites in mammalian mRNAs. eLife. 2015;4.

173. Nam JW, Rissland OS, Koppstein D, Abreu-Goodger C, Jan CH, Agarwal V, et al. Global analyses of the effect of different cellular contexts on microRNA targeting. Mol Cell. 2014;53(6):1031-43.
174. Shin C, Nam JW, Farh KK, Chiang HR, Shkumatava A, Bartel DP. Expanding the microRNA targeting code: functional sites with centered pairing. Mol Cell. 2010;38(6):789-802.
175. Paraskevopoulou MD, Georgakilas G, Kostoulas N, Vlachos IS, Vergoulis T, Reczko M, et al. DIANA-microT web server v5.0: service integration into miRNA functional analysis workflows. Nucleic Acids Res. 2013;41(Web Server issue):W169-73.
176. Reczko M, Maragkakis M, Alexiou P, Grosse I, Hatzigeorgiou AG. Functional microRNA targets in protein coding sequences. Bioinformatics. 2012;28(6):771-6.
177. Wang X, El Naqa IM. Prediction of both conserved and nonconserved microRNA targets in animals. Bioinformatics. 2008;24(3):325-32.
178. Wang X. miRDB: a microRNA target prediction and functional annotation database with a wiki interface. Rna. 2008;14(6):1012-7.
179. Wong N, Wang X. miRDB: an online resource for microRNA target prediction and functional annotations. Nucleic Acids Res. 2015;43(Database issue):D146-52.
180. Sethupathy P, Corda B, Hatzigeorgiou AG. TarBase: A comprehensive database of experimentally supported animal microRNA targets. Rna. 2006;12(2):192-7.
181. Vlachos IS, Paraskevopoulou MD, Karagkouni D, Georgakilas G, Vergoulis T, Kanellos I, et al. DIANA-TarBase v7.0: indexing more than half a million experimentally supported miRNA:mRNA interactions. Nucleic Acids Res. 2015;43(Database issue):D153-9.
182. Hsu SD, Tseng YT, Shrestha S, Lin YL, Khaleel A, Chou CH, et al. miRTarBase update 2014: an information resource for experimentally validated miRNA-target interactions. Nucleic Acids Res. 2014;42(Database issue):D78-85.
183. Nan Y, Han L, Zhang A, Wang G, Jia Z, Yang Y, et al. MiRNA-451 plays a role as tumor suppressor in human glioma cells. Brain Res. 2010;1359:14-21.

184. Li HY, Zhang Y, Cai JH, Bian HL. MicroRNA-451 inhibits growth of human colorectal carcinoma cells via downregulation of Pi3k/Akt pathway. Asian Pacific journal of cancer prevention : APJCP. 2013;14(6):3631-4.
185. Bian HB, Pan X, Yang JS, Wang ZX, De W. Upregulation of microRNA-451 increases cisplatin sensitivity of non-small cell lung cancer cell line (A549). J Exp Clin Cancer Res. 2011;30:20.
186. Wang T, Zang WQ, Li M, Wang N, Zheng YL, Zhao GQ. Effect of miR-451 on the biological behavior of the esophageal carcinoma cell line EC9706. Dig Dis Sci. 2013;58(3):706-14.
187. Chen H, Untiveros GM, McKee LAK, Perez J, Li J, Antin PB, et al. micro-RNA-195 and -451 regulate the LKB1/AMPK signaling axis by targeting MO25. PLoS One. 2012;7(7):e41574.
188. Li HY, Zhang, Y., Cai, J.H., Bian, H.L. MicroRNA-451 inhibits growth of human colorectal carcinoma cells via downregulation of Pi3k/Akt pathway. Asian Pac J Cancer Prev. 2013;14(6):3631-4.
189. Tian Y, Nan, Y., Han, L., Zhang, A., Wang, G., Jia, Z., Hao, J., Pu, P., Zhong, Y., Kang, C. MicroRNA miR-451 downregulates the PI3K/AKT pathway through CAB39 in human glioma. Int J Oncol 2012;40(4):1105-12.
190. Kuwabara Y, Horie T, Baba O, Watanabe S, Nishiga M, Usami S, et al. MicroRNA-451 exacerbates lipotoxicity in cardiac myocytes and high-fat diet-induced cardiac hypertrophy in mice through suppression of the LKB1/AMPK pathway. Circ Res. 2015;116(2):279-88.
191. Hur W, Lee JH, Kim SW, Kim JH, Bae SH, Kim M, et al. Downregulation of microRNA-451 in non-alcoholic steatohepatitis inhibits fatty acid-induced proinflammatory cytokine production through the AMPK/AKT pathway. Int J Biochem Cell Biol. 2015;64:265-76.
192. Zang WQ, Yang X, Wang T, Wang YY, Du YW, Chen XN, et al. MiR-451 inhibits proliferation of esophageal carcinoma cell line EC9706 by targeting CDKN2D and MAP3K1. World J Gastroenterol. 2015;21(19):5867-76.
193. Zhang F, Huang W, Sheng M, Liu T. MiR-451 inhibits cell growth and invasion by targeting CXCL16 and is associated with prognosis of osteosarcoma patients. Tumour biology : the journal of the International Society for Oncodevelopmental Biology and Medicine. 2015;36(3):2041-8.

194. Liu DL, C.; Wang, X.; Ingvarsson, S.; Chen, H. MicroRNA-451 suppresses tumor cell growth by down-regulating IL6R gene expression. Cancer Epidemiol 2014;38(1):85-92.
195. Liu NJ, N.; Guo, R.; Jiang, W.; He, Q.M.; Xu, Y.F.; Li, Y.Q.; Tang, L.L.; Mao, Y.P.; Sun, Y.; Ma, J. MiR-451 inhibits cell growth and invasion by targeting MIF and is associated with survival in nasopharyngeal carcinoma. Mol Cancer 2013;12(1):123.
196. Graham A, Falcone T, Nothnick WB. The expression of microRNA-451 in human endometriotic lesions is inversely related to that of macrophage migration inhibitory factor (MIF) and regulates MIF expression and modulation of epithelial cell survival. Hum Reprod. 2015;30(3):642-52.
197. Li X, Sanda T, Look AT, Novina CD, von Boehmer H. Repression of tumor suppressor miR-451 is essential for NOTCH1-induced oncogenesis in T-ALL. J Exp Med. 2011;208(4):663-75.
198. Yin P, Peng R, Peng H, Yao L, Sun Y, Wen L, et al. MiR-451 suppresses cell proliferation and metastasis in A549 lung cancer cells. Molecular biotechnology. 2015;57(1):1-11.
199. Zhang T, Sun Q, Liu T, Chen J, Du S, Ren C, et al. MiR-451 increases radiosensitivity of nasopharyngeal carcinoma cells by targeting ras-related protein 14 (RAB14). Tumour biology : the journal of the International Society for Oncodevelopmental Biology and Medicine. 2014;35(12):12593-9.
200. Krek A, Grun D, Poy MN, Wolf R, Rosenberg L, Epstein EJ, et al. Combinatorial microRNA target predictions. Nat Genet. 2005;37(5):495-500.
201. Song L, Su M, Wang S, Zou Y, Wang X, Wang Y, et al. MiR-451 is decreased in hypertrophic cardiomyopathy and regulates autophagy by targeting TSC1. J Cell Mol Med. 2014;18(11):2266-74.
202. Zhang Z, Luo, X., Ding, S., Chen, J., Chen, T., Chen, X., Zha, H., Yao, L., He, X., Peng, H. MicroRNA-451 regulates p38 MAPK signaling by targeting of Ywhaz and suppresses the mesangial hypertrophy in early diabetic nephropathy. FEBS Lett. 2012;586(1):20-6.
203. Rosenberger CM, Podyminogin RL, Navarro G, Zhao GW, Askovich PS, Weiss MJ, et al. miR-451 regulates dendritic cell cytokine responses to influenza infection. J Immunol. 2012;189(12):5965-75.

204. Wu LN, Wei XW, Fan Y, Miao JN, Wang LL, Zhang Y, et al. Altered expression of 14-3-3zeta protein in spinal cords of rat fetuses with spina bifida aperta. PLoS One. 2013;8(8):e70457.
205. Murata K, Yoshitomi H, Furu M, Ishikawa M, Shibuya H, Ito H, et al. MicroRNA-451 down-regulates neutrophil chemotaxis via p38 MAPK. Arthritis & rheumatology (Hoboken, NJ). 2014;66(3):549-59.
206. Joshi NR, Su RW, Chandramouli GV, Khoo SK, Jeong JW, Young SL, et al. Altered expression of microRNA-451 in eutopic endometrium of baboons (Papio anubis) with endometriosis. Hum Reprod. 2015.
207. Liu C, Zhao X. MicroRNAs in adult and embryonic neurogenesis. Neuromolecular medicine. 2009;11(3):141-52.
208. Shi Y, Zhao X, Hsieh J, Wichterle H, Impey S, Banerjee S, et al. MicroRNA regulation of neural stem cells and neurogenesis. J Neurosci. 2010;30(45):14931-6.
209. Kawahara H, Imai T, Okano H. MicroRNAs in Neural Stem Cells and Neurogenesis. Front Neurosci. 2012;6:30.
210. Lang MF, Shi Y. Dynamic Roles of microRNAs in Neurogenesis. Front Neurosci. 2012;6:71.
211. Follert P, Cremer H, Beclin C. MicroRNAs in brain development and function: a matter of flexibility and stability. Front Mol Neurosci. 2014;7:5.
212. Singh T, Jauhari A, Pandey A, Singh P, Pant AB, Parmar D, et al. Regulatory triangle of neurodegeneration, adult neurogenesis and microRNAs. CNS Neurol Disord Drug Targets. 2014;13(1):96-103.
213. Meza-Sosa KF, Pedraza-Alva G, Perez-Martinez L. microRNAs: key triggers of neuronal cell fate. Front Cell Neurosci. 2014;8:175.
214. Saugstad JA. MicroRNAs as effectors of brain function with roles in ischemia and injury, neuroprotection, and neurodegeneration. J Cereb Blood Flow Metab. 2010;30(9):1564-76.
215. Smirnova L, Gräfe A, Seiler A, Schumacher S, Nitsch R, Wulczyn FG. Regulation of miRNA expression during neural cell specification. Eur J Neurosci. 2005;21:1469-77.
216. Coolen M, Katz S, Bally-Cuif L. miR-9: a versatile regulator of neurogenesis. Front Cell Neurosci. 2013;7:220.

217. Sun Y, Luo ZM, Guo XM, Su DF, Liu X. An updated role of microRNA-124 in central nervous system disorders: a review. Front Cell Neurosci. 2015;9:193.
218. Rehfeld F, Rohde AM, Nguyen DT, Wulczyn FG. Lin28 and let-7: ancient milestones on the road from pluripotency to neurogenesis. Cell Tissue Res. 2015;359(1):145-60.
219. Yin J, Lin J, Luo X, Chen Y, Li Z, Ma G, et al. miR-137: a new player in schizophrenia. Int J Mol Sci. 2014;15(2):3262-71.
220. Hudish LI, Blasky AJ, Appel B. miR-219 regulates neural precursor differentiation by direct inhibition of apical par polarity proteins. Dev Cell. 2013;27(4):387-98.
221. Franzoni E, Booker SA, Parthasarathy S, Rehfeld F, Grosser S, Srivatsa S, et al. miR-128 regulates neuronal migration, outgrowth and intrinsic excitability via the intellectual disability gene Phf6. eLife. 2015;4.
222. Santos MC, Tegge AN, Correa BR, Mahesula S, Kohnke LQ, Qiao M, et al. miR-124, -128, and -137 Orchestrate Neural Differentiation by Acting on Overlapping Gene Sets Containing a Highly Connected Transcription Factor Network. Stem Cells. 2015.
223. Pathania M, Torres-Reveron J, Yan L, Kimura T, Lin TV, Gordon V, et al. miR-132 enhances dendritic morphogenesis, spine density, synaptic integration, and survival of newborn olfactory bulb neurons. PLoS One. 2012;7(5):e38174.
224. Coolen M, Bally-Cuif L. MicroRNAs in brain development and physiology. Curr Opin Neurobiol. 2009;19(5):461-70.
225. Liu C, Teng ZQ, Santistevan NJ, Szulwach KE, Guo W, Jin P, et al. Epigenetic regulation of miR-184 by MBD1 governs neural stem cell proliferation and differentiation. Cell Stem Cell. 2010;6(5):433-44.
226. Kisliouk T, Cramer T, Meiri N. Heat stress attenuates new cell generation in the hypothalamus: a role for miR-138. Neuroscience. 2014;277:624-36.
227. Yi Y, Noh MJ, Lee KH. Current advances in retroviral gene therapy. Current gene therapy. 2011;11(3):218-28.
228. Choong ML, Yang HH, McNiece I. MicroRNA expression profiling during human cord blood-derived CD34 cell erythropoiesis. Exp Hematol. 2007;35(4):551-64.

229. Rathjen T, Nicol C, McConkey G, Dalmay T. Analysis of short RNAs in the malaria parasite and its red blood cell host. FEBS Lett. 2006;580(22):5185-8.
230. Franceschetti T, Dole NS, Kessler CB, Lee SK, Delany AM. Pathway analysis of microRNA expression profile during murine osteoclastogenesis. PLoS One. 2014;9(9):e107262.
231. Dmitriev P, Barat A, Polesskaya A, O'Connell MJ, Robert T, Dessen P, et al. Simultaneous miRNA and mRNA transcriptome profiling of human myoblasts reveals a novel set of myogenic differentiation-associated miRNAs and their target genes. BMC Genomics. 2013;14:265.
232. Jin HL, Kim JS, Kim YJ, Kim SJ, Broxmeyer HE, Kim KS. Dynamic expression of specific miRNAs during erythroid differentiation of human embryonic stem cells. Mol Cells. 2012;34(2):177-83.
233. Kouhkan F, Soleimani M, Daliri M, Behmanesh M, Mobarra N, Mossahebi Mohammadi M, et al. miR-451 Up-regulation, Induce Erythroid Differentiation of CD133+cells Independent of Cytokine Cocktails. Iranian journal of basic medical sciences. 2013;16(6):756-63.
234. Kouhkan F, Hafizi M, Mobarra N, Mossahebi-Mohammadi M, Mohammadi S, Behmanesh M, et al. miRNAs: a new method for erythroid differentiation of hematopoietic stem cells without the presence of growth factors. Applied biochemistry and biotechnology. 2014;172(4):2055-69.
235. Qian X, Li G, Vass WC, Papageorge A, Walker RC, Asnaghi L, et al. The Tensin-3 protein, including its SH2 domain, is phosphorylated by Src and contributes to tumorigenesis and metastasis. Cancer Cell. 2009;16(3):246-58.
236. Lo SH. Tensin. Int J Biochem Cell Biol. 2004;36(1):31-4.
237. Lo SH. C-terminal tensin-like (CTEN): a promising biomarker and target for cancer. Int J Biochem Cell Biol. 2014 51:150-4.
238. Muharram G, Sahgal P, Korpela T, De Franceschi N, Kaukonen R, Clark K, et al. Tensin-4-dependent MET stabilization is essential for survival and proliferation in carcinoma cells. Dev Cell. 2014;29(4):421-36.
239. Chung BM, Rotty JD, Coulombe PA. Networking galore: intermediate filaments and cell migration. Curr Opin Cell Biol. 2013;25(5):600-12.
240. Zhang X, Fournier MV, Ware JL, Bissell MJ, Yacoub A, Zehner ZE. Inhibition of vimentin or beta1 integrin reverts morphology of prostate tumor cells

grown in laminin-rich extracellular matrix gels and reduces tumor growth in vivo. Molecular cancer therapeutics. 2009;8(3):499-508.
241. Zeng T, Peng L, Chao C, Fu B, Wang G, Wang Y, et al. miR-451 inhibits invasion and proliferation of bladder cancer by regulating EMT. Int J Clin Exp Pathol. 2014;7(11):7653-62.
242. Irollo E, Pirozzi G. CD133: to be or not to be, is this the real question? American journal of translational research. 2013;5(6):563-81.
243. Chen WS, Xu PZ, Gottlob K, Chen ML, Sokol K, Shiyanova T, et al. Growth retardation and increased apoptosis in mice with homozygous disruption of the Akt1 gene. Genes Dev. 2001;15(17):2203-8.
244. Cho H, Thorvaldsen JL, Chu Q, Feng F, Birnbaum MJ. Akt1/PKBalpha is required for normal growth but dispensable for maintenance of glucose homeostasis in mice. J Biol Chem. 2001;276(42):38349-52.
245. Hers I, Vincent EE, Tavare JM. Akt signalling in health and disease. Cell Signal. 2011;23(10):1515-27.
246. Sun C, Zhao J, Jin Y, Hou C, Zong W, Lu T, et al. PTEN regulation of the proliferation and differentiation of auditory progenitors through the PTEN/PI3K/Akt-signaling pathway in mice. Neuroreport. 2014;25(3):177-83.
247. Bruel-Jungerman E, Veyrac A, Dufour F, Horwood J, Laroche S, Davis S. Inhibition of PI3K-Akt signaling blocks exercise-mediated enhancement of adult neurogenesis and synaptic plasticity in the dentate gyrus. PLoS One. 2009;4(11):e7901.
248. Arno B, Grassivaro F, Rossi C, Bergamaschi A, Castiglioni V, Furlan R, et al. Neural progenitor cells orchestrate microglia migration and positioning into the developing cortex. Nat Commun. 2014;5:5611.
249. Conboy L, Varea E, Castro JE, Sakouhi-Ouertatani H, Calandra T, Lashuel HA, et al. Macrophage migration inhibitory factor is critically involved in basal and fluoxetine-stimulated adult hippocampal cell proliferation and in anxiety, depression, and memory-related behaviors. Mol Psychiatry. 2011;16(5):533-47.
250. Ohta S, Misawa A, Fukaya R, Inoue S, Kanemura Y, Okano H, et al. Macrophage migration inhibitory factor (MIF) promotes cell survival and proliferation of neural stem/progenitor cells. J Cell Sci. 2012;125(Pt 13):3210-20.

251. Kang X, Kang F, Yang B, Guo H, Quan Y, Dong S. [Micro RNA-451 promoting osteogenesis of mesenchymal stem cells by targeting regulatory calcium binding protein 39]. Zhongguo xiu fu chong jian wai ke za zhi = Zhongguo xiufu chongjian waike zazhi = Chinese journal of reparative and reconstructive surgery. 2013;27(9):1122-7.
252. Fazi F, Nervi C. MicroRNA: basic mechanisms and transcriptional regulatory networks for cell fate determination. Cardiovasc Res. 2008;79(4):553-61.
253. Rogers K, Chen X. Biogenesis, turnover, and mode of action of plant microRNAs. Plant Cell. 2013;25(7):2383-99.
254. Eulalio A, Behm-Ansmant I, Schweizer D, Izaurralde E. P-body formation is a consequence, not the cause, of RNA-mediated gene silencing. Mol Cell Biol. 2007;27(11):3970-81.
255. Vieira J, Messing, J. . Gene1982.
256. Leypoldt F, Lewerenz J, Methner A. Identification of genes up-regulated by retinoic-acid-induced differentiation of the human neuronal precursor cell line NTERA-2 cl.D1. J Neurochem. 2001;76(3):806-14.
257. Cheung WM, Fu WY, Hui WS, Ip NY. Production of human CNS neurons from embryonal carcinoma cells using a cell aggregation method. Biotechniques. 1999;26(5):946-8, 50-2, 54.
258. Owczarzy R, You Y, Groth CL, Tataurov AV. Stability and mismatch discrimination of locked nucleic acid-DNA duplexes. Biochemistry. 2011;50:9352-67.
259. You Y, Moreira BG, Behlke MA, Owczarzy R. Design of LNA probes that improve mismatch discrimination. Nucleic Acids Res. 2006;34(8):e60.
260. Tolstrup N, Nielsen PS, Kolberg JG, Frankel AM, Vissing H, Kauppinen S. OligoDesign: Optimal design of LNA (locked nucleic acid) oligonucleotide capture probes for gene expression profiling. Nucleic Acids Res. 2003;31(13):3758-62.
261. Hardikar AA, Farr RJ, Joglekar MV. Circulating microRNAs: understanding the limits for quantitative measurement by real-time PCR. Journal of the American Heart Association. 2014;3(1):e000792.

262. Karlsen F, Steen HB, Nesland JM. SYBR green I DNA staining increases the detection sensitivity of viruses by polymerase chain reaction. Journal of virological methods. 1995;55(1):153-6.
263. Schneeberger C, Speiser P, Kury F, Zeillinger R. Quantitative detection of reverse transcriptase-PCR products by means of a novel and sensitive DNA stain. PCR methods and applications. 1995;4(4):234-8.
264. Mestdagh P, Van Vlierberghe P, De Weer A, Muth D, Westermann F, Speleman F, et al. A novel and universal method for microRNA RT-qPCR data normalization. Genome Biol. 2009;10:R64.
265. Sarkar D, Parkin RK, Wyman S, Bendoraite A, Sather C, Delrow J, et al. Quality assessment and data analysis for microRNA expression arrays. Nucleic Acids Res. 2009;37(2):e17.
266. Vandesompele J, De Preter K, Pattyn F, Poppe B, Van Roy N, De Paepe A, et al. Accurate normalization of real-time quantitative RT-PCR data by geometric averaging of multiple internal control genes. Gen Biol. 2002;3(7).
267. Andersen CL, Jensen JL, Orntoft TF. Normalization of real-time quantitative reverse transcription-PCR data: a model-based variance estimation approach to identify genes suited for normalization, applied to bladder and colon cancer data sets. Cancer Res. 2004;64(15):5245-50.
268. Chen H, Shalom-Feuerstein, R., Riley, J., Zhang, S.D., Tucci, P., Agostini, M., Aberdam, D., Knight, R.A., Genchi, G., Nicotera, P., Melino, G., Vasa-Nicotera, M. miR-7 and miR-214 are specifically expressed during neuroblastoma differentiation, cortical development and embryonic stem cells differentiation, and control neurite outgrowth in vitro. Biochem Biophys Res Commun. 2010;394(4):921-7.
269. Meseguer S, Mudduluru, G., Escamilla, J.M., Allgayer, H., Barettino, D. MicroRNAs-10a and -10b contribute to retinoic acid-induced differentiation of neuroblastoma cells and target the alternative splicing regulatory factor SFRS1 (SF2/ASF). J Biol Chem. 2011;286(6):4150-64.
270. Patnaik SK, Kannisto, E., Yendamuri, S. Overexpression of microRNA miR-30a or miR-191 in A549 lung cancer or BEAS-2B normal lung cell lines does not alter phenotype. PLoS One. 2010;5(2):e9219.

271. Wang W, Peng, B., Wang, D., Ma, X., Jiang, D., Zhao, J., Yu, L. Human tumor microRNA signatures derived from large-scale oligonucleotide microarray datasets. Int J Cancer 2011;129(7):1624-34.
272. Foley NH, Bray, I., Watters, K.M., Das, S., Bryan, K., Bernas, T., Prehn, J.H., Stallings, R.L. MicroRNAs 10a and 10b are potent inducers of neuroblastoma cell differentiation through targeting of nuclear receptor corepressor 2. Cell Death Differ 2011;18(7):1089-98.
273. Lim QE, Zhou L, Ho YK, Wan G, Too HP. snoU6 and 5S RNAs are not reliable miRNA reference genes in neuronal differentiation. Neuroscience. 2011;199:32-43.
274. Zhang Z, Luo X, Ding S, Chen J, Chen T, Chen X, et al. MicroRNA-451 regulates p38 MAPK signaling by targeting of Ywhaz and suppresses the mesangial hypertrophy in early diabetic nephropathy. FEBS Lett. 2012;586(1):20-6.
275. Yan WH CM, Liu JR, Xu Y, Han XF, Xing Y, Wang JZ. Effects of EGF and bFGF on expression of microtubule-associated protein tau and MAP-2 mRNA in human umbilical cord mononuclear cells. Cell Biol Int 2005;29(2):153-7.
276. Galiveti CR, Rozhdestvensky, T.S., Brosius, J., Lehrach, H., Konthur, Z. Application of housekeeping npcRNAs for quantitative expression analysis of human transcriptome by real-time PCR. RNA. 2010;16(2):450-61.

6. Appendix

6.1. Transformation and restriction digestion

Small amounts of lentiviral vectors (AB.G.ct, termed hereafter Ct, AB.G.miR-451+, termed hereafter miR-451+), vector maps shown in Figure 13A and B) were a gift from Dr. Papapetrou (129). To increase these amounts, the first step was to transform super-competent bacteria with lentiviral vector DNA. In general, transformation of super-competent cells with our constructs yielded fewer transformed bacterial colonies than transformation with the pUC19 control (data not shown), which might be due to the relatively small size of the pUC19 plasmid (ca 2700bp). The lentiviral vectors have a size of about 10000bp. The next step was to grow the different transformed colonies in selective LB medium. Lentiviral vector DNA (minipreps) was isolated and identity of the constructs was checked with restriction analysis. The theoretical (A) and experimental restriction digestion pattern (B) of Ct and miR-451+ with *Eco*RI and *Xho*I is shown in Figure 44. This resulted in a distinct experimental restriction pattern for each vector and a congruency between the theoretical and experimental restriction patterns of Ct and miR-451+.

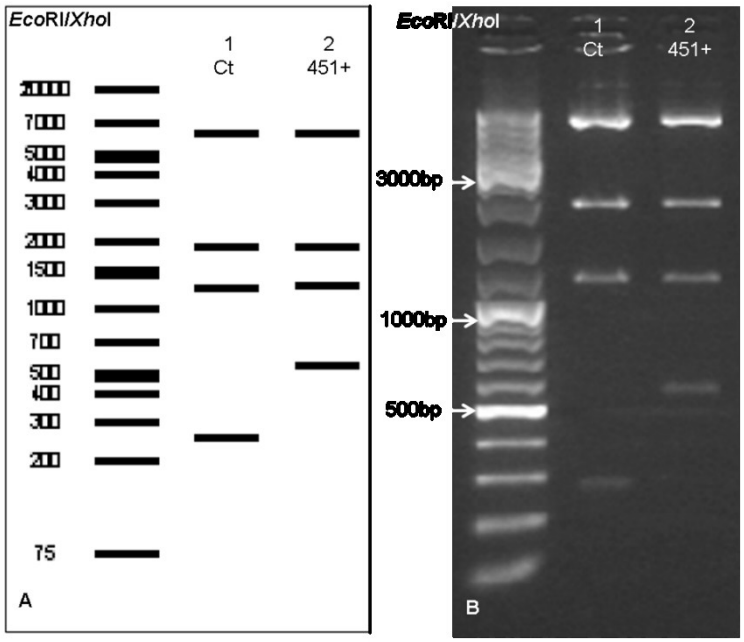

Figure 44

(A) Theoretical restriction digestion pattern (done with SerialCloner2.1) of the overexpressing lentiviral vectors (miR-451+) plus the control vector (Ct) digested with *Eco*RI and *Xho*I. (B) De facto restriction digestion pattern on a 1% agarose gel.

After we had confirmed the identity of the plasmid maxipreps were performed in order to increase the yield of lentiviral vector DNA for lentiviral transfection of HEK293T cells.

6.2. Transfection, lentiviral titer measurement and transduction

HEK293T cells were transfected with the lentiviral vectors (Ct, miR-451+) in order to generate potent lentiviral particles to transduce our cell line of interest (NT2). Lentiviral vectors are shown in Figure 13A, B. All vectors contain the sequence for expression of eGFP (enhanced green fluorescent protein). A transfection method based on using Lentifectin^{TM}, HEK293T cells (gift from Dr. Alexander Deutsch, Division of Hematology, Medical University of Graz) and a 3rd generation lentiviral packaging mix was performed. Fluorescent HEK293T cells (Figure 45B) as well as viral particles of all the described vectors were generated.

The approximate titer of the supernatant aspirated from transfected HEK293T was measured with Lenti-X p24 Rapid Titer Kit from Clontech. For each measurement a p24 standard curve with known concentrations of the p24 protein was included (Figure 45D). A trend line was fitted through the data points and the resulting formula was used to calculate the amount of p24 protein in the lentiviral supernatants. Then the approximate lentiviral titer was calculated with assumptions stated in the user manual and described in the methods sections (see 2.10). It was stated in the user manual, that the absorbance value for 0 pg/ml p24 protein (only media alone) should be around 0,03, but in all our measurements we obtained values between 0,172 and 0,233.

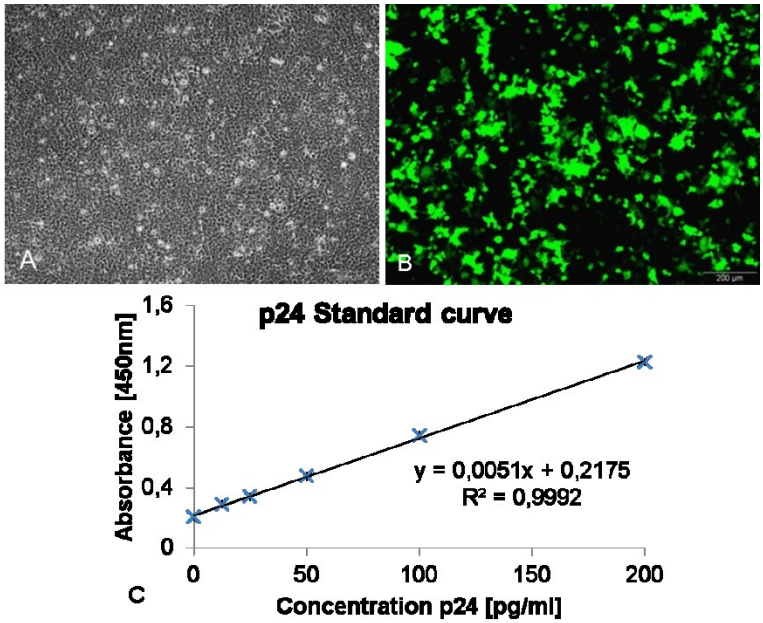

Figure 45

(A) Microscopic picture of HEK293T cells (10x) (B) Fluorescent and thereby transfected viral particle producing HEK293T cells (10x). Pictures were taken with a fluorescent microscope (Olympus, Vienna, Austria). (C) p24 standard curve

We performed 3 transductions of the same NT2 cells on 3 consecutive days. In order to increase transduction efficiency we used the transduction enhancer polybrene. After successful transduction (Figure 46B), cells were sorted by FACS into high, middle and low GFP expressing cells (Figure 46C). After FACS, only fluorescent cells were detectable (Figure 46E). We decided to work only with high GFP expressing cells. Middle and low GFP expressing cells were frozen in liquid N_2 and kept for future experiments.

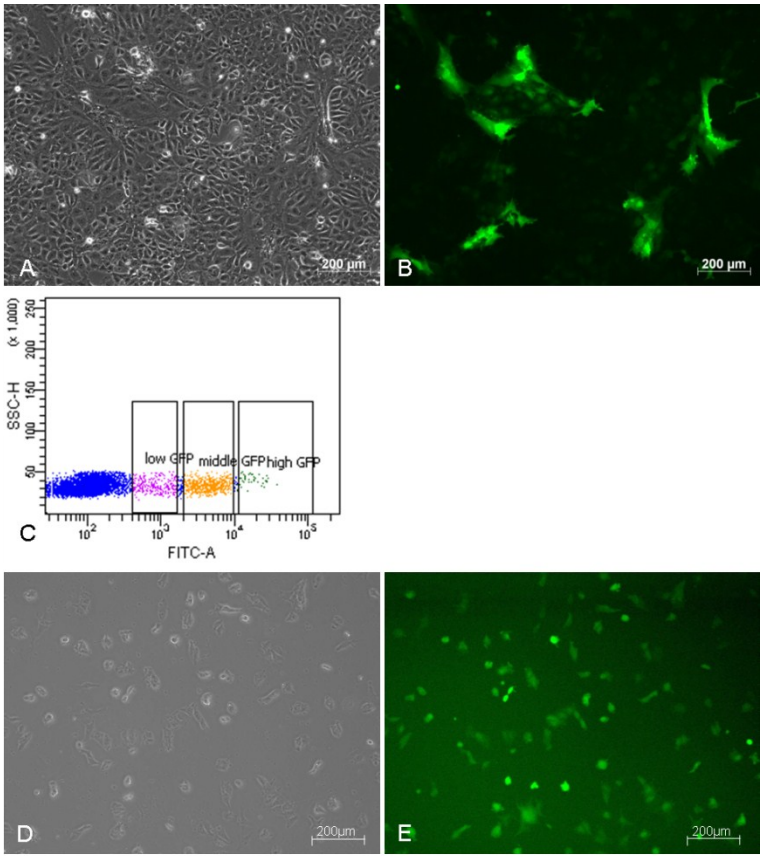

Figure 46

(A) Microscopic picture of transduced NT2 (10x)

(B) Fluorescent picture of eGFP positive transduced NT2 cells (10x). Pictures were taken with LSM, Zeiss, Oberkochen, Germany

(C) After successful transduction cells were sorted by FACS in high, middle and low eGFP positive cells.

(D) Microscopic picture of transduced NT2 after FACS (10x), (E) Fluorescent picture of transduced NT2 after FACS (10x). (D) and (E) were taken with a fluorescent microscope (Olympus, Vienna, Austria).

6.3. Normalisation method

6.3.1. miRNA analyses

The suitability of SNORD38b, 44, 48, 49A, 66, U1, 5s, U6 and 14s RNA for usage as normalisation genes in miRNA expression analyses in undifferentiated transduced and non-transduced cell lines (NT2, Ct, miR-451+) was investigated. Mean Ct-values of the different genes together with the standard deviation are shown on the y-axis in Figure 47. Ct-values for the different genes obtained in qRT-PCR were compared with the statistical program MultiD (GeNorm and NormFinder analysis (Figure 48A and B)) in order to find suitable normalization genes.

SNORD38b and 49A were chosen as the best normalisation combination in GeNorm, NormFinder selected SNORD49A as the best normalisation gene.

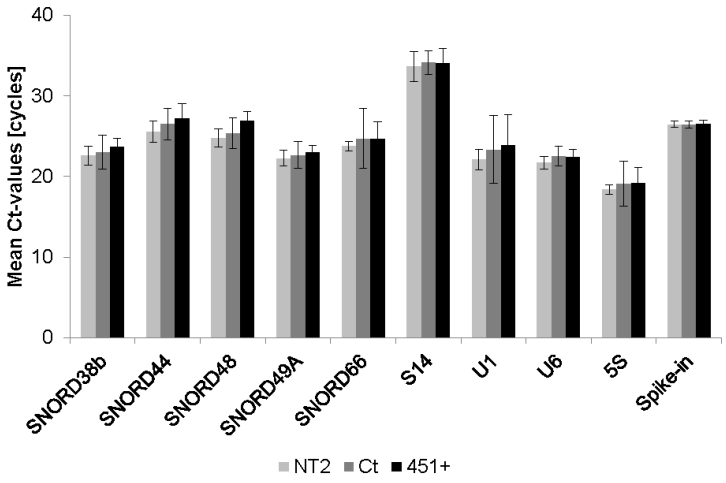

Figure 47

Normalisation genes SNORD38b, 44, 48, 49A, 66, S14, U1, U6, 5s, and Spike-in in undifferentiated transduced (miR-451+, Ct) and non-transduced cells. Error bars show the standard deviation (SD) (n=3).

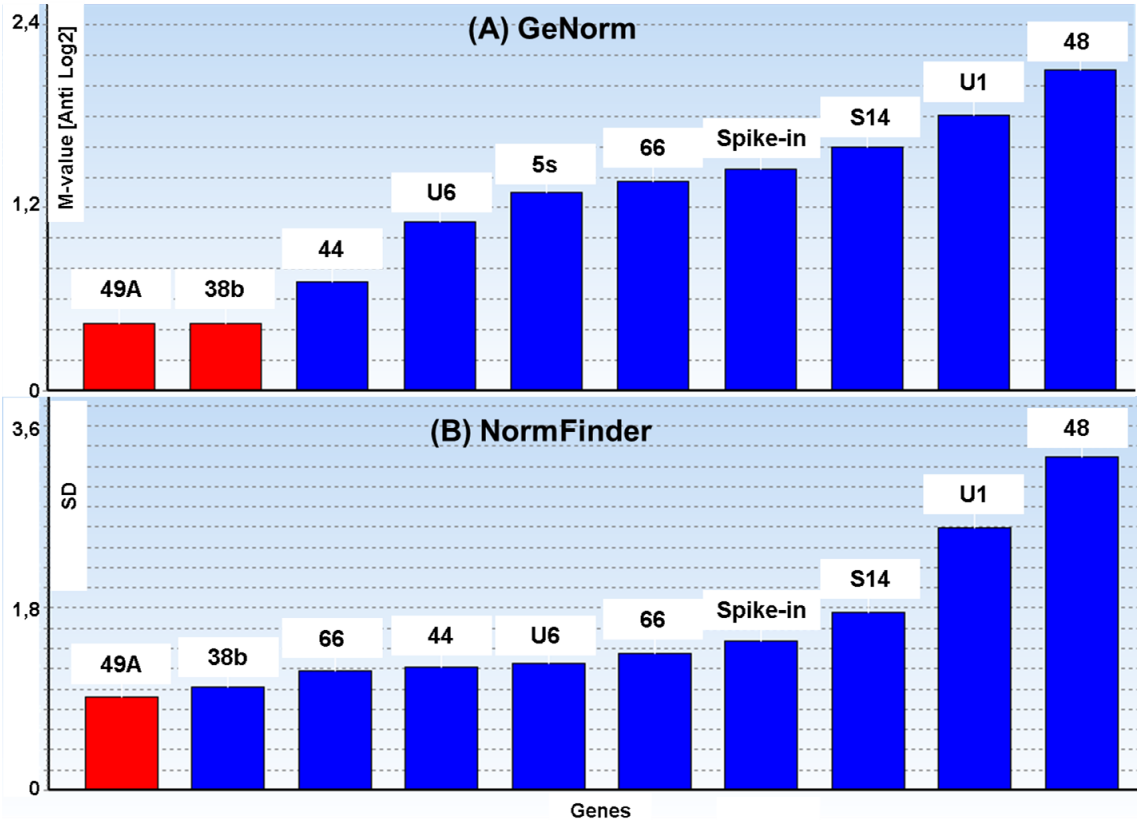

Figure 48

GeNorm (A) and NormFinder (B) analysis was done for SNORD38b, 44, 48, 49A, 66, S14, U1, U6, 5s, and Spike-in in different transduced and non-transduced undifferentiated cells (miR-451+, Ct, NT2). The optimum normalisation gene(s) is/are highlighted in red (n=3).

SNORD38b, SNORD49, U6 and Spike were used for evaluation of suitability as normalisers in miRNA analyses of differentiated transduced and non-transduced cells. Figure 49A-D illustrates mean Ct-values of SNORD38b (A), SNORD49A (B), U6 (C) and Spike-in (D) in non-transduced NT2, Ct cells (Control, Ct) and transduced miR-451+ cells. A significant difference was found between transduced miR-451+ and NT2 in SNORD38b and SNORD49A, whereas no significant difference between miR-451+ and control or NT2 and control was seen (non-parametric Kruskal-Wallis test for independent samples). No significant differences between the groups in U6 and Spike-in were detectable therefore we analysed these 2 genes in neuronal differentiation (Figure 50A-D).

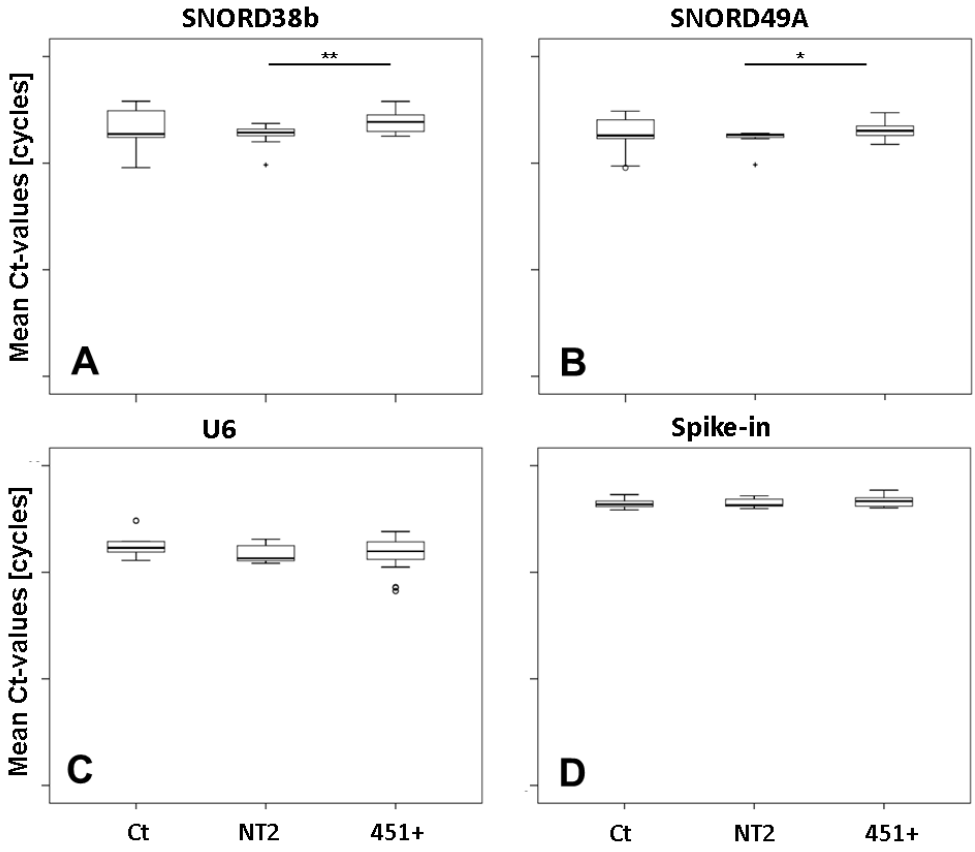

Figure 49

(A) qRT-PCR was done for different normalisation genes SNORD38b, SNORD49A, U6, and Spike-in in different undifferentiated transduced cells (miR-451+, Ct) and non-transduced NT2. The mean Ct-values together with the standard deviation on the y-axis are shown. (Kruskal-Wallis Test for independent samples). * $p \leq 0,05$, ** $p \leq 0,01$. + and ○ mark outlier, (n=3)

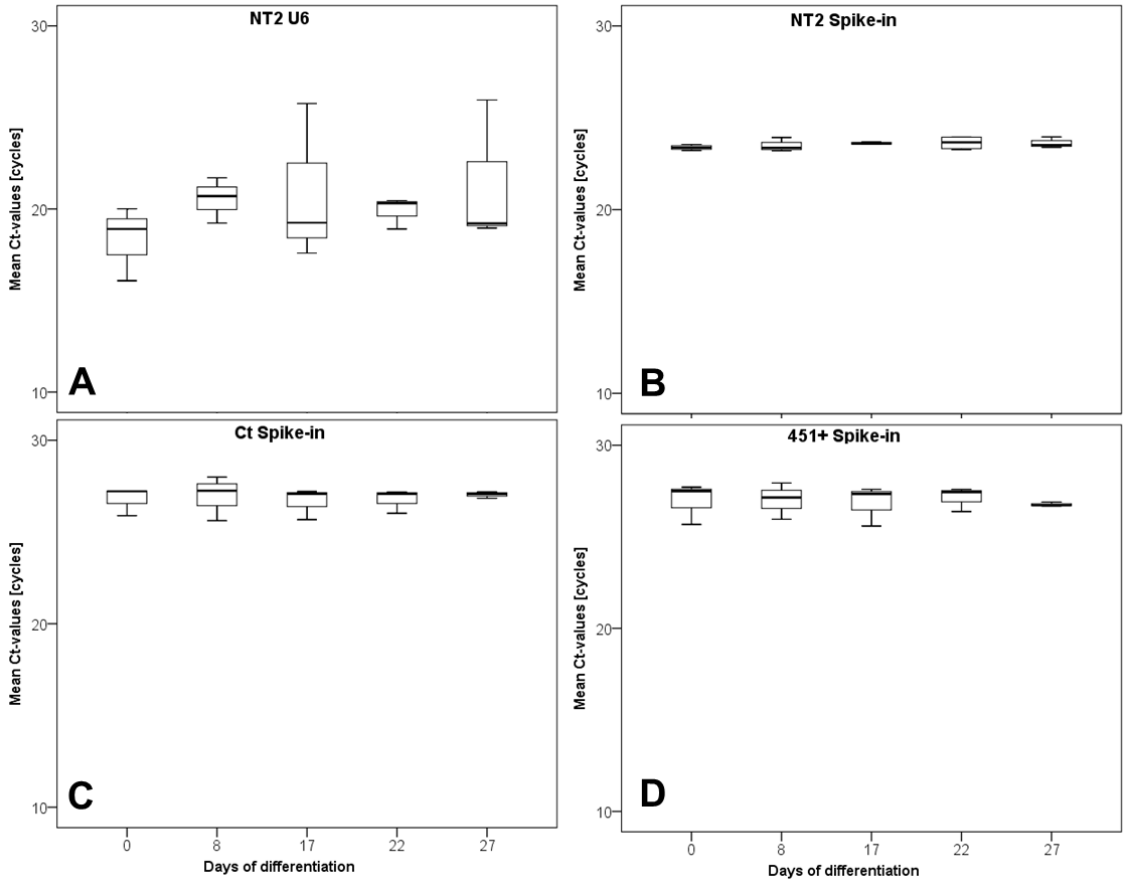

Figure 50

(A) Mean Ct-values on the y-axis for different normalisation genes U6 (A) and Spike-in (B) during neuronal differentiation of non-transduced NT2 (A and B), Ct cells (C) and transduced miR-451+ cells (D). The mean Ct-values together with the standard deviation are shown on the y-axis (n=3)

6.3.2. mRNA analyses

The suitability of different housekeeping genes (TOP1, B2M, UBC, SDHA, RPL13A, YWHAZ, GAPDH, U6, mRNA Spike-in) as normalisation genes in mRNA studies was tested in undifferentiated transduced and non-transduced NT2 (miR-451+ Ct, NT2). In Figure 51 the mean Ct-values together with the standard deviation of the different housekeeping genes are shown. Ct-values were compared statistically with the program MultiD for variability (GeNorm and NormFinder analysis, Figure 52A and B). UBC and YHWAZ were chosen as the best normalisation combination in GeNorm. NormFinder selected YHWAZ as the least variable gene.

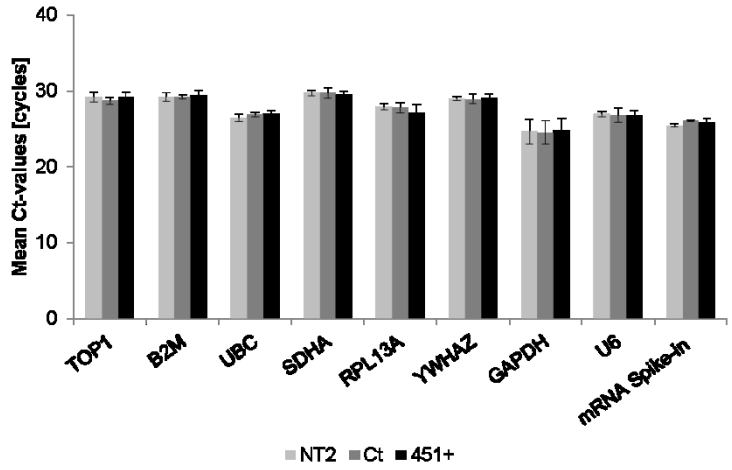

Figure 51

Mean values together with the standard deviation of TOP1, B2M, UBC, SDHA, RPL13A, YWHAZ, GAPDH, U6 and mRNA Spike-in in transduced and non-transduced undifferentiated cells (miR-451+, Ct, NT2). n=3.

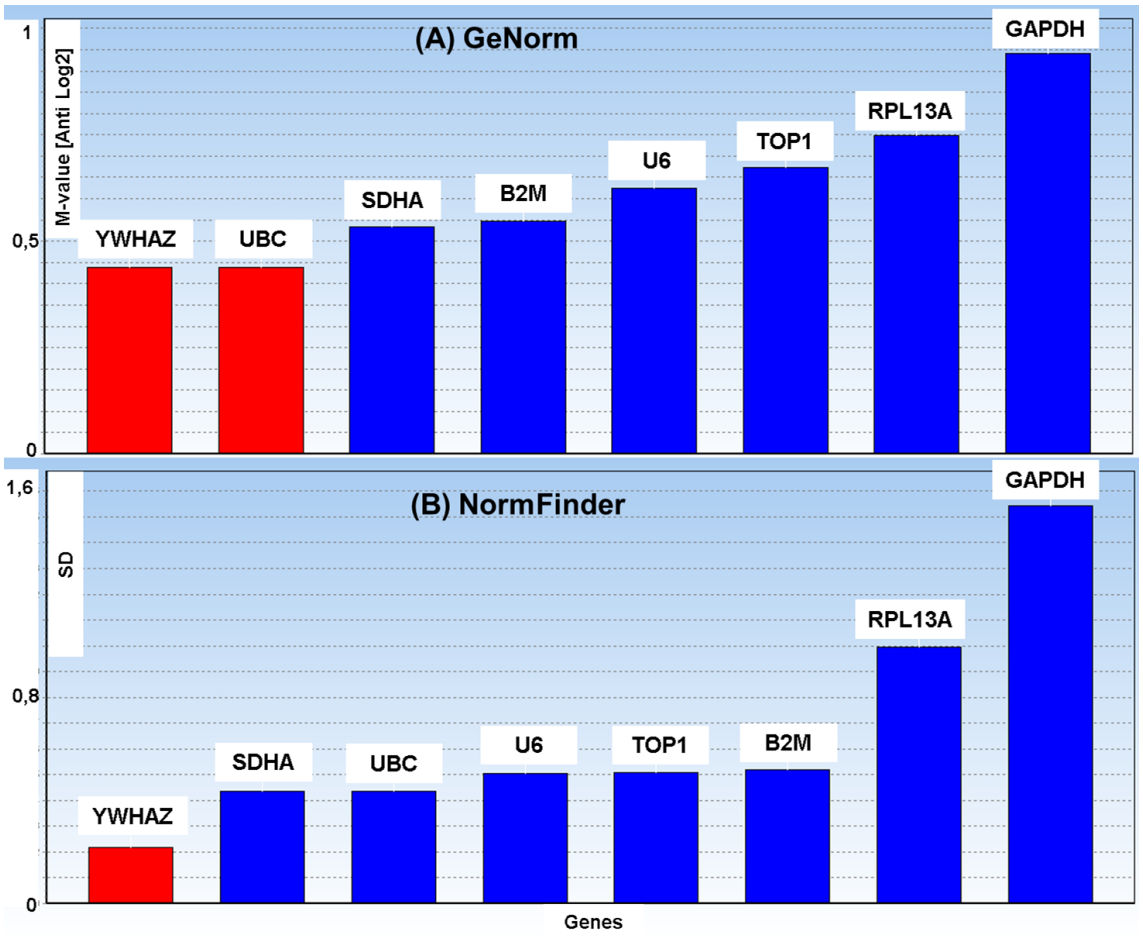

Figure 52

GeNorm (A) and NormFinder (B) analysis after qRT-PCR (n=6) was done for normalisation genes YWHAZ, UBC, SDHA, B2M, U6, TOP1, RPL13A and GAPDH in different transduced cells (miR-451+ and Ct). The optimum normalisation gene(s) is/are highlighted in red. (SD = standard deviation), (n=3)

UBC and mRNA Spike-in were chosen for further analyses in neuronal differentiation of non-transduced NT2 (A1, A2), Ct cells (Ct, B1, B2) and transduced miR-451+ cells (C1, C2) Figure 53. There are no significant differences in Ct-values at the different differentiation days in UBC and mRNA Spike-in. The standard deviation is higher in UBC compared to mRNA Spike-in.

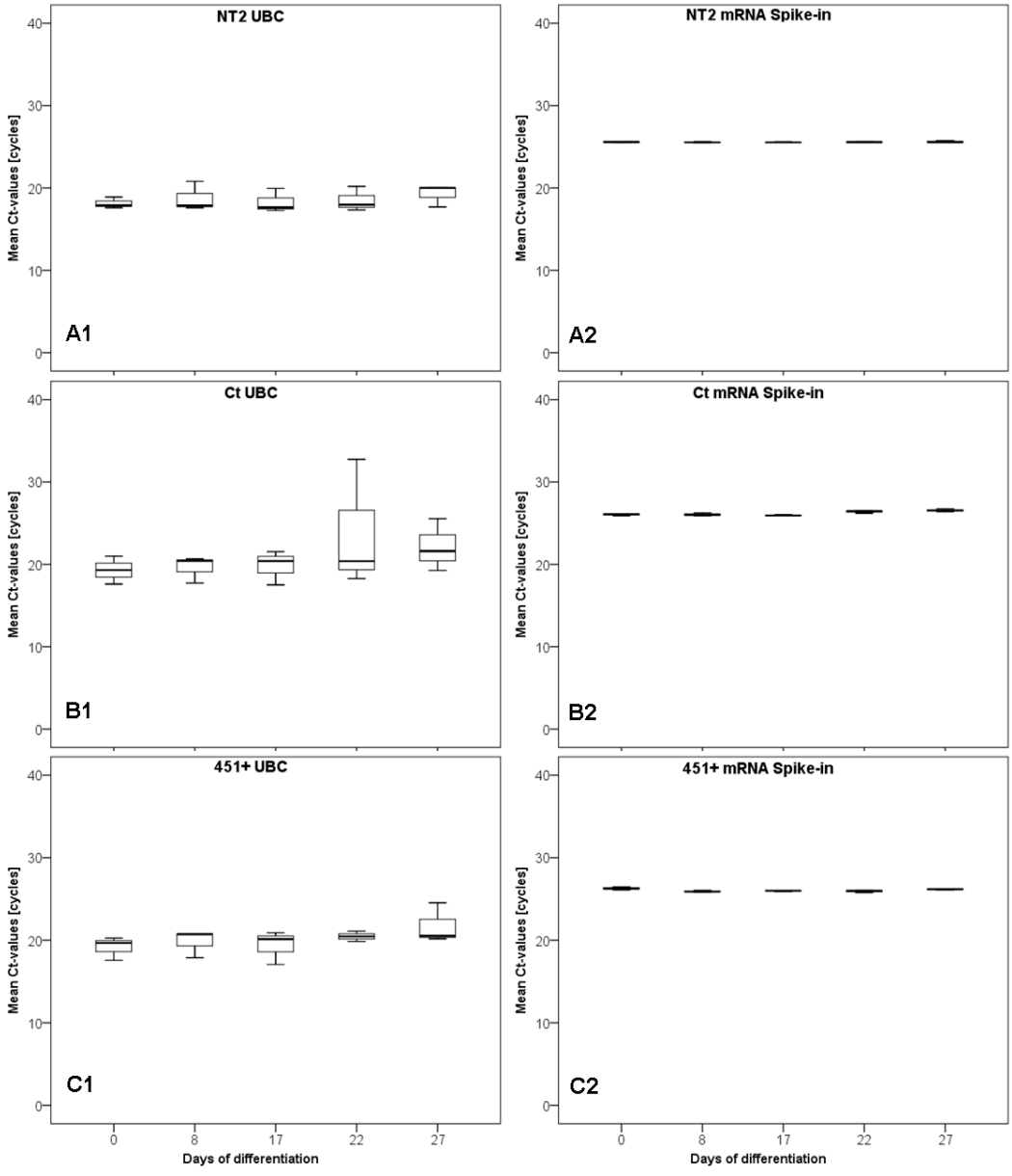

Figure 53

The mean Ct-value together with the standard deviation of UBC (A1, B1, C1) and mRNA Spike-in (A2, B2, C2) during neuronal differentiation of non-transduced NT2 (A1, A2), Ct cells (B1, B2) and transduced miR-451+ cells is shown.

6.4. Calculation of the copy number of miR-451

For the calculation of the copy number/20ng used miRNA we had to establish a standard curve with miR-451 mimics. Figure 54 shows the resulting graph and the formula, by which the copy number was calculated. Data was normalized as described as by (160).

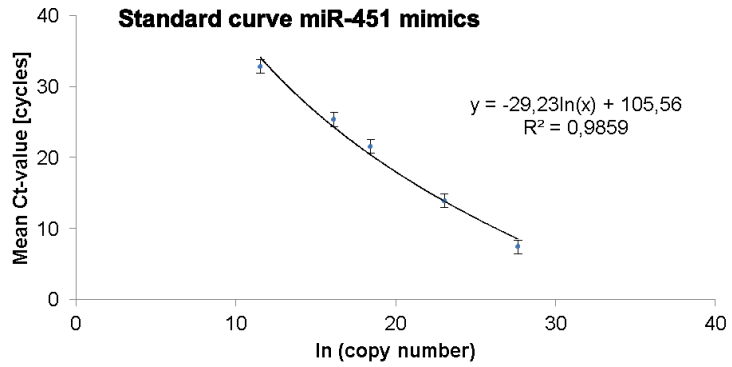

Figure 54
Standard curve of miR-451 mimics used for calculation of the copy number of miR-451 in the different non-transduced and transduced undifferentiated and differentiated NT2.

6.5. Neuronal differentiation of NT2

immuno-fluorescent stainings for DCX (A), Tuj1 (C), MAP2 (E) and NF (G) of differentiating NT2 cells at day 22 (Figure 55, Figure 57, Figure 59) and day 28 (Figure 56, Figure 58, Figure 60) were performed. A negative control (incubation only with the secondary antibody) was included in every condition.

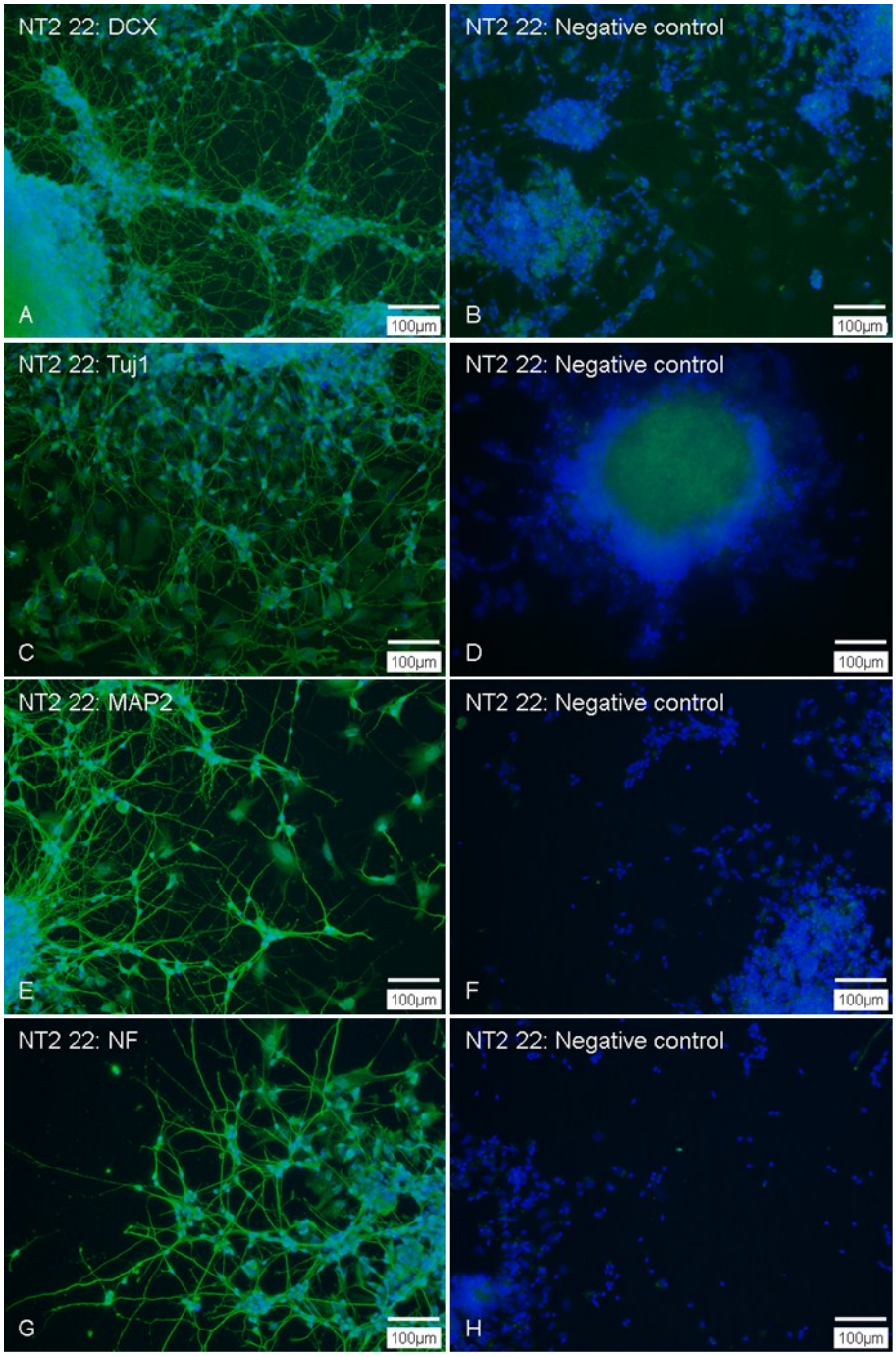

Figure 55

Immunostaining of markers (A) DCX, (B) Tuj1, (C) MAP2 and (D) NF in NT2 at day 22. (B), (D), (F) and (H) negative controls. Pictures are 20x and were taken with a fluorescence microscope (Olympus, Hicksville, New York, USA).

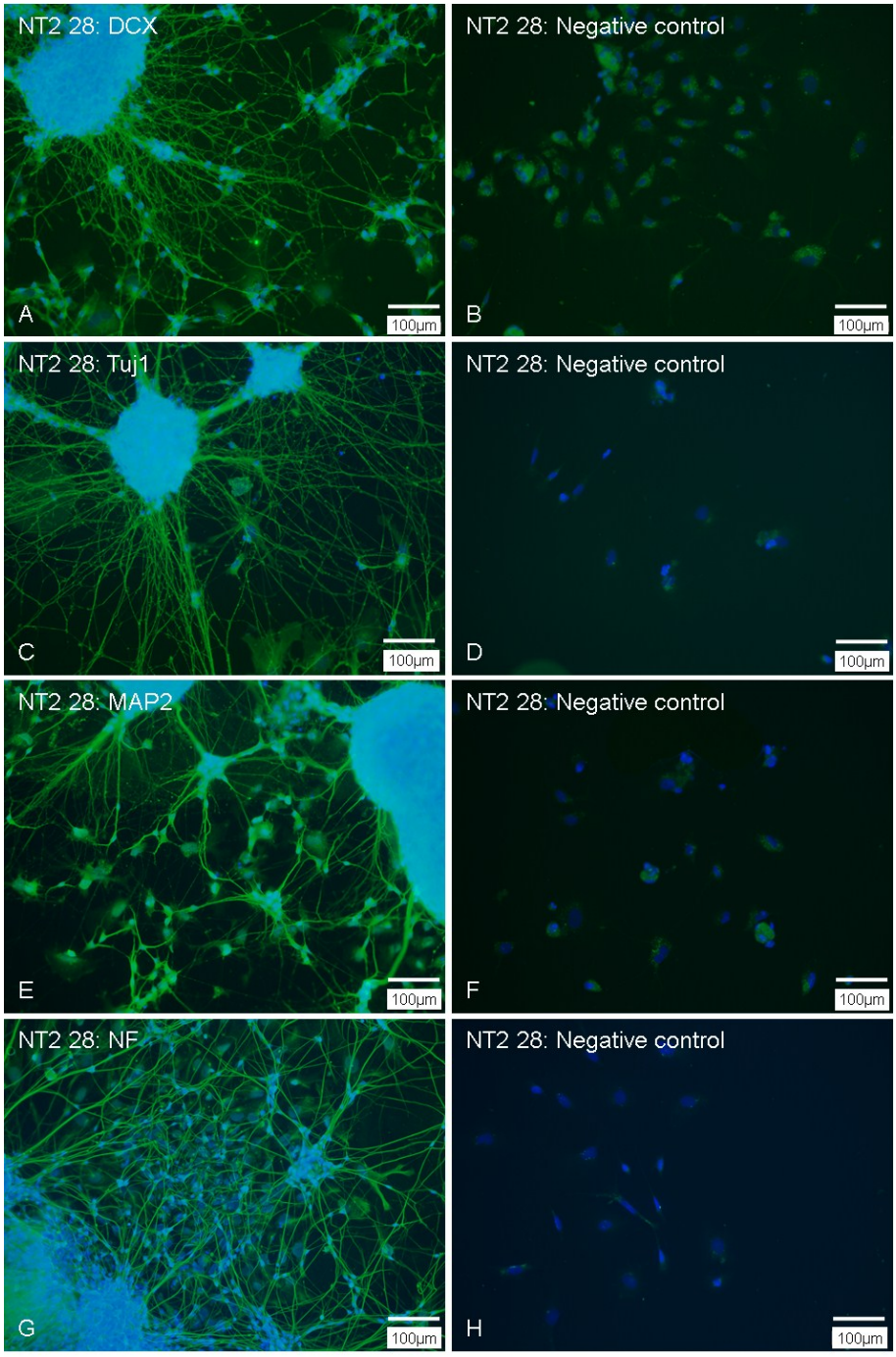

Figure 56

Immunostaining of markers (A) DCX, (B) Tuj1, (C) MAP2 and (D) NF in non-transduced NT2 at day 28. (B), (D), (F) and (H) negative controls. Pictures are 20x and were taken with a fluorescence microscope (Olympus, Hicksville, New York, USA).

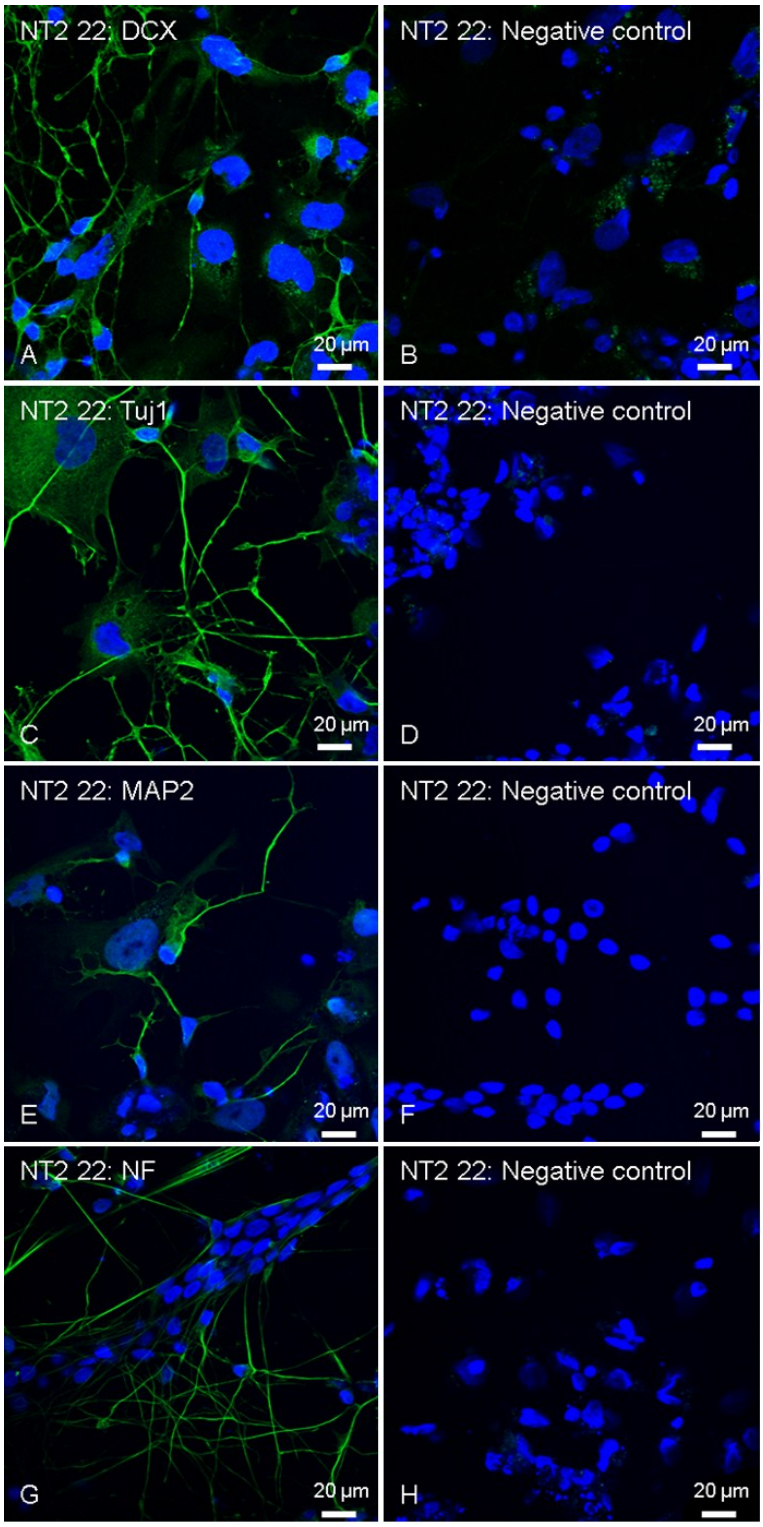

Figure 57

Immunostaining of markers (A) DCX, (B) Tuj1, (C) MAP2 and (D) NF in non-transduced NT2 at day 22. (B), (D), (F) and (H) negative controls. Pictures are 40x and were taken with LSM, Zeiss, Oberkochen, Germany).

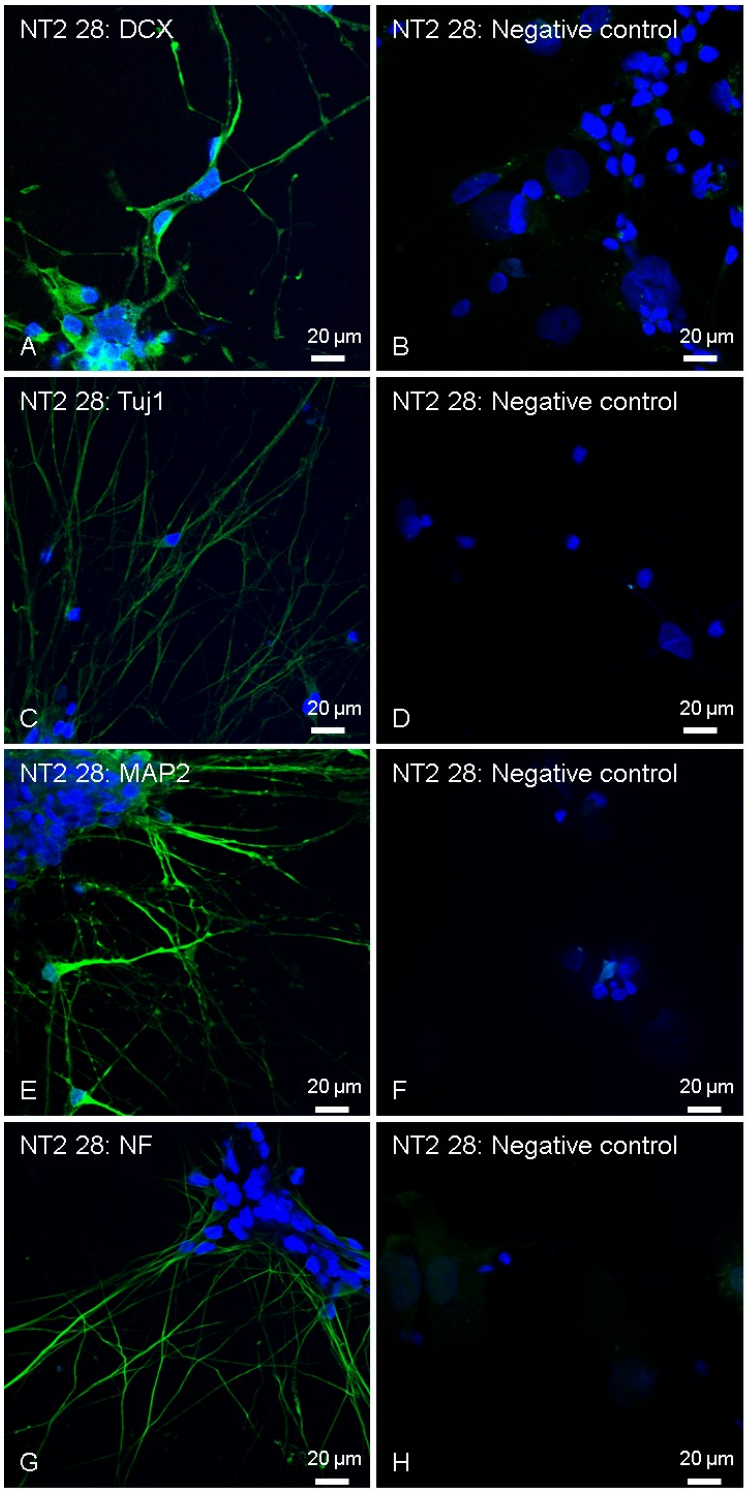

Figure 58

Immunostaining of markers (A) DCX, (B) Tuj1, (C) MAP2 and (D) NF in non-transduced NT2 at day 28. (B), (D), (F) and (H) negative controls. Pictures are 40x and were taken with LSM, Zeiss, Oberkochen, Germany).

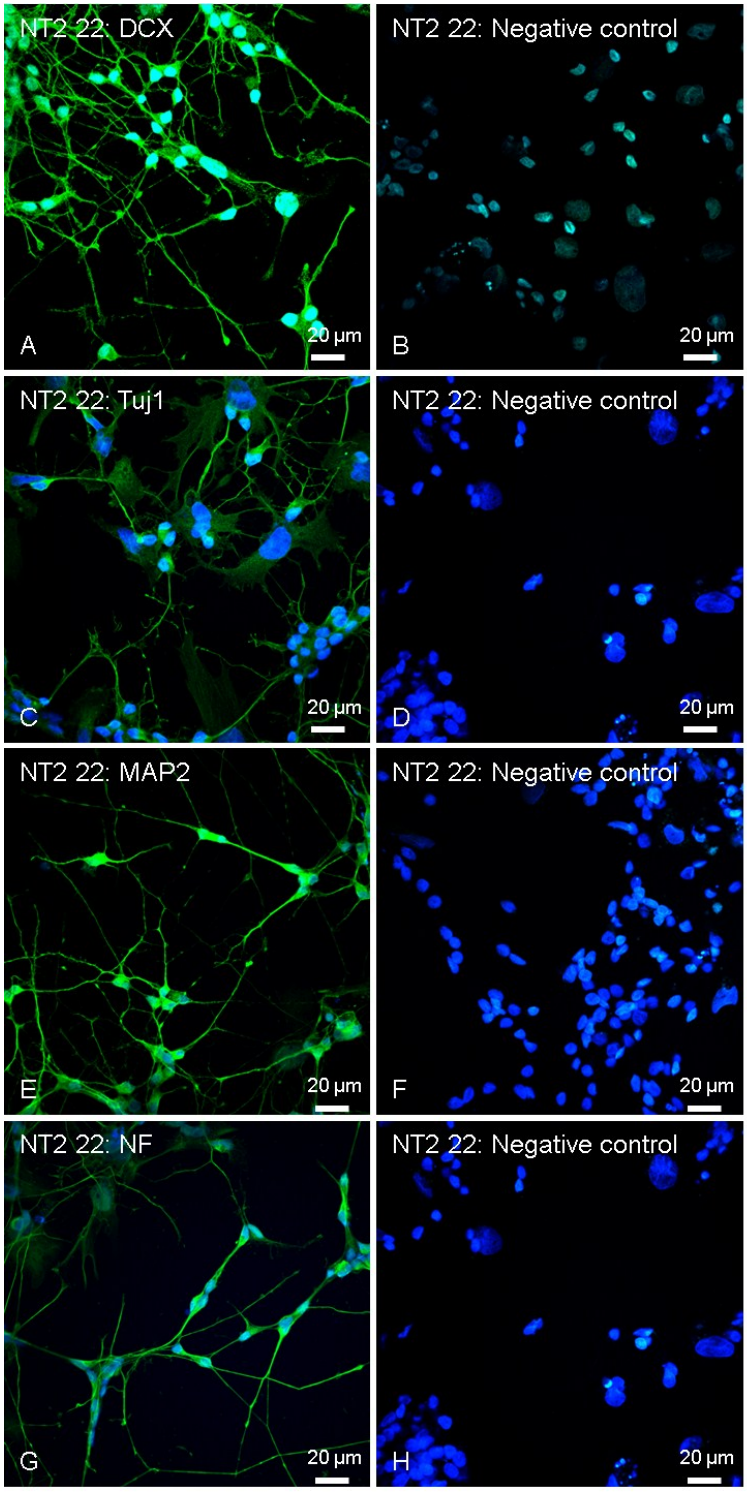

Figure 59

Immunostaining of markers (A) DCX, (B) Tuj1, (C) MAP2 and (D) NF NT2 at day 22. (B), (D), (F) and (H) negative controls. Pictures are 40x and were taken with LSM Nikon (Vienna, Austria).

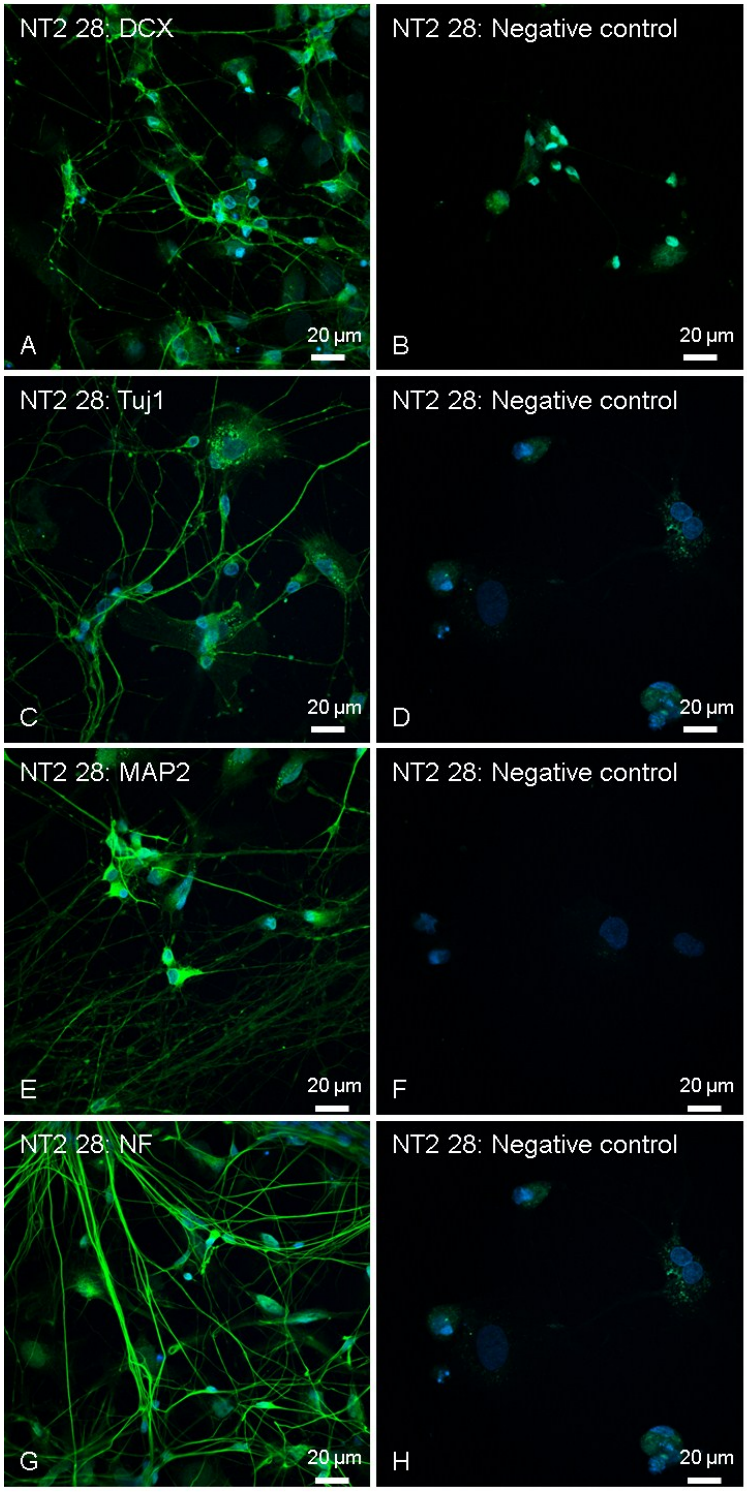

Figure 60

Immunostaining of markers (A) DCX, (B) Tuj1, (C) MAP2 and (D) NF in non-transduced NT2 at day 28. (B), (D), (F) and (H) negative controls. Pictures are 40x and were taken with Nikon (Vienna, Austria).

6.6. Immunofluorescence – differences between Ct and miR-451+

Immuno-fluorescent staining for DCX (Figure 61 until Figure 63), Tuj1 (Figure 64 until Figure 66), MAP2 (Figure 67 until Figure 69) and NF (Figure 70 until Figure 72) of differentiating transduced cells at day 22 (A, C, E and G) and day 28 (B, D, F and H) were performed. A negative control (incubation only with the secondary antibody) was included in every condition.

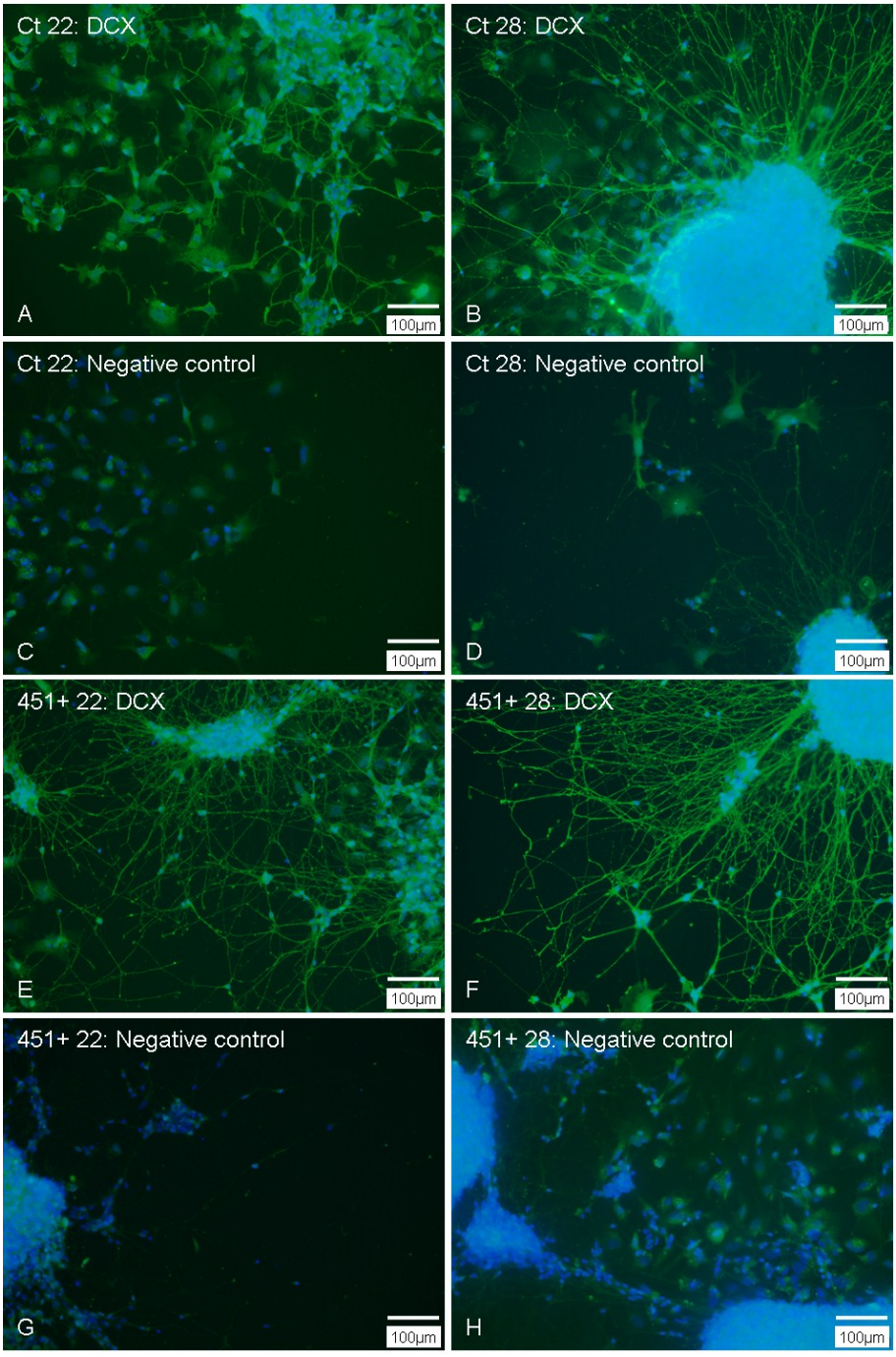

Figure 61 Immunostaining of DCX together with DAPI: Ct cells (A-D) and transduced miR-451+ cells (E-H) at day 22 (A, C, E, G) and 28 (B, D, F; H) Negative controls are shown in C, D, G and H. All pictures are 20x and were taken with a fluorescence microscope (Olympus, Hicksville, New York, USA)

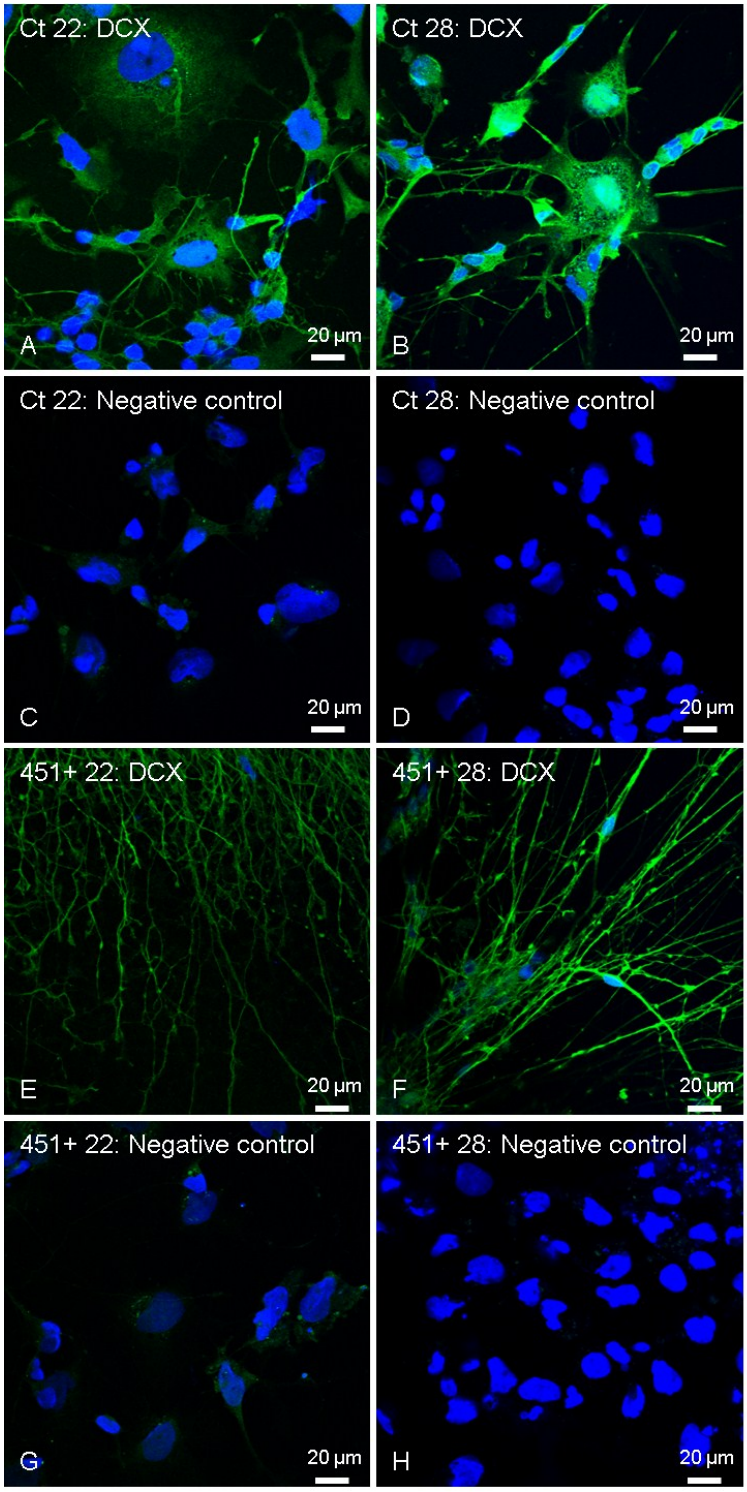

Figure 62

Immunostaining of DCX together with DAPI: Ct cells (A-D) and transduced miR-451+ cells (E-H) at day 22 (A, C, E, G) and 28 (B, D, F; H) Negative controls are shown in C, D, G and H. All pictures are 40x and were taken with LSM Zeiss, Oberkochen Germany).

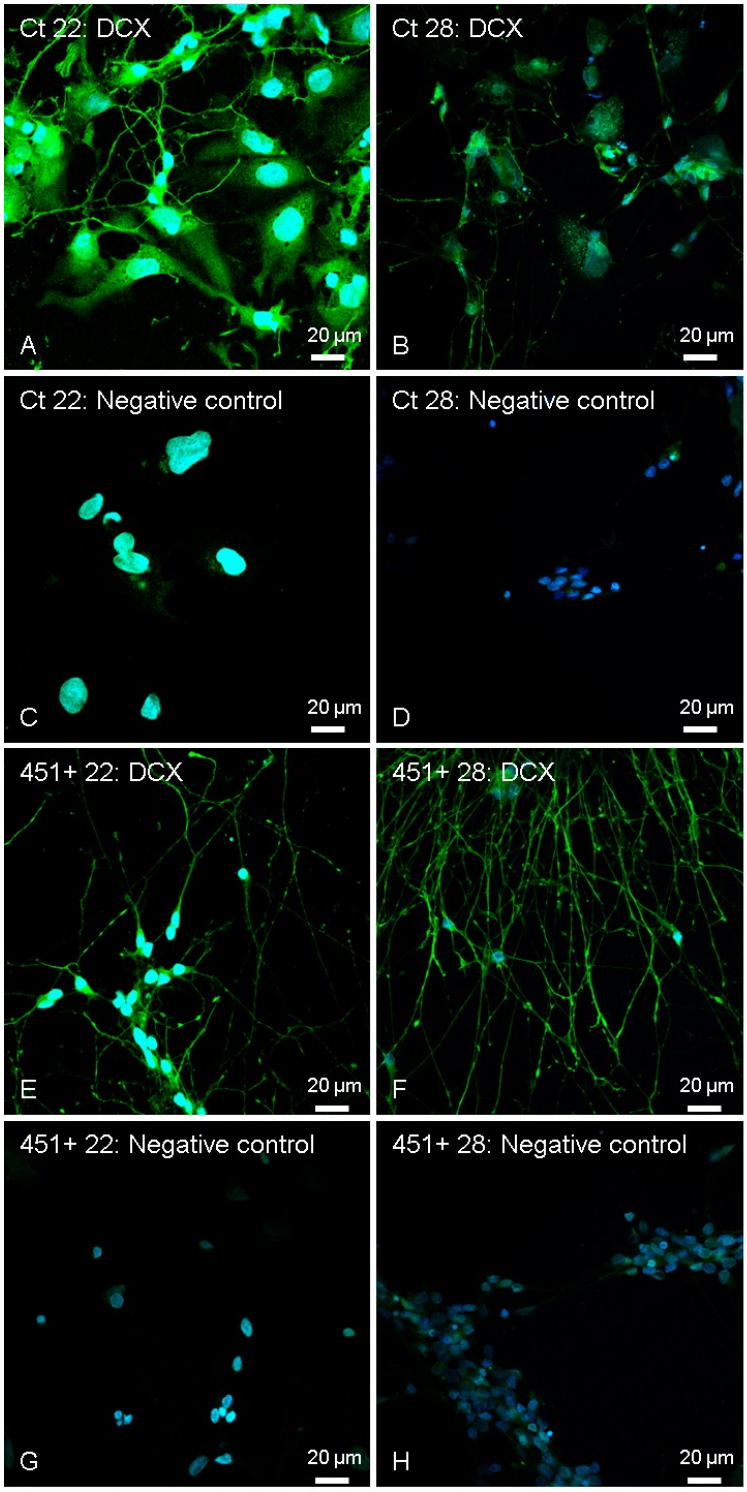

Figure 63

Immunostaining of DCX together with DAPI: Ct cells (A-D) and transduced miR-451+ cells (E-H) at day 22 (A, C, E, G) and 28 (B, D, F; H) Negative controls are shown in C, D, G and H. All pictures are 40x and were taken with Nikon, Vienna, Austria).

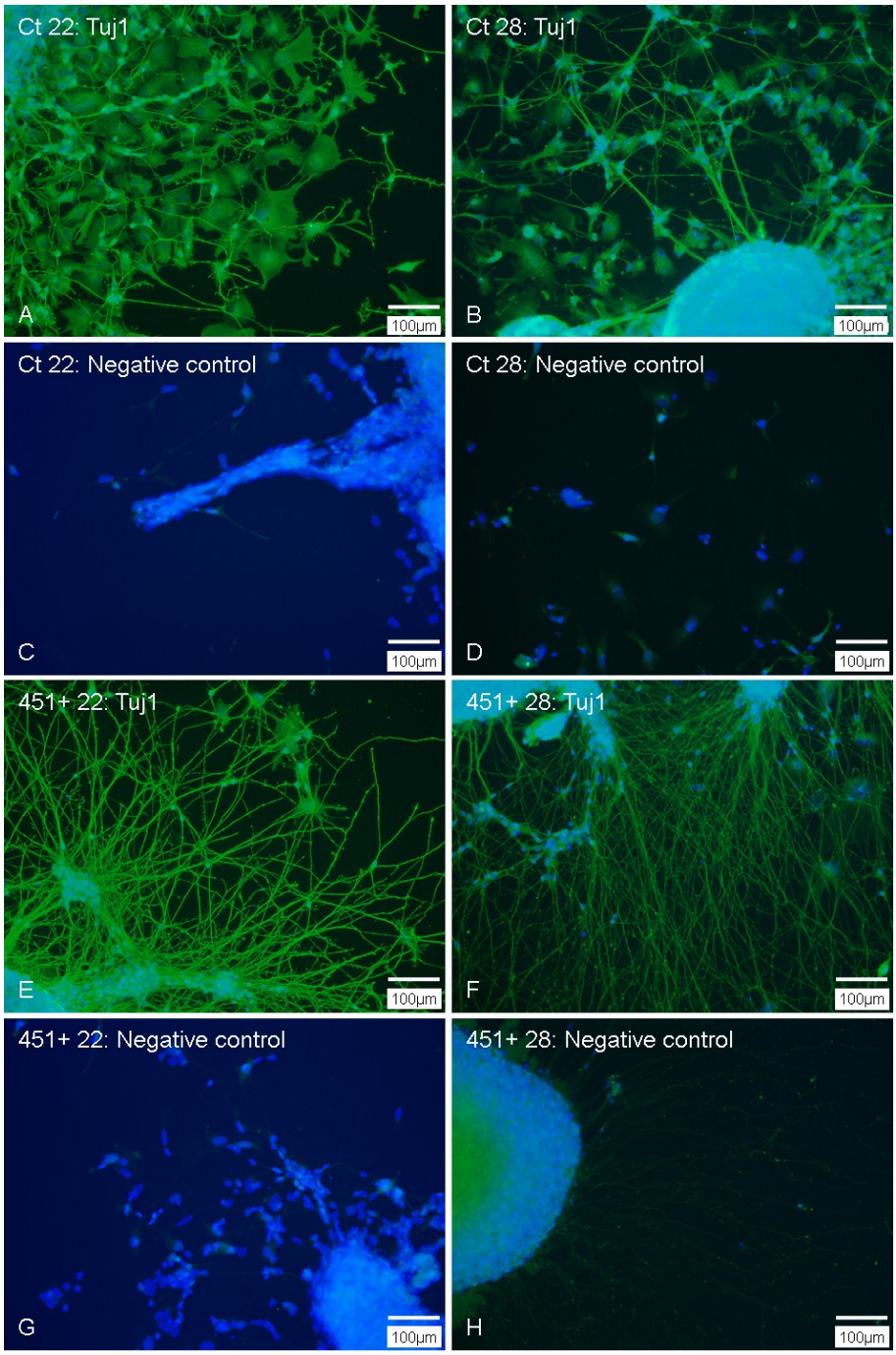

Figure 64

Immunostaining of Tuj1 together with DAPI: Ct cells (A-D) and transduced miR-451+ cells (E-H) at day 22 (A, C, E, G) and 28 (B, D, F; H) Negative controls are shown in C, D, G and H. All pictures are 20x and were taken with a fluorescence microscope (Olympus, Hicksville, New York, USA)

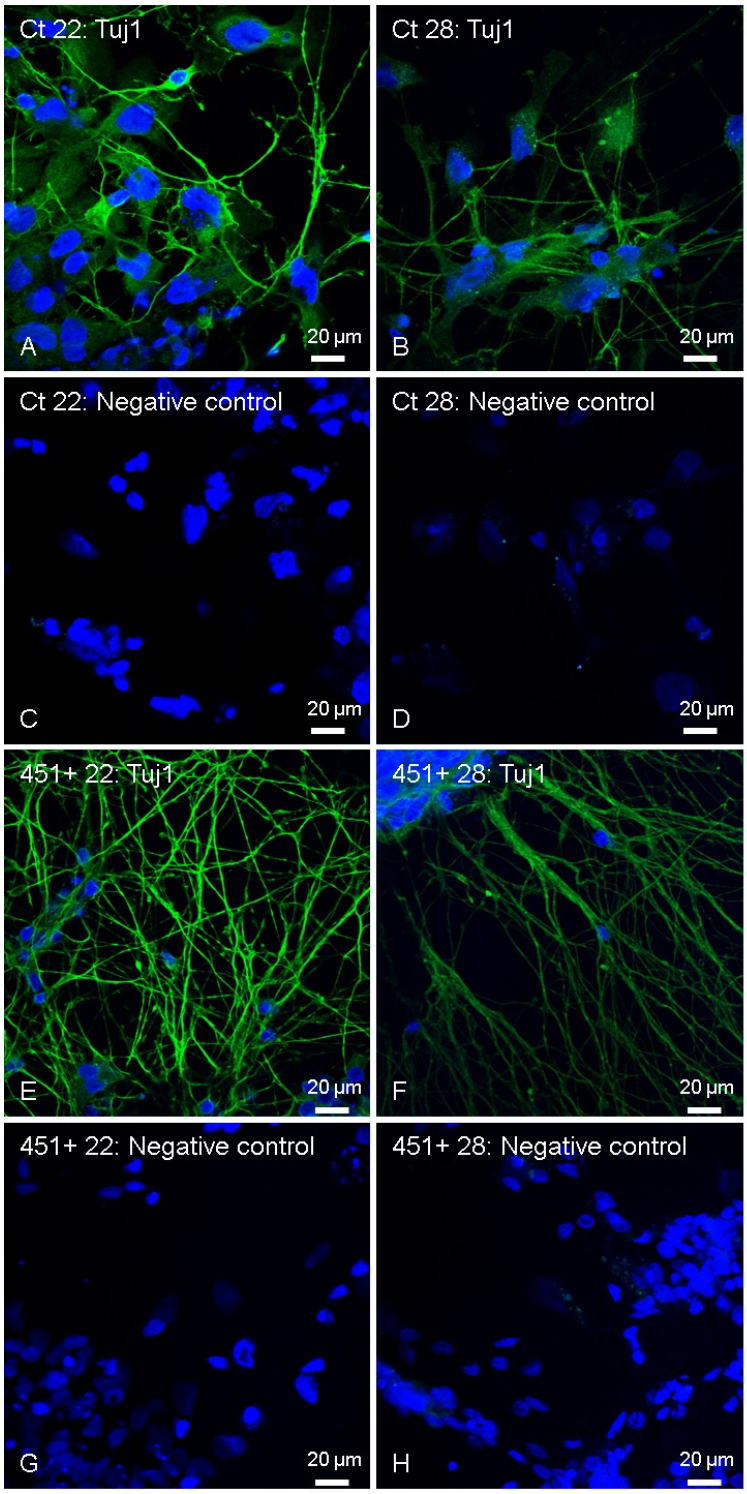

Figure 65

Immunostaining of Tuj1 together with DAPI: Ct cells (A-D) and transduced miR-451+ cells (E-H) at day 22 (A, C, E, G) and 28 (B, D, F; H) Negative controls are shown in C, D, G and H. All pictures are 40x and were taken with LSM Zeiss, Oberkochen Germany).

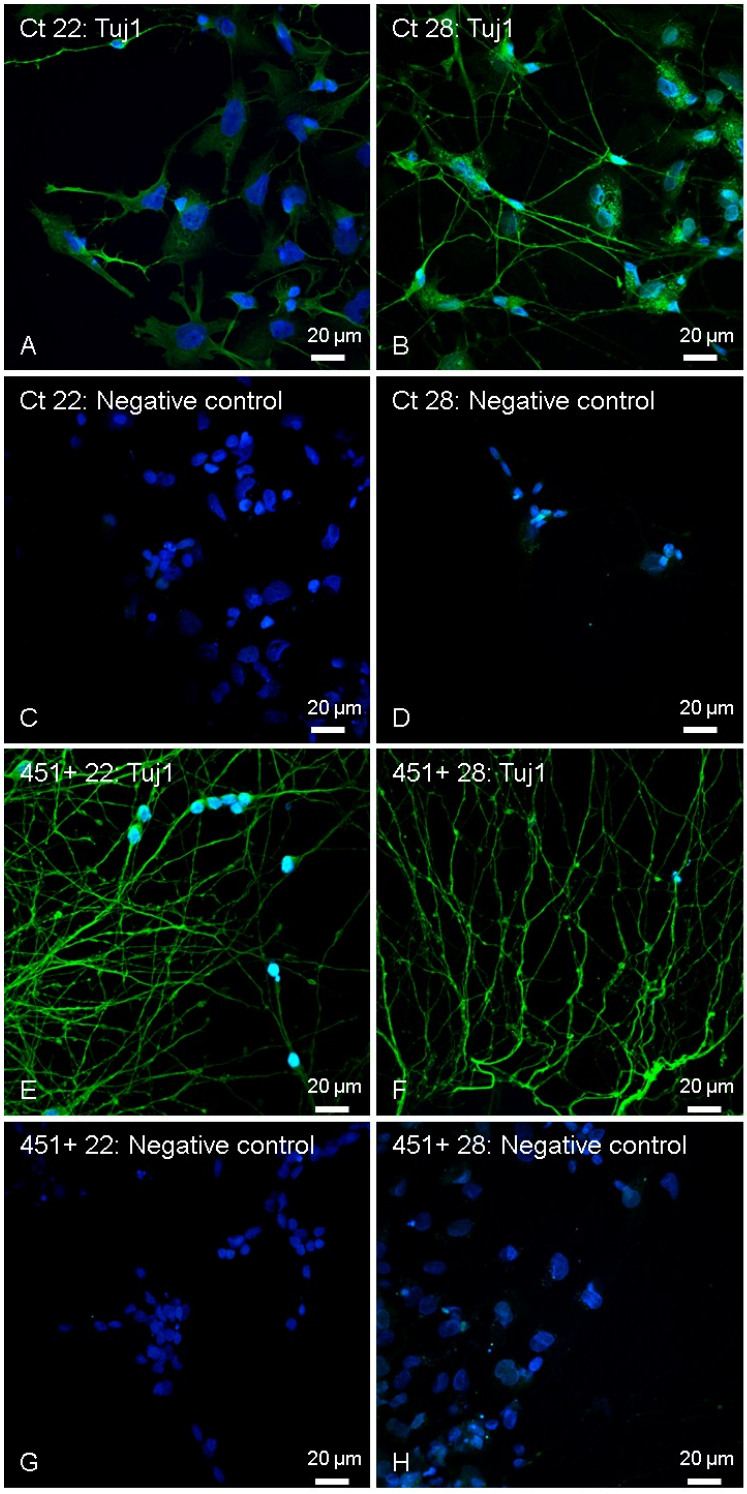

Figure 66

Immunostaining of Tuj1 together with DAPI: Ct cells (A-D) and transduced miR-451+ cells (E-H) at day 22 (A, C, E, G) and 28 (B, D, F; H) Negative controls are shown in C, D, G and H. All pictures are 40x and were taken with Nikon (Vienna, Austria)

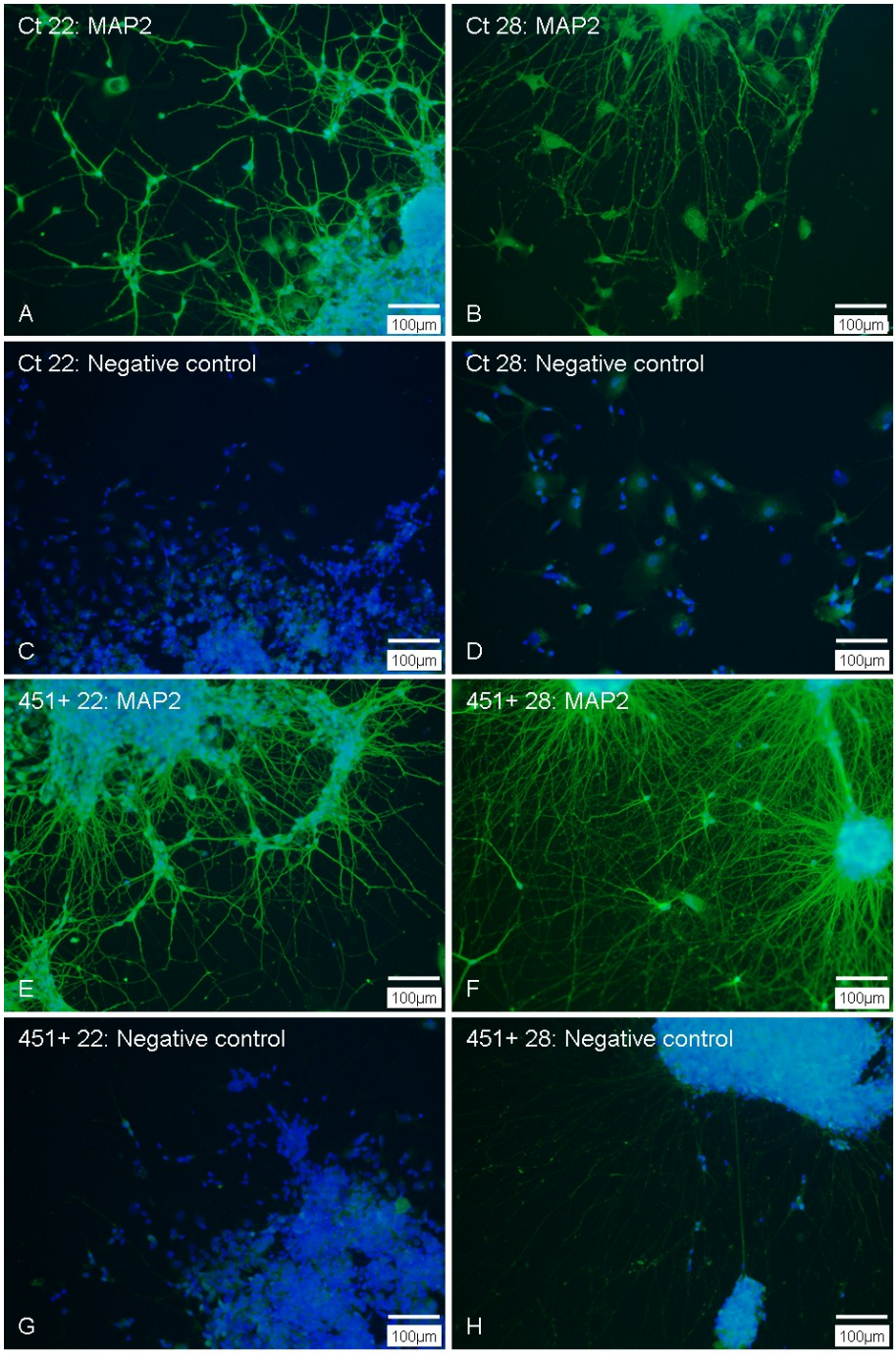

Figure 67

Immunostaining of MAP2 together with DAPI stain: Ct cells (A-D) and transduced miR-451+ cells (E-H) at day 22 (A, C, E, G) and 28 (B, D, F; H) Negative controls are shown in C, D, G and H. All pictures are 20x and were taken with a fluorescence microscope (Olympus, Hicksville, New York, USA)

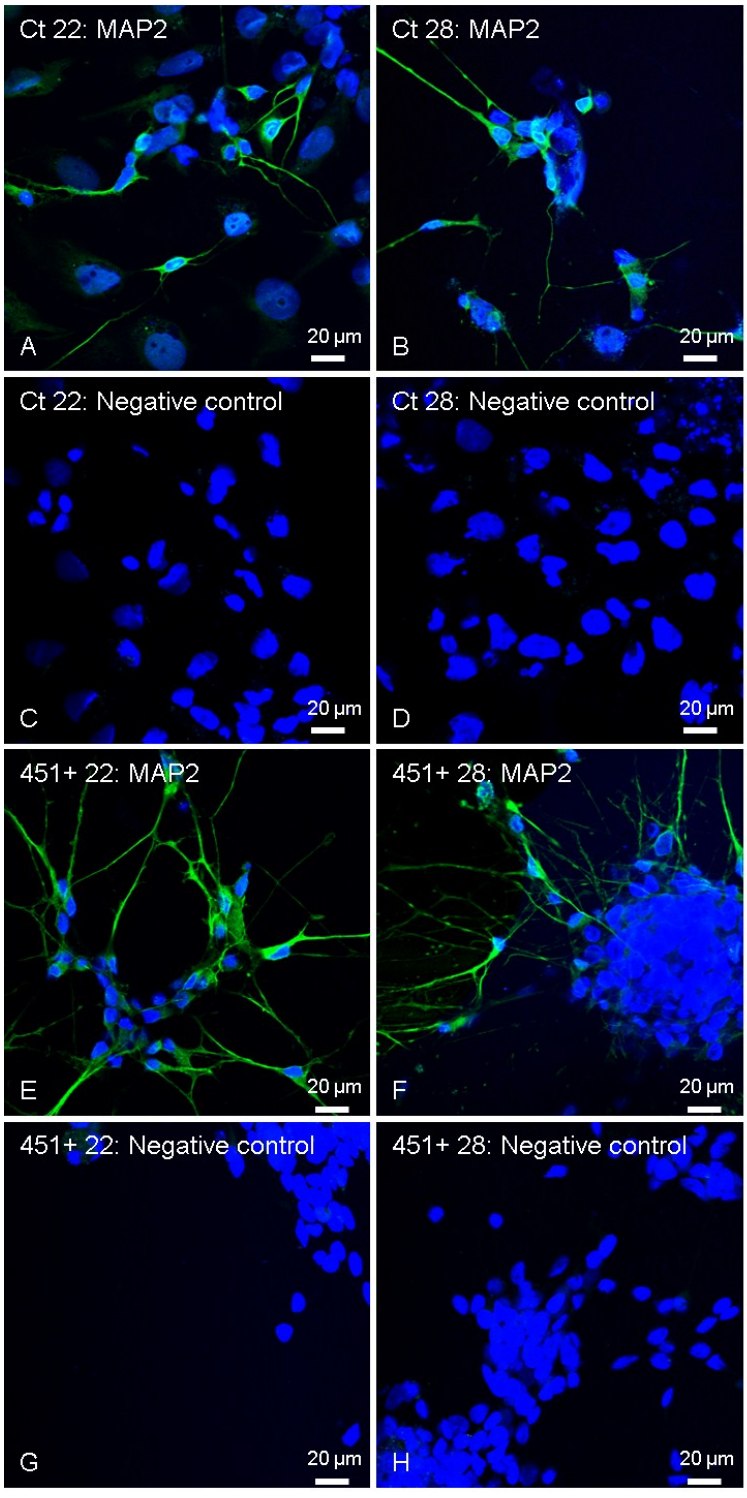

Figure 68

Immunostaining of MAP2 together with DAPI: Ct cells (A-D) and transduced miR-451+ cells (E-H) at day 22 (A, C, E, G) and 28 (B, D, F; H) Negative controls are shown in C, D, G and H. All pictures are 40x and were taken with LSM Zeiss, Oberkochen Germany).

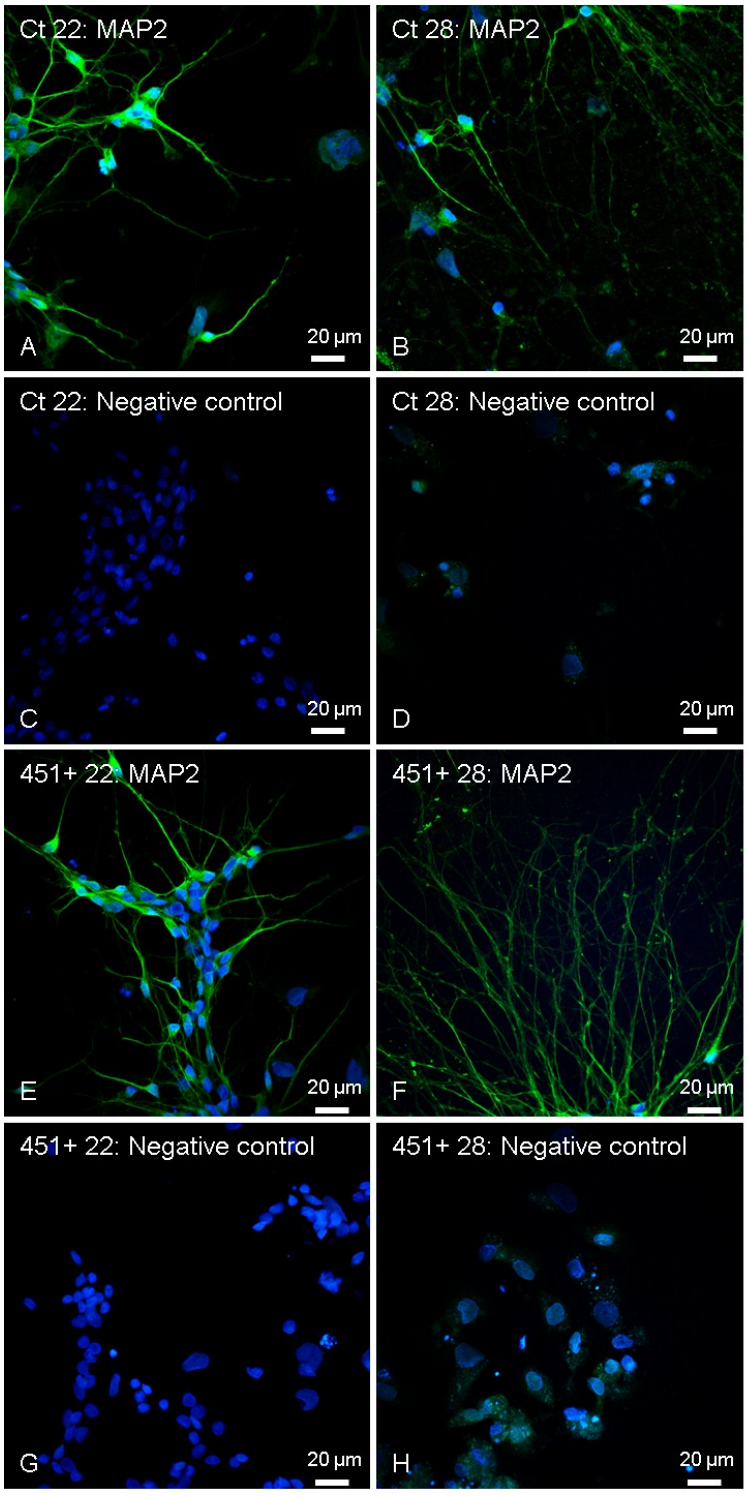

Figure 69

Immunostaining of MAP2 together with DAPI: Ct cells (A-D) and transduced miR-451+ cells (E-H) at day 22 (A, C, E, G) and 28 (B, D, F; H) Negative controls are shown in C, D, G and H. All pictures are 40x and were taken with LSM Nikon, Vienna, Austria).

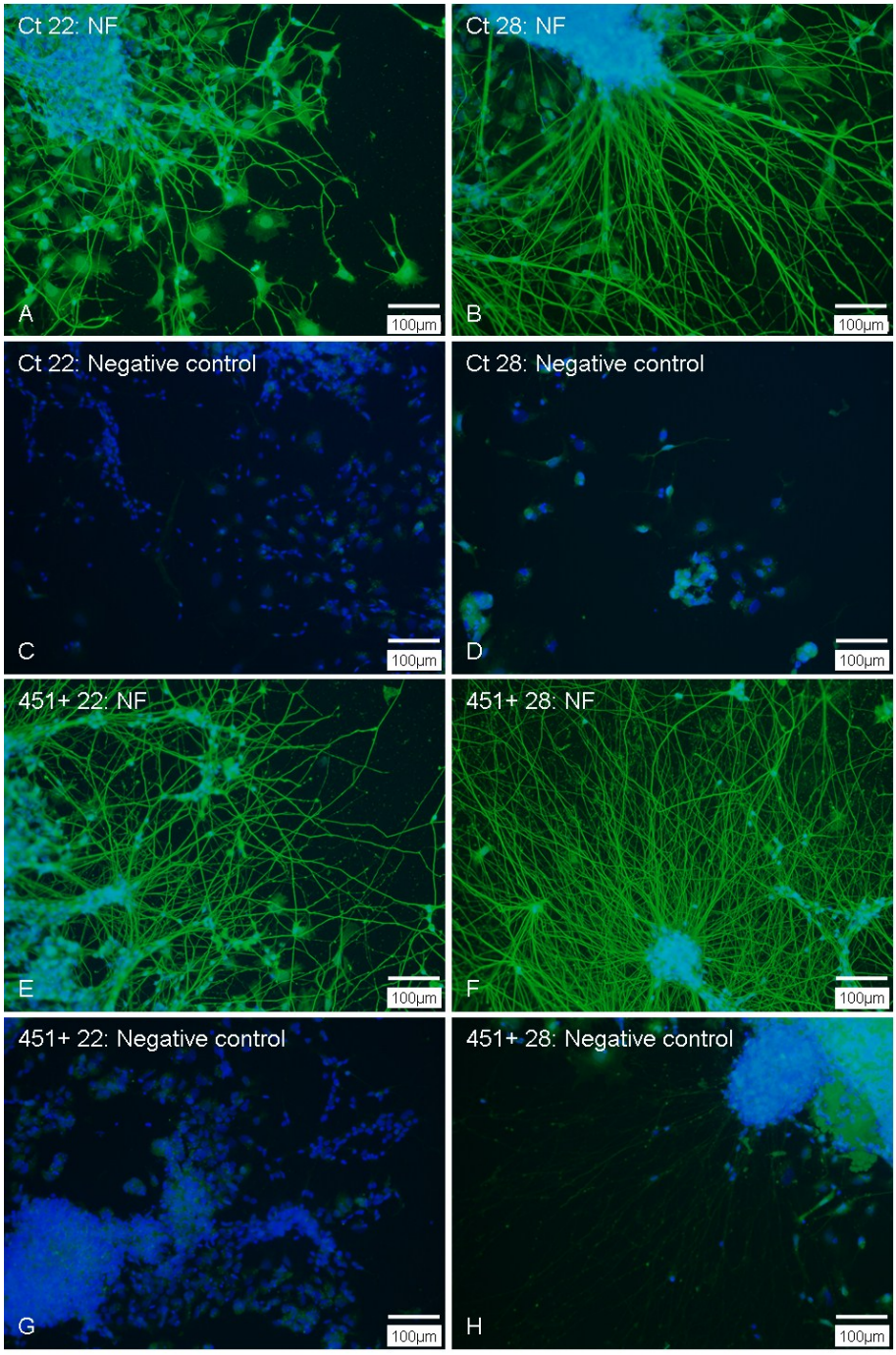

Figure 70

Immunostaining of NF together with DAPI stain: Ct cells (A-D) and transduced miR-451+ cells (E-H) at day 22 (A, C, E, G) and 28 (B, D, F; H) Negative controls are shown in C, D, G and H. All pictures are 20x and were taken with a fluorescence microscope (Olympus, Hicksville, New York, USA)

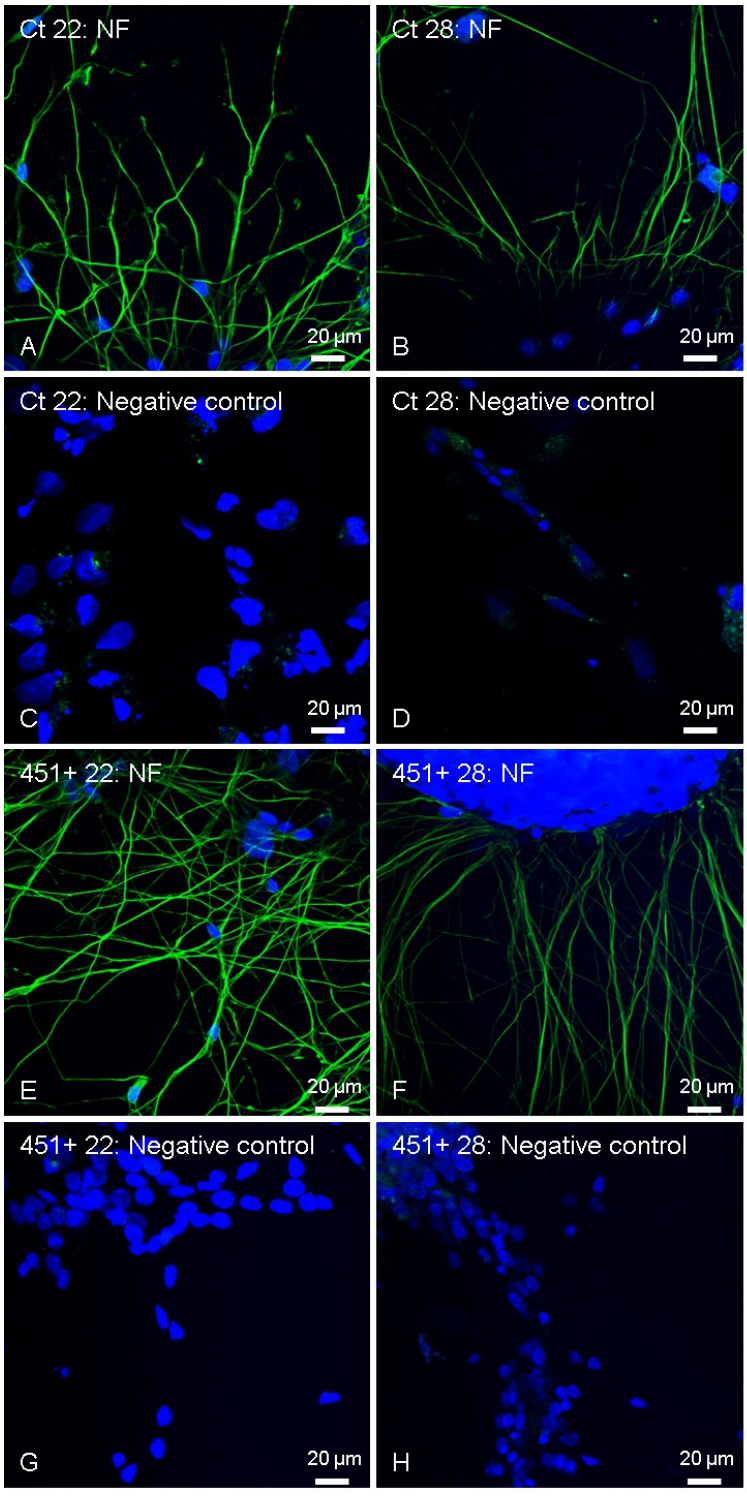

Figure 71

Immunostaining of NF together with DAPI: Ct cells (A-D) and transduced miR-451+ cells (E-H) at day 22 (A, C, E, G) and 28 (B, D, F; H) Negative controls are shown in C, D, G and H. All pictures are 40x and were taken with LSM Zeiss, Oberkochen Germany).

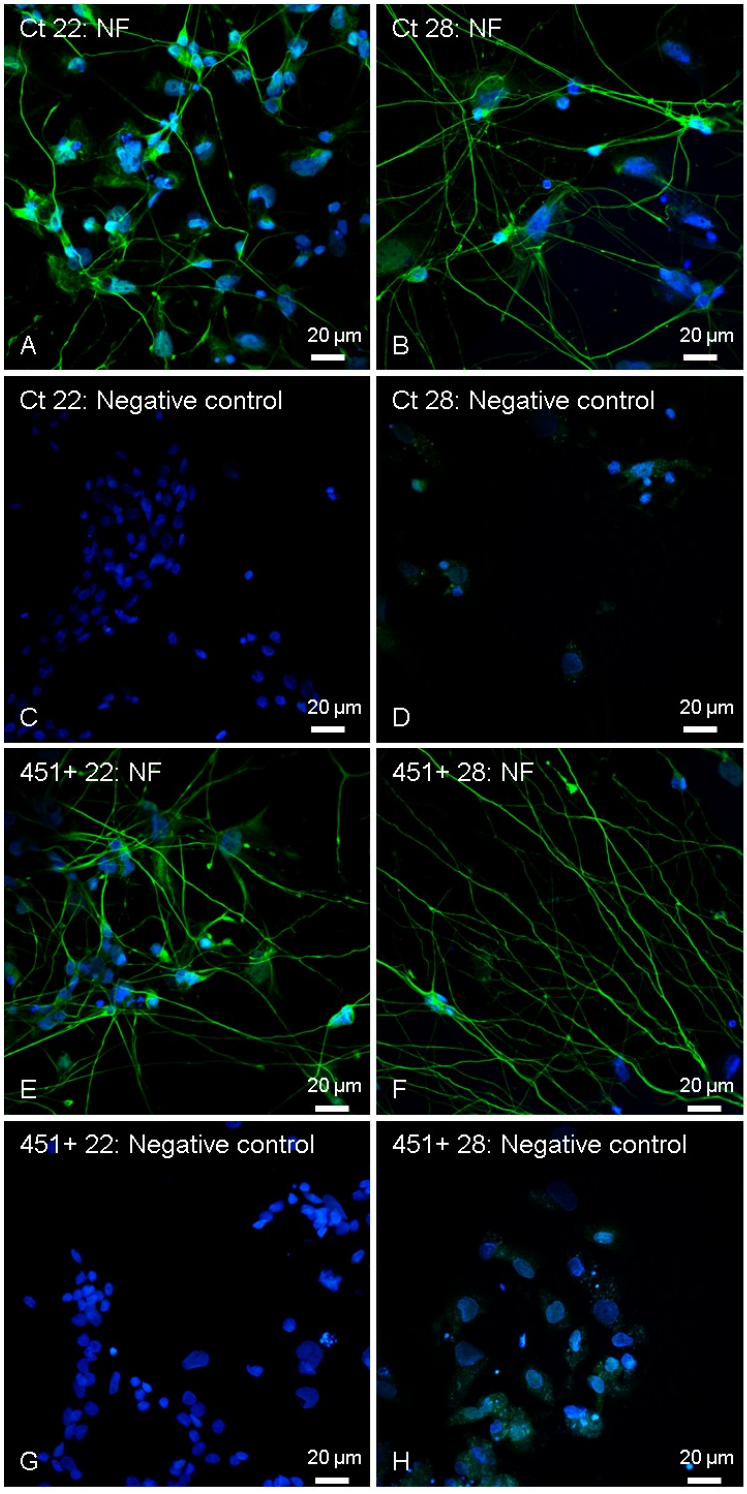

Figure 72

Immunostaining of NF together with DAPI: Ct cells (A-D) and transduced miR-451+ cells (E-H) at day 22 (A, C, E, G) and 28 (B, D, F; H) Negative controls are shown in C, D, G and H. All pictures are 40x and were taken with Nikon (Vienna, Austria)

6.7. Immunofluorescence – TNS4 Staining

Immunostaining was performed for TNS4 at day 22 and 28 of differentiating NT2 (A), Ct (C) and miR-451+ (E) cells.

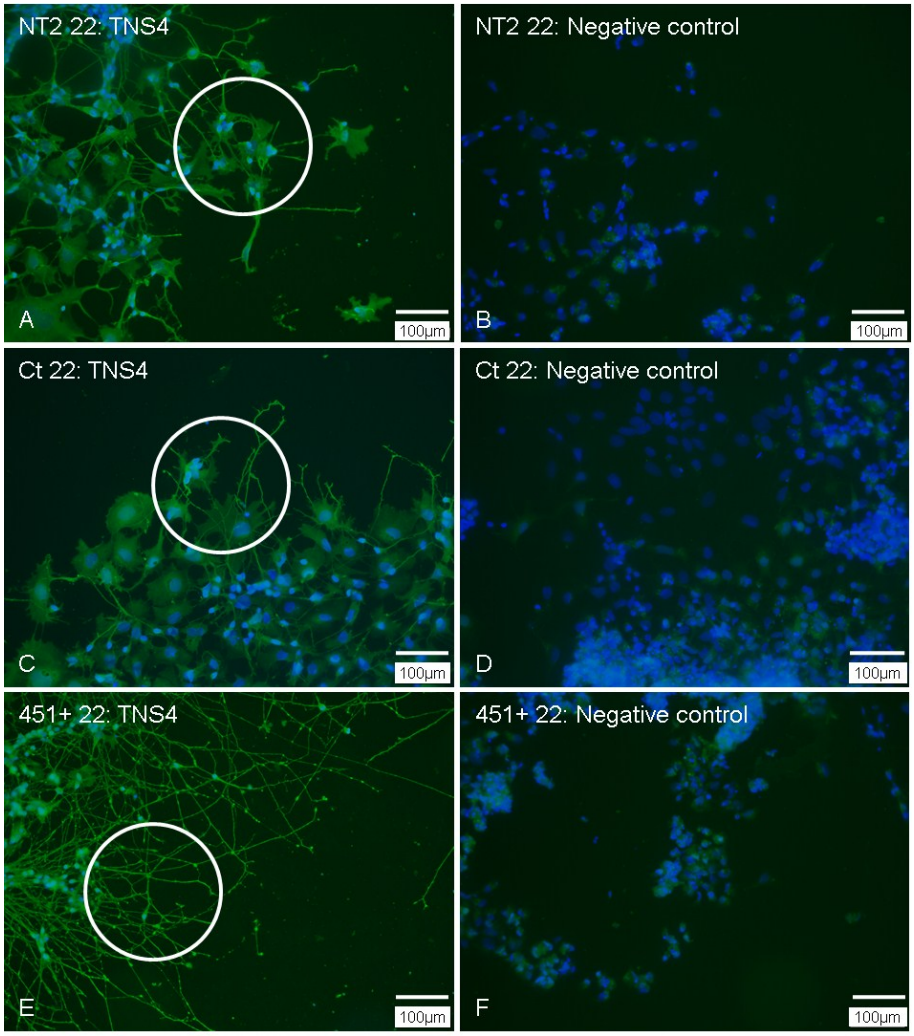

Figure 73

Immunostaining of TNS4 together with DAPI stain: non-Transduced NT2 cells (A-B), Ct cells (C-D) and transduced miR-451+ cells (E-F) at day 22. Negative controls are shown in B, D and F. All pictures are 20x taken with a fluorescence microscope (Olympus, Hicksville, New York, USA)

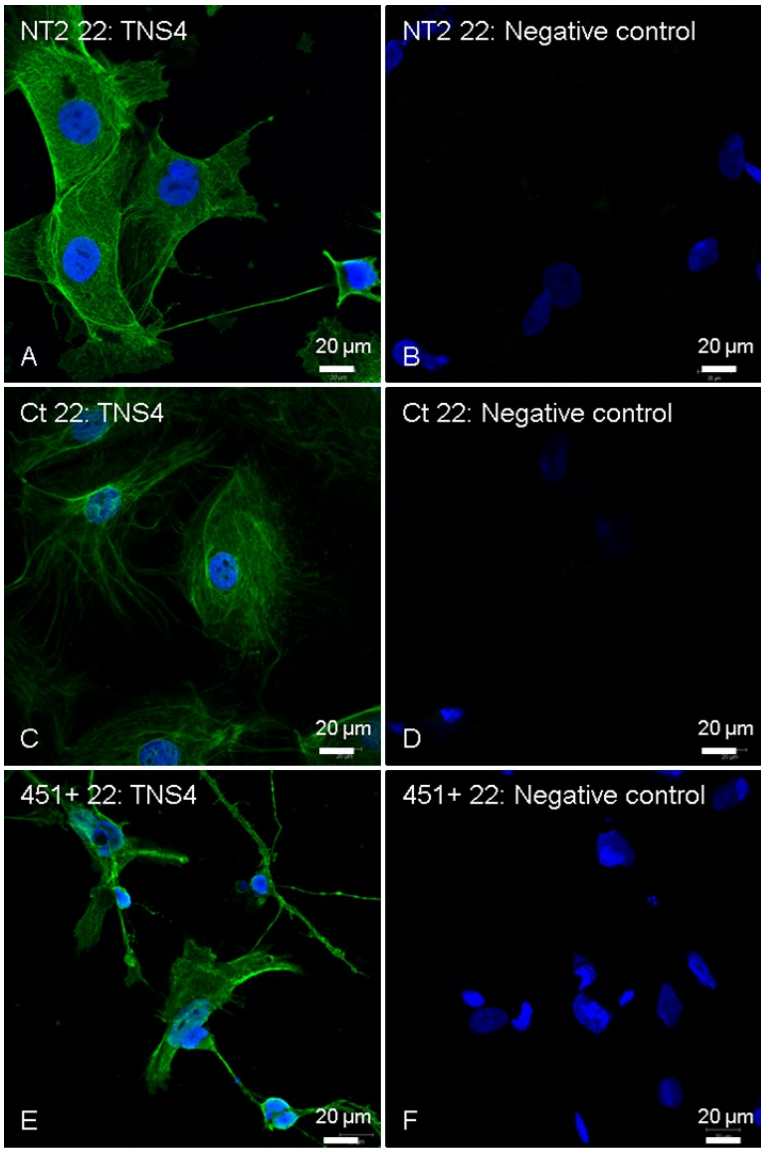

Figure 74

Immunostaining of TNS4 together with DAPI stain: non-Transduced NT2 cells (A-B), Ct cells (C-D) and transduced miR-451+ cells (E-F) at day 22. Negative controls are shown in B, D and F. All pictures are 40x taken with LSM (Zeiss, Oberkochen, Germany).

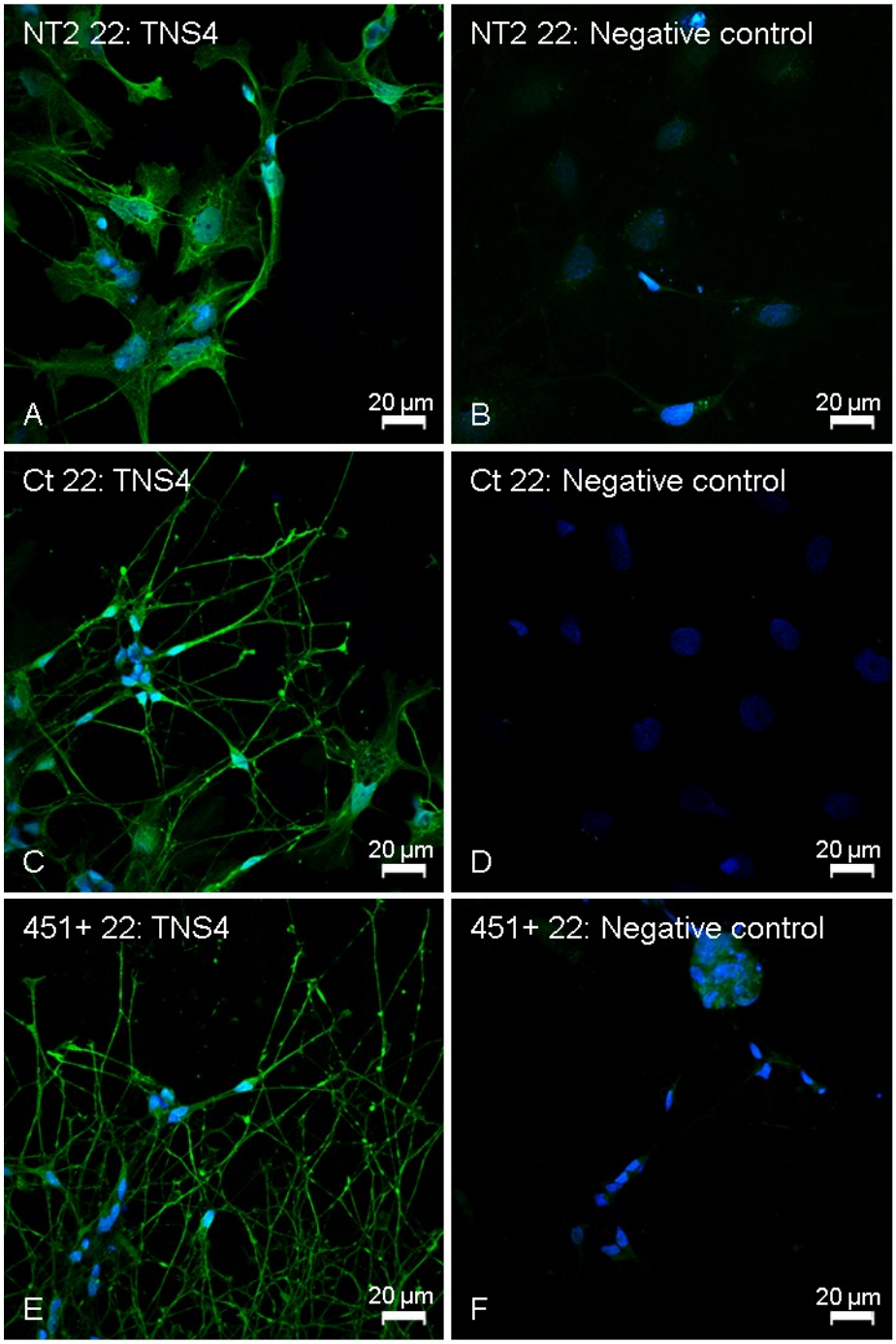

Figure 75

Immunostaining of TNS4 together with DAPI stain: non-Transduced NT2 cells (A-B), Ct cells (C-D) and transduced miR-451+ cells (E-F) at day 22. Negative controls are shown in B, D and F. All pictures are 40x taken with LSM Nikon (Vienna, Austria)

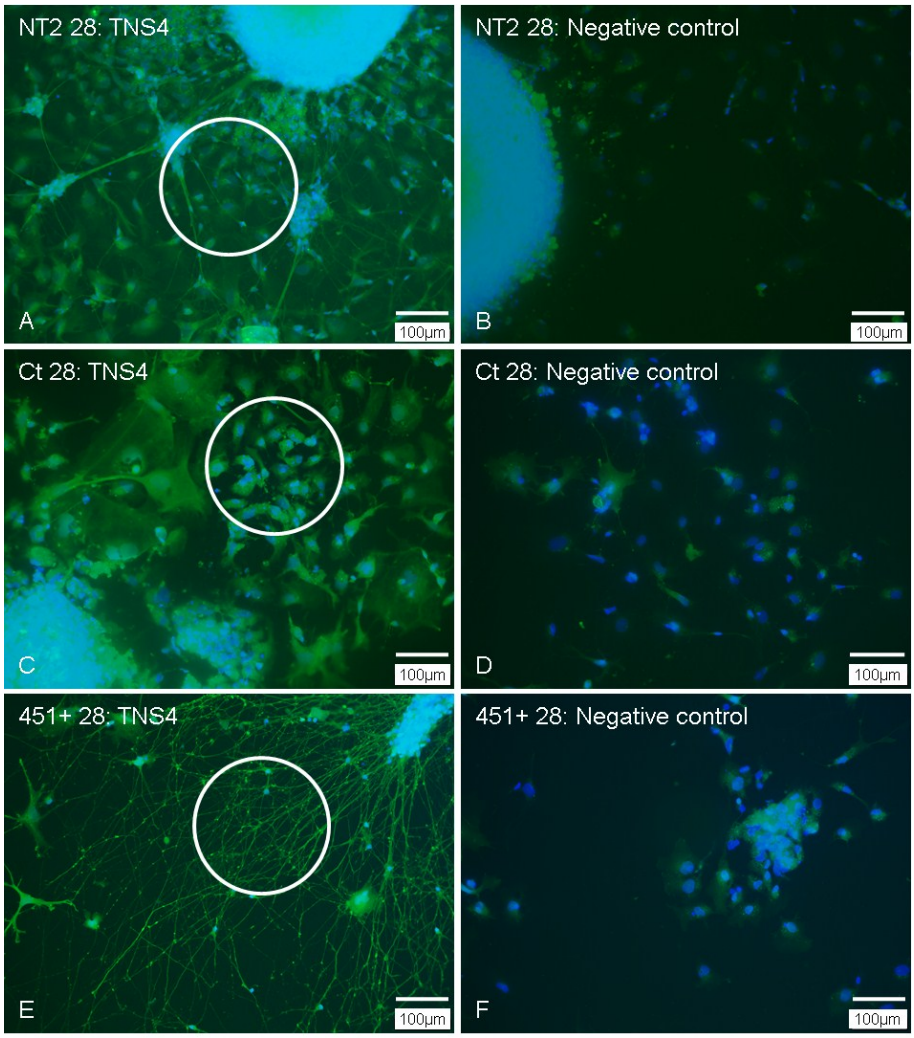

Figure 76

Immunostaining of TNS4 together with DAPI stain: non-Transduced NT2 cells (A-B), Ct cells (C-D) and transduced miR-451+ cells (E-F) at day 28. Negative controls are shown in B, D and F. All pictures are 20x taken with a fluorescence microscope (Olympus, Hicksville, New York, USA)

6.8. Comparison of marker expression in NT2 and Ct

There are differences in expression when comparing the expression of **Sox2** during neuronal differentiation of Ct cells to the expression in NT2 cells at day 0, 8, 22 and 27 (Figure 77A). At day 0, day 8 and day 22 the down-regulation of Sox2 expression is stronger in NT2 compared to control cells. But at day 27 we see a reverse effect and there is a significant higher down-regulation of Sox2 in the Ct cells.

Nestin expression in cells (NT2) was compared to Ct cells by setting the reference to day 0 of Ct cells (Figure 77B) When comparing the expression of Nestin in NT2 and Ct cells, there is a significant difference in expression at all examined days of differentiation. Whereas there is a tendency of down-regulation of Nestin expression at day 22 and 27 in NT2, we see an up-regulation of Nestin expression in Ct cells (Ct).

When comparing NT2 and Ct cells by referencing the values to day 0 of the Ct cells, we see again significant differences in expression of **DCX** (Figure 77C). DCX is significantly down-regulated in undifferentiated NT2 compared to Ct cells. At day 8, the expression level of DCX in cells and Ct seems to be similar at day 17, 22 and 27 there is a significant higher up-regulation of DCX expression in NT2 compared to Ct.

There is a significant difference in **Tuj1** expression, when comparing Ct and NT2 (Figure 77D). There are higher initial levels of Tuj1 in Ct cells, the same levels of expression at day 8, significant differences at day 17 and 22 and similar levels of expression at day 27.

MAP2 expression is significantly different between NT2 and Ct at day 0, 8, 17 and 27 (Figure 77E).

There is a lower expression of **NF** in NT2 compared to Ct cells (Figure 77F).

There is a significant difference in **GFAP** expression at day 22 between NT2 and Ct cells (Figure 77G). There are GFAP expressing cells present at day 22 in Ct cells, meaning that there seem to be more astrocytes in Ct.

Delta ct values of NT2 were referenced to the delta ct of day 0 of Ct cells in order to compare the marker expression between Ct and NT2 at day 0 and within the expression profile.

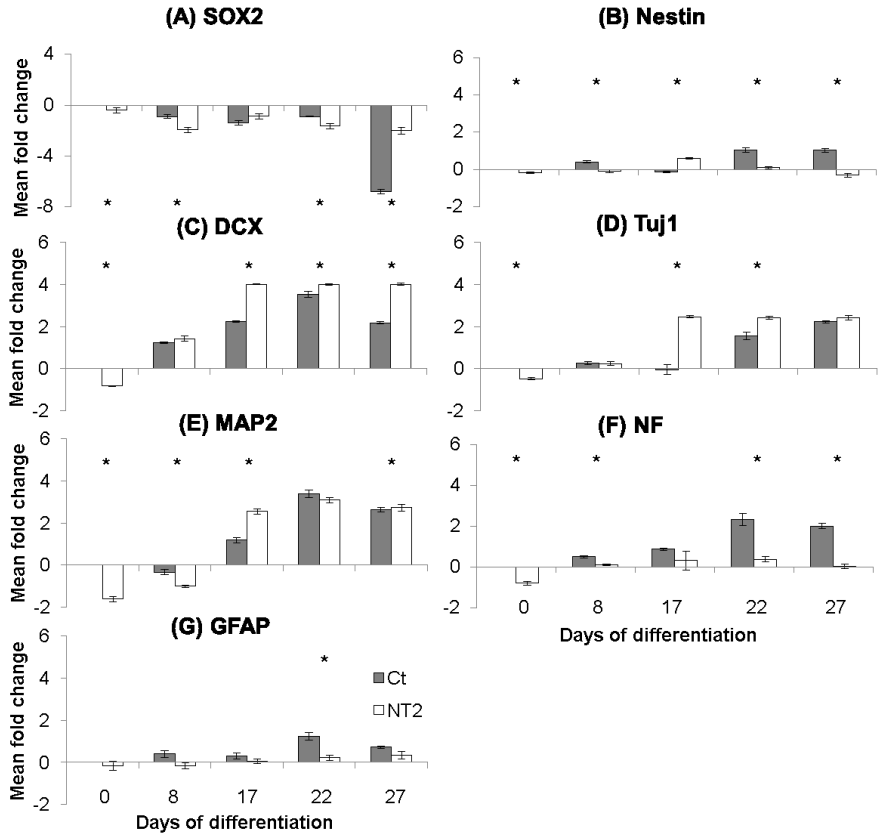

Figure 77

Expression pattern of different markers during neuronal differentiation of NT2 compared to Ct cells (Ct) (n=3). (A) Sox2, (B) Nestin, (C) DCX, (D) Tuj1, (E) MAP2, (F) NF, (G) GFAP. Mann-Whitney U-Test (* = $p \leq 0,05$)

Differences in marker expression imply that the transduction of the control vector into NT2 cells has an influence on the genotype. As the expression profiles of the markers show a similar pattern we conclude that there is no change of the general neuronal differentiation capacity of Ct cells.

6.9. Morphological comparison between NT2 and Ct during differentiation

NT2 cells at day 22 (A) and 27 (C) and Ct at 22 (B) and 27 (D) of neuronal differentiation in vitro are shown in Figure 78.

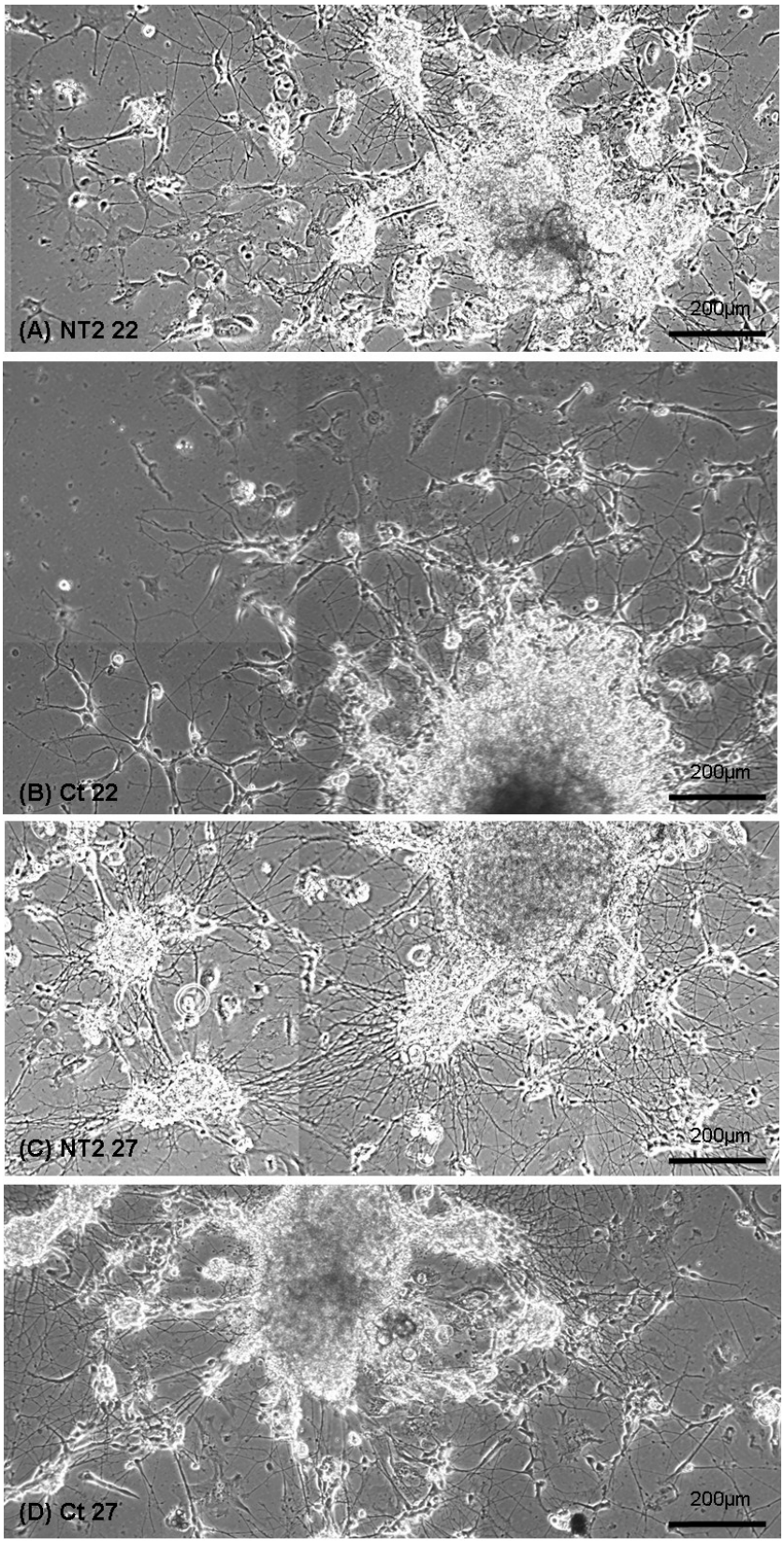

Figure 78

NT2 cells at day 22 (A) and 27 (C) and Ct at 22 (B) and 27 (D) of neuronal differentiation in vitro are shown.

6.10. Target gene analysis - expression in NT2

Figure 79 shows the gene expression profile of (A) AKT1, (B) CAB39, (C) CDKN2D, (D) CXCL16, (E) IL6R, (F) KIF24, (G) MIF, (H) MYC and (I) OSR1 (J) POU3F2, (K) PSMB8, (L) RAB14, (M) S1PR2, (N) TNS4, (O) TSC1, (P) VAPA and (Q) YWHAZ in neuronal differentiation of NT2 compared to day 0.

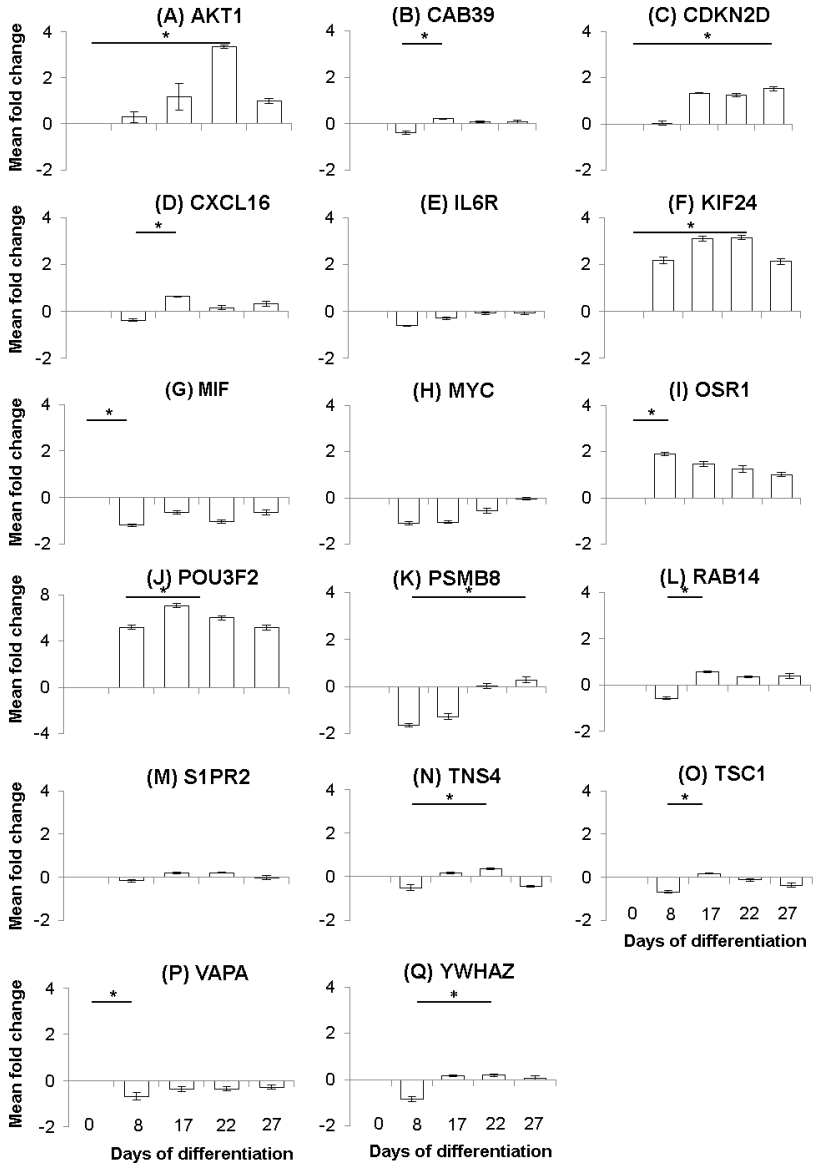

Figure 79

Expression pattern of various predicted and validated miR-451 target genes during neuronal differentiation of NT2 cells referenced to day 0 (n=3). (A) AKT1, (B) CAB39, (C) CDKN2D, (D) CXCL16, (E) IL6R, (F) KIF24, (G) MIF, (H) MYC and (I) OSR1 (J) POU3F2, (K) PSMB8, (L) RAB14, (M) S1PR2, (N) TNS4, (O) TSC1, (P) VAPA and (Q) YWHAZ. (Friedman's test, * = $p \leq 0{,}05$).

6.11. Target gene analysis – differences between NT2 and Ct

Figure 80 shows the gene expression of (A) AKT1, (B) CAB39, (C) CDKN2D, (D) CXCL16, (E) IL6R, (F) KIF24, (G) MIF, (H) MYC and (I) OSR1 (J) POU3F2, (K) PSMB8, (L) RAB14, (M) S1PR2, (N) TNS4, (O) TSC1, (P) VAPA and (Q) YWHAZ in neuronal differentiation of NT2 compared to Ct at day 0. There are significant differences in expression when comparing the target gene expression of NT2 to the expression in Ct at day 0.

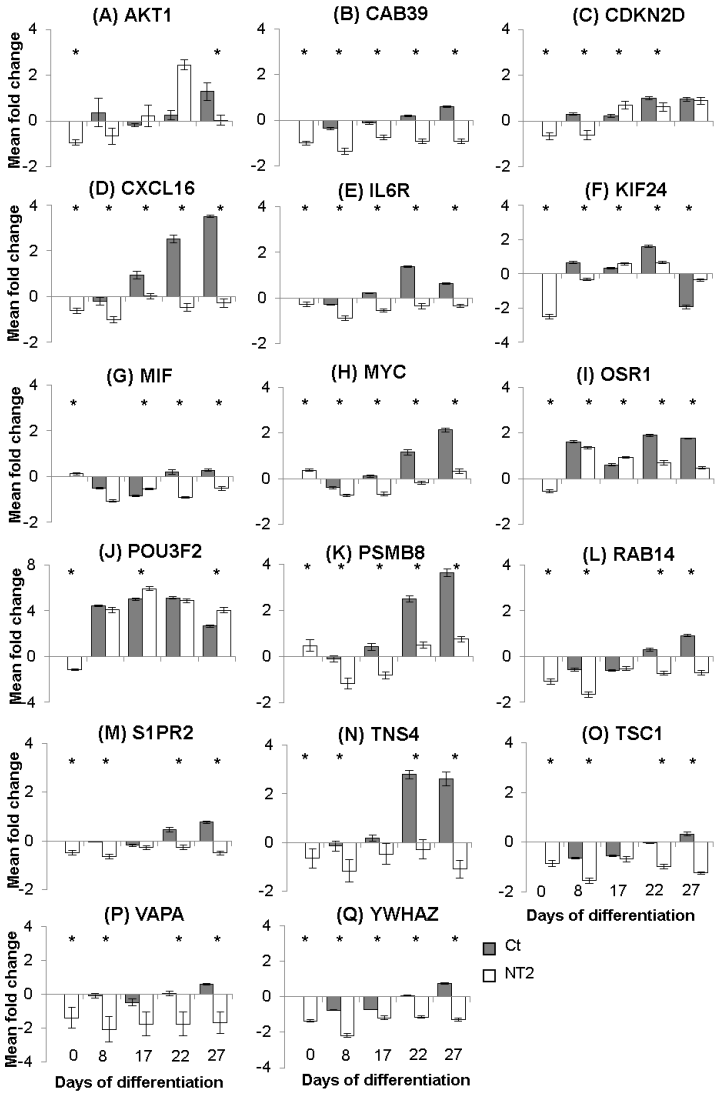

Figure 80

Expression pattern of various predicted and validated miR-451 target genes during neuronal differentiation of NT2 cells compared to Ct at day 0 (n=3). (A) AKT1, (B) CAB39, (C) CDKN2D, (D) CXCL16, (E) IL6R, (F) KIF24, (G) MIF, (H) MYC and (I) OSR1 (J) POU3F2, (K) PSMB8, (L) RAB14, (M) S1PR2, (N) TNS4, (O) TSC1, (P) VAPA and (Q) YWHAZ. Mann-Whitney U-Test (* = $p \leq 0{,}05$).

6.12. Buffers, media and solutions

6.12.1. Complete medium (10% DMEM) for NT2 and HEK293T cells

High glucose DMEM (Dulbecco modified Eagle medium, Sigma-Aldrich Handels GmbH, Vienna, Austria) was supplemented with 10% FBS (Fetal bovine serum, low in Endotoxin, Sigma-Aldrich Handels GmbH, Vienna, Austria), 1% Non Essential Amino Acids (NEAA, Sigma-Aldrich Handels GmbH, Vienna, Austria) and 1% Penicillin-Streptomycin solution (Sigma-Aldrich Handels GmbH, Vienna, Austria)

6.12.2. Retinoic acid, 10mM stock solution

50mg retinoic acid (Sigma-Aldrich Handels GmbH, Vienna, Austria) were dissolved in 16,7ml 100% ethanol (Sigma-Aldrich Handels GmbH, Vienna, Austria) and stored in 1ml aliquots protected from light at -20°C.

6.12.3. Freezing media

10 ml complete medium (6.12.1), 5ml FBS and 5ml DMSO (Dimethylsulfoxide, Lactan, Graz, Austria) were mixed.

6.12.4. DEPC-treated water

1ml/L of DEPC was added to deionized water (MilliQ, Millipore, Vienna, Austria), incubated overnight on a stirring plate (Laborpartner, Vienna, Austria) and then autoclaved (Fedegari Autoclavi spa, Albuzzano, Italy).

6.12.5. SOC medium

20g/L Tryptone (Sigma-Aldrich Handels GmbH, Vienna, Austria), 5g/L Yeast Extract (Sigma-Aldrich Handels GmbH, Vienna, Austria), 0,5g/L NaCl (Sigma-Aldrich Handels GmbH, Vienna, Austria) and 10ml/L 250mM KCl (Sigma-Aldrich Handels GmbH, Vienna) were dissolved in 800ml deionized H_2O (MilliQ, Millipore, Vienna, Austria). pH was adjusted to 7 with 1N NaOH (Sigma-Aldrich Handels GmbH, Vienna, Austria). Volume was adjusted to 1L with deionized H_2O and the solution was autoclaved (Fedegari Autoclavi spa, Albuzzano, Italy). The medium was cooled to 60°C or less and 18ml/L 20% filter-sterilized Glucose (100g of Glucose in 400 ml ddH_2O, Sigma-Aldrich Handels GmbH, Vienna, Austria, filter-sterilization through a 0.45µm filter (VWR International, Vienna, Austria) was added. Finally 5ml/L of a sterile solution of 2M $MgCl_2$ (Sigma-Aldrich Handels GmbH, Vienna, Austria) were added.

6.12.6. LB selective Agar

35g/L LB-Agar mixture (Sigma-Aldrich Handels GmbH, Vienna, Austria) were dissolved in 1L deionized water (MilliQ, Millipore, Vienna, Austria), autoclaved and cooled to 60°C. Ampicillin (Sigma-Aldrich Handels GmbH, Vienna, Austria) was added (ampicillin end concentration: 100µg/ml, stock concentration 10mg/ml, 10ml per 1L).

6.12.7. LB medium

For 500ml LB medium 5g Tryptone (Sigma-Aldrich Handels GmbH, Vienna, Austria), 5g NaCl (Sigma-Aldrich Handels GmbH, Vienna, Austria) and 2,5g yeast extract (Sigma-Aldrich Handels GmbH, Vienna, Austria) were dissolved in 500ml Aqua bidest and then autoclaved.

6.12.8. 0,5x TBE Buffer+GelRed®

50ml Rotiphorese 10x TBE Buffer (Lactan, Graz, Austria) plus 950ml MilliQ water and 100µl GelRed® (GelRedTM Nucleic Acid Gel Stain, VWR international, Vienna, Austria)

6.12.9. 10x DNA loading buffer

For 10ml 10x DNA loading buffer 5 ml Glycerol, 2ml MilliQ Water, 2ml 0,5M EDTA pH 8,0 and 1% Xylencyanol FF were used. 10x DNA loading buffer was diluted with ddH_2O to 1x DNA loading buffer.

6.12.10. 10x Formaldehyde Agarose Gel Buffer

200mM MOPS (N-morpholino]propanesulfonic acid (BDH biochemical, owned by VWR international, Vienna, Austria), 50mM sodium acetate (Sigma-Aldrich Handels GmbH, Vienna, Austria) and 10mM EDTA (Ethylenediaminetetraacetic acid, Sigma-Aldrich Handels GmbH, Vienna, Austria) were mixed in DEPC-treated water and autoclaved. pH was adjusted to 7 with (NaOH Sigma-Aldrich Handels GmbH, Vienna, Austria). For 1x Formaldehyde Buffer 100ml 10x Formaldehyde Agarose gel buffer, 20ml 37% Formaldehyde and 880 RNase free water (DEPC treated).

6.12.11. 5x RNA loading buffer

For 10ml 5x RNA loading buffer 16µl saturated aqueous bromphenol blue solution (Sigma-Aldrich Handels GmbH, Vienna, Austria), 80µl 500mM EDTA pH 8 (Sigma-Aldrich Handels GmbH, Vienna, Austria), 720µl 37% formaldehyde (Merck, Hohenbrunn, Germany), 2ml 100% glycerol (Sigma-Aldrich Handels GmbH, Vienna, Austria), 3084µl formamide (VWR International, Vienna, Austria) and 4ml 10x formaldehyde agarose gel buffer were mixed.

6.12.12. Blocking solution for immunofluorescence

1g BSA (Sigma-Aldrich Handels GmbH, Vienna, Austria) was dissolved in 100ml PBS (Sigma-Aldrich Handels GmbH, Vienna, Austria)

6.12.13. 10x TBS

For 2L of 10x TBS 121g Tris (Sigma-Aldrich Handels GmbH, Vienna, Austria) are dissolved in 500ml MilliQ water. pH is adjust to 7,4 by using 900ml 1N HCl (VWR, Vienna, Austria). Then 146 g NaCl (Sigma-Aldrich Handels GmbH, Vienna, Austria) are added and mixed. Volume is adjusted to 2000ml using MilliQ water. pH is checked again und then the solution is autoclaved.

6.12.14. 1x TBS

100 ml of 10x TBS are added to 900ml MilliQ water.

6.12.15. 10x Transfer Buffer

For 2L of 10x TBS 288g Glycin (Merck, Vienna, Austria) and 72,6 g Tris (Sigma-Aldrich Handels GmbH, Vienna, Austria) are dissolved in 1800ml MilliQ water. After dissolving, volume is adjusted to 2000ml using MilliQ water.

6.12.16. 1x Transfer Buffer

100ml of 10x Transfer Buffer and 700 ml of MilliQ water are mixed. 200ml of Methanol (VWR, Vienna, Austria) are added.

6.12.17. Blocking solution for Western Blot

5 g BSA are dissolved in 100ml TBS

6.13. Used Primers

Table 3

Primer	Sequence 5'- 3'	Size of Product	Source
Differentiation markers			
Nestin_new	fw: TCAAGATGTCCCTCAGCCTGGA rev: TCAAGATGTCCCTCAGCCTGGA		Origene
SOX2	fw: AGTCTCCAAGCGACGAAA AA rev: GCAAGAAGCCTCTCCTTGAA	141bp	Lit. (41)
NF200_new (heavy chain)	fw: CTGAGGAACACCAAGTGGGAGA rev: TCCGACACTCTTCACCTTCCAG		Origene
NeuN_new	fw: TACGCAGCCTACAGATACGCTC rev: TGGTTCCAATGCTGTAGGTCGC		Origene
MAP2	fw: TCAGAGGCAATGACCTTACC rev: GTGGTAGGCTCTTGGTCTTT	319bp	Lit. (275)
DCX	fw: ACCTGCCTCAGGGAGTGCGT rev: GGCCAGCTGTGGCTGATGGG	567bp	Primer3 Output
DCX_new	fw: TATGCGCCGAAGCAAGTCTCCA rev: CATCCAAGGACAGAGGCAGGTA		Origene
Tuj1	fw: GGCAACCAGATCGGGGCCAAGT rev: CCCTGCAGGCAGTCGCAGTTT	359bp	Primer3 Output
GFAP (transcript variant 2)	fw: GCCAAGCACGAAGCCAACGAC rev:GAGCCGGCGGCGTTCCATTTACAAT	457bp	Primer3 Output
House keeping genes (RNA)			
U6 snRNA	fw: CTCGCTTCGGCAGCACA rev: AACGCTTCACGAATTTGCGT	94bp	Lit.(276)
GAPDH	fw: CTGGTAAAGTGGATATTGTTGCCAT rev: TGGAATCATATTGGAACATGTAAACC	81bp	Lit.(276)
YWHAZ	Unknown		Primerdesign
UBC	Unknown		Primerdesign
TOP1	Unknown		Primerdesign
RPL13A	Unknown		Primerdesign
B2M	Unknown		Primerdesign
SDHA	Unknown		Primerdesign
House keeping genes (miRNA)			
SNORD38b	Unknown		Exiqon
SNORD44	Unknown		Exiqon
SNORD48	Unknown		Exiqon
SNORD49A	Unknown		Exiqon
SNORD66	Unknown		Exiqon
U1	fw: CCATGATCACGAAGGTGGTTT rev: ATGCAGTCGAGTTTCCCACAT	101bp	Lit.(276)
U6 snRNA	fw: CTCGCTTCGGCAGCACA	94bp	Lit.(276)

	rev: AACGCTTCACGAATTTGCGT		
5s	Unknown		Exiqon
miRNA Primer			
miR-451	Unknown		Exiqon
miR-144	Unknown		Exiqon
Target genes and interesting genes			
AKT1	fw: TGGACTACCTGCACTCGGAGAA rev: GTGCCGCAAAAGGTCTTCATGG		Origene
CAB39	fw: GAGCATGGCTGTTCTGGAAAAGC rev: GCTACTGCTTCTGTCTGAGGCT		Origene
CD133	Fw: TTACGGCACTCTTCACCT rev: TTACGGCACTCTTCACCT	172bp	Primer3 Output
CXCL16	fw: CCTATGTGCTGTGCAAGAGGAG rev: CTGGGCAACATAGAGTCCGTCT		Origene
CDKN2D	fw: GTGCATCCCGACGCCCTCAAC rev: TGGCACCTTGCTTCAGCAGCTC		Origene
FGFR1	fw: CCCGAAGACCCTCGCTGGGA rev: CCGCAGGTTGCCCTTGGAGG	315bp	Primer3 Output
IL6R	fw: GACTGTGCACTTGCTGGTGGAT rev: ACTTCCTCACCAAGAGCACAGC		Origene
Integrin-ß1	fw: GCCTTACATTAGCACAACAAC rev: CATCTCCAGCAAAGTGAAAC	284bp	Primer3 Output
KIF24	fw: GACAGAAATGCCAGCAATGATGG rev: GGAATCATCTGGTAGCATGTGTTC		Origene
MIF	fw: AGAACCGCTCCTACAGCAAGCT rev: GGAGTTGTTCCAGCCCACATTG		Origene
Myc	fw: CCTGGTGCTCCATGAGGAGAC rev: CAGACTCTGACCTTTTGCCAGG		Origene
OSR1	fw: CCTACACCTGTGACATCTGCCA rev: GTGAGTGTAGCGTCTTGTGGAC		Origene
POU3F2	fw: AAAGGCCAGTTCCCATACCT rev:TCATTTCCCCCAATGAATGT	93bp	Primer3 Output
PSMB8	fw: CCTTACCTGCTTGGCACCATGT rev: TTGGAGGCTGCCGACACTGAAA		Origene
RAB14	fw: GCGATTTAGGGCTGTTACACGG rev: CCTTGCATCTGTCAACCAGCTG		Origene
TSC1	fw: CTGGACAGACTGATACAGCAGG rev: TGCGGATCTCATCTGAAGGAGG		Origene
TNS4	fw: GGACAGCAATGACCTCATCCGA rev: AATGCTGGCACACGAAGGCAGA		Origene
VAPA	fw: CCTGCCAGTTATCACACGAAGG rev: CTGTGTGGTTTTGGCATAGGTCC		Origene
Vimentin	fw: GGCAGAAGAATGGTACAAATCC rev: CTTCCAGCAGCTTCCTGTAG	359bp	Primer3 Output
YHWAZ	fw: ACCGTTACTTGGCTGAGGTTGC rev: CCCAGTCTGATAGGATGTGTTGG		Origene

6.14. Used antibodies

Table 4

List of primary antibodies

Antibody	Dilution	Company
Anti-NF200 (chicken)	1:500	Abcam, Cambridge, United Kingdom
Anti-MAP2 (chicken)	1:1000	Abcam, Cambridge, United Kingdom
Anti-Doublecortin (goat)	1:250	Santa Cruz, Heidelberg, Germany
Anti-Tuj1 (chicken)	1:1000	Abcam, Cambridge, United Kingdom
Anti-TNS4 (mouse)	1:250	Abcam, Cambridge, United Kingdom
Anti-MIF (rabbit)	1:300	Santa Cruz, Heidelberg, Germany
Anti-CAB39 (rabbit)	1:20000	Abcam, Cambridge, United Kingdom

Table 5

List of secondary antibodies

Antibody	Dilution	Company
Rabbit anti chicken FITC	1:1000	Abcam, Cambridge, United Kingdom
Donkey anti goat FITC	1:1000	Abcam, Cambridge, United Kingdom
Goat anti mouse FITC	1:1000	Abcam, Cambridge, United Kingdom
Anti rabbit-HRP	1:3000	Santa Cruz, Heidelberg, Germany